Universitat de Lleida

Design of nanostructured delivery systems to enhance the functionality of food bioactive compounds

María Artiga Artigas

Universitat de Lleida

Design of nanostructured delivery systems to enhance the functionality of food bioactive compounds

Doctoral Thesis
(International Mention)

María Artiga Artigas

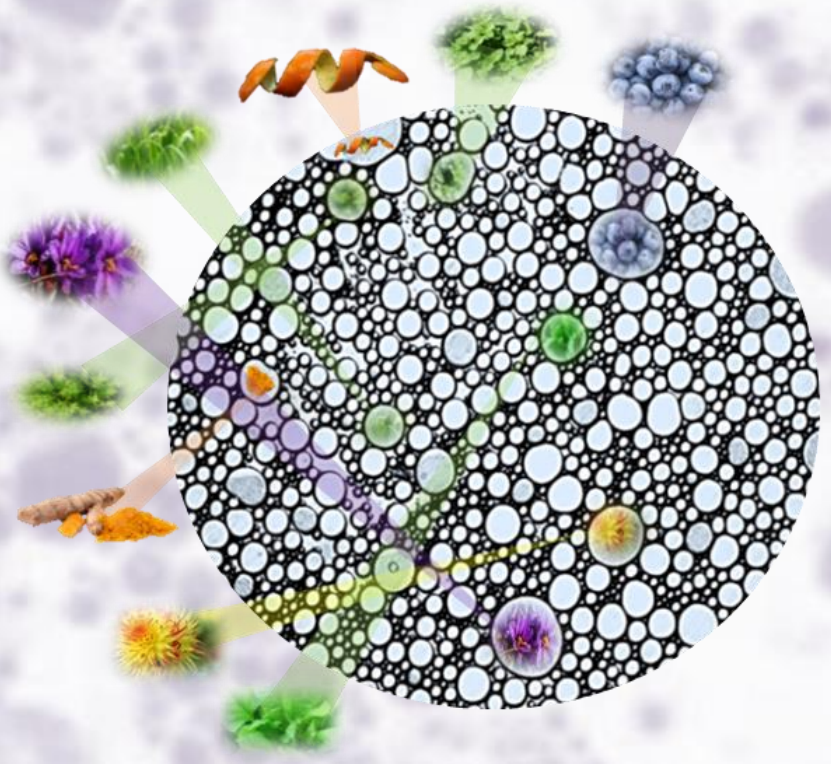

Universitat de Lleida

TESIS DOCTORAL

(MENCIÓN INTERNACIONAL)

Design of nanostructured delivery systems to enhance the functionality of food bioactive compounds

María Artiga Artigas

Memoria presentada para optar al grado de Doctor por la Universitad de Lleida

Programa de Doctorado en Ciencia y Tecnología Agraria y Alimentaria

Directoras:
Olga Martín Belloso
Laura Salvia Trujillo

Tutora:
Olga Martín Belloso

2018

The current research has been performed in the Laboratory of Novel Technologies for Food Processing and the Pilot Plant of the Department of Food Technology, under the supervision of Prof. Olga Martín Belloso and the co-direction of Dra. Laura Salvia Trujillo.
This Doctoral Thesis has been supported by the Spanish Ministry of Economy, Industry and Competitiveness (MINECO/FEDER, UE) through the following projects:

ALG2009-11475: 'Development of nanostructured edible coatings as carriers of active compounds'

ALG2012-35635: "Improving quality and functionality of food products by incorporating lipid nanoparticles into edible coatings"

AGL2015-65975-R: 'Design of nanostructured systems for protecting and releasing natural compounds with functional and technological activity'.

The PhD candidate granted a fellowship of the University of Lleida to pursue the PhD degree.

Chapter V, based on the formation of protein-polysaccharide complexes, was carried out in the Department of Food Physics and Meat Science at the Institute of Food Science and Biotechnology at the University of Hohenheim (Stuttgart, Germany), under the supervision of Prof. Jochen Weiss.

*“*Your work is going to fill a large part of your life, and the only way to be truly satisfied is to do what you believe is great work. And the only way to do great work is to love what you do. If you haven't found it yet, keep looking. Don't settle. As with all matters of the heart, you'll know when you find it*”*- *Steve Jobs*

*“*Remember to look up at the stars and not down at your feet. Try to make sense of what you see and wonder about what makes the universe exist. Be curious. And however difficult life may seem, there is always something you can do and succeed at. It matters that you don't just give up*” – Stephen Hawking*

*“*L’essentiel est invisible pour les yeux*”- Saint Exupéry*

A mis padres, Mª Pilar y Juan Ramón.

A mi yaya Montse.

A Eric.

A ti, Iñaki (19-05-2018). May your force be with me.

AGRADECIMIENTOS/ACKNOWLEDGEMENTS

En primer lugar, me gustaría dar las gracias a mis directoras, Olga y Laura. Especialmente a ti, Olga, por acompañarme en cada paso que he ido dando y por saber guiarme y templarme incluso en los tiempos difíciles. Gracias por confiar en mí desde el primer momento y darme la libertad necesaria para desarrollar mi pensamiento crítico. A ti, Laura, por aparecer en el momento preciso y contagiarme tu energía, gracias por implicarte así y enseñarme tanto. Me habéis ayudado a ampliar mis conocimientos y capacidad científica, pero también a crecer y a enfrentarme a este camino con tenacidad.

A todos mis compañeros *Novestec* por aportarme tantas cosas, por escucharme y apoyarme siempre. Os agradezco las risas, los abrazos, los bailes, los cafés y las patatas del Beat. Espero que sigamos celebrando momentos juntos. A vosotros, Gloria, Gustavo, Ariadna, Clara, Júlia y en especial a ti, Anna, muchas gracias por cuidarme y acompañarme en este último año tan difícil para mí. Gracias Manel y sobre todo a ti, Magda, por echarme un cable siempre que lo he necesitado. Muchas gracias también a ti María, por ser mi gran apoyo en una etapa de mi vida bastante complicada a nivel personal. Y a ti, Fabiola, por enseñarme a usar las herramientas que me han permitido llegar hasta aquí.

In addition, I would like to thank the Prof. Weiss, Ben and Corina for your patience and kindness during my stay at the University of Hohenheim. And, of course, I would like to thank all my lab mates, specially, Sandra, Isabel, Angelika, Ivonne, Linda, Julia, Lutz, Eva, Johannes, Juli, Laixin, Ines and Monise, for make me feel like home. Danke für Alles.

También quisiera agradecer todo el apoyo a mis amigos, a los que sí, siempre y a los que no pueden estar, pero son; que pese a la distancia se han esforzado porque los sienta cerca. Pablo, gracias por hacer el esfuerzo de leerte mis artículos, escucharme, hacerme reír y conseguir entenderme siempre. Gracias a ti Saroto por acompañarme al fin del mundo si hace falta, aunque sea para discutir, y por ser mi apoyo incondicional. Gracias por la amistad *Havaneros crew* y *Butasonas*, en especial a vosotras, Andrea y Aroa, que siempre habéis estado a una llamada de distancia. A mis hermanas de otros padres, Ambika, mi pequeña Sofía y las *Bolingas*: Raquel, Marina y sobre todo a ti, Elena. Nunca os podré agradecer lo suficiente los miles de recuerdos que creamos juntas y lo bonita que me habéis puesto la vida estos cuatro años. Os echo de menos y os querré siempre. Tampoco me olvido del resto de mis compañeros de piso de todos estos años: Johan, Alba, Helena, Sofi, Javi… Gracias por los momentazos, las largas conversaciones, el apoyo y hacer que todo sea más fácil y divertido. No podría haber tenido más suerte. A Xenia y a Estrella, así como a todas las personas que he ido conociendo por el camino y que, a día de hoy, todavía son capaces de arrancarme una sonrisa. Y de los creadores de "Comerse un Frankfurt en Frankfurt" y "Vamos a no comer al restaurante de Amelie", gracias a ti Ana, por ser mi "traveler in crime" y "compi-yogui" favorita. A mis amigos internacionales y excompañeros de unizar, en especial a Jose, por vuestros consejos y cariño. También a ti Mariajo, por empujarme a comenzar este camino y haber sido mi referente. Natalia, gracias por ser mi vía de escape y ayudarme en todo lo que estaba en tu mano. Gracias a mis segundas familias, la *Rufat-Muñoz*, la *Benito-Bailera* y la *García-Tena* y a las *Chicas de oro*, por aplaudir cada uno de mis logros y quererme como a una hija más.

Por último, a todas las personas, sin las que ninguno de los pasos que he dado en mi vida tendría sentido. A mis padres, os quiero y os admiro muchísimo. Gracias por ser mi motor cada día, respaldarme y estar siempre a mi lado. A mi yaya, a mis tíos Javi y Judith y mis pequeñas Zoe y Margarita, gracias por no soltarme nunca de la mano, confiar en mí y quererme tanto. De corazón, gracias por todo. Este logro es también vuestro. Gracias a ti, Eric por ser mi apoyo y mi compañero de viaje todos estos años; por recordarme de lo que soy capaz en los buenos y malos momentos y por enseñarme a entender la vida de otra manera. Nada hubiera sido lo mismo sin ti. Al resto de mis tíos, y principalmente a María y Luis, Mamen y Nacho, Salz y Juanjo; y a todos mis primos, gracias por haber estado siempre al pie del cañón.

En especial, quiero dar las gracias a mi tío Iñaki, al que querré toda mi vida, que siempre creyó en mí incluso más que yo misma, y que me enseñó que, en esta vida, pese a todo, hay que ser valiente.

RESUM

La incorporació dels pigments bioactius derivats de plantes, amb elevada capacitat antioxidant i/o antimicrobiana, té com a finalitat augmentar el seu valor nutricional i/o la seva vida útil, respectivament. Aquests pigments, són fàcilment degradables, per tant caldrà protegir-los dins de sistemes nanoestructurats. Depenent de la seva naturalesa (hidrofílica o lipofílica) i de l'aplicació desitjada, les nanoestructures requerides i les estratègies per a la seva estabilització interfacial seran diferents. L'objectiu principal d'aquesta tesi doctoral va ser dissenyar, preparar i caracteritzar nanoemulsions i emulsions dobles capaces d'actuar com a sistemes de transport i alliberament de pigments bioactius liofílics i hidrofílics, respectivament.

En primer lloc, es van preparar nanoemulsions contenint olis essencials (orenga, farigola, citronole·la o mandarina) com a fase lipídica, Tween 80 com surfactant i pectina en la fase aquosa, mitjançant microfluidització (5 cicles, 150 MPa). Es va observar que la pectina actuava com emulsificant fins i tot en absència de surfactant i va contribuir positivament a la reducció de la mida de partícula de les nanoemulsions que contenien citronel·la, suggerint que l'adsorció de la pectina en la interfase depenia del tipus d'oli. Així mateix, es van obtenir nanoemulsions portadores de curcumina (0.4% *p/p*) amb Tween 20, lecitina o monopalmitat de sacarosa com a surfactants (0.5-2% *p/p*) amb mides de partícula inferiors a 400 nm. Les nanoemulsions incloent lecitina (≥1% *p/p*) van resultar efectives per a la encapsulació i alliberament controlat de curcumina i es van mantenir estables durant almenys 3 mesos a temperatura ambient. El fet d'augmentar la concentració d'oli en emulsions altament concentrades (fracció en volum 0.5, i relació surfactant-oli = 0.1), preparades per ultrasons (100 micres, 200 s) o microfluidització (2 cicles, 800 bar) no va afectar l'eficiència dels sistemes formats. D'altra banda, es van preparar nanoemulsions a les quals es va incorporar alginat de sodi microfluiditzat o no, i es va demostrar que la microfluidització provocava el trencament parcial de les cadenes del biopolímer, permetent una disposició més homogènia al voltant de les gotes, reduint la mida de partícula, la polidispersitat i la viscositat de les nanoemulsions resultants. Una altra forma d'estabilització de nanoemulsions va ser l'ús de complexos proteïna de sèrum (WPI)-pectina de remolatxa sucrera (SBP), que va mostrar més efectivitat que WPI i SBP per separat enfront de la maduració d'Ostwald, retardant el creixement de les gotes durant més temps.

En segon lloc, es van dissenyar emulsions dobles (6-7 μm) per transportar clorofilina (pigment bioactiu hidrofílic) i/o oli essencial de citronella seguint un procediment en dues etapes: *(I)* formació de l'emulsió primària estabilitzada amb 4% *p/p* PGPR, per homogeneïtzació (11,000 rpm, 5 minuts) i *(II)* obtenció de l'emulsió doble estabilitzada amb lecitina (2% *p/p*) mitjançant homogeneïtzació (5,600 rpm, 2 min) i agitació magnètica (750 rpm, 24h).

Finalment, es van aplicar recobriments comestibles formats a partir de nanoemulsions amb oli essencial d'orenga com a agent antimicrobià sobre la superfície d'un formatge tallat baix en greix. Aquells recobriments amb una major concentració d'oli (2.5% *p/p*) van ser efectius davant *Staphylococcus aureus* i van retardar el creixement de fongs i llevats durant almenys 11 dies respecte al formatge no recobert.

RESUMEN

La incorporación de los pigmentos bioactivos derivados de plantas, con elevada capacidad antioxidante y/o antimicrobiana, tiene como fin aumentar su valor nutricional y/o su vida útil, respectivamente. Estos pigmentos son fácilmente degradables por lo que habrá que protegerlos dentro de sistemas nanoestructurados. Dependiendo de su naturaleza (hidrofílica o lipofílica) y de la aplicación deseada, las nanoestructuras requeridas y las estrategias para su estabilización interfacial serán diferentes. El objetivo principal de esta Tesis Doctoral fue diseñar, preparar y caracterizar nanoemulsiones y emulsiones dobles capaces de actuar como sistemas de transporte y liberación de pigmentos bioactivos lipofílicos e hidrofílicos, respectivamente.

En primer lugar, se prepararon nanoemulsiones conteniendo aceites esenciales (orégano, tomillo, hierba de limón o mandarina) como fase lipídica, Tween 80 como surfactante y pectina en la fase acuosa, mediante microfluidización (5 ciclos, 150 MPa). Se observó que la pectina actuaba como emulsificante incluso en ausencia de surfactante y contribuyó positivamente a la reducción del tamaño de partícula de las nanoemulsiones que contenían citronela, sugiriendo que la adsorción de la pectina en la interfase, dependía del tipo de aceite. Del mismo modo, se obtuvieron nanoemulsiones portadoras de curcumina (0.4% *p/p*) con Tween 20, lecitina o monopalmitato de sacarosa como surfactantes (0.5-2% *p/p*) con tamaños de partícula inferiores a 400 nm. Las nanoemulsiones incluyendo lecitina (≥1% *p/p*) resultaron efectivas para la encapsulación y liberación controlada de curcumina y se mantuvieron estables durante al menos 3 meses a temperatura ambiente. El hecho de aumentar la concentración de aceite en emulsiones altamente concentradas (fracción en volumen 0.5 y relación surfactante-aceite=0.1), preparadas por ultrasonidos (100 μm, 200 s) o microfluidización (2 ciclos, 800 bar) no afectó a la eficiencia de los sistemas formados. Por otra parte, se prepararon nanoemulsiones a las que se incorporó alginato de sodio microfluidizado o no y se demostró que la microfluidización provocaba la rotura parcial de las cadenas del biopolímero permitiendo una disposición más homogénea alrededor de las gotas, reduciendo el tamaño de partícula, la polidispersidad y la viscosidad de las nanoemulsiones resultantes. Otra forma de estabilización de nanoemulsiones fue el uso de complejos proteína de suero (WPI)-pectina de remolacha azucarera (SBP), que mostró mayor efectividad que WPI y SBP por separado frente a la maduración de Ostwald, retrasando el crecimiento de las gotas durante más tiempo.

En segundo lugar, se diseñaron emulsiones dobles (6-7 μm) para trasportar clorofilina (pigmento bioactivo hidrofílico) y/o aceite esencial de citronela siguiendo un procedimiento en dos etapas: *(I)* formación de la emulsión primaria estabilizada con 4% *p/p* PGPR, por homogenización (11,000 rpm, 5 min) y *(II)* obtención de la emulsión doble estabilizada con lecitina (2% *p/p*) mediante homogenización (5,600 rpm, 2 min) y agitación magnética (750 rpm, 24h).

Finalmente, se aplicaron recubrimientos comestibles formados a partir de nanoemulsiones con aceite esencial de orégano (OR-EO) como agente antimicrobiano sobre la superficie de un queso cortado bajo en grasa. Aquellos recubrimientos con una mayor concentración de OR-EO (2.5% *p/p*) fueron efectivos frente *Staphylococcus aureus* y retrasaron el crecimiento de hongos y levaduras durante al menos 11 días respecto al queso no recubierto.

ABSTRACT

The incorporation of plant-derived bioactive pigments, with high antioxidant and/or antimicrobial capacity, is intended to increase their nutritional value and/or their shelf-life, respectively. These pigments are easily degradable, so they should be protected within nanostructured systems. Depending on its nature (hydrophilic or lipophilic) and the desired application, the required nanostructures and strategies for interfacial stabilization will be different. The main objective of this Doctoral Thesis was to design, prepare and characterize nanoemulsions and double emulsions able to act as carriers and release systems of lipophilic and hydrophilic bioactive pigments, respectively.

Firstly, nanoemulsions containing essential oils (oregano, thyme, lemongrass or mandarin) as lipid phase, Tween 80 as a surfactant and pectin in the aqueous phase, were prepared by microfluidization (5 cycles, 150 MPa). It was observed that the pectin acted as an emulsifier even in the absence of surfactant and positively contributed to the reduction of the particle size of nanoemulsions prepared with lemongrass essential oil, suggesting that the adsorption of the pectin at droplets interface depended on the type of oil. Likewise, curcumin-loaded nanoemulsions (0.4% *w/w*) stabilized by Tween 20, lecithin or sucrose monopalmitate as surfactants (0.5-2% *w/w*) exhibited particle sizes below 400 nm. Those nanoemulsions containing lecithin (≥1% *w w*) were effective for the encapsulation and controlled release of curcumin and were stable for at least 3 months at room temperature. The fact of increasing the concentration of oil in highly concentrated emulsions (fraction in volume 0.5 and surfactant-oil ratio = 0.1), prepared by ultrasound (100 μm, 200 s) or microfluidization (2 cycles, 800 bar) did not affect the efficiency of the resultant delivery systems. On the other hand, nanoemulsions prepared with microfluidized or non-microfluidized sodium alginate and it was demonstrated that microfluidization caused the partial breakage of the biopolymer chains allowing a more homogeneous disposition around the drops, reducing the particle size, the polydispersity and the viscosity of the resulting nanoemulsions. Another form of stabilization of nanoemulsions was the use of whey protein (WPI)-sugar beet pectin (SBP) complexes, which showed greater effectiveness than WPI and SBP separately against Ostwald ripening, delaying the droplets growth during more time.

Secondly, double emulsions (6-7 μm) were designed to transport chlorophyllin (hydrophilic bioactive pigment) and/or lemongrass essential oil following a two-step procedure: *(I)* formation of the primary emulsion stabilized with 4% *w/w* PGPR, by homogenization (11,000 rpm, 5 min) and *(II)* preparation of double emulsion stabilized with lecithin (2% *w/w*) by homogenization (5,600 rpm, 2 min) and magnetic stirring (750 rpm, 24 h)

Finally, edible coatings formed from nanoemulsions with oregano essential oil (OR-EO) were applied as an antimicrobial agent onto the surface of a low-fat cheese. Coatings with a higher concentration of OR-EO (2.5% *w/w*) were effective against *Staphylococcus aureus* and delayed the growth of molds and yeasts for at least 11 days regarding the uncoated cheese.

TABLE OF CONTENTS

Introduction

LITERATURE REVIEW: *Nanoemulsions and double emulsions as delivery systems of plant-derived bioactive pigments*

Artiga-Artigas, M., Salvia-Trujillo, L. & Martín-Belloso, O.

(In preparation)

Background

Currently, there is an increasing interest in incorporating plant-derived bioactive pigments to food products in order to increase their quality and/or safety. Emulsion-based nanostructures are emerging as potential tools to protect, transport and controlled release of both lipophilic and hydrophilic plant-derived bioactive pigments with antimicrobials and nutraceuticals properties.

Scope and Approach

This review provides the most relevant advances in the interfacial stabilization of two types of emulsion-based nanostructures as carriers of plant-derived bioactive pigments for their further incorporation into foods. Depending on the nature of the plant-derived pigment, whether it is lipophilic or hydrophilic, different emulsion-based nanostructures should be designed. Lipophilic plant-derived pigments may be loaded into nanoemulsions, whereas those hydrophilic might be incorporated in the inner water phase of double emulsions.

Key Findings and Conclusions

The key point of these emulsion-based systems preparation is their stabilization, which in turn may help to avoid the degradation of the encapsulated compound. Therefore, it is necessary to deepen in the behavior of different emulsifiers including surfactants, single biopolymers and protein-polysaccharide complexes at inner droplets' interface. The resultant antimicrobial or bioactive emulsion-based nanostructures exhibit some promising capacity as food preservers and may represent a new strategy to produce functional foods. In addition, the properties of these systems can be modeled according to their subsequent application. However, their toxicological aspects when incorporated into food matrices after their intake should be also considered.

Keywords: Nanoemulsions; double emulsions; highly concentrated emulsions; protein-polysaccharide complexes; essential oils; natural pigments.

1. Introduction

Colored products are fashionable since they are more attractive to consumers. Nonetheless, there is an increasing demand for healthy and safe foods that goes beyond their sensorial quality. This worldwide interest in functional foods with higher nutritional value is stimulating innovation and new product development in the food industry (Lopez-Rubio, Gavara, & Lagaron, 2006). Plant-derived colored bioactive compounds, can be used as natural pigments providing an alternative to those synthetic satisfying the current consumers' concern. Moreover, these pigments have attracted scientist attention in recent times since it is reported that they own highly beneficial health properties (Rodriguez-Amaya, 2016). In this regard, the incorporation of certain plant-derived pigments including antimicrobials, antioxidants and flavorings among others to foods can enhance their safety, shelf stability and offering additional health benefits (Moschakis & Biliaderis, 2017). However, just a few of natural pigments have reached the market due to drawbacks such as their low stability, and thus, fast degradation, when exposed to external factors such as pH, temperature, light and interactions with food ingredients (Sigurdson, Tang, & Giusti, 2017). Moreover, these plant-derived bioactive compounds come in a variety of different molecular and physical forms such as polarities (polar, non-polar, amphiphilic), molecular weights (low to high), and physical states (solid, liquid, gas), which might difficult their direct incorporation into food matrices. In addition, since these ingredients are usually intensely colored and flavored, their direct incorporation may cause organoleptic changes in the original product (Bourbon, Cerqueira, & Vicente, 2016).

Emulsion-based nanostructures have the potential to act as carriers and delivery systems of plant-derived pigments both lipophilic and hydrophilic, protecting them against degradation. Indeed, the capacity of these systems to encapsulate bioactive compounds with different polarity depends on their interfacial characteristics. In this regard, oil-in-water nanoemulsions, which are colloidal dispersions consisting of a lipid core in an aqueous phase, are attractive to be used as delivery systems for lipophilic bioactive compounds. Oppositely, a water-in-oil-in-water ($W_1/O/W_2$) double emulsion, which is defined as an emulsion containing a nanoemulsion itself (Dickinson, 2011), is presented as a great alternative for the encapsulation of hydrophilic bioactive compounds. These systems are able not only to carry hydrophilic functional compounds within the inner aqueous compartment (W_1) but also be loaded with lipophilic compounds in their oil intermediate phase (O), simultaneously.

2. Plant-derived pigments

Plant-derived compounds can be classified as lipophilic or hydrophilic according to their low or high affinity to water, respectively. And as nutraceuticals (related to health benefits) such as curcumin, carotenoids, anthocyanins, betalains, chlorophyllins and phytoesterols; or antimicrobials (*e.g.* essential oils and their main components) regarding their functionality (Salvia-Trujillo, Rojas-Graü, Soliva-Fortuny, & Martín-Belloso, 2014c). Figure 1 summarizes the most common plant-derived colored bioactive compounds chemical structure along with the source from which can be derived.

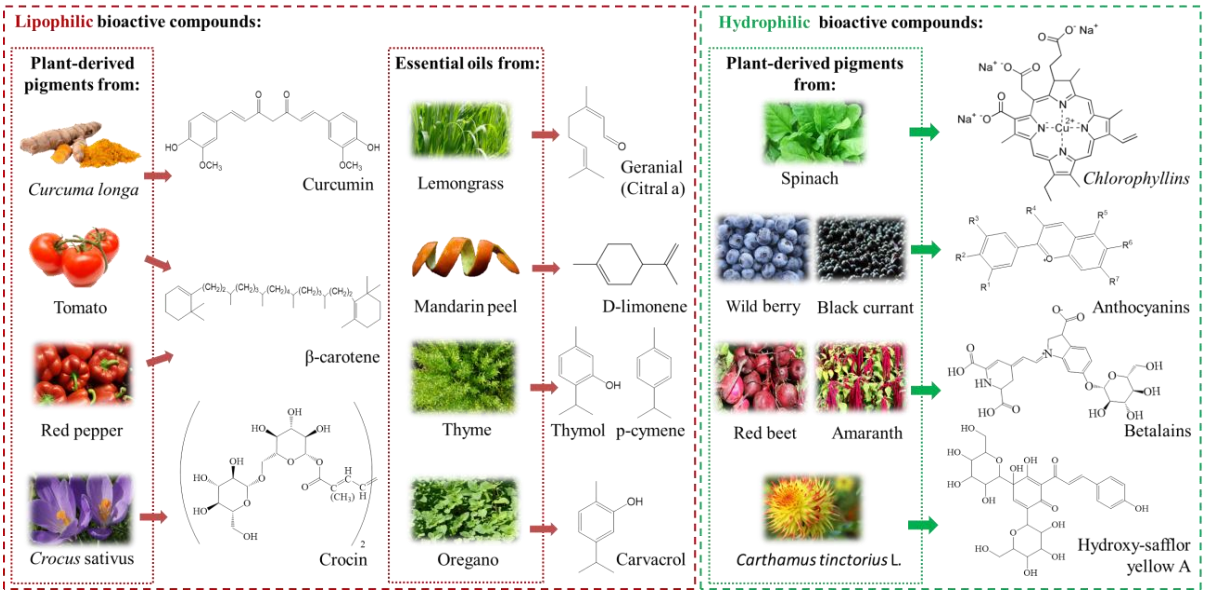

Figure 1. Lipophilic and hydrophilic plant-derived bioactive pigments that can be incorporated to food matrices.

Lipophilic compounds are those able to dissolve in fats, oils, lipids and non-polar solvents. Within this group, the main components of essential oils (*i.e.* quinones, saponins, flavonoids, phenolic acids, tannins, terperoids, coumarins and alkaloids), carotenes including β-carotene and crocin; and curcumin are included (Artiga-Artigas, Lanjari-Pérez, & Martín-Belloso, 2018; Donsì & Ferrari, 2016; Salvia-Trujillo, Qian, Martín-Belloso, & McClements, 2013). Oppositely, natural pigments such as cholophyllins, betalains, anthocyanins or hydroxy-safflor are catalogued as hydrophilic compounds due to their high solubility in water (Stintzing & Carle, 2004).

Essential oils (EOs) are secondary metabolites of plants with antioxidant activity that show high efficacy against different pathogens responsible for food spoilage and foodborne illnesses (Acevedo-Fani, Soliva-Fortuny, & Martín-Belloso, 2017; Salvia-Trujillo, Rojas-Graü, Soliva-Fortuny, & Martín-Belloso, 2013a; Solórzano-Santos & Miranda-Novales, 2012). In fact, Acevedo-Fani, Salvia-Trujillo, Rojas-Graü, & Martín-Belloso, (2015), Rojas-Graü, Soliva-Fortuny, & Martín-Belloso (2009) and Artiga-Artigas, Acevedo-Fani, & Martín-Belloso (2017) observed that edible coatings based on nanoemulsions containing thyme, lemongrass or oregano essential oils, respectively, showed a great effectiveness against external pathogens such as *Escherichia coli* and *Staphylococcus aureus*. Although EOs are not pigments as such, they are rich in some colored bioactive compounds like tannins and coumarins as mentioned above (Bilia et al., 2014; Burt, 2004). Moreover, the most of the EOs are obtained from fruits and/or vegetables, usually colored and hence, some of their pigmented compounds can be transferred to them during the process leading to colored oils. This is the case of mandarin EO extracted from the mandarin peel, which is orange-colored (Artiga-Artigas, Guerra-Rosas, Morales-Castro, Salvia-Trujillo, & Martín-Belloso, 2018). Nevertheless, their incorporation to

foods has some limitations regarding their poor water solubility, partitioning behavior, mass transfer, volatility or reactivity that may reduce EOs efficacy (Donsì, Annunziata, Sessa, & Ferrari, 2011). For this reason, their encapsulation within oil-in-water nanoemulsion is a usual practice to enhance EOs functionality (Bilia et al., 2014; Guerra-Rosas, Morales-Castro, Cubero-Márquez, Salvia-Trujillo, & Martín-Belloso, 2017).

Yellowish pigments such as β-carotene, crocin and curcumin are also obtained from fruits and vegetables (*e.g.* tomato, red pepper), plants (*e.g. Crocus sativus*) and roots (*e.g. Curcuma longa)* (Figure 1). The main characteristic of these lipophilic plant-derived pigments is their high antioxidant and anti-carcinogenic capacity, which makes them potentially effective to prevent several diseases like cancer, obesity, infectious disease, and cardiovascular illnesses (Gasa-Falcon, Odriozola-Serrano, Oms-Oliu, & Martín-Belloso, 2017; Pulido-Moran, Moreno-Fernandez, Ramirez-Tortosa, & Ramirez-Tortosa, 2016). The study performed by Park (2010) demonstrated the exciting possibility of curcumin as a chemopreventive agent for colorectal cancer. Also the capacity of crocin, one of the main components of saffron, to scavenge free radicals, especially superoxide anions, and hence, to protect cells from oxidative stress responsible for many neurodegenerative disorders is well reported (Bolhassani, 2018; Esfanjani, Jafari, Assadpoor, & Mohammadi, 2015). Moreover, since carotenoids (β-carotene, crocin, croacetin…) and curcuminoids are harmlessness even at high concentrations (Table 1), their incorporation to food matrices as natural flavoring additives, pigments and/or preservatives is of great interest for the food industry ([EC] European Commission, 2000; Lehto et al., 2017). Nonetheless, the hydrophobic nature of these bioactive compounds hinders their incorporation in non-fatty foods and causes their fast elimination from the body after its intake, with little absorption in the gastrointestinal tract (GIT) (Bourbon et al., 2016). Aditya et al. (2013) reported that the solubility of curcumin increased from 10 to 70% when it was incorporated within nanostructured lipid carriers regarding the *in vitro* digestion assay enhancing its bioavailability. Therefore, emulsion-based nanostructures containing a lipid core, as nanoemulsions, especially those highly concentrated (oil volume fraction $\geq$ 0.4) that allow the entrapping of more quantity of pigment, may be a good alternative to encapsulate and carry these lipophilic bioactive compounds.

Likewise, some hydrophilic bioactive compounds such as chlorophyllins, betalains and anthocyanins have been also used as food dyes for decades. Chlorophyllin, which is a water-soluble sodium copper salt derived from chlorophyll exhibits potential capacity as wound-healing accelerant without any known human toxicity (Figure 1) (Das, Samadder, Mondal, Abraham, & Khuda-Bukhsh, 2016). Indeed, Gradecka-Meesters et al. (2011) and Thiyagarajan et al. (2012) observed that this green-colored pigment has anti-carcinogenic activity preventing DNA-damage since it can bind to environmental mutagens twenty times better than resveratrol and about a thousand times better than xanthenes.

Meanwhile, betalains and anthocyanins, which are responsible for orange, red, purple and bluish hues of flowers, fresh and processed fruits or vegetables and grains, develop two different functions according to Stintzing & Carle (2004). The first one is the improvement of the general outer appearance of the product and the second, their contribution to increase consumers' health and well-being according to their high antioxidant capacity. Hydroxysafflor yellow A (HSYA) is the main bioactive flavonoid derived and isolated from the flower of *Carthamus tinctorius* L., which has widely used in traditional Chinese medicine for the treatment of myocardial and cerebral ischemia. Recently, this pigment is attracting the interest of food scientist due to its anti-inflammatory, anti-oxidative and neuroprotective effects (Zhao et al., 2018). In fact, studies performed by Wang et al. (2017) and Wei et

al. (2005) concluded that HSYA improved motor dysfunction in their rotenone-induced Parkinson disease model and has a protective effect on brain injury after focal cerebral ischemia reperfusion, respectively.

Table 1. European regulation of the most common plant-derived bioactive pigments.

Plant-derived Bioactive Pigments	**EU number**	**Limit of use (european Union)**	**Polarity**
Curcumin	E 100	*Quantum Satis*	Lipophilic
Carotenes	E 160a	*Quantum Satis* (20 mg/Kg for sausages), pates and terrines	Lipophilic
Saffron	Coloring food	*Quantum Satis*	Lipophilic
Betalains	E 162	*Quantum Satis* (200 mg/Kg for cereals)	Hydrophilic
Anthocyanins from Reed beet	E 163	*Quantum Satis* (200 mg/Kg for fruit-flavored cereals)	Hydrophilic
Anthocyanins from Amaranth	E 123	30-100 mg/Kg individually or in combination	Hydrophilic
Chlorophyllins	E 141	*Quantum Satis*	Hydrophilic

Adapted from Lehto et al. (2017).

Chlorophyllins, anthocyanins, betalains and HSYA present poor intestinal membrane permeability, resulting in low oral bioavailability (Rodriguez-Amaya, 2016; Zhao et al., 2018). Additionally, metabolic inactivation of some plant-derived pigments occurs in the gastrointestinal tract, and further restricts its oral absorption, as it is the case of HSYA (Li et al., 2010). Moreover, their susceptibility to photodegradation and instability in acidic pH (3.5–5) make the direct incorporation of these hydrophilic pigments to food products, often limited (Ferruzzi & Schwartz, 2005). In order to overcome these problems, recent works have been focus on developing stable double emulsions able to encapsulate, protect and release hydrophilic compounds (Matos, Gutiérrez, Martínez-Rey, Iglesias, & Pazos, 2018; Shaddel et al., 2018).

In this regard, the design and preparation of the appropriated emulsion-based nanostructured system has to be related with the polarity of the pigment as well as its further application in order to preserve their activity without causing the lost in quality of the resultant food products.

3. Emulsion-based nanostructures

Emulsion-based nanostructures are emerging as a great alternative to encapsulate, protect, transport and release plant-derived pigments. However, these systems have to accomplish certain requirements regarding the nature of the bioactive compound that is going to be encapsulated and concerning the final application of the mentioned nanostructures. Despite the fact that most emulsion-based systems present kinetic stability, from a thermodynamical point of view they are unstable systems. Indeed, some authors such as Salvia-Trujillo et al. (2014) have reported that emulsion-based nanostructures can be thermodynamically unstable since the separated oil and water phases have a lower free energy than the emulsified oil and water phases. Several factors namely: surfactant concentration, water content, shear rate, shear stress, temperature, and rotational speed may compromise emulsion-based systems stability. Therefore, it may be required to find the most suitable formulation and processing to ensure their stability during a certain period of time. In this regard, the present work is focused on reviewing the most common strategies for emulsion-based nanostructures stabilization. Figure 2 illustrates the emulsion-based nanostructures discussed in this work to encapsulate lipophilic compounds such as nanoemulsions and/or hydrophilic bioactive compounds like double emulsions.

3.1.Nanoemulsions

Nanoemulsions contain at least two immiscible liquid phases -normally water and oil- in which one of them is dispersed as small spherical droplets (diameter < 100 nm) within the other as can be observed in Figure 2 (Qian & Mcclements, 2011). Theoretically, an oil-in-water nanoemulsion consists of a lipophilic core (dispersed phase) surrounded by an interface of adsorbed material with opposite polarity (continuous phase). This peculiarity makes them interesting delivery systems for lipophilic plant-derived pigments. Nanoemulsions interface can be formed by one or more materials like low-weight surfactants, polysaccharides, proteins or protein-polysaccharide complexes acting as emulsifiers and/or texturing agents. According to Yamashita & Sakamoto (2017) interfacial rheology has been found to be a key factor in the stability of emulsions. Indeed, in most practical applications, the interfaces are subject to external mechanical perturbations such as change in shape or size. For instance, Mendoza et al. (2014) observed that the Ostwald-ripening mechanism of emulsion destabilization would be coupled to the interface viscosity and to the adsorption/desorption kinetics of surfactant. The principal advantage of using nanoemulsions instead of conventional emulsions is the small droplet size, which provides a higher surface area that allows the adsorption of more emulsifier molecules reducing droplets interfacial tension and favoring their disruption (Chung, Sher, Rousset, & McClements, 2017). Therefore, the smaller the particle size, the higher the stability of nanoemulsions and also the higher the transparency, since small droplets scatter the light weakly because their sizes are smaller than the wavelength of light (Salvia-Trujillo, Rojas-Graü, Soliva-Fortuny, & Martín-Belloso, 2014). This is of special importance to incorporate lipophilic bioactive compounds into aqueous-based foods or beverages such as soft drinks that need to remain transparent (Salvia-Trujillo et al., 2013a). In this regard, nanoemulsions can be incorporated to food matrices without altering the outer appearance of the final product.

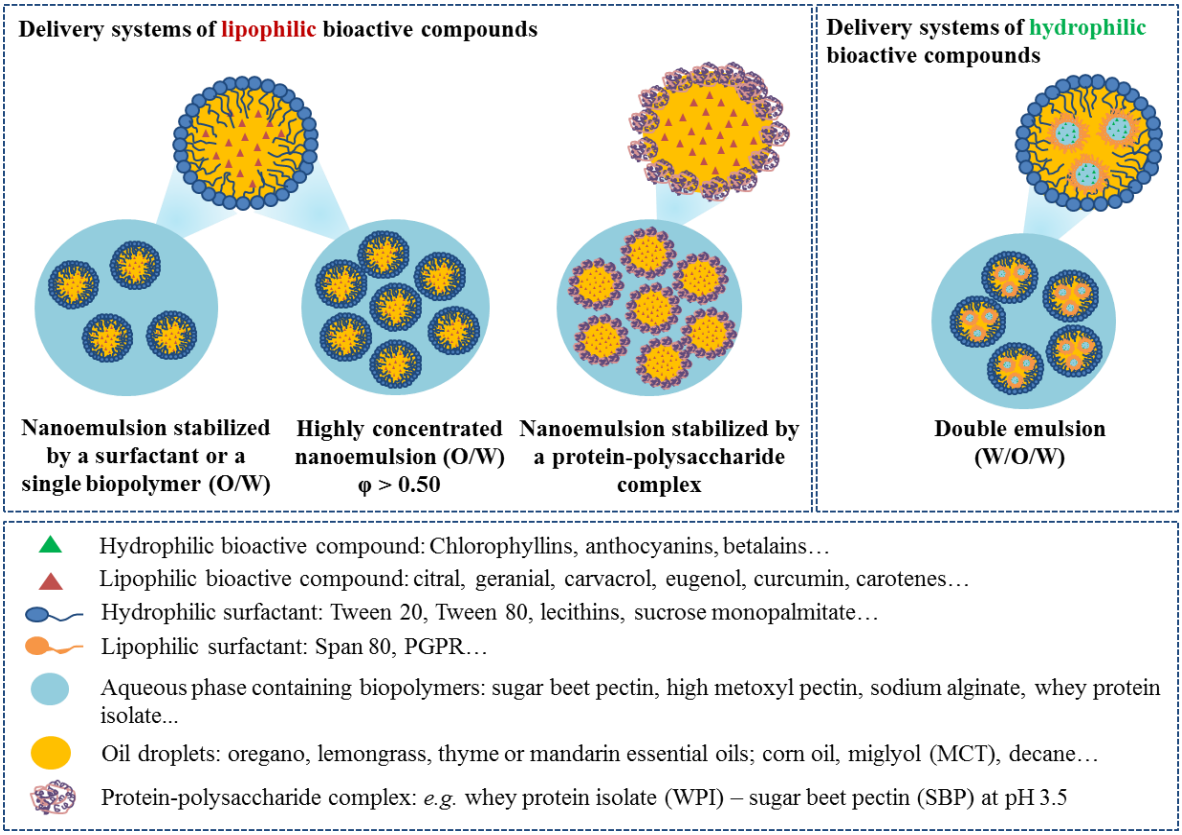

Figure 2. Oil-in-water (O/W) nanoemulsions and water-in-oil-in-water (W/O/W) double emulsions as delivery systems of lipophilic and hydrophilic bioactive compounds.

3.1.1. Nanoemulsion formation

Nanoemulsions are prepared by homogenizing both lipid and aqueous phases through the application of energy to increase the surface are of the dispersed phase (Acevedo-Fani et al., 2017). The reduction of emulsions particle size is the result of a high interfacial tension that may cause the decrease of the oil-water interfacial area. Therefore, the applied procedure to prepare nanoemulsions may affect their particle size and formation (Silva, Cerqueira, & Vicente, 2012). High energy methods are performed using microfluidizers, high pressure valve homogenizers and sonicators able to generate intense disruptive forces leading to the formation of oil droplets with particle sizes bellow 500 nm (Otoni et al., 2014). Despite the fact that ultrasonications is a powerful technique that has been widely used, microfluidizers are considered as a more gentle technique since it is able to produce smaller particle sizes with narrower distribution (Salvia-Trujillo et al., 2013). Actually, Maa & Hsu (1999) reported that their microfluidized nanoemulsions exhibited lower particle sizes (<1 μm) than those ultrasonicated with values around 30 μm. Qian & Mcclements (2011) prepared nanoemulsions with particle sizes around 32 nm by passing the coarse emulsions through an air-driven microfluidizer (1-14 cycles, 4-14 kbar). Likewise, nanoemulsions obtained by Salvia-Trujillo et al. (2013) after a microfluidization process consisting of 10 cycles at 150 MPa showed particles of 6 nm. However, each formulation may determine the election of the most suitable procedure for nanoemulsions

formation since viscous oil phases difficult droplet disruption by mechanical forces (Zeeb, Gibis, Fischer, & Weiss, 2012).

One alternative is the use of low energy methodologies such as spontaneous emulsification (SE), phase inversion temperature (PIT), phase inversion composition (PIC), and emulsion inversion point (EIP) approaches. They depend on the spontaneous formation of minuscule oil droplets (< 100 nm) within mixed oil–water–emulsifier systems after alterations of solution or environmental conditions (McClements, 2011; Solans & Solé, 2012). In the study performed by Bilbao-Sáinz and others (2010), PIC emulsification led to nanoemulsions with particle sizes ranging between 120 and 190 nm, which reached a size below 100 nm at increasing surfactant concentration. Similarly, as observed by Forgiarini, Esquena, González, & Solans (2001) it is also possible to obtain nanoemulsions with average droplet size of 50 nm and high kinetic stability at oil weight fractions lower than 0.3 by stepwise addition of water to a solution of the surfactant in oil.

3.1.2. Nanoemulsions stabilization

Emulsifiers, which are amphiphilic molecules able to stabilize two immiscible liquids, are required to the preparation of appropriate interfaces according to the desirable characteristics of the resultant nanostructured system and its further application. Diverse types of emulsifiers can be utilized to stabilize nanoemulsions including *(i)* surfactants, *(ii)* biopolymers and *(iii)* protein-polysaccharide complexes. Surfactants are able to form a protective interfacial layer around droplets reducing the interfacial tension and protecting them from flocculation or coalescence. Biopolymers are macromolecules located at droplets interface that are usually generating electrostatic and steric forces preventing droplets recoalescence. Finally, the electrostatic interaction of two biopolymers such as proteins and polysaccharides has the formation of protein-polysaccharide complexes as a result. In this regard, oil-in-water interfaces could be modeled depending on the type of emulsifier used since these molecules will have a different behavior at droplets interface. However, besides the type of emulsifier, another important parameter as their concentration should be considered. In fact, there have to be enough molecules of emulsifier to cover all the droplets of the dispersed phase leading to smaller particle sizes, higher stability and avoiding coalescence. Nonetheless, as pointed out by Neumann, Schmitt, & Iamazaki (2003), when there are more surfactant molecules than available droplets surface to cover, this non-adsorbed surfactant chains located in the continuous phase may interact with each other leading to aggregates formation. As a consequence, these aggregates might sediment causing phase separation and thus, nanoemulsions destabilization. On the other hand, the election of the most suitable emulsifier has to be related with the physical characteristics of the lipid phase used such as its polarity, water solubility, interfacial tension and rheology, together with the chemical nature of the bioactive compound that is going to be encapsulated (Surassmo, Min, Bejrapha, & Choi, 2010).

(i) Surfactants

Surfactants are amphiphilic molecules that consist of a polar head group bounded to one or more non-polar chains and have been widely used in the formation of nanoemulsions since they are able to adsorb quickly at droplets interface reducing interfacial tension thus leading to small oil droplets during homogenization (Degner et al., 2014; Salvia-Trujillo, Rojas-Graü, Soliva-Fortuny, & Martín-Belloso, 2013). The classification and characteristics of the most commonly used surfactants in the food industry are shown in Table 2. The emulsifying capacity of surfactants is attributed to their

hydrophilic-lipophilic balance (HLB), which usually ranged from 1 to 20 (Kralova & Sjöblom, 2009). This is defined as the ratio of the weight percentage of hydrophilic groups to the weight percentage of hydrophobic groups in the molecule. In this regard, lipophilic plant-derived pigments (*i.e.* EOs, carotenoids or curcumin) may be loaded into stable oil-in-water (O/W), in which surfactants with a high HLB (8-16) such as phospholipids or polyoxyethylene fatty acid esters, among others may be required. The head group of surfactant molecules can be cationic, anionic or non-ionic, whereas the length and grade of unsaturation of non-polar chains may vary (Degner et al., 2014). According to Tadros (2013) the most effective surfactants are those non-ionic since repulsion between the head groups is smaller than with those ionic and adsorption may occur from dilute solutions (Figure 3). This is the case of polyoxyethylene sorbitan esters also called Tweens, and sucrose esters, whose high HLB allows the formation of long-term stable oil-in-water (O/W) emulsions (Wei, Liu, San, Wong, & Quan, 2017). These non-toxic surfactants might encapsulate lipid compounds when surfactant-oil ratios are high due to their surface-tension-reducing capacity, dispersion, and foaming capability (Zhao et al., 2013). Actually, sucrose monoesters and, in particular, sucrose monopalmitate, are increasingly utilized by the food and beverage industry since they are biodegradable, with good taste and aroma profile (Szuts & Szabó-Révész, 2012). In a recent study accomplished by Lee, Liu, Wong, & Liu, (2017) sucrose monopalmitate-stabilized nanoemulsions exhibited lower mean droplet diameters (≈ 100 nm) than those containing modified starch (> 250 nm) and promoted the release of volatile sulfur flavor compounds (potent odorants of coffee aroma), which may translate into positive sensory perception of instant coffee. Oppositely, Artiga-Artigas et al. (2018) reported that in spite of the encapsulation efficiency of curcumin-loaded nanoemulsions stabilized by sucrose monopalmitate was as high as that of those Tween or lecithin-stabilized, they suffered phase separation during the first hours after their preparation. This fact, along with the loss of antioxidant capacity of curcumin, suggests that curcumin is not entrapped but hold in sucrose monopalmitate chains by H-bonding being exposed to degradation. Therefore, for the election of the most suitable surfactant, the chemical properties of the encapsulated compound should be also taken into account.

Ionic surfactants such as lecithins, which are amphiphilic molecules consisting of a mixture of phospholipids whose polar head groups contain ionizable phosphate and nitrogen moieties, can also be used as emulsifiers. However, their adsorption is more complicated than in the case of those non-ionic because they are very sensitive to the presence of electrolytes. Hence, the adsorption may depend on the repulsion between the head groups and the addition of indifferent electrolyte (Figure 3) (Tadros, 2013). Nonetheless, results reported by Nash & Erk (2017) and Artiga-Artigas et al. (2018) concluded that concentrations of lecithin over 1% *w/w* were more effective than Tween 20 or sucrose monopalmitate (non-ionic surfactants) in stabilizing nanoemulsions loaded with EOs or curcumin, respectively. In this regard, despite ionic surfactant adsorption onto droplets surface is less easy than that of non-ionic, lecithin may form a viscoelastic interface resisting deformation and contributing to enhance nanoemulsions stability. This behavior had been previously observed by Klang & Valenta (2011), who established that lecithin was able to form a mechanical barrier around the droplets protecting them against destabilization phenomena such as coalescence or flocculation.

Since the majority of surfactants are synthetic and within them only a restricted number are food-labeled limiting their application in food and beverage products, the use of lecithin or sucrose esters as emulsifiers can be a good alternative.

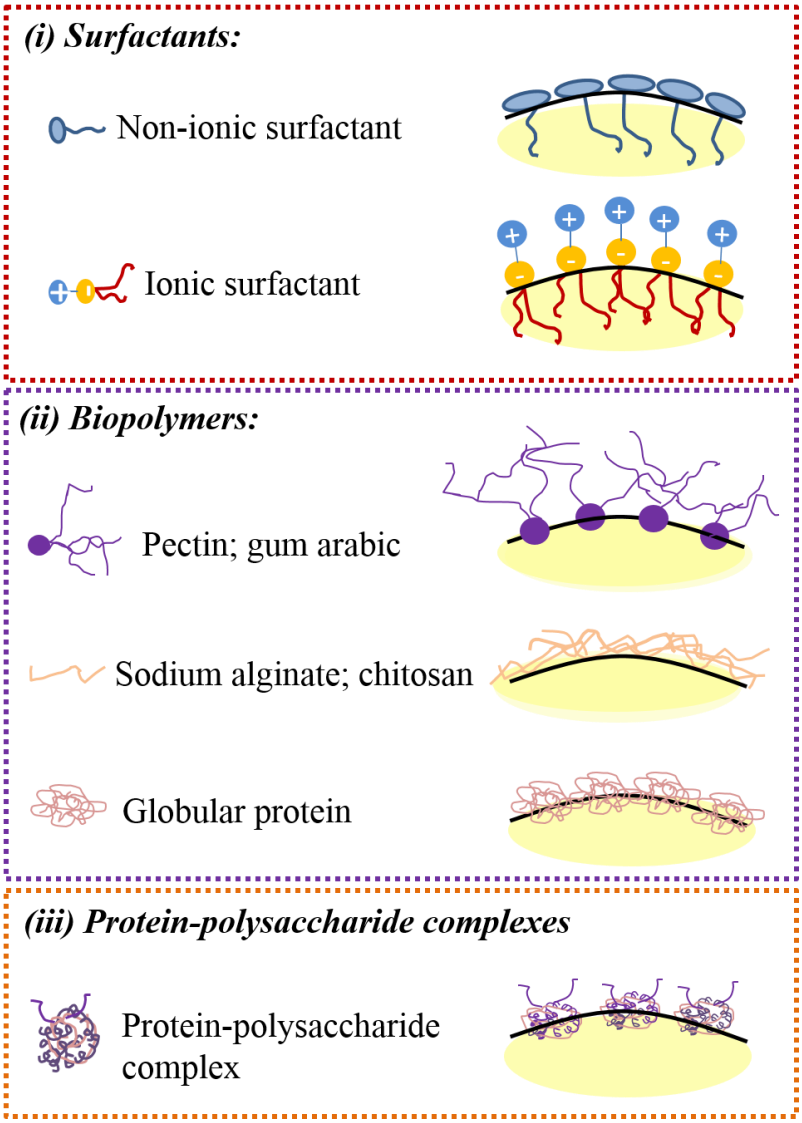

Figure 3. Proposed adsorption mechanism of different emulsifiers: *(i)* surfactants, *(ii)* biopolymers and *(iii)* protein-pectin complexes at droplets interface.

Table 2. Classification, characteristics and European regulation of the most common surfactants used in the food industry.

Surfactant	Abreviation	EU number	Limit of use (European Union)	HBL	Emulsion type	Charge
Polyoxyethylene sorbitan monoesters	Polisorbates (20, 80, 60,65) Tweens ® (20, 80, 60,65)	E 432-436	*Quantum satis*	16.7; 15; 14.9; 10.5	o/w	Non-ionic
Lecithin		E 322	*Quantum satis*	< 9	o/w and w/o	Amphoteric to anionic
Mono and dyglycerides		E 471	*Quantum satis*	3-6	w/o	Non-ionic
Sucrose esters of fatty acids		E 473	50 mg/Kg (except beverages)	1-18	o/w and w/o	Non-ionic
Sorbitan monoesters	Spans (60, 65, 20, 80)	E 491-494	*Quantum satis*	4.7; 2.1; 8.6; 4.3	w/o	Non-ionic
Polyglycerol esters of fatty acids	PGE	E 475	*Quantum satis*	6-11	o/w	Non-ionic
Polyglycerol polyricinoleate	PGPR	E 476	4000 mg/Kg 5000 mg/Kg (Cocoa-based confectionery, including chocolate)	≤ 4	w/o	Non-ionic

Adapted from Genot, Kabri, & Meynier (2013).

(ii) Biopolymers

Natural biopolymers are edible polymeric molecules produced by living organisms such as plants, animals or microorganisms. There are two major types of biopolymers that are normally used in food formulations being proteins and polysaccharides (Figure 3). Proteins including gelatin, casein or insulin, which are polymers of aminoacids, have been traditionally as emulsifying agents due to their great binding affinities and surface activities, as well as their low saturation surface (Dickinson, 2009). Oppositely, polysaccharides have been commonly used as thickening and gelling agents since their incorporation to the aqueous phase of emulsions and nanoemulsions cause the increase in viscosity preventing their destabilization by decreasing oil droplets gravitational movement (Guerra-Rosas et al., 2016). However, progressively more studies are demonstrating the capacity of polysaccharides to act as emulsifiers consolidating themselves as potential alternative to synthetic surfactants (Artiga-Artigas et al., 2018). Some of the most used polysaccharides as emulsifiers for food applications are pectin (*e.g.*citrus), alginate, chitosan, gum arabic (*Acacia senegal*), intact or modified starches and some galactomannans (Dickinson, 2009).

Biopolymers can adopt many configurations in aqueous solution depending on electrostatic and hydrophobic interactions, hydrogen bonding, van der Waals forces and entropic effects (Dror, Cohen, & Yerushalmi-Rozen, 2007). For instance, gum arabic has been traditionally used as stabilizer agent of flavor oils in soft drinks due to its ability to form an adsorbed film at the oil-water interface, whose surface viscoelasticity is rather insensitive to dilution of the aqueous phase (Yao et al., 2013). The structure of this biopolymer consists of a main highly branched region and a smallest fraction of arabinogalactan–protein complex in which arabinogalactan chains are covalently linked to a protein chain through serine and hydroxyproline groups (Dror et al., 2007). Although gum arabic is negatively charged, is not the electrostatic but rather the steric repulsion that plays a dominant role in nanoemulsion stabilization. Traditionally, the emulsifying and stabilizing properties of the gum arabic have been attributed to the protein moieties. In spite of the specific action and conformation of gum arabic at droplets interface are not clear yet, in the study of Yao et al. (2013), three gum arabic samples with the same nitrogen content showed different emulsifying properties confirming that the nature and distribution of the proteinaceous component of gum arabic confer the emulsifying capacity and no its concentration. In previous works also had been observed that arabinogalactan from gum arabic and Fenugreek gum, which is a type of galactomannan obtained by ground fenugreek seeds, were able to adsorb on the oil interface forming a relatively thick interfacial film preventing destabilization (Dickinson, Elverson, & Murray, 1989; Garti, Madar, Aserin, & Sternheim, 1997).

Likewise, pectin, which is a natural biopolymer mainly present in fruits and vegetables, recently has shown adsorption capacity at oil-water interfaces and may enhance the stability of emulsions (Alba & Kontogiorgos, 2017). Pectins contain smooth regions (also called linear regions) primarily made up of a polymer of a-1,4-linked D-galacturonic acid (GalpA) residues and hairy, branched regions also referred to as rhamnogalacturonan-I. Some of these GalpA residues are partially esterified with methanol at the C-6 carboxyl group and may be esterified with acetyl groups at C-2 or C-3 (Liu, Fishman, & Hicks, 2006). In fact, Artiga-Artigas et al. (2018) observed that citrus pectin at specific concentrations over 1% *w/w* led to the formation of submicron nanoparticles in absence of small-molecule surfactants evidencing its capacity to act as emulsifier. Other pectins such as those from sugar beet also have shown capacity as emulsifiers. This capacity is attributed to the hydrophobic character of its acetyl groups (Schmidt, Schütz, & Schuchmann, 2017). There is a direct relationship between the degree of methyl esterification (DM) and emulsifying capacity of pectin, by increasing

the DM from ~70% to ~80% (Schmidt et al., 2017). These groups with interfacial activity are able to act as hydrophobic anchors that facilitate adsorption of pectin chains at the interface resulting in reduction of interfacial tension as is illustrated in Figure 3 (Alba & Kontogiorgos, 2017). Nonetheless, other authors as Funami et al. (2007) reported that proteinaceous moieties present in pectin, which are bound to the carbohydrate, may adsorb onto the O/W interface. In this regard, the carbohydrate portion of pectin might form a hydrated layer around oil droplets preventing flocculation (Figure 3).

Oppositely to gums and pectins, alginate -extracted from marine brown algae (Phaeophyta) by treatment with aqueous alkali solutions- is a linear polysaccharide, which consist of β-D-mannuronic (M) acid and α-L-guluronic (G) acid linked by 1/4 bonds (Rivera, Pinheiro, Bourbon, Cerqueira, & Vicente, 2015). Their capacity to absorb large amount of water may lead to the formation of hydrogels and hence, facilitate the solubility of the alginate chains in the aqueous phase (Artiga-Artigas, Acevedo-Fani, & Martín-Belloso, 2017). In addition, alginates contain functional groups such as carboxylates, which can easily dissociate in the aqueous phase and, as a result, provide negative charge to the emulsions (Pereira et al., 2013). Therefore, these chains may form a protective layer around oil droplets preventing coalescence being even more effective after microfluidization (Figure 3) (Artiga-Artigas et al., 2017). Sellimi et al. (2015) studied the emulsifying activity of sodium alginate and observed that the higher the concentration of biopolymer, the higher their emulsifying capacity. Additionally, the emulsifying capacity of sodium alginate was influenced by the type of oil used during emulsions formation. Indeed, this biopolymer exhibited a higher emulsifying capacity (around 76%) with corn oil than with other vegetable oils (*i.e.* olive oil, sunflower, soybean oil, ricin oil, almond oil and argan oil).

Other linear biopolymers such as chitosan, which is positively charged and it is present in the cuticles of crustacean, insects and molluscs and the cell walls of microorganisms; have shown potential ability to act as emulsifier agents (Rinaudo, 2006). Certainly, Schulz, Rodríguez, Del Blanco, Pistonesi, & Agulló (1998) observed that although chitosan was inactive at the air/solution interface, it could adsorb at the oil/water interface providing both mechanical and electrostatic stability to the droplets.

Therefore, differences in emulsification capacity among polysaccharides are not only attributed to their molecular characteristics (molecular weight, polarity, hydrophobicity) but also it may depend on their flexibility and the conformation that they adopt in aqueous solution.

(iii)Protein-polysaccharide complexes

Emulsion-based nanostructures containing short-chain oils are very prone to suffer Ostwald ripening in spite of using surfactants or single biopolymers as emulsifiers. However, protein-polysaccharide complexes, from the interaction between two oppositely charged biopolymers have presented considerable surface activity (Ifeduba & Akoh, 2016). Thus, they have emerged as a promising alternative to be used as emulsions stabilizers. Complexation toughly depends on the pH and ionic strength of the implicated biopolymers (Zeeb, Mi-Yeon, Gibis, & Weiss, 2018). Polysaccharides including pectin, sodium alginate or gums, among others, contain anionic functional groups such as acetyls or carboxylates with delocalized electrons, which confer the negative charge to the biopolymers (Artiga-Artigas et al., 2017). Nevertheless, proteins such as whey protein isolate (WPI) change their charge approximately from -30 mV to +30 mV when the pH was reduced from 7 to 3, respectively (Zeeb, Stenger, Hinrichs, & Weiss, 2016). In this regard, the procedure for

assembling complexed biopolymers at the liquid–liquid interface consists of pre-forming the complex by putting in contact both biopolymers and varying the pH of the media progressively. In addition, their physicochemical properties can be modified by the addition of crosslinking agents like transglutaminase or facilitating Maillard reaction (Moschakis & Biliaderis, 2017). Thus, the complex at a specific concentration will be incorporated into the emulsion mixture being able to adsorb at the interface increasing its thickness and the steric forces. Indeed, Zeeb et al. (2012) stabilized short-chain oils (*e.g.* alkanes or essential oils) with protein-polysaccharide complexes. These oils tend to migrate quickly towards the aqueous phase due to the hydrophilic compounds present in their composition leading to Ostwald ripening or coalescence phenomena (Artiga-Artigas et al., 2018). Therefore, they cannot be easily stabilized either by conventional surfactants or by natural biopolymers.

Complex-stabilized emulsions stabilization can be even more sensitive than other emulsifiers to the homogenization procedure, stirring speed, temperature, viscosity of solution as well as concentration and type of biopolymers together with pH and ionic strength (Zeeb et al., 2018). The proposed adsorption mechanism of the complexes at the interface can be observed in Figure 3. The protein fraction of the complex (mostly pure protein and the protein moieties from the polysaccharide) would be directly adsorbed at the interface as in the case of pure protein, whereas the polysaccharide chains would be oriented towards the bulk aqueous phase. Thus, pectin situated at the surface of complexes on one hand, may provide negative charge to the interface and on the other hand, cause electrostatic repulsions favoring the attenuation of destabilization phenomena such as flocculation.

3.2.Double emulsions

Double emulsions, also known as duplex or multiple emulsions, are emulsions in which the dispersed phase is an emulsion itself (Dickinson, 2011). In this regard, in a double emulsion the inner phase is usually miscible with the final external phase due to they owe the same polarity. Nevertheless, the intermediate phase is immiscible with the other two leading to systems such as water-in-oil-in-water ($W_1/O/W_2$) or oil-in-water-in-oil ($O_1/W/O_2$) (Wang, Zhang, & Hu, 2006). In $W_1/O/W_2$ emulsions, water is first dispersed in oil, which is then dispersed in another external water phase (Muschiolik & Dickinson, 2017). The other described morphology consists of an oil-continuous system containing water droplets with smaller oil droplets inside them ($O_1/W/O_2$). Therefore, double emulsions have three distinct main phases and two oil–water interfaces (Dickinson, 2011). In this regard, at least two different emulsifiers are required in order to formulate a double emulsion for the stabilization of each interface.

The main particularity of double emulsions is their ability to carry two or more active compounds with different polarity simultaneously. The design and preparation of $W_1/O/W_2$ emulsions result of special interest since these systems can, on the one hand, encapsulate and protect hydrophilic plant-derived pigments (*e.g.* chlorophyllins, anthocyanins or betalains) in their most internal phase and, on the other hand, be loaded with other active compound with opposite polarity in the intermediate compartment (*e.g.* essential oils, vitamins, carotenes or curcuminoids) (Muschiolik & Dickinson, 2017). Indeed, Frank et al. (2012) showed that it was possible to stabilize anthocyanins in the inner (W_1) phase of double emulsions preventing the loss of its functionality during the release of the pigment under gastrointestinal *in vitro* conditions. Likewise, Kaimainen, Marze, Järvenpää, Anton, & Huopalahti (2015) observed that oil in $W_1/O/W_2$ emulsions can act as a barrier to protect hydrophilic bioactives such as betalains, which gradually released during oil digestion. They also concluded that whether the encapsulation of the hydrophilic pigment can improve its chemical

stability along the gastrointestinal tract in the *in vitro* study the following step should be to evaluate the pigment shelf-life within food applications. Moreover, either Frank et al. (2012) or Kaimainen et al. (2015) proposed that the structural changes of the inner and outer droplets influenced the pigment release, induced by coalescence of the inner droplets and reduced by outer droplets aggregation.

According to Lamba, Sathish, & Sabikhi (2015) there are three major types of double emulsions regarding the number of internal droplets (Figure 4). Type A is also called "core-shell" type multiple emulsion and it is characterized by the presence of just one large internal droplet. Oppositely, types B and C multiple emulsions contain few or several small droplets within the inner phase, respectively. Nonetheless, $W_1/O/W_2$ emulsions of type C, have shown the best capacity to be applied as delivery systems (Pal, 2008).

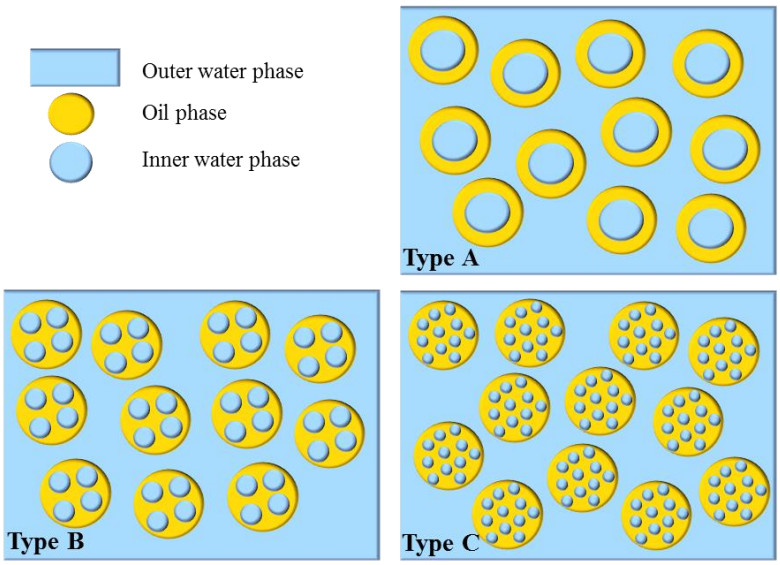

Figure 4. Types of water-in-oil-in-water double emulsions. Figure adapted from Lamba, Sathish, & Sabikhi (2015b).

3.2.1. Double emulsions formation

The major issue of $W_1/O/W_2$ emulsions is their low stability on manufacture and high susceptibility to breakdown during storage and on exposure to environmental stresses including mechanical forces, thermal processing, freezing or dehydration (Lamba et al., 2015). Therefore, several parameters need to be controlled during the preparation of double emulsions including homogenization method, shear applied, number of passes, temperature of operation, type and concentration of emulsifier, ratio of dispersed emulsion to continuous phase, osmotic balance between inner and outer aqueous phase and final desired droplet size, among others (Lamba et al., 2015). Double emulsions can be prepared by one-step or two-step emulsification procedures. One-step method implies the application of heat to an emulsion containing a non-ionic surfactant or a mixture of surfactants, causing the phase inversion needed to form a double emulsion (Xu, Ge, Chen, & Luo,

2014). However, the two step procedure that consists of two sequentially steps is considered as the standard method for the obtaining of $W_1/O/W_2$ emulsions (Muschiolik & Dickinson, 2017). The first stage is the formation of a primary water-in-oil (W_1/O) emulsion produced by the homogenization of water, oil and a low HLB surfactant. For this first homogenization, high shear devices including ultrasonicators, high pressure homogenizers, high shear mixers or microfluidizers are commonly used (Muschiolik & Dickinson, 2017). All of them are based on the production of cavitation, collision and turbulence forces, which causes breakdown of the droplets and uniform dispersion of the dispersed phase. However, some works have revealed the fact that, under certain conditions, high shear stress can cause an over-processing of the emulsions provoking coalescence due to an increase in the surface area, thus favoring their destabilization (Jafari, He, & Bhandari, 2007). This suggests that homogenization processing conditions are required to be controlled in order to ensure a stable primary emulsion formation. The second step consists of dispersing the W_1/O emulsion in an aqueous continuous phase containing a high HLB or hydrophilic surfactant leading to a $W_1/O/W_2$ emulsion. Several authors agree with that the second step of the procedure is crucial for a good $W_1/O/W_2$ emulsion formulation since intense homogenization forces may cause the undesired breakdown of the primary emulsion (O'Regan & Mulvihill, 2010). Therefore, in order to allow the inclusion of more quantity of droplets in the outer phase the application of moderated energies such as ultrasonication at low amplitudes or magnetic stirring is required. Actually, recent works reported the formation of double emulsions with particle sizes ranging from 3.36 ± 0.69 to 8.39 ± 0.83 μm depending on the hydrophilic surfactant (Tween 20 or lecithin, respectively), by applying ultrasonication during 180 s at a frequency of 24 kHz and amplitude of 40% (Teixé-Roig, Oms-Oliu, Velderrain-Rodríguez, Odriozola-Serrano, & Martín-Belloso, 2018).

Oppositely, Vladisavljević, Nuumani, & Nabavi (2017) directly prepared small micron-sized double emulsions (20-300 μm) with firmly controlled structures by the use of microfluidic channel devices as an alternative procedure. This device differs from others high shear homogenizers such as microfluidizers or sonicators in that the preparation of a $W_1/O/W_2$ emulsion consists of the injection of water into oil followed by the injection of this emulsion into water (McClements, 2012). Similar results can be achieved by using a series of concentric cylinders through which the different liquids flow: the inner water phase (W_1) flows through the innermost channel; the oil phase (O) flows through the middle channel; and, the outer water phase (W_2) flows through the outermost channel (McClements, 2012). The main advantage of preparing double emulsions by microfluidic channel devices is that it allows large scale production, whereas conventional two-step procedures can be only applied for preparation of small quantities of material in fundamental studies.

According to Muschiolik & Dickinson (2017) as well as choosing the appropriated emulsification equipment and processing conditions for the second step, the stability problems of $W_1/O/W_2$ emulsions can be addressed by finding the most suitable emulsions formulation. Certainly, an important parameter to characterize the effectiveness of $W_1/O/W_2$ emulsions formulation is the "yield." This is defined as the percentage of the W_1 retained as internal droplets in the W_1O/W_2 (Dickinson, 2011). In this sense, the yield can be controlled by using a different ratio of W_1 to oil phase or of W_1/O emulsion to W_2 phase. Herzi, Essafi, Bellagha, & Leal-Calderon (2014) studied the influence of the inner droplet fraction on the release rate of $W_1/O/W_2$ emulsion and found an indirect correlation between the W_1 or W_1/O droplets and the release. That is, the higher the weight fraction of aqueous droplets (W_1) in the globules (W_1/O) or the globules in W_2, the lower the encapsulated compound release rate. This is related to the phase ratio, which may determine the resulting

physicochemical properties of the final $W_1/O/W_2$ emulsion. Actually, Yildirim, Sumnu, & Sahin (2017) have recently found that samples with the same ratio of W_1/O emulsion/W_2 phase had similar characteristics in terms of particle size, stability, viscosity, encapsulation efficiency and rheology; regardless the ratio between W_1 and O using for the W_1/O emulsion formation. Despite the fact that there is not a rule for the election of phase ratio, the greater the ratio between W_1/O and W_2 concentrations, the higher apparent viscosity and stability of the resultant $W_1/O/W_2$ may be.

3.2.2. Double emulsions stabilization

The stabilization of double emulsions represents a higher challenge than in the case of nanoemulsions, due to the physicochemical characteristics of the interfaces, the kinetics of the complex structure and the presence of various phases with different compositions (Muschiolik & Dickinson, 2017). There are four principal forms of double emulsions instability including coalescence of inner water droplets, coalescence of oil droplets, the rupture of oil film that separates the inner and outer phases due to high packing density both causing the leakage of the encapsulated bioactive compound and migration of inner water droplets or their water soluble materials through a process called "reverse micellar transport" (Lamba et al., 2015). Moreover, another practical concern is that inner droplets are prone to suffer swelling and rupture induced by osmotic transport and hence, it is necessary to control these phenomena in order to avoid their coalescence.

The most accepted strategies to enhance $W_1/O/W_2$ emulsions stability are: the reduction of inner droplets size (W_1) by forming an internal microemulsion; the increase of W_2 phase viscosity (Özer, Muguet, Roy, Grossiord, & Seiller, 2000); the formation of an interfacial complex; the modification of the solubility and polarity of the oil phase to make it less water soluble (Tedajo, Seiller, Prognon, & Grossiord, 2001); the addition of oil-insoluble electrolytes to the W_1 in order to balance the Laplace and osmotic pressures between the inner aqueous phase and the outer aqueous phase (Kanouni, Rosano, & Naouli, 2002) and the incorporation of stabilizing agents such as biopolymers, surfactants or colloidal particles in the outer aqueous phase (W_2) (Mezzenga, 2007). Indeed, Özer et al. (2000) concluded that the increase of viscosifying agents concentration (from 5 to 20% *w/w*) caused the rise of W_2 aqueous phase viscosity contributing to improve stability of $W_1/O/W_2$ emulsions against temperature changes. Nonetheless, normally these strategies are not cost effective or may require the use of non-food grade ingredients making these emulsion-based structures unsuitable for human consumption and less attractive for the food industry (O'Regan & Mulvihill, 2010). Therefore, the incorporation of natural and food grade emulsifiers (alone or in combination) is gaining attention as a potential tool to enhance $W_1/O/W_2$ emulsions stability. Overall, the most common emulsifiers used for the stabilization of double emulsions are *(i)* surfactants, *(ii)* biopolymers and *(iii)* protein-polysaccharide complexes.

(i) Surfactants

Lipophilic surfactants (HLB ≈ 3-6) are required for the stabilization of the first water-in-oil interface, which is the most critical step for the preparation of double emulsions (Dickinson, 2011). Within this group, there are glycerol esters, propylene glycol fatty acid esters, polyglycerol esters and sorbitan fatty acid esters such as Span 80 being this one the most commonly used (Table 2). Span 80 as other small molecule surfactants are able to rapidly adsorb to water droplets thus reducing the interfacial tension and avoiding coalescence. However, Surh et al. (2007) observed that although Span

80 was soluble in vegetable oils such as corn oil at room temperature, the resultant W_1/O rapidly separated after the homogenization process. Thus, in order to obtain water-in-oil emulsions with particle sizes sufficiently small to be re-encapsulated during the second step, Span 80 needs to be at very high concentrations in the oil (Dickinson, 2011). Weiss & Muschiolik (2007) reported that double emulsions' stability may increase as increasing the viscosity of the oil phase. This has been attributed to an enhancement of inner water droplets stability against the shear-induced stress applied during the second step of double emulsion preparation. In this regard, polymeric surfactants and especially PGPR is presented as a potential alternative to stabilize multiple emulsions (Surh et al., 2007; Teixé-Roig et al., 2018). In fact, in agreement with Altuntas, Sumnu, & Sahin (2017), there is a direct dependence between the type and concentration of surfactant and the resultant particle size of the $W_1/O/W_2$ emulsions. The results provided by Musashino, Hasegawa, Imaoka, Adachi, & Matsuno (2001) revealed that in order to obtain W_1/O particle sizes bellow 1 μm, Span 80 had to be at concentration of 20% *w/w,* whereas Frank et al. (2012) used only a 2.5% *w/w* of PGPR to obtain similar results. This can be explained because vegetal oils are able to interact better with PGPR due to its higher hydrophobicity compared to Span 80 forming a kinetic barrier protecting the emulsion against destabilization phenomena such as coalescence or Ostwald ripening (Tabibiazar & Hamishehkar, 2015).

However, there is a limitation of using PGPR for food applications since several studies have related PGPR intake with a liver enlargement thus restricting the acceptable diary intake to 7.5 mg/kg body weight (Altuntas et al., 2017; Wilson, Van Schie, & Howes, 1998). One alternative to reduce PGPR concentration consists of its combination with other surfactants. Indeed, Garti, Aserin, Tiunova, & Binyamin (1999) observed that W_1/O emulsions stabilized by a mixture of fully hydrogenated tristearin and PGPR in a ratio 1:1 (in weight) showed a very minor coalescence than those stabilized by tristearin or PGPR. Likewise, $W_1/O/W_2$ emulsions prepared by Altuntas et al. (2017) with a 1.5% *w/w* lecithin and 1.5% *w/w* PGPR as emulsifiers for the first W_1/O emulsion, exhibited higher instant and storage stability (56.1 ± 1.7 and 93.6 ± 0.5 %, respectively) than those prepared by only PGPR (44.4 ± 0.1 and 80 ± 1% respectively). Moreover, the addition of lecithin contributed to decrease the mean volume droplet diameter (d[4;3]) of $W_1/O/W_2$ emulsions from 23.8 ± 0.1 to 16.5 ± 0.1 μm.

According to Table 2, for the stabilization of the second interface, which is oil-in-water, hydrophilic surfactants (HLB ≈ 8-18) may be required (Scherze, Knoth, & Muschiolik, 2006). Moreover, particle size of the final emulsions has to be large enough to be able to contain as many W_1/O droplets as possible. Therefore, the concentration and type of hydrophilic surfactant may be decisive in double emulsions' formation. Concerning the surfactant concentration, it has to be enough surfactant molecules to cover the whole droplets surface as in the case of single-interface emulsions in order to avoid coalescence. Consequently, the surfactant-oil-ratio (SOR) has to be higher than 1 (Salvia-Trujillo, Rojas-Graü, Soliva-Fortuny, & Martín-Belloso, 2013a) Regarding the type of hydrophilic surfactant, the most commonly used are those small-molecular weight ones as polysorbitan-monolaurate (Tween) or lecithin and several proteins (Andrade, 2016). Actually, several studies have been performed with Tween 80 due to its known protective capacity of lipid nanoparticles from degradation in the stomach due to acidic conditions, the action of pepsin, and lipid oxidation, because of its molecular structure (Aditya et al., 2015). Nonetheless, depending on the hydrophobic surfactant chosen for primary emulsion formation, the concentration of Tween is restricted. Jiao & Burgess (2003) realized that high concentrations of Tween 80 solubilized Span 83 rendering it useless to stabilize the W_1/O emulsion. For this reason and based on the current consumer demand of natural

ingredients places lecithin as the preferred one to be used as hydrophilic surfactant (Degner et al., 2014; Muschiolik & Dickinson, 2017).

(ii) Biopolymers

The effect of natural biopolymers incorporation in the stabilization of double emulsions by the two-step procedure has been widely considered (Dickinson, 2011). Weiss & Muschiolik (2007) reported that the incorporation of biopolymers such as proteins (*e.g.* gelatin, whey protein isolate, pea protein isolate, caseinates) or polysaccharides (*e.g.* sodium alginate, carboxymethyl cellulose, pectins, gums) causes a critical impact in the stabilization of W_1/O emulsions. It is believed that the origin of this enhancement of stability is due to the interaction between polysaccharide and lipophilic surfactant, which provides a viscoelastic barrier thus preventing droplets coalescence (Dickinson, 2011). However, Teixé-Roig et al. (2018) observed a synergetic effect between carboxymethyl cellulose and hydrophilic surfactant (lecithin) in the stabilization of double emulsions, whose combination inhibited the aggregation of the outer aqueous droplets during 21 days of storage.

Nonetheless, the strategy to improve the stability of $W_1/O/W_2$ emulsions that is currently booming is the immobilization of W_1 by a gelation mechanism (Andrade, Wright, & Corredig, 2018; Muschiolik & Dickinson, 2017). Actually, Surh, Vladisavljević, Mun, & McClements (2007) prepared $W_1/O/W_2$ emulsions by microfluidization and high pressure homogenization containing 6.4% *w/w* of polyglycerol polyricinoate (PGPR) and 0-15% *w/w* of whey protein isolate (WPI), whose internal water droplets were gelled due to a thermal treatment of WPI. These double emulsions were able to highly retain the water droplets and showed long-term stability due to resulted more effective in inhibiting coalescence or Ostwald ripening. Similarly, $W_1/O/W_2$ emulsions studied by Oppermann, Renssen, Schuch, Stieger, & Scholten (2015), in which the inner water droplets were gelled with gelatin or WPI resulted less sensitive towards an imbalance in osmotic pressure compared to their counterparts without gelling agents.

Mezzenga (2007) also described that the use of small quantities of electrolytes (*e.g.* NaCl), sugars (*e.g.* glucose) or polysaccharides including pectins, sodium alginate, chitosan, carrageenan, xanthan and gellan among others, is a common practice to preserve the stability of double emulsions. They provided coalescence resistance and additional stability to the internal water droplets of PGPR-stabilized $W_1/O/W_2$ emulsions. Moreover, Muschiolik & Dickinson (2017) observed that the interaction between electrolytes (typically NaCl) and polysaccharide also improved the stability and release behavior of the double emulsion. Likewise, other authors as Li, Fang, Al-Assaf, Phillips, & Jiang (2012) showed that the incorporation of polysaccharides or electrolytes like NaCl to both aqueous phases of double emulsions can improve their thermodynamic stability due to the control of the osmotic balance. Therefore, the incorporation of salts such as NaCl in both inner and outer aqueous phases seems to be essential for the maintenance of the optimal osmotic balance (Muschiolik & Dickinson, 2017). Scherze et al. (2006) reported that the presence of NaCl maintained a balance between Laplace pressure, defined as the pressure difference between inside and outside of the curved surface, and osmotic pressure. This may improve emulsification efficiency leading to long-term stable double emulsions.

In addition, Oppermann, Noppers, Stieger, & Scholten (2018) studied the influence of incorporating different emulsifiers including sodium caseinate and WPI in the outer aqueous phase (W_2) of $W_1/O/W_2$ emulsions. They concluded that the use of these biopolymers led to higher oil droplets sizes and lower yields than emulsions stabilized by small molecular surfactants (≈ 67 μm

against 51 μm). In fact, they observed that protein-stabilized $W_1/O/W_2$ emulsions exhibited yields between 60-75%, whereas they reached the 100% in those Tween 20-stabilized; which is in accordance with previous studies (Oppermann et al., 2015; Surh et al., 2007). Thus, it can be hypothesized that since proteins adsorption kinetics during emulsion breakup is slow, inner water droplets can migrate during the placement of biopolymer chains at droplets interface. Moreover, the observed behavior of the two proteins was also different since they are structurally different. Sodium caseinate- emulsions yielded smaller oil droplets than WPI since caseinates are more flexible and can rearrange at droplets interface favoring adsorption throughout emulsification.

(iii)Protein-polysaccharide complexes

Protein-polysaccharides complexes are gaining attention for the stabilization of $W_1/O/W_2$ emulsions. Indeed, according to Li et al. (2012), protein and polysaccharides show a synergistic effect on the functionality of $W_1/O/W_2$ emulsions when they are complexed. They observed that a combination of bovine serum albumin and sugar beet pectin under specific conditions exhibited better emulsifying capacity than the individual components alone. Likewise, Li et al. (2012) reported that protein-polysaccharide complexes such as those of whey protein with low methoxyl pectin (LMP) and κ-carrageenan (KCG) showed the ability to improve encapsulation efficiency (61.7-94.3% depending on the biopolymers ratio) of emulsion-based nanostructures acting as selective non pH- dependent barriers preventing enzyme attack in upper GTI. Possibly because LMP and KCG interacted effectively with positive groups of whey protein isolate in the mixture to make stable double emulsions (Lamba et al., 2015). Moreover, the particle size of pure KCG-stabilized $W_1/O/W_2$ emulsions was 147.4 ± 4.2 μm, whereas it ranged from 18.8 ± 4.2 to 84.9 ± 7.6 μm in those WPI-KCG complex-stabilized (Li et al., 2012). Therefore, the higher the concentration of polysaccharide in the complex, the greater the $W_1/O/W_2$ emulsions particle size.

Shaddel et al., (2018), which effectively encapsulated anthocyanins from black raspberry (*Rubus occidentalis L.*) within $W_1/O/W_2$ emulsions containing PGPR and Tween 80 as lipophilic and hydrophilic surfactant, respectively (Table 2) by a two-step procedure followed by gum Arabic-gellatin complexation observed the same trend. The increase of protein concentration with regards the polysaccharide, resulted in the reduction of emulsions particle size and the improvement of encapsulation efficiency.

4. Functionality and applications of emulsion-based nanostructures

Emulsion-based nanostructures have to be effective enough on the one hand, to protect the bioactive compounds either nutraceuticals (*e.g.* plant-derived pigments) or antimicrobials (*e.g.* essential oils) encapsulated within them in order to avoid the loss of their functional activity; and on the other hand, to allow their controlled release. Actually, in the case of nutraceuticals, the main objective is to ensure the absorption of the encapsulated bioactive compound in the target organ, whereas regarding antimicrobials encapsulation, the focus is on enhancing the quality and safety of high perishable foods in order to extend their shelf-life. Thus, the design of the emulsion-based nanostructures should be related with the polarity of the functional compound in order to favor its diffusion and to the desired application of the prepared systems.

On the other hand, the small particle size of these nanostructured delivery systems (<500 nm) also enhance its functionality with regards to conventional systems since the superficial area is higher

thus improving its effectiveness. Indeed, Salvia-Trujillo & McClements (2016) reported that small droplets were fully digested within the small intestine phase, and these emulsions showed 2.5 and 5% bioaccessibility higher than those containing large droplets emulsion-free samples, respectively. Thus, the smaller the nanostructures particle size, the higher the bioavailability of the encapsulated bioactive compound. In addition, its small size allows reducing the amount of compound incorporated in the dietary matrices, minimally affecting its organoleptic properties. However, it must be taken into account that emulsion-based nanostructures are normally incorporated to both liquid and solid food matrices, which causes their dilution as a result. Consequently, the concentration of bioactive compound may be too low to have a significant impact on the organism in the case of neutraceuticals, or in the prevention of food spoilage if the bioactive compounds are antimicrobials. For this reason, there is a special interest in prepare highly concentrated emulsion-based systems in which the inner volume fraction is at least 0.4 and hence, they are able to be loaded with more concentration of bioactive compound (Luo et al., 2017).

Furthermore, although these delivery systems can be directly incorporated in liquid products (*e.g.* beverages, yogurts, purees), the application of emulsion-based nanostructures onto solid foods requires the presence of biopolymers capable of gelling on the surface fixing the bioactive compound. Edible coatings are able to transport antioxidants and antimicrobials such as EOs to the food matrix by diffusion release (Aloui & Khwaldia, 2016). Thus, they can not only act as physical barriers against moisture, gas and solute but also extend the shelf-life of high perishable foods when they contain antimicrobial agents within (Rojas-Graü et al., 2009). There are different techniques for the application of edible coatings to food matrices including dipping, enrobing, spraying or electronic spraying. According to Zhong et al. (2014), dipping and enrobing coating methods led to more homogeneous film structures, whereas those obtained by spraying and electrostatic spraying coating methods were thinner film thickness. Nonetheless, edible coatings based on EO-loaded nanoemulsions prepared onto high perishable foods surface by Artiga-Artigas et al. (2017) and Salvia-Trujillo, Rojas-Graü, Soliva-Fortuny, & Martín-Belloso (2015) using dipping technique resulted potentially effective in extending the shelf-life of low-fat cut cheese and fresh-cut fruit, respectively.

Moreover, the incorporation of biopolymers such as proteins or polysaccharides and natural surfactants as emulsifiers may promote the scaling of these delivery systems to the industry. Recently, nanostructures containing protein-polysaccharide complexes have been developed as a tool to produce specific microstructures and novel functionalities with potential application in foods (Martins et al., 2013; Salminen & Weiss, 2014). Bosnea, Moschakis, & Biliaderis, (2017) directly incorporated complex-stabilized nanoemulsions in a yogurt matrix without practically affecting their mechanical properties and sensorial attributes. Likewise, Ifeduba & Akoh (2016) concluded that gelatin-gum arabic complexes prepared by Maillard-reaction-modified for stearidonic acid soybean oil encapsulation incorporated in a yoghurt matrix delayed the development of rancidity and improved its storage and oxidative stability during 14 days of yoghurt storage at 4 °C.

Regardless the incorporation procedures of these emulsion-based nanostructures all their components must be safe to eat or have the generally recognized as safe (GRAS) status since they are considered as food products, food ingredients or food contact substances. Thus, as "food ingredients" their preparation should follow the corresponding regulations allowing reaching safe, stable, nutritious and high quality foods according to the current consumers demand (Rojas-Graü et al., 2009). Food matrices are complex multi-component systems containing different macromolecules such as proteins, lipids and hydrocolloids that can compete with those biopolymers from nanostructures causing their

destabilization (Guichard, 2015). Likewise, if the food matrix contains some charged biopolymers, they could adsorb to the surfaces of oppositely charged emulsion droplets through electrostatic interactions (Zeeb et al., 2016). These biopolymers are able to promote droplet flocculation due to charge neutralization and bridging effects (Dickinson, 2009). Therefore, the control of pH and ionic strength is also required after the incorporation of emulsion-based nanostructures to foods during storage.

In this regard, the selection of the most suitable emulsion-based system and its formulation may be crucial in order to get the most out of them.

5. Toxicological aspects

Emulsion-based structured delivery systems are increasingly reaching the market and some of them have really small particle sizes (nanometric scale). This particularity is remarkable because it is associated with their greater reactivity, higher bioavailability and a better cellular transport than those conventional. However, nanoparticles might have an impact in the human body and hence, there is also a great concern about the potential toxicological effects related to their intake through food products. This could be the case of EOs-loaded nanostructures, which have some toxic effects at high doses associated to their potential ability to interact with the human cellular membranes as they act on microbial membranes (Fandohan et al., 2008). However, the concentration of each encapsulated compound can be accurately controlled within nanostructures due to their small sizes and homogeneity. On the other hand, particle size has a direct effect in the digestibility suggesting that nanoparticles could be able to pass across the cell membranes without being digested (Salvia-Trujillo, Qian, Martín-Belloso, & McClements, 2013). In this regard, emulsion-based nanostructures might reach biological tissues triggering unpredictable reactions in the target organs. There, they should be completely degraded and solubilized in the GIT in order to reduce the toxicity risk to a large extent.

Furthermore, since all the structures mentioned in the present work present potential qualities to be applied as delivery systems for food products, their preparation should follow all required regulations pertinent to food ingredients (Rojas-Graü et al., 2009). This means that all the components that conform nanoemulsions and double emulsions must be safe to eat and they have to be prepared following good manufacturing practices (GMP) (Rojas-Graü et al., 2009). Moreover, all of these delivery systems can contain biopolymers in their aqueous phase like sodium alginate, pectin or proteins. As it has been discussed previously, these biopolymers may enhance the stability of the delivery systems and modify the textural properties of the final product. Therefore, it is necessary to study the behavior and digestibility of these biopolymers during the GIT. Incorporation of biopolymers into emulsion-based nanostructures also results interesting from the environment point of view. In fact, there is a "green-packaging" initiative that consists of encouraging the use of delivery systems biopolymer-based as edible coatings or films among others. The US EPA (US Environmental Protection Agency) suggests using these coatings or films instead of synthetic plastics to reduce the amount of environmental toxic materials used in packaging and make them easier to reuse or compost. In addition, these edible coatings or films can be carrying antimicrobial compounds able to extend the shelf-life of packaged foods reducing their damage or spoilage and improving their quality (Espitia, Du, Avena-Bustillos, Soares, & McHugh, 2014).

6. Concluding remarks

Plant-derived bioactive compounds including pigments and essential oils are potential natural additives that can be incorporated to food matrices in order to satisfy the current consumers demand. That can explain the notable interest in designing, preparing and characterizing emulsion-based nanostructures able to encapsulate, protect and enhance functionality of these bioactive compounds. It is of vital importance to choose the most suitable system for each bioactive compound and its final application. In addition, the prepared emulsion-based nanostructures have to be stable in order to be applied to food matrices. Therefore, their preparation should be carefully controlled considering several factors such as the viscosity of the aqueous media, pH or ionic strength. Moreover, the selection of the most suitable type and concentration of emulsifier is crucial to obtain stable nanostructures. However, there is a current challenge about unraveling the fundamental mechanisms of emulsifiers' interfacial assembly. Thus, a deeper study of emulsifiers (*i.e.* surfactants, polysaccharides or protein-polysaccharide complexes) interaction at droplets interface is necessary to create novel complex structures with controlled mechanical and functional properties.

In spite of being demonstrated that emulsion-based nanostructures incorporation to food products contributes to enhance their quality and safety, more research is required about the consequences of nanostructures intake in the body. Therefore, future investigations should be focused on studying emulsion-based nanostructures stability in food matrices during storage, their behavior during digestion and their potential toxicological effects. And last but not least, the study of the costs involved in bringing these systems to industrial scale it is also of great importance.

7. Acknowledgments

This study was funded by the Ministry of Economy, Industry and Competitiveness (MINECO/FEDER, UE) throughout project **AGL2015-65975-R**. Author María Artiga-Artigas thanks the University of Lleida for their pre-doctoral fellowship. Author Laura Salvia-Trujillo thanks the "Secretaria d'Universitats i Recerca del Departament d'Empresa i Coneixement de la Generalitat de Catalunya" for the Beatriu de Pinós post-doctoral grant **BdP2016 00336**.

8. References

[EC] European Commission. (2000). Regulation (EC) No. 258/ 97 of the European Parliament and of the Council of 27 January 1997 concerning novel foods and novel food ingredients. *Official Journal of the European Communities*, *L 269*(September 2000), 1–15.

Acevedo-Fani, A., Salvia-Trujillo, L., Rojas-Graü, M. A., & Martín-Belloso, O. (2015). Edible films from essential-oil-loaded nanoemulsions: Physicochemical characterization and antimicrobial properties. *Food Hydrocolloids*, *47*, 168–177.

Acevedo-Fani, A., Soliva-Fortuny, R., & Martín-Belloso, O. (2017). Nanostructured emulsions and nanolaminates for delivery of active ingredients: Improving food safety and functionality. *Trends in Food Science & Technology*, *60*, 12–22.

Aditya, N. P., Aditya, S., Yang, H., Kim, H. W., Park, S. O., & Ko, S. (2015). Co-delivery of hydrophobic curcumin and hydrophilic catechin by a water-in-oil-in-water double emulsion.

Food Chemistry, *173*, 7–13.

Aditya, N. P., Shim, M., Lee, I., Lee, Y., Im, M.-H., & Ko, S. (2013). Curcumin and genistein coloaded nanostructured lipid carriers: In vitro digestion and antiprostate cancer activity. *Journal of Agricultural and Food Chemistry*, *61*(8).

Alba, K., & Kontogiorgos, V. (2017). Pectin at the oil-water interface: Relationship of molecular composition and structure to functionality. *Food Hydrocolloids*, *68*, 211–218.

Aloui, H., & Khwaldia, K. (2016). Natural Antimicrobial Edible Coatings for Microbial Safety and Food Quality Enhancement. *Comprehensive Reviews in Food Science and Food Safety*, *15*(6), 1080–1103.

Altuntas, O. Y., Sumnu, G., & Sahin, S. (2017). Preparation and characterization of W/O/W type double emulsion containing PGPR–lecithin mixture as lipophilic surfactant. *Journal of Dispersion Science and Technology*, *38*(4), 486–493.

Andrade, J. (2016). Food-based multiple emulsions as carriers of bioactive compounds: interactions at the interface and physical and chemical changes during in vitro digestion, 124.

Andrade, J., Wright, A. J., & Corredig, M. (2018). In vitro digestion behavior of water-in-oil-in-water emulsions with gelled oil-water inner phases. *Food Research International*, *105*(October 2017), 41–51.

Artiga-Artigas, M., Acevedo-Fani, A., & Martín-Belloso, O. (2017). Effect of sodium alginate incorporation procedure on the physicochemical properties of nanoemulsions. *Food Hydrocolloids*, *70*, 191–200.

Artiga-Artigas, M., Acevedo-Fani, A., & Martín-Belloso, O. (2017). Improving the shelf life of low-fat cut cheese using nanoemulsion-based edible coatings containing oregano essential oil and mandarin fiber. *Food Control*, *76*, 1–12.

Artiga-Artigas, M., Guerra-Rosas, M. I., Morales-Castro, J., Salvia-Trujillo, L., & Martín-Belloso, O. (2018). Influence of essential oils and pectin on nanoemulsion formulation: A ternary phase experimental approach. *Food Hydrocolloids*, *81*, 209–219.

Artiga-Artigas, M., Lanjari-Pérez, Y., & Martín-Belloso, O. (2018). Curcumin-loaded nanoemulsions stability as affected by the nature and concentration of surfactant. *Food Chemistry*, *266*(June), 466–474.

Bilbao-Sáinz, C., Avena-Bustillos, R. J., Wood, D. F., Williams, T. G., & McHugh, T. H. (2010). Nanoemulsions prepared by a low-energy emulsification method applied to edible films. *Journal of Agricultural and Food Chemistry*, *58*(22), 11932–11938.

Bilia, A. R., Guccione, C., Isacchi, B., Righeschi, C., Firenzuoli, F., & Bergonzi, M. C. (2014). Essential oils loaded in nanosystems: A developing strategy for a successful therapeutic approach. *Evidence-Based Complementary and Alternative Medicine*.

Bolhassani, A. (2018). *Bioactive Components of Saffron and Their Pharmacological Properties*. *Studies in Natural Products Chemistry* (1st ed., Vol. 58). Elsevier B.V.

Bosnea, L. A., Moschakis, T., & Biliaderis, C. G. (2017). Microencapsulated cells of Lactobacillus paracasei subsp. paracasei in biopolymer complex coacervates and their function in a yogurt matrix. *Food Funct.*, *8*(2), 554–562.

Bourbon, A. I., Cerqueira, M. A., & Vicente, A. A. (2016). Encapsulation and controlled release of bioactive compounds in lactoferrin-glycomacropeptide nanohydrogels: Curcumin and caffeine as model compounds. *Journal of Food Engineering*, *180*, 110–119.

Burt, S. (2004). Essential oils: their antibacterial properties and potential applications in foods--a review. *International Journal of Food Microbiology*, *94*(3), 223–53.

Chung, C., Sher, A., Rousset, P., & McClements, D. J. (2017). Influence of homogenization on physical properties of model coffee creamers stabilized by quillaja saponin. *Food Research International*, *99*(April), 770–777.

Das, J., Samadder, A., Mondal, J., Abraham, S. K., & Khuda-Bukhsh, A. R. (2016). *Nano-encapsulated chlorophyllin significantly delays progression of lung cancer both in in vitro and in vivo models through activation of mitochondrial signaling cascades and drug-DNA interaction*. *Environmental Toxicology and Pharmacology*. Elsevier B.V.

Degner, B. M., Chung, C., Schlegel, V., Hutkins, R., & Mcclements, D. J. (2014). Factors influencing the freeze-thaw stability of emulsion-based foods. *Comprehensive Reviews in Food Science and Food Safety*, *13*(2), 98–113.

Dickinson, E. (2009). Hydrocolloids as emulsifiers and emulsion stabilizers. *Food Hydrocolloids*, *23*(6), 1473–1482.

Dickinson, E. (2011). Double Emulsions Stabilized by Food Biopolymers. *Food Biophysics*, *6*(1), 1–11.

Dickinson, E., Elverson, D. J., & Murray, B. S. (1989). On the film-forming and emulsion-stabilizing properties of gum arabic: dilution and flocculation aspects. *Topics in Catalysis*, *3*(2), 101–114.

Donsì, F., Annunziata, M., Sessa, M., & Ferrari, G. (2011). Nanoencapsulation of essential oils to enhance their antimicrobial activity in foods. *LWT - Food Science and Technology*, *44*(9), 1908–1914.

Donsì, F., & Ferrari, G. (2016). Essential oil nanoemulsions as antimicrobial agents in food. *Journal of Biotechnology*, *233*, 106–120.

Dror, Y., Cohen, Y., & Yerushalmi-Rozen, R. (2007). Structure of Gum Arabic in Aqueous Solution. *Journal of Polymer Science Part B: Polymer Physics*, *45*(April), 1390–1398.

Esfanjani, A. F., Jafari, S. M., Assadpoor, E., & Mohammadi, A. (2015). Nano-encapsulation of saffron extract through double-layered multiple emulsions of pectin and whey protein concentrate. *Journal of Food Engineering*, *165*, 149–155.

Espitia, P. J. P., Du, W. X., Avena-Bustillos, R. de J., Soares, N. de F. F., & McHugh, T. H. (2014). Edible films from pectin: Physical-mechanical and antimicrobial properties - A review. *Food Hydrocolloids*, *35*, 287–296.

Fandohan, P., Gnonlonfin, B., Laleye, A., Gbenou, J. D., Darboux, R., & Moudachirou, M. (2008). Toxicity and gastric tolerance of essential oils from Cymbopogon citratus, Ocimum gratissimum and Ocimum basilicum in Wistar rats. *Food and Chemical Toxicology*, *46*(7), 2493–2497.

Ferruzzi, M. G., & Schwartz, S. J. (2005). Thermal degradation of commercial grade sodium copper chlorophyllin. *Journal of Agricultural and Food Chemistry*, *53*(18), 7098–7102.

Forgiarini, A., Esquena, J., González, C., & Solans, C. (2001). Formation of nano-emulsions by low-energy emulsification methods at constant temperature. *Langmuir*, *17*(7), 2076–2083.

Frank, K., Walz, E., Gräf, V., Greiner, R., Köhler, K., & Schuchmann, H. P. (2012). Stability of Anthocyanin-Rich W/O/W-Emulsions Designed for Intestinal Release in Gastrointestinal Environment. *Journal of Food Science*, *77*(12).

Funami, T., Zhang, G., Hiroe, M., Noda, S., Nakauma, M., Asai, I., … Phillips, G. O. (2007). Effects of the proteinaceous moiety on the emulsifying properties of sugar beet pectin. *Food Hydrocolloids*, *21*(8), 1319–1329.

Garti, N., Aserin, A., Tiunova, I., & Binyamin, H. (1999). Double emulsions of water-in-oil-in-water stabilized by α-form fat microcrystals. Part 1: Selection of emulsifiers and fat microcrystalline particles. *JAOCS, Journal of the American Oil Chemists' Society*, *76*(3), 383–389.

Garti, N., Madar, Z., Aserin, A., & Sternheim, B. (1997). Fenugreek galactomannans as food emulsifiers. *LWT - Food Science and Technology*, *30*(3), 305–311.

Gasa-Falcon, A., Odriozola-Serrano, I., Oms-Oliu, G., & Martín-Belloso, O. (2017). Influence of mandarin fiber addition on physico-chemical properties of nanoemulsions containing β-carotene under simulated gastrointestinal digestion conditions. *LWT - Food Science and Technology*, *84*, 331–337.

Genot, C., Kabri, T., & Meynier, A. (2013). *Stabilization of omega-3 oils and enriched foods using emulsifi ers*. *Food enrichment with omega-3 fatty acids*. Woodhead Publishing Limited.

Gradecka-Meesters, D., Palus, J., Prochazka, G., Segerbäck, D., Dziubaltowska, E., Kotova, N., … Stepnik, M. (2011). Assessment of the protective effects of selected dietary anticarcinogens against DNA damage and cytogenetic effects induced by benzo[a]pyrene in C57BL/6J mice. *Food and Chemical Toxicology*, *49*(8), 1674–1683.

Guerra-Rosas, M. I., Morales-Castro, J., Cubero-Márquez, M. A., Salvia-Trujillo, L., & Martín-Belloso, O. (2017). Antimicrobial activity of nanoemulsions containing essential oils and high methoxyl pectin during long-term storage. *Food Control*, *77*, 131–138.

Guichard, E. (2015). *Interaction of aroma compounds with food matrices*. *Flavour Development, Analysis and Perception in Food and Beverages*. Elsevier Ltd.

Herzi, S., Essafi, W., Bellagha, S., & Leal-Calderon, F. (2014). Influence of the inner droplet fraction on the release rate profiles from multiple W/O/W emulsions. *Colloids and Surfaces A: Physicochemical and Engineering Aspects*, *441*, 489–495.

Ifeduba, E. A., & Akoh, C. C. (2016). Microencapsulation of stearidonic acid soybean oil in Maillard

reaction-modified complex coacervates. *Food Chemistry*, *199*, 524–532.

Jafari, S. M., He, Y., & Bhandari, B. (2007). Production of sub-micron emulsions by ultrasound and microfluidization techniques. *Journal of Food Engineering*, *82*(4), 478–488.

Jiao, J., & Burgess, D. J. (2003). Rheology and stability of water-in-oil-in-water multiple emulsions containing Span 83 and Tween 80. *AAPS PharmSci*, *5*(1), 62–73.

Kaimainen, M., Marze, S., Järvenpää, E., Anton, M., & Huopalahti, R. (2015). Encapsulation of betalain into w/o/w double emulsion and release during invitro intestinal lipid digestion. *LWT - Food Science and Technology*, *60*(2), 899–904.

Kanouni, M., Rosano, H. L., & Naouli, N. (2002). Preparation of a stable double emulsion (W1/O/W2): Role of the interfacial films on the stability of the system. *Advances in Colloid and Interface Science*, *99*(3), 229–254.

Kralova, I., & Sjöblom, J. (2009). Surfactants used in food industry: A review. *Journal of Dispersion Science and Technology*, *30*(9).

Lamba, H., Sathish, K., & Sabikhi, L. (2015). Double Emulsions: Emerging Delivery System for Plant Bioactives. *Food and Bioprocess Technology*, *8*(4), 709–728.

Lee, L. W., Liu, X., Wong, W. S. E., & Liu, S. Q. (2017). Effects of sucrose monopalmitate (P90), Tween 80 and modified starch on coffee aroma retention and release in coffee oil-based emulsions. *Food Hydrocolloids*, *66*, 128–135.

Lehto, S., Buchweitz, M., Klimm, A., Straßburger, R., Bechtold, C., & Ulberth, F. (2017). Comparison of food colour regulations in the EU and the US: a review of current provisions. *Food Additives and Contaminants - Part A Chemistry, Analysis, Control, Exposure and Risk Assessment*, *34*(3), 335–355.

Li, B., Jiang, Y., Liu, F., Chai, Z., Li, Y., Li, Y., & Leng, X. (2012). Synergistic effects of whey protein-polysaccharide complexes on the controlled release of lipid-soluble and water-soluble vitamins in W1/O/W2double emulsion systems. *International Journal of Food Science and Technology*, *47*(2), 248–254.

Li, J.-R., Sun, M.-J., Ping, Q.-N., Chen, X.-J., Qi, J.-P., & Han, D.-E. (2010). Metabolism, Excretion and Bioavailability of Hydroxysafflor Yellow A after Oral Administration of Its Lipid-Based Formulation and Aqueous Solution in Rats. *Chinese Journal of Natural Medicines*, *8*(3), 233–240.

Li, X., Fang, Y., Al-Assaf, S., Phillips, G. O., & Jiang, F. (2012). Complexation of bovine serum albumin and sugar beet pectin: Stabilising oil-in-water emulsions. *Journal of Colloid and Interface Science*, *388*(1), 103–111.

Liu, L., Fishman, M. L., & Hicks, K. B. (2006). Pectin in controlled drug delivery – a review. *Cellulose*, *14*, 15–24.

Lopez-Rubio, A., Gavara, R., & Lagaron, J. M. (2006). Bioactive packaging: turning foods into healthier foods through biomaterials. *Trends in Food Science and Technology*, *17*(10), 567–575.

Luo, X., Zhou, Y., Bai, L., Liu, F., Zhang, R., Zhang, Z., … McClements, D. J. (2017). Production of highly concentrated oil-in-water emulsions using dual-channel microfluidization: Use of individual and mixed natural emulsifiers (saponin and lecithin). *Food Research International*, *96*, 103–112.

Maa, Y. F., & Hsu, C. C. (1999). Performance of sonication and microfluidization for liquid-liquid emulsification. *Pharmaceutical Development and Technology*, *4*(2), 233–240.

Martins, A. F., Bueno, P. V. A., Almeida, E. A. M. S., Rodrigues, F. H. A., Rubira, A. F., & Muniz, E. C. (2013). Characterization of N-trimethyl chitosan/alginate complexes and curcumin release. *International Journal of Biological Macromolecules*, *57*, 174–184.

Matos, M., Gutiérrez, G., Martínez-Rey, L., Iglesias, O., & Pazos, C. (2018). Encapsulation of resveratrol using food-grade concentrated double emulsions: Emulsion characterization and rheological behaviour. *Journal of Food Engineering*, *226*, 73–81.

McClements, D. J. (2011). Edible nanoemulsions: fabrication, properties, and functional performance. *Soft Matter*, *7*(6), 2297–2316.

McClements, D. J. (2012). Advances in fabrication of emulsions with enhanced functionality using structural design principles. *Current Opinion in Colloid and Interface Science*, *17*(5), 235–245.

Mendoza, A. J., Guzmán, E., Martínez-Pedrero, F., Ritacco, H., Rubio, R. G., Ortega, F., … Miller, R. (2014). Particle laden fluid interfaces: Dynamics and interfacial rheology. *Advances in Colloid and Interface Science*, *206*, 303–319.

Mezzenga, R. (2007). Equilibrium and non-equilibrium structures in complex food systems. *Food Hydrocolloids*, *21*(5–6), 674–682.

Moschakis, T., & Biliaderis, C. G. (2017). Biopolymer-based coacervates: Structures, functionality and applications in food products. *Current Opinion in Colloid and Interface Science*, *28*, 96–109.

Musashino, K., Hasegawa, Y., Imaoka, H., Adachi, S., & Matsuno, R. (2001). Preparation of W/O/W multiple emulsions with polymers in the outer aqueous phase. *Food Sci.Technol.Res.*, *7*(1), 78–83.

Muschiolik, G., & Dickinson, E. (2017). Double Emulsions Relevant to Food Systems: Preparation, Stability, and Applications. *Comprehensive Reviews in Food Science and Food Safety*, *16*(3), 532–555.

Nash, J. J., & Erk, K. A. (2017). Stability and interfacial viscoelasticity of oil-water nanoemulsions stabilized by soy lecithin and Tween 20 for the encapsulation of bioactive carvacrol. *Colloids and Surfaces A: Physicochemical and Engineering Aspects*, *517*, 1–11.

Neumann, M. G., Schmitt, C. C., & Iamazaki, E. T. (2003). A fluorescence study of the interactions between sodium alginate and surfactants. *Carbohydrate Research*, *338*(10), 1109–1113.

O'Regan, J., & Mulvihill, D. M. (2010). Sodium caseinate-maltodextrin conjugate stabilized double emulsions: Encapsulation and stability. *Food Research International*, *43*(1), 224–231.

Oppermann, A. K. L., Noppers, J. M. E., Stieger, M., & Scholten, E. (2018). Effect of outer water phase composition on oil droplet size and yield of (w1/o/w2) double emulsions. *Food Research International*, *107*(February), 148–157.

Oppermann, A. K. L., Renssen, M., Schuch, A., Stieger, M., & Scholten, E. (2015). Effect of gelation of inner dispersed phase on stability of (w1/o/w2) multiple emulsions. *Food Hydrocolloids*, *48*, 17–26.

Otoni, C. G., Moura, M. R. de, Aouada, F. A., Camilloto, G. P., Cruz, R. S., Lorevice, M. V., … Mattoso, L. H. C. (2014). Antimicrobial and physical-mechanical properties of pectin/papaya puree/cinnamaldehyde nanoemulsion edible composite films. *Food Hydrocolloids*, *41*, 188–194.

Özer, O., Muguet, V., Roy, E., Grossiord, J. L., & Seiller, M. (2000). Stability Study of W / O / W Viscosified Multiple Emulsions, *26*(11), 1185–1189.

Pal, R. (2008). Viscosity models for multiple emulsions. *Food Hydrocolloids*, *22*(3), 428–438.

Park, J. (2010). Anti-carcinogenic properties of curcumin on colorectal cancer. *World Journal of Gastrointestinal Oncology*, *2*(4), 169.

Pulido-Moran, M., Moreno-Fernandez, J., Ramirez-Tortosa, C., & Ramirez-Tortosa, M. C. (2016). Curcumin and health. *Molecules*, *21*(3), 1–22.

Qian, C., & Mcclements, D. J. (2011). Food Hydrocolloids Formation of nanoemulsions stabilized by model food-grade emulsi fi ers using high-pressure homogenization : Factors affecting particle size. *Food Hydrocolloids*, *25*(5), 1000–1008.

Rinaudo, M. (2006). Chitin and chitosan: Properties and applications. *Progress in Polymer Science (Oxford)*, *31*(7), 603–632.

Rivera, M. C., Pinheiro, A. C., Bourbon, A. I., Cerqueira, M. A., & Vicente, A. A. (2015). Hollow chitosan/alginate nanocapsules for bioactive compound delivery. *International Journal of Biological Macromolecules*, *79*, 95–102.

Rodriguez-Amaya, D. B. (2016). Natural food pigments and colorants. *Current Opinion in Food Science*, *7*, 20–26.

Rojas-Graü, M. A., Soliva-Fortuny, R., & Martín-Belloso, O. (2009). Edible coatings to incorporate active ingredients to fresh-cut fruits: a review. *Trends in Food Science & Technology*, *20*(10), 438–447.

Salminen, H., & Weiss, J. (2014). Electrostatic adsorption and stability of whey protein-pectin complexes on emulsion interfaces. *Food Hydrocolloids*, *35*, 410–419.

Salvia-Trujillo, L., & McClements, D. J. (2016). Enhancement of lycopene bioaccessibility from tomato juice using excipient emulsions: Influence of lipid droplet size. *Food Chemistry*, *210*, 295–304.

Salvia-Trujillo, L., Qian, C., Martín-Belloso, O., & McClements, D. J. (2013). Influence of particle size on lipid digestion and β-carotene bioaccessibility in emulsions and nanoemulsions. *Food*

Chemistry, *141*(2).

Salvia-Trujillo, L., Rojas-Graü, A., Soliva-Fortuny, R., & Martín-Belloso, O. (2013a). Physicochemical characterization of lemongrass essential oil-alginate anoemulsions: effect of ultrasound processing parameters. *Food and Bioprocess Technology*, *6*(9), 2439–2446.

Salvia-Trujillo, L., Rojas-Graü, M. A., Soliva-Fortuny, R., & Martín-Belloso, O. (2013b). Effect of processing parameters on physicochemical characteristics of microfluidized lemongrass essential oil-alginate nanoemulsions. *Food Hydrocolloids*, *30*(1), 401–407.

Salvia-Trujillo, L., Rojas-Graü, M. A., Soliva-Fortuny, R., & Martín-Belloso, O. (2014). Formulation of Antimicrobial Edible Nanoemulsions with Pseudo-Ternary Phase Experimental Design. *Food and Bioprocess Technology*, *7*(10).

Salvia-Trujillo, L., Rojas-Graü, M. A., Soliva-Fortuny, R., & Martín-Belloso, O. (2014). Impact of microfluidization or ultrasound processing on the antimicrobial activity against Escherichia coli of lemongrass oil-loaded nanoemulsions. *Food Control*, *37*(1), 292–297.

Salvia-Trujillo, L., Rojas-Graü, M. A., Soliva-Fortuny, R., & Martín-Belloso, O. (2015). Use of antimicrobial nanoemulsions as edible coatings: Impact on safety and quality attributes of fresh-cut Fuji apples. *Postharvest Biology and Technology*, *105*, 8–16.

Scherze, I., Knoth, A., & Muschiolik, G. (2006). Effect of emulsification method on the properties of lecithin- and PGPR-stabilized water-in-oil-emulsions. *Journal of Dispersion Science and Technology*, *27*(4), 427–434.

Schmidt, U. S., Schütz, L., & Schuchmann, H. P. (2017). Interfacial and emulsifying properties of citrus pectin: Interaction of pH, ionic strength and degree of esterification. *Food Hydrocolloids*, *62*, 288–298.

Schulz, P. C., Rodríguez, M. S., Del Blanco, L. F., Pistonesi, M., & Agulló, E. (1998). Emulsification properties of chitosan. *Colloid and Polymer Science*, *276*(12), 1159–1165.

Sellimi, S., Younes, I., Ayed, H. Ben, Maalej, H., Montero, V., Rinaudo, M., … Nasri, M. (2015). Structural, physicochemical and antioxidant properties of sodium alginate isolated from a Tunisian brown seaweed. *International Journal of Biological Macromolecules*, *72*, 1358–1367.

Shaddel, R., Hesari, J., Azadmard-Damirchi, S., Hamishehkar, H., Fathi-Achachlouei, B., & Huang, Q. (2018). Double emulsion followed by complex coacervation as a promising method for protection of black raspberry anthocyanins. *Food Hydrocolloids*, *77*, 803–816.

Sigurdson, G. T., Tang, P., & Giusti, M. M. (2017). Natural Colorants: Food Colorants from Natural Sources. *Annual Review of Food Science and Technology*, *8*(1), 261–280.

Silva, H. D., Cerqueira, M. Â., & Vicente, A. a. (2012). Nanoemulsions for Food Applications: Development and Characterization. *Food and Bioprocess Technology*, *5*(3), 854–867.

Solans, C., & Solé, I. (2012). Nano-emulsions: Formation by low-energy methods. *Current Opinion in Colloid and Interface Science*, *17*(5), 246–254.

Solórzano-Santos, F., & Miranda-Novales, M. G. (2012). Essential oils from aromatic herbs as antimicrobial agents. *Current Opinion in Biotechnology*, *23*(2), 136–141.

Stintzing, F. C., & Carle, R. (2004). Functional properties of anthocyanins and betalains in plants, food, and in human nutrition. *Trends in Food Science and Technology*, *15*(1), 19–38.

Surassmo, S., Min, S. G., Bejrapha, P., & Choi, M. J. (2010). Effects of surfactants on the physical properties of capsicum oleoresin-loaded nanocapsules formulated through the emulsion-diffusion method. *Food Research International*, *43*(1), 8–17.

Surh, J., Vladisavljević, G. T., Mun, S., & McClements, D. J. (2007). Preparation and characterization of water/oil and water/oil/water emulsions containing biopolymer-gelled water droplets. *Journal of Agricultural and Food Chemistry*, *55*(1), 175–184.

Szuts, A., & Szabó-Révész, P. (2012). Sucrose esters as natural surfactants in drug delivery systems - A mini-review. *International Journal of Pharmaceutics*, *433*(1–2), 1–9.

Tabibiazar, M., & Hamishehkar, H. (2015). Formulation of a food grade water-in-oil nanoemulsion: Factors affecting on stability. *Pharmaceutical Sciences*, *21*(4), 220–224.

Tadros, T. F. (2013). Emulsion Formation , Stability , and Rheology.

Tedajo, G. M., Seiller, M., Prognon, P., & Grossiord, J. L. (2001). pH compartmented w/o/w multiple emulsion: A diffusion study. *Journal of Controlled Release*, *75*(1–2), 45–53.

Teixé-Roig, J., Oms-Oliu, G., Velderrain-Rodríguez, G. R., Odriozola-Serrano, I., & Martín-Belloso, O. (2018). The Effect of Sodium Carboxymethylcellulose on the Stability and Bioaccessibility of Anthocyanin Water-in-Oil-in-Water Emulsions.

Thiyagarajan, P., Senthil Murugan, R., Kavitha, K., Anitha, P., Prathiba, D., & Nagini, S. (2012). Dietary chlorophyllin inhibits the canonical NF-κB signaling pathway and induces intrinsic apoptosis in a hamster model of oral oncogenesis. *Food and Chemical Toxicology*, *50*(3–4), 867–876.

Vladisavljević, G. T., Al Nuumani, R., & Nabavi, S. A. (2017). Microfluidic production of multiple emulsions. *Micromachines*, *8*(3).

Wang, T., Wang, L., Li, C., Han, B., Wang, Z., Li, J., … Fu, F. (2017). Hydroxysafflor Yellow A Improves Motor Dysfunction in the Rotenone-Induced Mice Model of Parkinson's Disease. *Neurochemical Research*, *42*(5), 1325–1332.

Wang, Y., Zhang, T., & Hu, G. (2006). Structural evolution of polymer-stabilized double emulsions. *Langmuir*, *22*(1), 67–73.

Wei, L., Liu, X., San, W., Wong, E., & Quan, S. (2017). Food Hydrocolloids Effects of sucrose monopalmitate (P90), Tween 80 and modi fi ed starch on coffee aroma retention and release in coffee oil-based emulsions, *66*, 128–135.

Wei, X., Liu, H., Sun, X., Fu, F., Zhang, X., Wang, J., … Ding, H. (2005). Hydroxysafflor yellow A protects rat brains against ischemia-reperfusion injury by antioxidant action. *Neuroscience*

Letters, *386*(1), 58–62.

Weiss, J., & Muschiolik, G. (2007). Factors affecting the droplet size of water-in-oil emulsions (W/O) and the oil globule size in Water-in-oil-in-water emulsions (W/O/W). *Journal of Dispersion Science and Technology*, *28*(5), 703–716.

Wilson, R., Van Schie, B. J., & Howes, D. (1998). Overview of the preparation, use and biological studies on polyglycerol polyricinoleate (PGPR). *Food and Chemical Toxicology*, *36*(9–10), 711–718.

Xu, J.-H., Ge, X.-H., Chen, R., & Luo, G.-S. (2014). Microfluidic preparation and structure evolution of double emulsions with two-phase cores. *RSC Advances*, *4*(4), 1900.

Yamashita, Y., & Sakamoto, K. (2017). Structural Analysis of Formulations. *Cosmetic Science and Technology: Theoretical Principles and Applications*, 635–655.

Yao, X., Wang, N., Fang, Y., Phillips, G. O., Jiang, F., Hu, J., … Tian, D. (2013). Impact of surfactants on the lipase digestibility of gum arabic-stabilized O/W emulsions. *Food Hydrocolloids*, *33*(2), 393–401.

Yildirim, M., Sumnu, G., & Sahin, S. (2017). The effects of emulsifier type, phase ratio, and homogenization methods on stability of the double emulsion. *Journal of Dispersion Science and Technology*, *38*(6), 807–814.

Zeeb, B., Gibis, M., Fischer, L., & Weiss, J. (2012). Influence of interfacial properties on Ostwald ripening in crosslinked multilayered oil-in-water emulsions. *Journal of Colloid and Interface Science*, *387*(1), 65–73.

Zeeb, B., Mi-Yeon, L., Gibis, M., & Weiss, J. (2018). Growth phenomena in biopolymer complexes composed of heated WPI and pectin. *Food Hydrocolloids*, *74*, 53–61.

Zeeb, B., Stenger, C., Hinrichs, J., & Weiss, J. (2016). Formation of concentrated particles composed of oppositely charged biopolymers for food applications - impact of processing conditions. *Food Structure*, *10*, 10–20.

Zhao, B., Gu, S., Du, Y., Shen, M., Liu, X., & Shen, Y. (2018). Solid lipid nanoparticles as carriers for oral delivery of hydroxysafflor yellow A. *International Journal of Pharmaceutics*, *535*(1–2), 164–171.

Zhao, L., Wei, Y., Huang, Y., He, B., Zhou, Y., & Fu, J. (2013). Nanoemulsion improves the oral bioavailability of baicalin in rats: In vitro and in vivo evaluation. *International Journal of Nanomedicine*, *8*, 3769–3779.

Zhong, Y., Cavender, G., & Zhao, Y. (2014). Investigation of different coating application methods on the performance of edible coatings on Mozzarella cheese. *LWT - Food Science and Technology*, *56*(1), 1–8.

Hypothesis and Objectives

The hypothesis of this Doctoral Thesis was that food-grade nanostructured delivery systems based on emulsions may be suitable carriers of plant-derived bioactive compounds. In this regard, the design of the appropriated nanostructure for each bioactive compound is of great importance for its effective incorporation into foods.

The main objective of this Doctoral Thesis was to find stabilization strategies for the formulation of food-grade emulsion-based nanostructures, as nanoemulsions and double emulsions, to carry and deliver plant-derived pigments, whether bioactives or antimicrobials and to be further incorporated into food products.

To achieve this goal, the following specific objectives were proposed:

i. To elucidate the impact of each component concentration (*i.e.* oil, surfactant, biopolymer and water) in the formation of food-grade nanoemulsions containing antimicrobial lipids (*i.e.* essential oils) using Ternary phase diagrams.
ii. To assess the influence of the type and concentration of three different surfactants (Tween 20, lecithin and sucrose monopalmitate) on the physicochemical characteristics of nanoemulsions and the ability of these systems to encapsulate lipophilic bioactive compounds (*i.e.* curcumin).
iii. To settle the effect of the homogenization procedure, as well as oil and surfactant concentration on the formation of highly concentrated nanoemulsions as carriers of lipophilic bioactive compounds (*i.e.* curcumin).
iv. To find the impact of microfluidization on the molecular structure of sodium alginate acting as emulsion stabilizer and the effect of the biopolymer incorporation before or after microfluidization on their physicochemical properties.
v. To determine the effectiveness of sugar beet pectin-whey protein isolate complexes used as emulsifiers in the stabilization of short-chain oil-in water nanoemulsions to prevent Ostwald ripening.
vi. To optimize the methodology for the formation of double emulsions and assess their ability as template carriers of hydrophilic and/or lipophilic bioactive compounds (*i.e.* cholophyllin and/or lemongrass essential oil, respectively).
vii. To prove the feasibility of using oregano essential oil-in water nanoemulsions as antimicrobial edible coatings onto low-fat cut cheese and their effect on the quality and safety attributes.

Materials and Methods

MATERIALS

Table 1. Materials required to produce the nanostructured delivery systems.

System	Active ingredients	Materials
Nanoemulsions	Essential oils: Oregano, Thyme, Lemongrass, Mandarin Pigments: Curcumin	***Disperse phase:*** *essential oils, corn oil, miglyol (MCT), decane* ***Emulsifier:*** *(i)* Surfactants: *Tween 20, Tween 80, Soy lecithin, sucrose monopalmitate* *(ii)* Biopolymers: *sodium alginate, high-methoxyl pectin.* *(iii)* Protein-polysaccharide complexes*: whey protein isolate-sugar beet pectin complexes*
Double emulsions	Essential oils: Lemongrass Pigments: Chlorophyllin	***Disperse phase****: essential oils, corn oil* ***Hydrophobic emulsifier****: span 80, PGPR* ***Hydrophilic emulsifier****: Tween 20, Soy lecithin* ***Stabilizer:*** *sodium alginate, NaCl salt*

METHODS

SECTION I. Designing nanoemulsions as carriers of lipophilic plant-derived bioactive compounds.

Nanoemulsions formation

The continuous phase was prepared by dissolving the surfactant and/or biopolymer in hot ultrapure water (70ºC). In the case of using natural biopolymers, the aqueous phase was stirred during at least 4h to ensure their complete hydration. The disperse phase was an essential oil and/or corn oil. All the components were homogenized using a high-speed blender (T25 digital Ultra-Turrax, IKA, Staufen, Germany). The resulting coarse emulsions were treated in a microfluidizer (M110P, Microfluidics, Massachusetts, USA), with 150 MPa and 5 passes, in order to obtain the subsequent nanoemulsions.

Characterization of nanoemulsions

Nanoemulsions were characterized in terms of droplet size, droplet charge, viscosity, color and morphology. The particle size (nm) of nanoemulsions was measured by dynamic light scattering and ζ-potential (mV) by phase-analysis light scattering (PALS) using a laser diffractometer (Zetasizer NanoZS, Malvern Instruments, U.K.). For all the measurements, samples were prior diluted in a ratio of 1/9 sample-to-solvent.

Apparent viscosity of nanoemulsions was measured in a vibro-viscometer SV-10 (A&D Company, Tokyo, Japan), from aliquots of 10 mL, vibrating at 30 MHz and constant amplitude. The temperature of samples was recorded simultaneously by the same equipment.

The color of nanoemulsions was determined in a Minolta CR-400 colorimeter (Konica Minolta Sensing, Inc., Osaka, Japan), using an illuminant D65 and the 10º observer angle. Whiteness index was calculated from the CIE L^*, a^* and b^* parameters, according to eq.(1) (Salvia-Trujillo, Rojas-Graü, Soliva-Fortuny, & Martín-Belloso, 2014a):

$$WI = 100-((100-L^*)^2+(a^{*2}+b^{*2}))^{0.5} \quad \textbf{eq. (1)}$$

Nanoemulsions turbidity is related to destabilization phenomena such as coalescence, creaming or flocculation, which were monitored by a Turbiscan Classic (Formulaction, Toulouse, France) during a maximum of 86 days of storage at room temperature. Tests were performed in duplicate.

Nanoemulsions were observed by negative-staining electron microscopy as a direct measurement of their droplet size and shape. Conventional emulsions and nanoemulsions were diluted with ultrapure water using a factor of 1:10, and they were adsorbed onto carbon-coated copper/palladium grids for 1 min. Then, the grids were washed three times by floating it face-down on drops of sterilized, deionized water for 1 min. Finally, the sample was negatively stained by floating the grids face-down on a drop of 2% (w/w) ammonium molybdate at pH 6.5 for 1 min. The grids were observed in a transmission electron microscope (Jeol 2100, FEI Company, Netherlands) at an acceleration voltage of 100 kV.

Encapsulation efficiency (EE, %) and curcumin release of nanoemulsions

Curcumin-loaded nanoemulsion aliquots of 10 mL were placed inside a dialysis tubing cellulose membrane of 43 mm x 27 mm (Sigma-Aldrich, Darmstadt, Germany) and submerged in 20 mL of food grade ethanol. After centrifugation (2000 rpm, 10 min) with a Hettich® Universal 320 centrifuge (Sigma-Aldrich, Darmstadt, Germany) the non-encapsulated curcumin content (free curcumin) was quantified spectrophotometrically with a V-670 spectrophotometer (Jasco, Tokyo, Japan) at 425 nm. Encapsulation efficiency (%) of the obtained nanoemulsions was calculated by eq.(2) (Surassmo et al., 2010):

$$EE = \frac{Total\ amount\ of\ curcumin - Free\ curcumin}{Total\ amount\ of\ curcumin} \text{x } 100 \qquad \textbf{eq. (2)}$$

where the total amount of curcumin is the initial concentration of this bioactive compound added to the mixture and the free curcumin is the concentration of compound that was not loaded in nanoemulsions.
All the measurements were performed in triplicate.

In order to monitor the curcumin rate release, aliquots of the samples were taken at times 0, 3, 6 and 24 h and quantified spectrophotometrically with a V-670 spectrophotometer (Jasco, Tokyo, Japan) at 425 nm. The curcumin release was calculated with equation (3) according to Surassmo et al. (2010) and fitted to a rectangular hyperbolic curve according to equation (4):

$$CR = (100 - \frac{Total\ amount\ of\ curcumin\ (t{=}0) - Released\ curcumin(t{=}t)}{Total\ amount\ of\ curcumin\ (t{=}0)})\text{x } 100 \qquad \textbf{eq. (3)}$$

$$CR = \frac{CRmax \cdot t}{k + t} \qquad \textbf{eq. (4)}$$

where CR is the curcumin release expressed in %, t is the time (h), CRmax is the maximum curcumin release (%) and k is a kinetic constant (h).

Antioxidant capacity of curcumin-loaded nanoemulsions

The antioxidant capacity of curcumin-loaded nanoemulsions was determined by the α, α-diphenyl-β-picrylhydrazyl (DPPH) free radical scavenging method and the Ferric Reducing Antioxidant Power (FRAP) assay. Although both methods can properly evaluat the antioxidant potential of curcumin, the main difference between them is that DPPH assay is based on the presence

of radicals (DPP·), whereas FRAP consists of an electrons exchange (Thaipong, Boonprakob, Crosby, Cisneros-Zevallos, & Hawkins Byrne, 2006).

DPPH procedure was conducted according to the method of Brand-Williams; Cuvelier, & Berset, (1995) with some modifications. The DPPH radical solution was prepared by dissolving 2.5 mg of DPPH radical in 100 mL of methanol. The absorbance of solution was adjusted to 0.7 ± 0.02 at 515 nm. Aliquots of 20 µL of sample were placed in a microplate and 280 µL of DPPH radical solution was added to each sample. Samples were incubated for 30 min in the dark and the absorbance was measured.

FRAP assay was carried out as described by Benzie & Strain (1996) where 20 µL of sample were placed into each tube and mixed with 280 µL of FRAP solution. The samples were incubated at room temperature in the dark for 30 min and the absorbance was measured at 630 nm after prior filtration.

Results were reported as mg of Trolox equivalents per mL of solution (mg TE/mL) using a standard curve of Trolox (Velderrain-Rodríguez et al., 2015). In both methods, triplicate determinations were made at each dilution of the standard.

Statistics

All the experiments were assayed at least in duplicate, and three replicate analyses were carried out for each parameter. SigmaPlot 12.0 Systat Software was used to perform the analysis of variance. Tukey test was chosen to determine significant differences among the use of different surfactants and concentrations, at a 5% significance level.

Correlation analyses were performed with statistical analysis software (SigmaPlot 12.0 Systat Software, London, UK).

Curcumin release curve was generated and statistically analyzed at a 5% significance level using Statgraphics Centurion XVII (Statgraphics Technologies INC, Virginia, USA). The output showed the results of fitting a nonlinear regression model to describe the relationship between CR and t independent variables. The R-Squared statistic indicates that the model as fitted explains 100.0% of the variability in CR.

Highly concentrated emulsions formation

Highly concentrated coarse emulsions contained at least a 40% *w/w* of oil as dispersed phase. Therefore, the aqueous phase containing the hydrophilic surfactant and corn oil, where the oil volume fraction (φ) ranged from 0.4 to 0.7 and the surfactant-to-oil ratio (SOR) from 0.01-0.2; were mixed with a T25 digital Ultra-Turrax (IKA, Staufen, Germany) at 11,000 during 2 min. Afterwards, highly concentrated nanoemulsions were obtained by ultrasonication with a UP 400S Hielscher sonifier (Hielscher Ultrasound Technology, Teltow, Germany) at 100 µm of amplitude and during 20-240 s or by microfluidization with a microfluidizer (M110P, Microfluidics, Massachusetts, USA) at 800 bar and 1-5 cycles.

Characterization of highly concentrated emulsions

The emulsion droplet size in terms of volume and surface diameter (d[4;3] and d[3;2], respectively) of all coarse emulsions and nanoemulsions expressed in μm was measured by the laser diffraction technique with a Mastersizer 3000^{TM} (Malvern Instruments Ltd., Worcestershire, UK). Refractive index of corn oil is 1.47. For the measurement of particle sizes, highly concentrated coarse and nanoemulsions were dispersed in distilled water.

The ζ-potential (mV), was measured by phase-analysis light scattering (PALS) with a Zetasizer Nano-ZS laser diffractometer (Malvern Instruments Ltd, Worcestershire, UK). It determines the electrical charge at the interface of the droplets dispersed in the aqueous phase. Samples were prior diluted in ultrapure water using a dilution factor of 1/150 sample-to-solvent.

Viscosity measurements (mPa·s) were performed by using a vibro-viscometer (SV-10, A&D Company, Tokyo, Japan) vibrating at 30 Hz, with constant amplitude and working at room temperature. Aliquots of 10 mL of each emulsion and nanoemulsion were used for determinations.

Microscopy images of fresh highly concentrated coarse and nanoemulsions were taken with an optical microscope (BX41, Olympus, Göttingen, Germany) equipped with UIS2 optical system. Phase contrast and bright field images were obtained without diluting the samples in order to maintain oil droplets packaging. All images were processed using the instrument software (Olympus cellSense, Barcelona, Spain).

Encapsulation efficiency (EE, %) and curcumin release of highly concentrated emulsions

The curcumin encapsulation efficiency (EE) was measured following the method of Lin et al. (2018) in which 0.5 mL of each emulsion is poured in 2 mL of ethanol absolute and 3 mL of n-hexane, and vortexed (MS 2, Fisher Scientific, Leicestershire, UK). The curcumin was collected in the ethanol fraction and subsequently quantified. The curcumin absorbance was measured with a V-670 spectra photometer (Jasco, Tokyo, Japan) at a 425 nm wavelength and the concentration was calculated from the calibration curve. EE (%) of the obtained emulsions was calculated by eq.(2) (Surassmo et al., 2010).

The curcumin release was measured following the method of Behbahani, Ghaedi, Abbaspour, & Rostamizadeh (2017). Aliquots of 10 mL of each sample were loaded into the dialysis bags, which were subsequently submerged in a 100 mL mixture of distilled water and ethanol (50:50), at room temperature and constant agitation (100 rpm). A 2-mL aliquot of the outer extraction medium was used to determine the curcumin concentration at 0.5, 1, 3, 5, 8, 24 and 48 h. In order to maintain the volume constant during the whole experiment, 2 mL of dissolution medium were added to replace each extracted aliquot. Samples were measured with a V-670 spectra photometer (Jasco, Tokyo, Japan) at a 425 nm wavelength. The curcumin release was calculated with eq.(5):

$$Release\ (\%) = \frac{released\ curcumin\ (mg)}{total\ amount\ of\ encapsulated\ curcumin\ (mg)} x100 \qquad \textbf{eq.(5)}$$

where the released curcumin expressed in mg is the amount of curcumin found in each sample and the total amount of encapsulated curcumin is the quantity of compound that was loaded in the emulsions according to encapsulation efficiency results, also expressed in mg.

Curcumin release curve was generated and statistically analyzed at a 5% significance level using JMP 12 Pro 12 software (Statistical Discovery™, North Carolina, USA). The output showed the results of fitting a non-linear regression model to describe the relationship between CR and t independent variables as shown in eq.(6). The R-Squared statistic (0.99) indicates that the model as fitted explains almost 100.0% of the variability in CR.

$$CR = CRmax \cdot (1 - e^{-kt}) \qquad \textbf{eq.(6)}$$

where CR is the curcumin release expressed in %, t is the time (h), CR_{max} is the maximum estimated curcumin release (%) and k is the kinetic constant (h^{-1}).

Statistics

All the experiments were assayed in duplicate, and at least three replicate analyses were carried out for each parameter. JMP Pro 12 software (Statistical Discovery™, North Carolina, USA) was used to perform the statistical analysis. Tukey-Kramer test was chosen to determine significant differences among treatments, at a 5% significance level.

Protein-polysaccharide complex formation

WPI and SBP used during the experiment were characterized in terms of ζ-potential with a Zetasizer Nano-ZS laser diffractometer (Malvern Instruments Ltd, Worcestershire, UK) and optical microscopy with an Axio Scope optical microscope (A1, Carl Zeiss Microimaging GmbH, Göttingen, Germany) over a pH range of 7 to 3, measured with a laboratory pH meter (inoLab, pH Level 1, WTW, Weilheim, Germany), in order to set the accurate conditions for associative complex formation. Initially, the single biopolymers were dissolved in distilled water with magnetic stirring overnight at room temperature to obtain two stock solutions at 2% *w/w* of biopolymer and ensure their complete hydration. Afterwards, solutions were adjusted to pH 7 with 0.1M and 1M of NaOH or HCl (Zeeb et al., 2016). Stock solutions were mixed in a WPI/SBP ratio of 1/1 and the complex formation was induced by decreasing the pH to 3 at regular intervals. Soluble complexes were obtained in a pH range 5-3.5.

Complex-stabilized nanoemulsions formation

Two stock solutions, one containing 2 % *w/w* of whey protein isolate (WPI) and the other 2 % *w/w* of sugar beet pectin (SBP), were prepared in citrate buffer (3.5 pH). Both solutions were magnetically stirred overnight to ensure complete hydration of the biopolymers at room temperature and pH was readjusted to 3.5. Afterwards, both solutions were mixed 1/1 (WPI/SBP) ratio and 20% w/w of decane was added. The different mixtures were homogenized using a high shear laboratory

blender (Standard Unit, IKA Werk GmbH, Germany) at 15.000 rpm for 2 min followed by three passes at 1,000 bar (100 MPa) through a high pressure homogenizer (LM10, Microfluidics™, Westwood, MA).

Characterization of complex-stabilized nanoemulsions

The particle size (μm) and particle size distribution of emulsions were measured using a static light scattering instrument (Horiba LA-950, Retsch Technology GmbH, Haan, Germany) periodically during 21 days of room temperature. Samples were diluted to a droplet concentration of approximately 0.005% *w/w* with citrate buffer (pH 3.5) to prevent multiple scattering effects. The instrument measured the angular dependence of the intensity of the laser beam scattered by the dilute emulsions and then used the Mie theory to calculate the droplet size distributions that gave the best fit between theoretical predictions and empirical measurements. Refractive index ratio for decane-in-water nanoemulsions was calculated with the light scattering equipment and had a value of 1.48. The particle size measurements are reported as volume frequency distributions and as the number-average droplet diameter D[4;·3]. Particle radii were calculated as the average of measurements made on at least two freshly prepared samples. Afterwards, Ostwald ripening rate can be calculated from the change in mean droplet size with time using the equation 7 according to Weiss, Herrmann, & McClements (1999):

$$r_t^3 - r_0^3 = \omega t = (8\gamma D c_\infty V_m^2 t)/(9RT) \qquad \textbf{eq.(7)}$$

where, ω is the Ostwald ripening rate, r_t is the mean number droplet radius after time t, r_0 is the initial mean number droplet radius, γ is the interfacial free energy of the oil-water interface, D is the diffusion coefficient of the solute within the aqueous phase, T is the absolute temperature, c_∞ is the molecular solubility of the solute in the aqueous phase, V_m is the molar volume of the solute, and R is the molar gas constant. In this equation it is assumed that the emulsion is diluted and that there is no influence of interfacial rheology on the ripening rate.

The ζ-potential (mV) was measured by phase-analysis light scattering (PALS) with a Zetasizer Nano-ZS laser diffractometer (Malvern Instruments Ltd, Worcestershire, UK). It determines the electrical charge at the interface of the droplets dispersed in the aqueous phase. In all the determinations, samples were prior diluted in citrate buffer (3.5 pH) using a dilution factor of 1:30 sample-to-solvent.

The accelerated creaming test was performed by centrifuging 2.5 mL aliquots of nanoemulsions, diluted to 1% in citrate buffer, using a Heraeus Centrifuge (Biofuge 28RS, Osterode, Germany). Samples were centrifuged at 2500 rpm during 1, 5, 10, 15, 30 or 50 min. Pictures of the emulsions were taken periodically with a digital camera (Canon Powershot G10, Tokyo, Japan) and the creaming index provoked by centrifugation was calculated with eq.(8):

$$\text{Creaming index (\%)} = (h_{\text{creaming (t)}} - h_{\text{creaming (t0)}})/h_{t0} * 100 \qquad \textbf{eq.(8)}$$

Rheological measurements were conducted using a rheometer MCR 502 (Anton Paar GmbH, Graz, Austria; Software: Rheoplus) and were performed with a bicone measuring geometry, where the edge of the disk is located in the interfacial region between the two immiscible liquids. The influence of the bulk and upper phase of the flow field in the bicone system is compensated in an analysis performed using the rheometer software after the measurement. An amplitude sweep was conducted with 100 measuring points in the strain range between 0.01 to 100 % (frequency f = 0.01 Hz; ϑ = 25 °C). At the beginning of each measurement, a relaxation time of 15 min was applied. Each sample was measured in duplicate, whereas the interfacial storage modulus G_i' and loss modulus G_i'' were utilized as a key parameters to determine the rheological properties of the mixtures containing WPI solution (2% *w/w*), SBP solution (2% *w/w*) or complex WPI/SBP (1/1) solution (2% *w/w*) at pH 3.5 and decane as the upper fluid.

Statistics

All the experiments were performed in duplicate, and at least three replicate analyses were carried out for each parameter. SigmaPlot 11.0 Systat Software was used to perform the analysis of variance. Tukey test was chosen to determine significant differences among the different emulsions, at a 5% significance level.

Molecular characterization of sodium alginate

Infrared spectroscopy through attenuated total reflectance (ATR) was applied to freeze-dried samples of coarse emulsions, nanoemulsions and alginate solutions in order to avoid the interferences caused by water in the –OH signal (3400-3600 cm^{-1}). After freeze-dried process with a Cryodos 50 freeze drier (Telstar Cryodos, Terrassa, Spain) working with a vacuum pressure of 0.128 mBar and a temperature of -45.6 ºC, emulsions and alginate solutions were directly measured in solid state by using an infrared spectrometer (FT-IR 6300 Jasco Series, Easton, USA) in a range of 4000-600 cm^{-1}. All tests were performed in triplicate and data were processed using SpectraManager Software (Jasco Analitica Spain S.L, Madrid, Spain).

For the performing of proton nuclear magnetic resonance (^{1}H-NMR), samples of emulsions, nanoemulsions and alginate solutions were freeze-dried using a Cryodos 50 freeze drier (Telstar Cryodos, Terrassa, Spain), weighed in a precision scale (Denver Instrument S-234, Germany) and dissolved in 7.5 mL of D_2O in order to be analyzed with a NMR spectrometer (Mercury Plus AS 400 MHz, Varian; California, USA). Data were processed with MestReNova 10.0.2 Software (Mestrelab Research, Santiago de Compostela, Spain).

Gel permeation chromatography (GPC) of the alginate solutions was used to study the breaking of alginate molecules. Microfluidized and non-microfluidized alginate solutions were prior diluted in water by a 1:1 factor and compared with different dextran solutions of 2 mg/mL acting as patterns (Sigma-Aldrich, USA).
The chromatograph (Waters Alliance 2695, Waters, Barcelona, Spain) was composed by a refraction index detector (Waters 2414, Barcelona, Spain) and a weighing scale (Mettler Toledo AT261 Delta Range, Barcelona, Spain). Chromatographic conditions consisted of an Ultrahydrogel 1000 + Ultrahydrogel 250, 300x7.8 mm column (Waters, Barcelona, Spain) using $NaNO_3$ 0.1M as eluent at

30ºC and the injection volume was 50 µl with a flux of 1.0 mL/min. Data were processed with the Empower GPC Software (Waters, Mildford, USA).

Statistics

All the procedures were assessed in duplicate, and at least three measurements of each parameter were carried out. The statistical software SigmaPlot 11.0 (Systat Software Inc., Pennsylvania, USA) was used to perform the analysis of variance. To determine differences among means of the different procedures, Tukey test (Two Way ANOVA) was run at a 5% significance level. In the case of comparing microfluidized and non-microfluidized alginate solutions, a Rank Sum test (One Way ANOVA) was run at a 5% significance level as well.

SECTION II. Designing double emulsions as carriers of hydrophilic plant-derived bioactive compounds.

Water-in-oil emulsions formation (W_1/O)

Water-in-oil emulsions (W_1/O) were prepared in a ratio aqueous phase (W_1)/lipid phase (O) of 30/70. First of all, alginate (1-2% *w/w*) was added to ultrapure water at 70ºC and stirred during 3 hours to ensure complete hydration of biopolymer. After reaching room temperature, the accurate quantity of c*hlorophyllin* (27 ppm) and NaCl (0-0.25 M) were added to the alginate solution until their dissolution. This aqueous phase was dispersed into a lipid phase containing 0-1% *w/w* Lemongrass essential oil (LG-EO) in corn oil; and Span 80 (4, 6 or 10% *w/w*) or PGPR (4, 6 or 10% *w/w*) as hydrophobic surfactants. Both phases were mixed through three different procedures: *i)* high shear homogenization with a T25 digital Ultra-Turrax (IKA, Staufen, Germany) at 11,000 or 22,000 rpm and during 1, 2, 3 or 5 min; *ii)* high shear homogenization (11,000 rpm, 5 min) followed by ultrasonication with a UP 400S Hielscher sonifier (Hielscher Ultrasound Technology, Teltow, Germany) testing amplitudes of 30, 60 or 100 µm and for 1, 3 or 5 min and *iii)* high shear homogenization (11,000 rpm, 5 min) followed by microfluidization with a microfluidizer (M110P, Microfluidics, Massachusetts, USA) at 150 MPa and 1-5 cycles to the formation of W_1/O.

Double emulsions formation (W_1/O/W_2)

After the formation of the primary W_1/O, these were dispersed in a second alginate solution (2% *w/w*) also containing NaCl (0-0.25 M) with a ratio of 1/4 (W_1O/W_2) and mixed again by a high shear homogenizer (T25 digital Ultra-Turrax, IKA, Staufen, Germany) at 5,600 rpm and during 2 min followed by magnetic stirring at 750 rpm, during 3, 5, 18 and 24h in order to obtain the W_1/O/W_2 emulsions.

Characterization of double emulsions

The emulsion droplet size was measured by the laser diffraction technique with a Mastersizer 3000^{TM} (Malvern Instruments Ltd., Worcestershire, UK). The measured droplet size was expressed as volume-weight and surface-weight diameter (d[4;3] and d[3;2] in µm. Refractive indexes (RI) of corn oil and lemongrass essential oil were 1.47 and 1.48, respectively. For the measurement of particle

sizes of W_1/O emulsions, sunflower oil, whose RI was the same as corn oil, was used as dispersant, whereas $W_1/O/W_2$ emulsions were dispersed in distilled water (RI=1.33).

A vibro-viscometer (SV-10, A&D Company, Tokyo, Japan) vibrating at 30 Hz was used to measure the viscosity (mPa·s) of 10 mL aliquots of the W_1/O and $W_1/O/W_2$ emulsions. Moreover, the viscosity of water, which was used as dispersant phase, was 0.91 mPa·s. This value was considered with regard to DLS measurements, which were all performed at 25 ± 2 ºC.

The color of W_1/O and $W_1/O/W_2$ emulsions was measured with a colorimeter (Minolta CR-400, Konica Minolta Sensing, Inc., Osaka, Japan) at room temperature set up for illuminant D65 and 10° observer angle and calibrated with a standard white plate. CIE L^*, a^* and b^* values were determined, and the whiteness index (WI) was calculated with eq.(1) (Salvia-Trujillo, Rojas-Graü, Soliva-Fortuny, & Martín-Belloso, 2013a).

The stability of the prepared W_1/O and $W_1/O/W_2$ emulsions containing CHL and/or LG-EO was performed in duplicate through a turbidity study with a Turbiscan Classic (Formulaction, Toulouse, France) during 21 days of refrigerated storage at 4ºC. The turbidity measurement allows the detection of the most common destabilization mechanisms of emulsions such as creaming, sedimentation, flocculation or coalescence by multiple light scattering.

Confocal microscopic images were Fresh double emulsions containing CHL and/or LG-EO were observed with an Olympus Spectral Confocal Microscope (Olympus FV1000, Melville, NY) with 100x oil immersion objective lens. Double emulsions were previously dyed with Nile red (Sigma Aldrich, Merk, Darmstadt, Germany), a fat-soluble fluorescent dye that was previously dissolved at 0.1% (w/v) in polyethilenglycol (Sigma Aldrich, Merk, Darmstadt, Germany) in order to capture the images. All images were taken and processed using the instrument software program (Olympus FV10-ASW viewer, Melville, NY).

Encapsulation efficiency of double emulsions ($W_1/O/W_2$) containing chlorophyllin

In order to calculate the CHL encapsulation efficiency (EE) of $W_1/O/W_2$ emulsion, aliquots of 10 mL were placed inside a centrifuge tube and 20 mL of food grade methanol were added. After centrifuging (3000 g, 10 min) with a Hettich® Universal 320 centrifuge (Sigma-Aldrich, Darmstadt, Germany) the outer aqueous phase with the non-encapsulated CHL (free CHL) was filtered through a 0.22 mm Vinylidene Polyfluoride (PVDF) syringe filter and quantified by analyzing the solvent spectrophotometrically with a V-670 spectrophotometer (Jasco, Tokyo, Japan) at 405 nm. The EE of the obtained $W_1/O/W_2$ emulsions was calculated by equation (9) (Giroux et al., 2013):

$$EE = \frac{C(W1)*X(W1) - Cs*(V+X(W2))}{C(W1)*X(W1)} \text{ x } 100 \qquad \textbf{eq.(9)}$$

where $C(w_1)$ is the initial CHL concentration in the internal aqueous phase of the emulsion (27 ppm), C_S is the CHL concentration in the subphase collected after centrifugation of the diluted emulsion, $X(W_1)$ and $X(W_2)$ are, respectively, the mass fractions of the internal (0.06) and external (0.8) aqueous phases for 1Kg (V) of emulsion. All the measurements were performed in triplicate.

Antioxidant capacity of double emulsions ($W_1/O/W_2$)

The antioxidant capacity of CHL and lemongrass essential oil (LG-EO) both solved in methanol (used as controls), as well as, CHL- and CHL/LG-EO-loaded emulsions was determined by DPPH and FRAP assays.

The DPPH procedure was conducted according to the method of Brand-Williams; Cuvelier, & Berset, (1995) with some modifications. The DPPH radical solution was prepared by dissolving 3.75 mg of DPPH radical in 100 mL of methanol. The absorbance of the solution was adjusted to a value between 0.7-0.8 ± 0.02 (measured at 515 nm). Aliquots of 10 μL of sample were placed in a microplate with 90 μL of Milli-Q water and 3900 μL of DPPH radical solution was added to each sample. Samples were incubated for 30 min in the dark and the absorbance at 405 nm was measured.

FRAP assay was carried out as described by Benzie & Strain (1996) with some modifications where 150 μL of sample were placed into each tube and mixed with 2850 μL of FRAP solution. The samples were incubated at room temperature in the dark for 30 min and the absorbance was measured at 630 nm after prior filtration.

Results were reported as mg of Trolox equivalents per mL of solution (mg TE/mL) using a standard curve of Trolox (Velderrain-Rodríguez et al., 2015). In both methods, triplicate determinations were made at each dilution of the standard.

Statistics

All the procedures were assessed in duplicate, and at least three measurements of each parameter were carried out. The statistical software SigmaPlot 11.0 (Systat Software Inc., Pennsylvania, USA) was used to perform the analysis of variance. To determine differences among means of the different procedures, Dunn's test (One Way ANOVA) was run at a 5% significance level.

SECTION III. Application of emulsion-based nanostructures to foods

Formation of edible coatings from nanoemulsions

The coating forming solutions were oil-in-water nanoemulsions containing OR-EO (1.5-2.5% w/w), Tween 80 (2.5% w/w), sodium alginate (2.0% w/w) and mandarin fiber (0.5% w/w). The aqueous phase was prepared by solving sodium alginate in ultrapure water at 70 ºC for 3 h. After reaching room temperature, mandarin fiber was added to alginate solution and mixed using a laboratory high-shear homogenizer (T25 digital Ultra-Turrax, IKA, Staufen, Germany) at 9600 rpm for 3 min. Ultimately, the aqueous phase was filtered in order to remove the fiber in excess. An accurate amount of the lipid phase consisted of the mixture of OR-EO and Tween 80 at room temperature was added to the aqueous phase, and blended with the high-shear homogenizer at 11,000 rpm for 2 min, leading to coarse emulsions. Lastly, nanoemulsions were formed passing the respective coarse emulsion through a microfluidizer (M110P, Microfluidics, Massachusetts, USA) at 150 MPa for 5 cycles.

Identical cylindrical cheese pieces (diameter: 1.5 cm, height: 2.4 cm) were immersed into the corresponding nanoemulsion for 1 min, and allowed to dry at room temperature for 5 min. The

addition of $CaCl_2$, which acts as cross-linker, was not needed since cheese contains calcium itself. A quantity of 50 g of coated cut cheese were packed polypropylene (PP) trays (ATS packaging, Barcelona, Spain) of 170 mm length x 25 mm height x 110 mm width, using a tray sealer (Basic V/G, Ilpra systems, Barcelona, Spain). Afterwards a cover film made of polyamide and polyethylene (Tecnopack, Girona, Spain) was used to heat seal the trays. Lastly, sealed trays were stored at 4 ºC during 15 days. Separate trays were prepared with cheese pieces inoculated with Staphylococcus aureus to evaluate the antimicrobial effect of the coating and to assess the changes in quality attributes along 24 days of refrigerated storage. Two trays of each set were prepared, and two replicates for each sealed package were performed.

Physical characterization of edible coatings

Water vapor resistance (WVR) of cheese pieces was evaluated gravimetrically at 25 ºC using a modified version of ASTM standard method E96-00 (ASTM, 2000). The method and experimental set up following to determine the water loss of coated cheese pieces was described by García, Jergel, Conde-Gallardo, Falcony, and Plesch (1998). Cheese cylinders were placed in small test cups (internal diameter of 2.7 cm and depth of 1.3 cm) and weighed in an analytical laboratory scale (AT261 Delta Range, Mettler Toledo, Barcelona, Spain). Initial weights of coated cheese pieces were 8.3 ± 0.12 g, 8.4 ± 0.23 g and 8.5 ± 0.20 g for coatings with 1.5% OR-EO, 2.0% OR-EO and 2.5% OR-EO, respectively and 7.8 ± 0.14 g for those uncoated. Cheese cylinders were placed in sealed chambers that were equilibrated at 33% RH with a saturated MgCl2·6H2O solution (Panreac Quimica SA, Barcelona, Spain) at 25 ºC. Cups weights were recorded at 60 min intervals during 6 h. Weight loss was calculated by difference using eq.(10) and plotted versus time. Data were analyzed by lineal regression to obtain the slope (ds/dt) of the curve in g/s. Water activity (a_w) of the coated and uncoated cheese pieces (0.974 ± 0.001 and 0.947 ± 0.001, respectively) was measured twice for each sample with a water activity meter (Acqualab CX-2, Decagon Devices Inc., Pullman, WA).

$$WL = W_i - W_f \qquad \textbf{eq.(10)}$$

where WL is the weight loss of cheese pieces (in mg); W_i and W_f, are initial and final weights (mg) of cheese pieces. Afterwards, WVR of the coatings was calculated using a modified Fick's first law equation as described in eq.(11) and (13) (Ben-Yehoshua et al. 1985; Kaya and Kaya 2000; Rojas-Graü et al. 2007; Rojas-Graü et al. 2007):

$$\Delta C = (P_i - P_a)/(R_c \cdot T) \qquad \textbf{eq.(11)}$$

$$A = \pi \cdot r \cdot (2 \cdot h + r) \qquad \textbf{eq.(12)}$$

$$WVR = (A \cdot \Delta C)/(d_s/d_t) \qquad \textbf{eq.(13)}$$

where P_i - P_a is the difference in water vapor pressure (Pa) inside and outside of the cheese piece ($P_i = a_w$ of the cheese x P_0). P_0 is the vapor pressure (Pa) of liquid water at 25ºC and P_a = partial water pressure in the environment (with 33.3% RH at 25ºC) x P_0, expressed in Pa; ΔC is the concentration of gas (g/cm^3) inside and outside the cheese piece at time t; A is the exposed area of cylindrical cheese pieces (5.65 cm^2) taking into account that only one of the bases was in contact with the environment; (d_s/d_t) is the rate of gas exchange (slope) in g/s; Rc is the universal gas constant (3.46 L·mmHg/K g) and T is the temperature in degrees Kelvin.

The composition of the headspace of each tray was analyzed with a gas chromatograph (Varian 490-CG) equipped with a thermal conductivity detector (Micro-GC CP 2002 gas analyzer, Chromatography Systems, Middelburg, The Netherlands). A 10 mL sample was automatically withdrawn from the tray headspace atmosphere and injected in the gas chromatograph. The oxygen (O_2) content expressed in percentage was analyzed with a 10 m packed column (CP-Molsieve 5Å, Varian, Middelburg, The Netherlands) at 60 ºC and 100 kPa. For quantification of carbon dioxide (CO_2) expressed in percentage, and ethanol (C_2H_5OH) concentration reported in ppm, a column PoraPLOT Q (Varian, Middelburg, The Netherlands) (10 m x 0.32mm, df = 10 mm) held at 70 ºC and 200 kPa was used.

The color of coated and uncoated cheese pieces was measured with a colorimeter (CR-400, Konica Minolta Sensing Inc., Osaka, Japan) set up for illuminant D65 and 10º observer angle and calibrated with a standard white plate. Measurements were taken at room temperature. CIE *L**, *a** and *b** values were determined and the Whiteness Index (WI) was calculated through eq. (1).

TPA of cheese pieces was carried out using a texture analyzer (TA-TX2, Stable Micro Systems, Goldaming, UK) equipped with a 5 kg load cell and the 36R probe, operating with two compression-decompression cycles and 2 $mm \cdot s^{-1}$ of crosshead speed (Diamantino et al., 2014). The hardness, cohesiveness, gumminess, elasticity, adhesiveness and chewiness of the cylindrical cheese pieces were calculated according to Szczesniak (2002). Eight replicates of each tray were performed at each sampling time.

Antimicrobial capacity of edible coatings against Staphylococcus aureus

A strain of *Staphylococcus aureus* (CECT 240) (University of Valencia, Spain) was provided by the culture collection of the Department of Food Technology, University of Lleida, Spain. The *Staphylococcus aureus* culture was kept in slant tubes with Tryptone Soy Agar (TSA) (Biokar Diagnostics, France) at 5 ºC. The strain was then inoculated in Tryptone Soy Broth (TSB) (Biokar Diagnostics, France) and incubated at 35 ºC, 200 rpm for 6 h, to obtain cells in stationary growth phase. The inoculum concentration was diluted from 10^8 CFU/mL to 10^6 CFU/mL for cheese inoculation. Cheese pieces (10 g) were inoculated with 50 µL aliquots of the culture and left dry for 20 min. Cheese pieces were coated with nanoemulsions that contained OR-EO, packed in heat sealed PP trays and stored at 4ºC for 15 days. In order to corroborate that no one of the other components of edible coating had also antimicrobial activity, nanoemulsions containing corn oil instead of OR-EO in the same concentrations were prepared and applied onto cheese pieces. The content of each tray (10 g) was put into a sterile stomacher bag (Strainer bag stomacher® lab system, Seward, UK) with 90 mL of buffer peptone (Biokar Diagnostics, France). Bags were homogenized for 1 min in a Stomacher blender (BagMixer®, Interscience, France). Serial dilutions with saline peptone (Peptic Digest of meat USP, Biokar, Diagnostics, France) were prepared and spread onto Baird-Parker agar (BP) (Biokar Diagnostics, France). Plates were incubated at 37 ºC for 48 h and colonies were counted. Results were expressed as $\log_{10}$ CFU/g. Psychrophilic bacteria and molds and yeasts growth in cheese pieces was examined along 24 days under refrigeration. Cheese samples of 10 grams randomly chosen in aseptic conditions were put into sterile bags with 90 mL of peptone buffer (Biokar Diagnostics, France). Bags were homogenized for 1 min in a Stomacher blender (BagMixer®, Interscience, France). Serial dilutions with saline peptone (Peptic Digest of meat USP, Biokar, Diagnostics, France) were prepared, and 100 µL were spread onto Plate Count Agar (PCA) (Biokar Diagnostics, France) and Cloranfenicol Glucosa Agar (CGA) (Biokar Diagnostics, France) for psychrophilic bacteria and molds and yeast

counts, respectively. PCA plates were incubated at 4 ºC for 15 days, whereas CGA plates were maintained at room temperature during 5 days. Afterwards, colonies were counted and the results were expressed as $\log_{10}$ CFU/g.

Statistics

All the experiments were assayed in duplicate, and at least three replicate analyses were carried out for each parameter. SigmaPlot 11.0 Systat Software was used to perform the analysis of variance. Tukey test was chosen to determine significant differences among treatments, at a 5% significance level.

Correlation analyses were performed with statistical analysis software (JMP Pro 12, Statistical Discovery™, North Carolina, USA).

References

Behbahani, E. S., Ghaedi, M., Abbaspour, M., & Rostamizadeh, K. (2017). Optimization and characterization of ultrasound assisted preparation of curcumin-loaded solid lipid nanoparticles: Application of central composite design, thermal analysis and X-ray diffraction techniques. *Ultrasonics Sonochemistry*, *38*, 271–280.

Ben-Yehoshua, S., Burg, S. P., & Young, R. (1985). Resistance of citrus fruit to mass transport of water vapor and other gases. *Plant Physiology*, *79*(4), 1048–1053.

Benzie, I. F. F., & Strain, J. J. (1996). The Ferric Reducing Ability of Plasma (FRAP) as a Measure of "Antioxidant Power": The FRAP Assay. *Analytical Biochemistry*, *239*(1), 70–76.

Brand-Williams, W.; Cuvelier, M. E.; Berset, C. (1995). Use of a free radical method to evaluate antioxidant activity. *Lebensmittel Wissenschaft Und Technologie*, *30*, 25–30.

Diamantino, V. R., Beraldo, F. A., Sunakozawa, T. N., & Penna, A. L. B. (2014). Effect of octenyl succinylated waxy starch as a fat mimetic on texture, microstructure and physicochemical properties of Minas fresh cheese. *LWT - Food Science and Technology*, *56*(2), 356–362.

Giroux, H. J., Constantineau, S., Fustier, P., Champagne, C. P., St-Gelais, D., Lacroix, M., & Britten, M. (2013). Cheese fortification using water-in-oil-in-water double emulsions as carrier for water soluble nutrients. *International Dairy Journal*, *29*(2), 107–114.

Kaya, S., & Kaya, A. (2000). Microwave drying effects on properties of whey protein isolate edible films. *Journal of Food Engineering*, *43*(2), 91–96.

Lin, C., Zhang, X., Chen, H., Bian, Z., Zhang, G., Riaz, M. K., … Yang, Z. (2018). Dual-ligand modified liposomes provide effective local targeted delivery of lung-cancer drug by antibody and tumor lineage-homing cell-penetrating peptide. *Drug Delivery*, *25*(1), 256–266.

Rojas-Graü, M. A., Avena-Bustillos, R. J., Olsen, C., Friedman, M., Henika, P. R., Martín-Belloso, O., … McHugh, T. H. (2007). Effects of plant essential oils and oil compounds on mechanical, barrier and antimicrobial properties of alginate–apple puree edible films. *Journal of Food Engineering*, *81*(3), 634–641.

Rojas-Graü, M. a., Tapia, M. S., Rodríguez, F. J., Carmona, a. J., & Martin-Belloso, O. (2007). Alginate and gellan-based edible coatings as carriers of antibrowning agents applied on fresh-cut Fuji apples. *Food Hydrocolloids*, *21*(1), 118–127.

Salvia-Trujillo, L., Rojas-Graü, A., Soliva-Fortuny, R., & Martín-Belloso, O. (2013). Physicochemical Characterization of Lemongrass Essential Oil-Alginate Nanoemulsions: Effect of Ultrasound Processing Parameters. *Food and Bioprocess Technology*, *6*(9).

Salvia-Trujillo, L., Rojas-Graü, A., Soliva-Fortuny, R., & Martín-Belloso, O. (2014). Food Hydrocolloids Physicochemical characterization and antimicrobial activity of food- grade emulsions and nanoemulsions incorporating essential oils. *Food Hydrocolloids*, *43*, 1–10.

Surassmo, S., Min, S. G., Bejrapha, P., & Choi, M. J. (2010). Effects of surfactants on the physical properties of capsicum oleoresin-loaded nanocapsules formulated through the emulsion-diffusion method. *Food Research International*, *43*(1), 8–17.

Szczesniak, A. S. (2002). Texture is a sensory property, *13*, 215–225.

Thaipong, K., Boonprakob, U., Crosby, K., Cisneros-Zevallos, L., & Hawkins Byrne, D. (2006). Comparison of ABTS, DPPH, FRAP, and ORAC assays for estimating antioxidant activity from guava fruit extracts. *Journal of Food Composition and Analysis*, *19*(6–7), 669–675.

Velderrain-Rodríguez, G. R., Ovando-Martínez, M., Villegas-Ochoa, M., Ayala-Zavala, J. F., Wall-Medrano, A., Álvarez-Parrilla, E., … González-Aguilar, G. A. (2015). Antioxidant Capacity and Bioaccessibility of Synergic Mango (cv. Ataulfo) Peel Phenolic Compounds in Edible Coatings Applied to Fresh-Cut Papaya. *Food and Nutrition Sciences*, *6*(6), 365–373.

Weiss, J., Herrmann, N., & McClements, D. J. (1999). Ostwald ripening of hydrocarbon emulsion droplets in surfactant solutions. *Langmuir*, *15*(20), 6652–6657.

Zeeb, B., Stenger, C., Hinrichs, J., & Weiss, J. (2016). Formation of concentrated particles composed of oppositely charged biopolymers for food applications - impact of processing conditions. *Food Structure*, *10*, 10–20.

Publications

SECTION I. Designing nanoemulsions as carriers of lipophilic plant-derived bioactive compounds

CHAPTER I: *Influence of essential oils and pectin on nanoemulsion formulation: a ternary phase experimental approach*

Artiga-Artigas, M.; Guerra-Rosas, M.I.; Morales-Castro, J., Salvia-Trujillo, L.; Martín-Belloso, O.

Food Hydrocolloids (2018); 81: 209-219

Abstract

A pseudo-ternary phase experimental approach was used to model the influence of the mixture components concentration on the nanoemulsions properties as ternary systems. For this, several types of essential oils (EO) were used as lipid phase, being oregano (OR-EO), thyme (TH-EO), lemongrass (LG-EO) and mandarin (MN-EO), while pectin and Tween 80 were studied as emulsifiers. All formulations were processed by microfluidization at 150MPa and 5 cycles. Polynomial models were fitted to experimental data and their adjusted R^2 and p-values were obtained. Remarkably, a pectin concentration of 1 % (*w/w*) allowed the formation of submicron emulsions between 350 and 850 nm in the absence of Tween 80 for all the studied EOs, thus confirming its emulsification capacity. In general, increasing the pectin concentration up to 2 % (*w/w*) enlarged the particle size of emulsions and their viscosity thus suggesting decreased emulsification efficiency during microfluidization. Nonetheless, nanoemulsions with particle sizes below 500 nm were obtained when a minimum Tween 80 concentration of 1.8% (*w/w*) was used, regardless the pectin or EO concentrations. The modest decrease in the ζ-potential that was observed depending on the type of EO at increasing pectin concentrations indicated that pectin is not or weakly adsorbed at the oil-water interface. All nanoemulsions were transparent at high concentrations of surfactant and low EO concentrations due to a weak light scattering of the nano-sized oil droplets. Thus, this work contributes in elucidating the role of pectin and small molecule non-ionic surfactants on the formation of submicron emulsions and nanoemulsions containing essential oils.

Keywords: Nanoemulsions, essentials oils, droplet size, ζ-potential, pseudo-ternary phase diagram.

1. Introduction

Essential oils (EOs) are natural compounds that contain a complex mixture of terpenoids, with non-volatile and volatile nature produced by aromatic plants as secondary metabolites (Fisher & Phillips, 2008; Salvia-Trujillo, Rojas-Graü, Soliva-Fortuny, & Martín-Belloso, 2014). EOs have been traditionally used as natural flavorings and more recently as natural antimicrobials for food preservation (Guerra-Rosas et al., 2016). Due to their lipophilic nature, they are able to interact with biological membranes of microbial cells causing the leakage of cytoplasmatic content and the subsequent cell collapse (Burt, 2004; Guerra-Rosas et al., 2016). Besides the benefits of adding EOs to food matrices, their poor water solubility, their intense aroma or their potential toxicity at high concentrations needs consideration (Svoboda, Brooker, & Zrustova, 2006). Therefore, the design of adequate delivery systems able to encapsulate, protect and release lipophilic bioactive compounds into food matrices more efficiently represents a challenge for the food technology field.

Recently, nanoemulsions have been described as colloidal dispersions of oil droplets with particle size diameters lower than 500 nm, which are suspended within an aqueous phase (Otoni, Avena-Bustillos, Olsen, Bilbao-Sáinz, & McHugh, 2016). Nanoemulsions seem to be a promising tool for incorporating antimicrobial EOs in foods and they have been reported to present several potential advantages in comparison with conventional emulsions. Nanoemulsions present a higher active surface area/volume ratio due to their small droplet size, thus enhancing the transport of active compounds through biological membranes. Therefore, the use of nanoemulsions as carriers of antimicrobial essential oils would allow reducing the concentration to be used in order to achieve equivalent microbial inactivation levels of those of conventional emulsions or bulk oils. This, would help overcoming the low threshold values of essential oil incorporation for consumer acceptance (McClements, 2012; Salvia-Trujillo et al., 2014a; Solans, Izquierdo, Nolla, Azemar, & Garcia-Celma, 2005).

The fabrication of nanoemulsions requires the use of surfactants in order to stabilize the oil droplets in the aqueous phase. Surfactants are able to adsorb at the oil-water interface thus lowering the interfacial tension of oil in water, which facilitates the emulsification process and prevents different destabilization phenomena such as aggregation, flocculation or coalescence (Kralova & Sjöblom, 2009). In addition, natural biopolymers are gaining importance for their use as emulsifiers and thickening agents. The increase in viscosity of the aqueous phase prevents the destabilization of emulsions and nanoemulsions due to a diminished gravitational movement of oil droplets, which may retard or avoid droplets coalescence (Guerra-Rosas et al., 2016). However, some biopolymers may also present surface active properties thus having emulsifying capacity. For instance, pectin is a natural biopolymer mainly present in fruits and vegetables that has shown certain adsorption capacity at oil-water interfaces and may enhance the stability of emulsions (Alba & Kontogiorgos, 2017; Chan et al., 2017; Ozturk & McClements, 2016). The lipid fraction also plays an important role in the physicochemical properties, which depend on the characteristics of the different EOs including their chemical composition and the hydrocarbon chain length (Hopkins, Chang, Lam, & Nickerson, 2015). In fact, it is reported that short chain fatty acids, such as EOs, are prone to destabilization phenomena due to Oswald ripening effect since they consist on an aromatic carbon ring, which makes them slightly water-soluble oils (Suriyarak & Weiss, 2014). In this context, differences between nanoemulsion stability incorporating different EOs may be rather affected by their chemical composition (Salvia-Trujillo, Rojas-Graü, Soliva-Fortuny, & Martín-Belloso, 2015a).

The selection of the appropriate concentration of each individual ingredient in the formulation of nanoemulsions is of crucial importance in order to obtain systems with the desired physicochemical characteristics (Salvia-Trujillo, Rojas-Graü, Soliva-Fortuny, & Martín-Belloso, 2014b). Building conventional pseudo-ternary phase diagrams has been explored as a strategy to optimize the formulation of multi-component emulsions. However, determining the region where nanoemulsions are formed requires performing a large number of experimental combinations and formulations. Oppositely, the ternary phase experimental design, and specifically D-optimal models, is a methodology which allows to evaluate the effect of multiple factors, alone or in combination, with a minimum number of experiments (Ramsey, 1997; Salvia-Trujillo et al., 2014b). Consequently, the combination of pseudo-ternary phase diagrams and response surface methodologies can improve the understanding of the influence of the emulsion components concentration and their interactions as well as predicting optimized multi-component formulations with controlled physicochemical and functional properties (Ren, Mu, Alchaer, Chtatou, & Müllertz, 2013). To the best of our knowledge, there is a lack of research works using this strategy for the formulation of nanoemulsions containing several emulsifying agents, such as Tweens and pectin. This would allow to fully map the behavior of the different components and their interactions on nanoemulsion characteristics.

Thus, the aim of this work was to study the influence of four different essential oils (EOs) such as oregano (OR-EO), thyme (TH-EO), lemongrass (LG-EO) and mandarin (MN-EO) essential oils on the properties (oil droplet size, ζ-potential, viscosity and whiteness index) of nanoemulsions. Moreover, the use of a small molecule surfactant (Tween 80) and a natural biopolymer (pectin) were studied as emulsifiers.

2. Material and Methods

2.1. Materials

Oregano (Origanum compactum), thyme (Thymus vulgare) and lemongrass (Cymbopogon citratus) essential oils (EOs) were purchased from Essential'aroms® (Dietetica Intersa, Lleida, Spain) and had a 100% purity. Oregano EO was composed of 26-45% carvacrol, 9-30% thymol, 9-26% p-cymene, 12-20% γ-terpinene and traces of α-terpinene and β-mircene. Thyme EO mainly contained thymol (30-47%) and p-cymene (15-35%) with traces of carvacrol and linalool. Lemongrass had 39-47.1% of geranial, 28.9-35.7% of neral, 0.5-8.3% of limonene, 0.9-6.9% of geranyl acetate, 0-5.3% of geraniol and traces of citronelol, eugenol and linalool among others. Mandarin EO (Citrus reticulata) 100% pure, was kindly donated by Indulleida, S.A. (Lleida, Spain) and contained 74.4% of D-limonene, a 13.6% of oxygenated monoterpenes and traces of cis-oxide limonene, cis-para-mentha-2,8-dien-1-ol, carvone, trans-carveol and and z-patchenol (>1%). Food-grade high methoxyl pectin (Unipectine QC100 from citrus source) with a degree of methylesterification (DM) from 69 to 75% and a particle size of the dry powder at least 99% less than 315 μm (ASTM Screen N°45) was kindly provided by Cargill Inc. (Reus, Spain). Tween 80 (Polyoxyethylenesorbitan Monoesterate) (Lab Scharlab, Barcelona, Spain) was used as food-grade non-ionic surfactant. Ultrapure water, obtained from Millipore Milli-Q filtration system (0.22μm) was used for the formulation and analysis of nanoemulsions.

2.2. Pseudo-Ternary Phase Experimental Design

An experimental mixture design, specifically a D-optimal design, was used to study the influence of the essential oil (EO), Tween 80 and pectin concentrations on the oil droplet diameter (nm), ζ-potential (mV), viscosity (mPa·s) and color of emulsions. For the experimental design, the software Design Expert 7.0.0 (Stat Ease Inc., Minneapolis, MN) was used. Posteriorly, pseudo-ternary phase diagrams were built in order to predict and identify the regions where stable nanoemulsions are formed. Firstly, for the experimental design setup, the concentration of each component was set according to the following constraints expressed as weight fraction in the aqueous phase (% *w/w*): $0.12 \leq EO \leq 1$ in case of OR-EO and TH-EO but $0.1 \leq EO \leq 2$ for LG-EO and $0.05 \leq EO \leq 3$ in case of MN-EO; $0 \leq$ Tween 80 ≤ 6, $1 \leq$ pectin ≤ 2 and for all the cases: EO + Tween 80 + pectin +water = 1. The minimum concentration of EO was set above its minimum inhibitory concentration against the most common pathogenic microorganisms that proliferate in foods such as *Escherichia coli, Listeria monocytogenes or Staphylococcus aureus* (Burt, 2004; Hammer, Carson, & Riley, 1999), whereas the maximum concentration was set regarding the toxicity of EOs at high concentrations (Svoboda et al., 2006). Tween 80 concentration was set to reach a maximum oil:surfactant ratio of 1:3 (expressed in weight), which ensures that enough surfactant molecules are available to be adsorbed at the oil-water interface (Qian & McClements, 2011; Salvia-Trujillo et al., 2014b). Pectin is generally recognized as safe (GRAS) thus its only limitation regarding its addition to nanoemulsions is the increase of viscosity of the mixtures in order to pass through the microfluidizer (Laurent & Boulenguer, 2003).

After running the statistical software, a series of mixture combinations were generated as an output of the D-optimal design. All oil-in-water emulsions were prepared in random order and analyzed the same day of preparation without further storage. Three replicate analyses of each formulation and physicochemical parameter were performed, and the mean value with its

corresponding standard deviation was calculated and used for modeling. The empirical data of the experimental designs related with high methoxyl pectin, Tween 80 and EOs – oregano (OR-EO), thyme (TH-EO), lemongrass (LG-EO) and mandarin (MN-EO)- are shown in the supplementary material (Tables 2, 3, 4 and 5). Afterwards, experimental data were represented graphically with pseudo-ternary phase diagrams and modeled with a Scheffe polynomial equation (Eq. 1) for the four components – EO, Tween 80, Pectin and water- in each formulation. Nevertheless, in some cases data did not follow a normal distribution and a power transformation recommended by de Box-Cox method was needed to stabilize variance and improve the validity of measures of association between variables (Table 1). A power transform is a family of functions that are applied to ensure the usual assumptions for linear model hold (P. Li, 2005). The statistical significance of the models for each response was evaluated regarding their adjusted R^2 and p-values that were obtained through the ANOVA analysis.

$$Y = \sum\beta_i A+\sum\sum \beta_{ij} AB+\sum\sum\sum \beta_{ijk} ABC+\sum\sum\sum\sum \beta_{ijkl} ABCD \qquad \textbf{eq.(1)}$$

where Y is the response variable, i, j and k are the number of ingredients in the mixture, β_i is the first-order coefficient, β_{ij} is the second-order coefficient, β_{ijk} is the third-order coefficient, $\beta_{ijkl}$is the fourth-order coefficient…; A,B, C and D are the corresponding EO, Tween 80, pectin and water concentrations, respectively.

Contour plots obtained from the ternary phase diagrams were generated by setting the concentration of water at 0.98 (Figures 1, 3, 4 and 5). However, for contour plots of particle size, water content was also fixed at 0.94 to highlight the regions where smallest particle sizes values were found (Figure 2).

Table 1. Coded polynomial equation coefficients: A essential oil, B Tween 80, C pectin and D water; of the Scheffe model for L-pseudo-components and statistical significance of droplet diameter (nm), ζ –potential (mV), viscosity (mPa·s) and whiteness index.

Mean Droplet diameter	**A**	**B**	**C**	**D**	**AB**	**AC**	**AD**	**BC**	**BD**	**CD**	**ABC**	**ABD**	**ACD**	**BCD**	**R^2**	**p-value**
Oregano	1317.37	317.93	11054.58	537.70	9784.96	$2.97 \cdot 10^5$	-1040.29	-13580.21	-646.58	-11532.48	$-4.66 \cdot 10^5$	-29870.35	$-3.72 \cdot 10^5$	15963.93	0.98895	0.0123
Thyme	-598.90	-6.95	2215.25	532.81	-	-	-	-	-	-	-	-	-	-	0.6184	0.0053
Lemongrass	-2548.84	548.13	-11501.86	510.02	371.28	31677.86	5365.65	11692.84	-1239.98	13109.77	-	-	-	-	0.9714	0.0057
Mandarin (log_{10})*	18.91	3.37	-42.66	2.75	-30.12	22.50	-20.44	51.55	-4.80	52.00	-	-	-	-	0.9435	0.0089
ζ -potential	A	B	C	D	AB	AC	AD	BC	BD	CD	ABC	ABD	ACD	BCD	R^2	p-value
Oregano	43.71	-8.05	-18.72	-15.38	-	-	-	-	-	-	-	-	-	-	0.7645	0.0002
Thyme	27.34	-14.69	4.19	-16.36	-	-	-	-	-	-	-	-	-	-	0.4985	0.0257
Lemongrass	-72.70	-3.50	-460.82	-13.62	39.27	783.87	121.35	469.41	-22.43	470.55	-	-	-	-	0.8952	0.0459
Mandarin	5.57	-12.22	-12.27	-11.18	-	-	-	-	-	-	-	-	-	-	0.4689	0.0364
Viscosity	A	B	C	D	AB	AC	AD	BC	BD	CD	ABC	ABD	ACD	BCD	R^2	p-value
Oregano (log_{10})*	1.59	1.37	8.46	1.12	-	-	-	-	-	-	-	-	-	-	0.9805	< 0.0001
Thyme	333.65	28.52	8813.87	24.33	-229.23	-9788.36	-467.55	-8601.44	-41.96	-8873.03	-	-	-	-	0.9926	< 0.0001
Lemongrass	-329.92	8.82	7751.40	13.24	423.89	-6681.54	440.31	-7423.38	28.59	-7813.82	-	-	-	-	0.9973	0.0003
Mandarin	326.02	-3.25	8906.58	13.66	-369.29	-9011.88	-360.27	-8509.85	71.63	-9025.94					0.9939	0.0031
Whiteness index	A	B	C	D	AB	AC	AD	BC	BD	CD	ABC	ABD	ACD	BCD	R^2	p-value
Oregano	1153.49	36.82	-937.01	33.111	-1440.65	560.80	-868.00	1065.83	-50.96	1092.75	-	-	-	-	0.9777	0.0009
Thyme	484.29	60.26	-1128.68	37.005	-819.41	2001.38	-246.52	1144.33	-102.39	1326.46	-	-	-	-	0.9315	0.0026
Lemongrass	-258.32	67.42	-2007.32	37.067	122.63	3504.76	582.78	2092.66	-131.97	2211.07	-	-	-	-	0.9531	0.0015
Mandarin	334.22	69.14	144.34	53.88	-537.67	-247.98	-269.28	-297.99	-149.81	-56.90	-	-	-	-	0.9580	0.0138

***Required log_{10} transformation recommended by the Box-Cox method.**

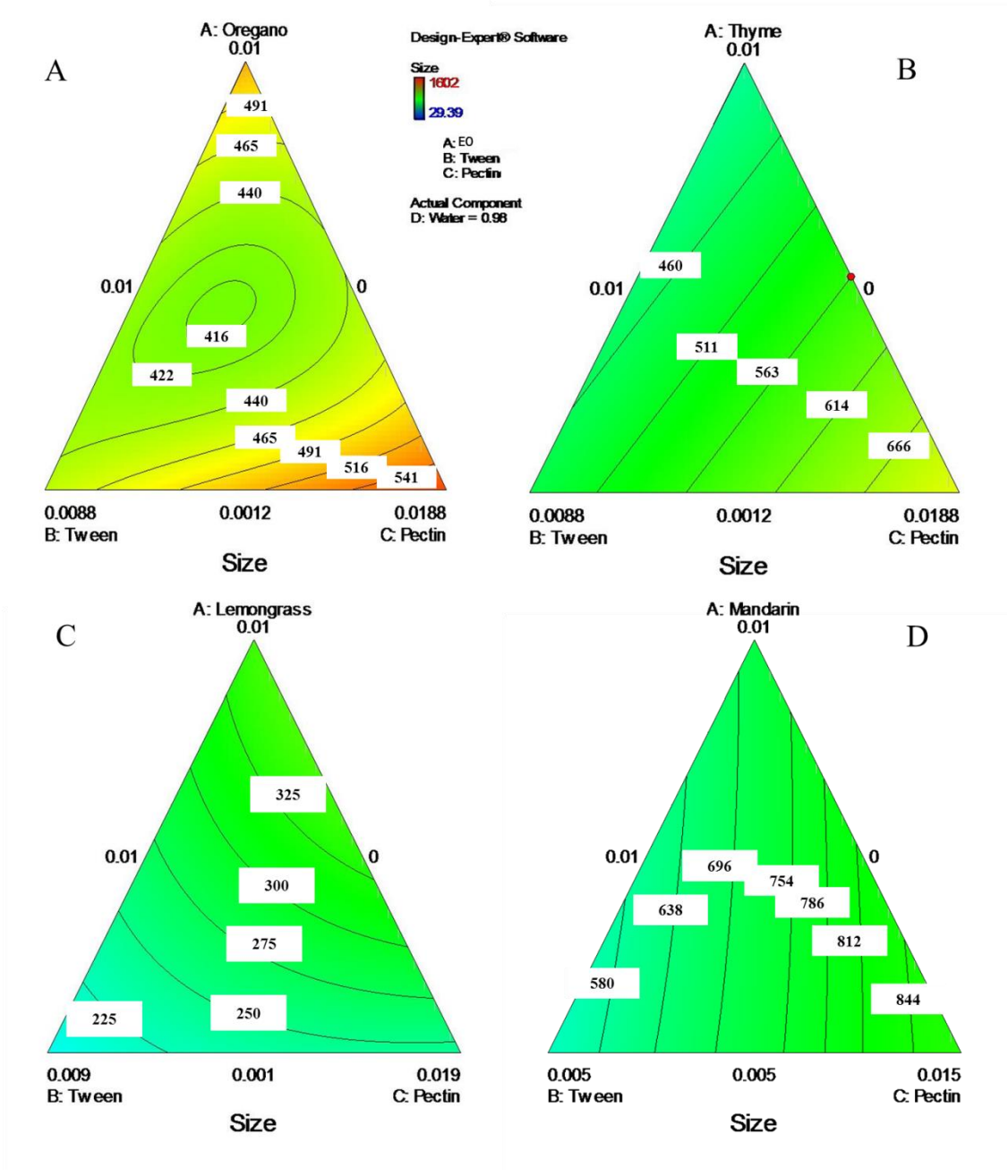

Figure 1 Contour plots of average droplet diameter (nm) of mixtures containing four different EOs: oregano oil (A), thyme oil (B), lemongrass (C) and mandarin oil (D), Tween 80 as surfactant and pectin. In the contour plots the water content was set at 0.98.

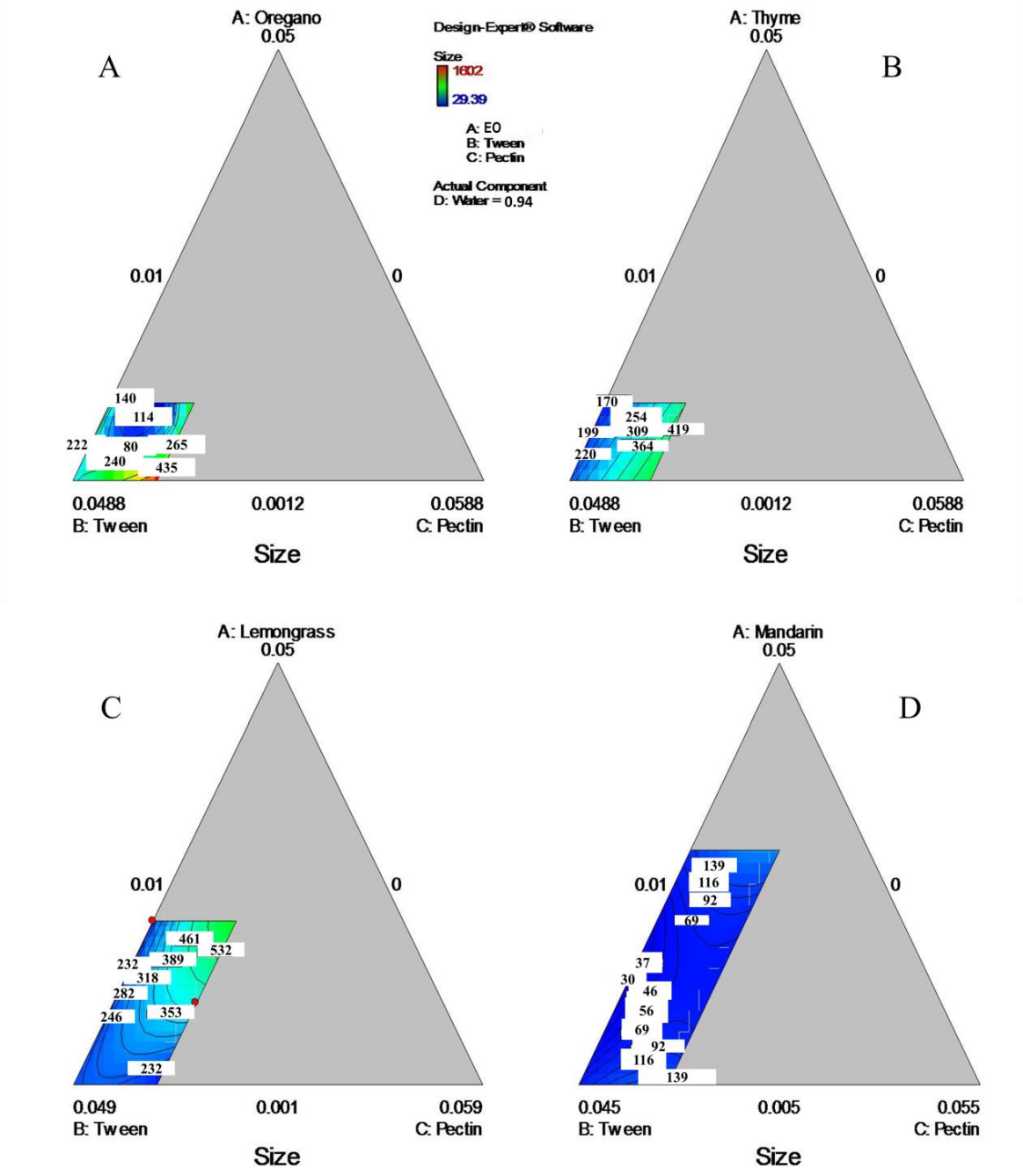

Figure 2. Enlargements of the contour plots of average droplet diameter (nm) of mixtures containing four different EOs: oregano oil (A), thyme oil (B), lemongrass (C) and mandarin oil (D), Tween 80 as surfactant and pectin. In the contour plots the water content was set at 0.94.

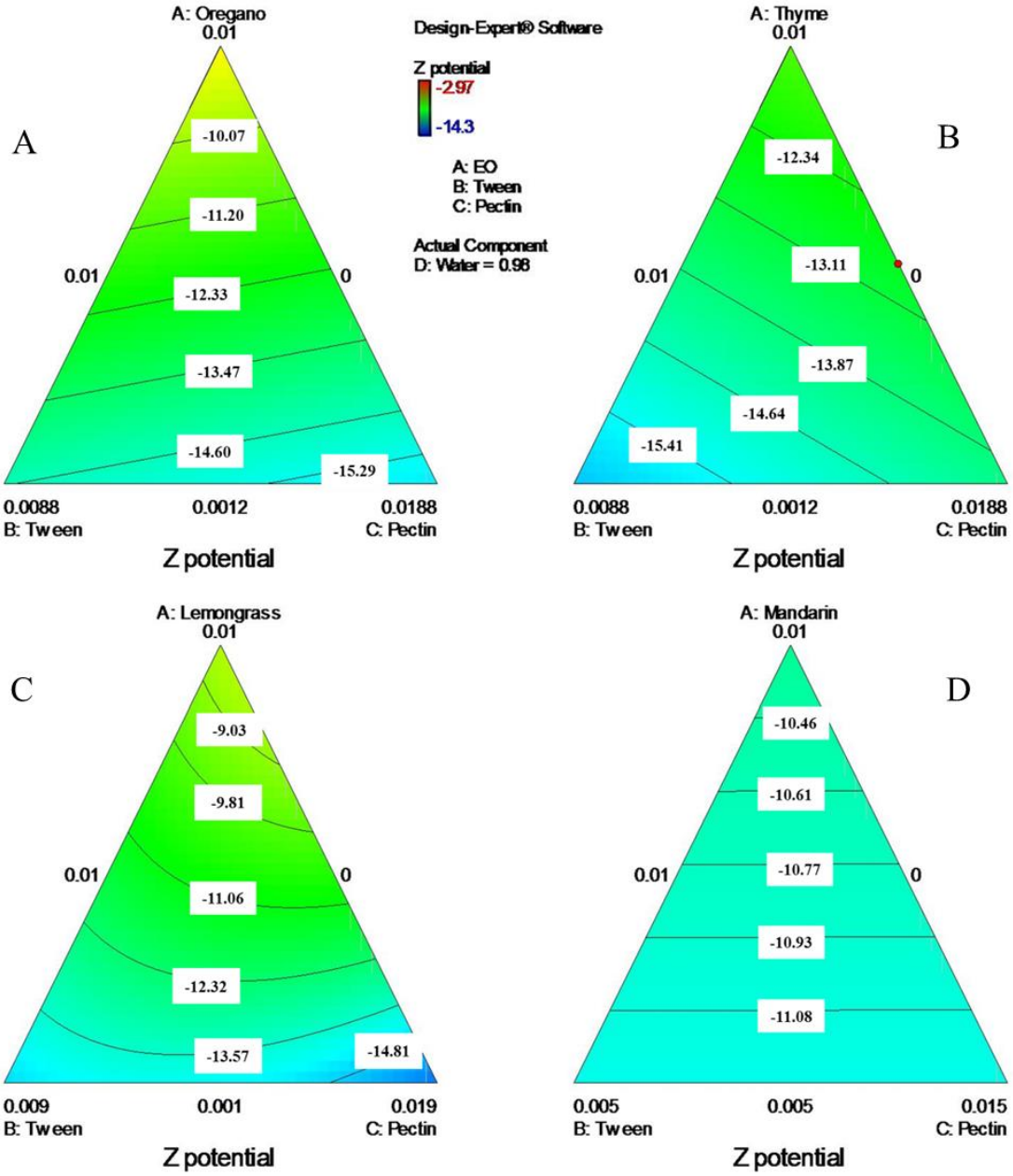

Figure 3. Contour plots of ζ -potential (mV) of mixtures containing four different EOs: oregano oil (A), thyme oil (B), lemongrass (C) and mandarin oil (D), tween 80 as a surfactant and pectin. The water content was set at 0.98.

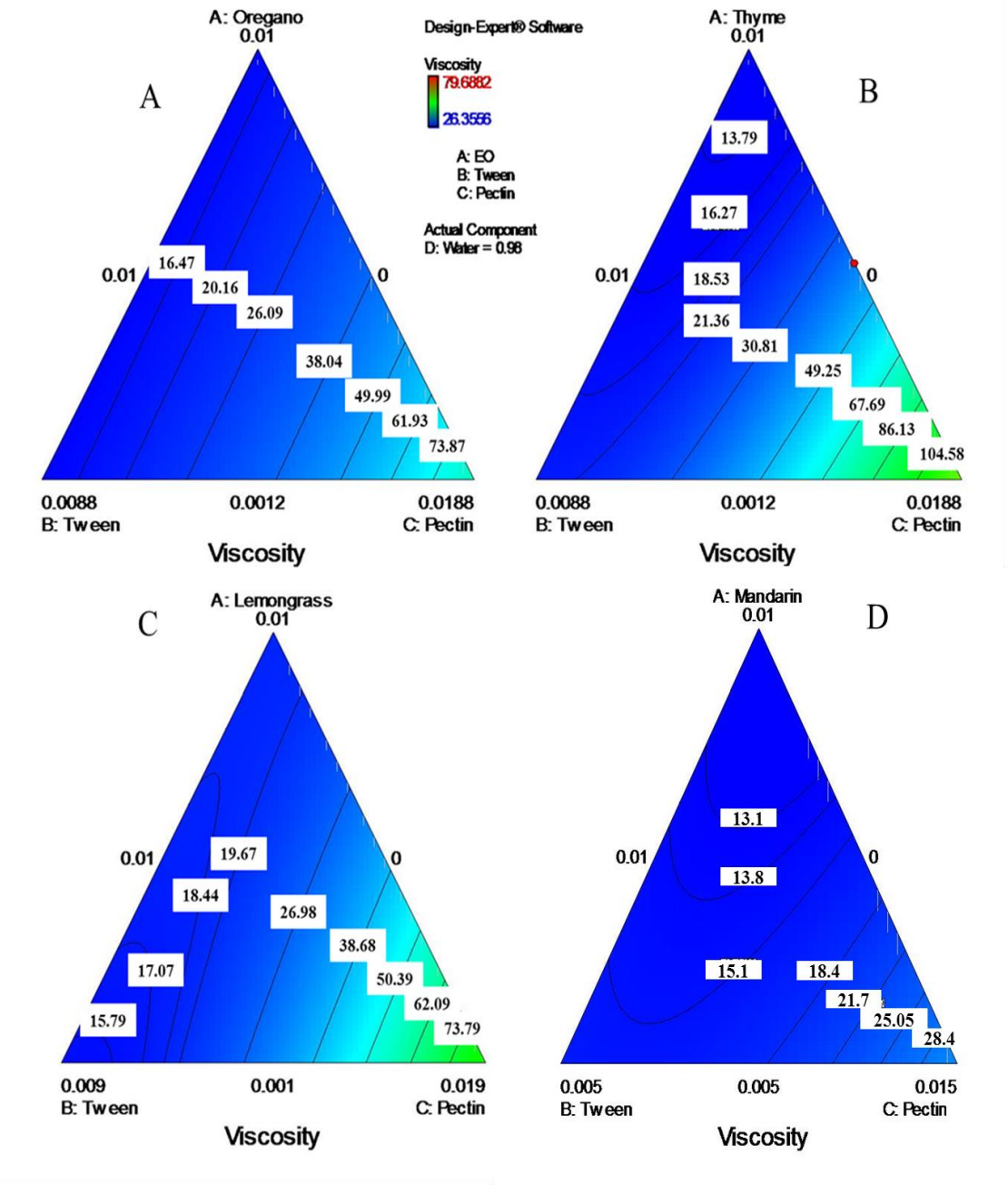

Figure 4. Contour plots of viscosity (mPa·s) of mixtures containing four different EOs: oregano oil (A), thyme oil (B), lemongrass (C) and mandarin oil (D), tween 80 as surfactant and pectin. The water content was set at 0.98.

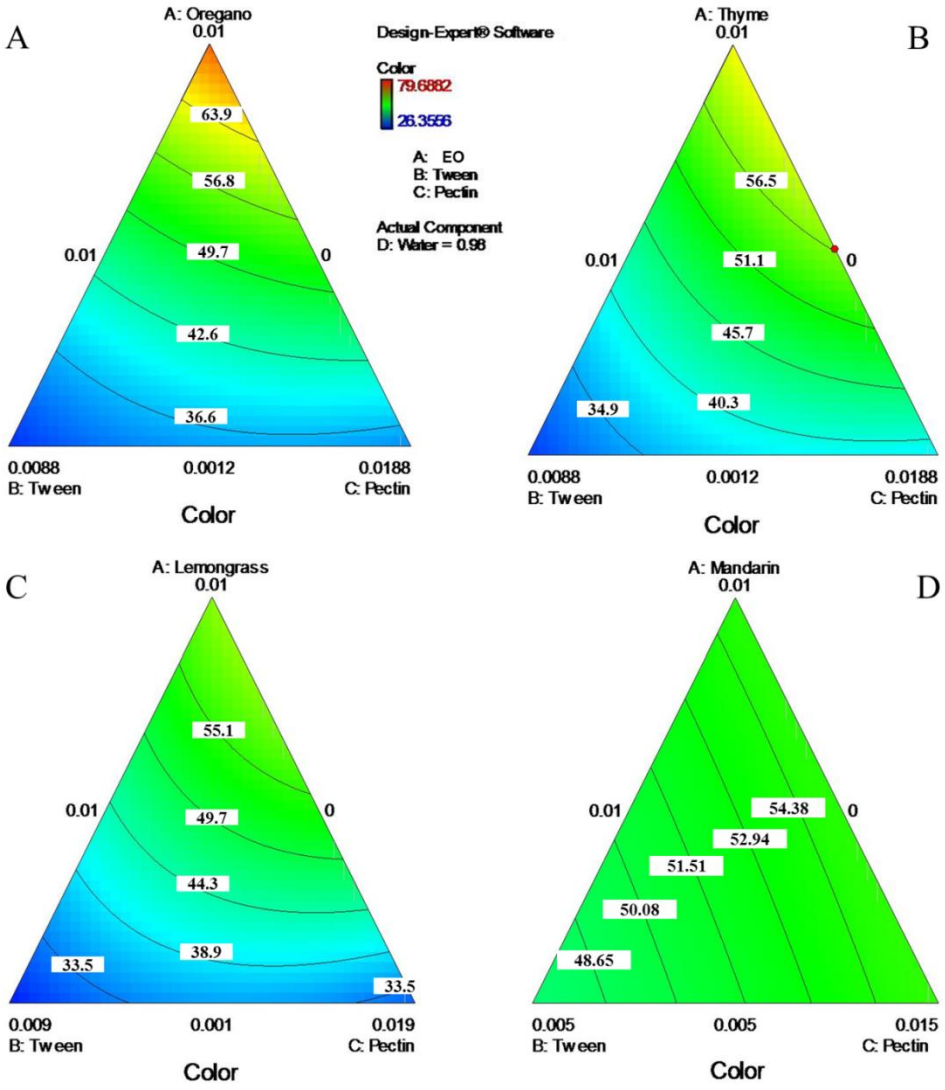

Figure 5. Contour plots of color (WI) of mixtures containing four different EOs: oregano oil (A), thyme oil (B), lemongrass (C) and mandarin oil (D), tween 80 as surfactant, and pectin. The water content was set at 0.98.

2.3. Nanoemulsions formation

All the formulations used for the D-optimal experimental design were prepared and their physicochemical properties tested. To achieve this, powdered pectin was added slowly to ultrapure water at 70ºC until its total dissolution and stored under refrigeration overnight to ensure the complete hydration of the biopolymer. Afterwards, a lipid phase was formed by adding the required Tween 80 amount to the corresponding EO. Then, the lipid phase and the aqueous phase were mixed by using a laboratory mixer (T25 digital Ultra-Turrax, IKA, Staufen, Germany) at 9600 rpm and 2 minutes, which led to the formation of a coarse emulsion. Nanoemulsions were obtained by passing the coarse emulsions through a microfluidizer (M-110P, Microfluidics, USA) at 150 MPa for 5 cycles (Qian & McClements, 2011) and were cooled down at the outlet of the microfluidization unit through an external coil immersed in a water bath with ice, so that temperature was kept at 10 ºC.

2.4. Nanoemulsions characterization

2.4.1. Particle Size and ζ-Potential

The emulsion droplet diameter (Z-average in nm) was measured by dynamic light scattering technique (DSL) with a Zetasizer laser diffractometer (NanoZS, Malvern Instruments Ltd., Worcestershire, UK) working at 633 nm at 25 °C and equipped with a back- scatter detector (173°) (Brar & Verma, 2011). Average droplet diameter (nm) and size distribution curves in intensity (%) were used to characterize the nanoemulsions. Particle size was calculated with the Mie Theory, which correlates the Brownian motion of the dispersed particles with their particle size by using the optical properties of the oil and the aqueous dispersant phase. Refractive indexes of OR-EO, TH-EO, LG-EO and MN-EO measured with a refractometer (ABBE-2WAJ, optic ivymen system®, Comecta SA, Barcelona, Spain) were 1.501, 1.497, 1.484 and 1.475, respectively; and their absorbance measured with a spectrophotometer (Jasco V-670, Tokyo, Japan) at 633 nm were 0.002, 0.002, 0.024 and 0.004, respectively.

The electrophoretic mobility of oil droplets, also reported as ζ-potential (mV), was measured by phase analysis light scattering (PALS) with a Zetasizer laser diffractometer (NanoZS, Malvern Instruments Ltd., Worcestershire, UK). It determines the surface charge at the interface of the droplets dispersed in the aqueous solution. Samples were diluted prior to particle size and ζ-potential measurements in ultrapure water with a dilution factor of 1:9 sample-to-dilutant.

2.4.2. Viscosity

A vibro-viscometer (SV-10, A&D Company, Tokyo, Japan) vibrating at 30 Hz was used to measure the viscosity (mPa·s) of 10 mL aliquots of the emulsions. Moreover, the viscosity of water, which was used as dispersant phase, was 0.89 mPa·s. The viscosity of water was considered as the viscosity of the aqueous phase for the particle size measurements, conducted at 25 ± 2 ºC.

2.4.3. Whiteness Index

The color of emulsions and nanoemulsions was measured with a colorimeter (Minolta CR-400, Konica Minolta Sensing, Inc., Osaka, Japan) at room temperature set up for illuminant D65 and 10° observer angle and calibrated with a standard white plate (Y=94.0; x=0.3133; y=0.3194). CIE L^*, a^* and b^* values were determined, and the whiteness index (WI) was calculated with Eq. 2 (Salvia-Trujillo et al., 2013b):

$$WI = 100-((100-L)^2+(a^2+b^2))^{0.5} \quad \textbf{eq.(2)}$$

3. Results and Discussion

3.1. Particle Size

The experimental values for the average oil droplet size of emulsions containing OR-EO, TH-EO, LG-EO and MN-EO are shown in the supplementary material (Tables 2, 3, 4 and 5, respectively); and the coefficients of the polynomial equation regarding particle size are shown in Table 1. On the one hand, a special cubic model fit the droplet size diameter experimental values of OR-EO whereas a linear or a quadratic model without transformations was needed for nanoemulsions containing TH-EO or LG-EO, respectively. On the other hand, for nanoemulsions with MN-EO, a quadratic model with a $\log_{10}$ power law transformation was required. The polynomial model to predict the particle size for each type of oil was statistically significant (p-values ≤ 0.01) and with a good fit as indicated by the coefficients of determination (R^2) for OR-EO, LG-EO and MN-EO formulations with values of 0.99, 0.97 and 0.94, respectively; being lower in nanoemulsions containing TH-EO (0.62). The minimum average droplet size observed for OR-EO, TH-EO, LG-EO and MN-EO nanoemulsions was 120 ± 9, 113 ± 3, 146 ± 6, and 29 ± 1 nm, respectively.

Contour plots obtained from the ternary phase diagrams regarding particle size were represented setting the concentration of water at 0.98 to facilitate the visualization of the data in a two-dimensional plane (Figure 1). However, in order to highlight the regions in which smallest particle size values were found, enlargements of Figure 1 were also represented setting the water concentration to 0.94 (Figure 2). Tween 80 is a low-mass surfactant, which has a molar mass of 1.310 g/mol and rapidly coats the surface of the created oil-water interface during emulsification (Kralova et al., 2011; Salvia-Trujillo et al., 2014b). Therefore, there must be enough amounts of surface-active molecules to cover the surface area of oil droplets generated during the formation of nanoemulsions (Acevedo-Fani, Salvia-Trujillo, Rojas-Graü, & Martín-Belloso, 2015). In this regard, the higher the concentration of surfactant, the lower the particle size would be, which is in accordance with previous works (Kralova & Sjöblom, 2009). However, a remarkable decrease in nanoemulsion particle size when concentration of Tween 80 increased only was observed in the contour plot of LG-EO. Actually, which it is shown in Figures 1 and 2 is the formation of submicron nanoparticles (350-850 nm) with concentrations of pectin between 1 and 2% *w/w* even in absence of surfactant. This highlights the capacity of pectin to act as emulsifier. Furthermore, in contrast with LG-EO nanoemulsions, in Figures 1A, 1B and 1D (OR-EO, TH-EO and MN-EO, respectively) the isolines are oriented parallely to the pectin axis, which means that the particle size was mainly dominated by pectin concentration. This affirmation agrees with positive coefficients in the pectin concentration for the OR-EO, TH-EO and MN-EO nanoemulsions (Table 1). It is considered that the higher the magnitude of the coefficient parameter of the corresponding terms in the fitted equation, the higher the response effect on the measured parameter (Salvia-Trujillo et al., 2014b). In this regard, an increase in pectin concentration in the aqueous phase caused the enlargement of nanoemulsion particle size of OR-EO, TH-EO and MN-EO nanoemulsions, which might be caused by a number of reasons. Firstly, the increase in biopolymer concentration may raise the viscosity of the continuous phase and therefore low the efficiency of the microfluidizer device in reducing the oil droplet size (Schmidt, 2016). Secondly, pectin might present certain surface activity at oil-water interfaces since it contains functional units including acetyl and methyl groups. Some authors have demonstrated a direct relationship between the DM and emulsifying capacity of citrus pectin by increasing the DM from ~70% to ~80% (Schmidt et al., 2017). These groups with interfacial activity are able to act as hydrophobic anchors that facilitate adsorption

of pectin chains at the interface resulting in reduction of interfacial tension (Alba & Kontogiorgos, 2017). Hence, pectin chains present in the bulk aqueous phase can compete with Tween 80 molecules, and cause the displacement of these previously-adsorbed surface active species (Jafari, He, & Bhandari, 2007a). And finally, pectin molecules have shown to induce depletion flocculation and subsequent coalescence in emulsions, thus causing an increase in nanoemulsions particle size (McClements, 2005; Neumann, Schmitt, & Iamazaki, 2003; Robins, 2000).

In general, the EOs concentration did not dominate the nanoemulsion particle size especially in the case of MN-EO nanoemulsions, where isolines were closely perpendicular to the oil axis. Thus, differences among the droplet size of EOs-loaded nanoemulsions has been attributed to different chemical composition of the volatile compounds forming each oil phase (supplementary material Figure 6) (Guerra-Rosas et al., 2016; L. Salvia-Trujillo et al., 2015a). Principally OR-EO and TH-EO nanoemulsions, whose major components carvacrol and thymol contain a phenolic group, are prone to suffer Ostwald ripening since are highly water soluble. During this process larger droplets grow at the expense of smaller ones leading to an increase of mean droplet diameters of emulsions (Zeeb et al., 2012). Nonetheless, LG-EO nanoemulsions have been reported to be stable against Ostwald ripening (Guerra-Rosas et al., 2016) and pectin seems to contribute positively in their emulsification. In fact, positive coefficients of the quadratic terms of LG-EO nanoemulsions indicate a synergistic effect among oil concentration and the other three components or between Tween 80 and pectin (Ramsey, 1997; Salvia-Trujillo et al., 2014; Cornel, 2002). Being the largest coefficient that of the interaction between the essential oil (component A) and pectin (component C) with an AC value of 31677.86 (Table 1).

3.2. ζ-potential

The electrical charge experimental values of OR-EO, TH-EO, LG-EO and MN-EO nanoemulsions are shown in the supplementary material (Tables 2, 3, 4 and 5, respectively). The ζ-potential varied significantly depending on the concentration of the different components of the emulsions and the type of oil used. They ranged between values around -5 ± 1 mV and -18 ± 2 mV depending on the type and concentration of EO used and the concentration of pectin.

A linear model was fitted to experimental data in all cases except for the emulsions with LG-EO, in which a quadratic model was used. The p-values and a R^2 for the four types of formulations are shown in Table 1. Consistently, the negative coefficients for Tween 80 (-8.05; -14.69; -3.50 and -12.22; in case of using OR-EO, TH-EO, LG-EO and MN-EO, respectively) as well as pectin coefficients of -18.72, 4.19, -460.82 and -12.27 (OR-EO, TH-EO, LG-EO and MN-EO, respectively), indicated their contribution to decrease the ζ-potential of the emulsions and nanoemulsions. On the one hand, it is known that, in the absence of any anionic biopolymer, non-ionic surfactants such as Tween 80 may confer negative charge to oil droplets probably due to the orientation towards the oil/water interface of OH^- ions from the aqueous phase or HCO_3^- and CO_3^{2-} ions from the dissolved atmospheric CO_2 (Marinova et al., 1996). Moreover, since Tween 80 is a small molecule surfactant, it adsorbs at the oil/water interface very quickly stabilizing the newly created oil droplets. On the other hand, pectin is a linear polysaccharide consisting of covalently linked galacturonic acid (GalA) units with methylester groups along the backbone. The ionization of the carboxylic groups of the methyesters contributes to the negative charge of pectin (D. Lin, Lopez-Sanchez, & Gidley, 2016). It has been recently described that pectin may adsorb at the oil/water interface but the exact mechanism of adsorption still needs to be elucidated (Alba & Kontogiorgos, 2017). In this regard, a different behavior of the emulsion ζ-potential was observed after the addition of pectin into the system depending on the type of EO

(Figure 3). In the contour plots of TH-EO and MN-EO, ζ-potential values remained practically unaltered after increasing the concentration of pectin from 1 to 2% w/w, ranging from -12 to -15 mV (Figure 3B) and from -10 to -11 mV (Figure 3D), respectively. This suggests that, despite the anionic nature of pectin, it may not be adsorbed at the oil/water interface due to a preferential adsorption of Tween 80 at the oil droplet surface. Oppositely, contour plots of OR-EO and LG-EO showed a decrease of ζ-potential values becoming more negative with an increase in the concentration of pectin. For instance, the ζ-potential of OR-EO or LG-EO nanoemulsions decreased from -10 to -15 mV (Figure 3A) or from -9 to -15 mV (Figure 3C), respectively, with an increase of the pectin concentration from 1% to 2% w/w. This suggests that pectin might have been partially adsorbed at the oil/water interface with its hydrophilic part in the continuous water phase and the hydrophobic part in contact with the oil drops (Nambam & Philip, 2012). This is in accordance with other studies that had described a competitive adsorption between negative biopolymers and low mass surfactants on the oil/water interface. If the concentration of surfactant molecules is not enough to cover the oil water interface, it might lead the adsorption of polymer molecules conferring a more negative ζ-potential (Gasa-Falcon et al., 2017; Goddard, 2002; Salvia-Trujillo et al., 2014b).

3.3. Viscosity

The viscosity values are presented in the supplementary material (Tables 2, 3, 4 and 5 for OR-EO, TH-EO, LG-EO and MN-EO, respectively). A linear model with a $\log_{10}$ transformation power law, recommended by the Box-Cox method was successfully fitted experimental data of OR-EO nanoemulsions (Table 1). Those formulations showed p-values lower than 0.0001 and a R^2 value higher or equal than 0.98. However, TH-EO, LG-EO and MN-EO fitted to a quadratic model that was based on R^2 values of 0.99 and p-values statistically significant (≤ 0.01).

The apparent viscosity values ranged from 19.9 ± 0.4 to 129.3 ± 0.5 mPa·s, from 24.9 ± 0.5 to 197 ± 3 mPa s; from 15.15 ± 0.4 to 137 ± 7 mPa·s and from 12.98 ± 0.05 to 147 ± 1 in case of using OR-EO, TH-EO, LG-EO and MN-EO, respectively. In fact, the parallel trend of OR-EO, TH-EO, LG-EO and MN-EO contour lines regarding the segment between EO and Tween 80 vertexes indicates a poor influence of these compounds on the nanoemulsion viscosity. Nonetheless, specifically in the case of LG-EO nanoemulsion a slight decrease of viscosity was observed when the concentration of surfactant increased (Figure 4C), which was linked with a smaller particle size in those regions (Figure 1C). It is well known that an increased concentration of surfactant may lead to a decrease in the particle size (Tadros et al., 2004) and this might have an impact on emulsion viscosity (McClements & Rao, 2011). In addition to this, MN-EO nanoemulsions, present lower overall viscosity values (Figure 4D) in comparison with the rest of the EOs, being also the ones having the smallest droplet sizes (Figure 1D). Thus, the lower viscosity values due to smaller droplets might be attributed to the higher flow properties when a stress is applied. In fact, droplet size has been reported to impact the rheology of emulsions and depends on the properties of the dispersed phase (Pal, 2000). Despite this, our results suggest that nanoemulsion viscosity was mainly determined by pectin concentration as the contour plot isolines are almost parallel to the pectin concentration axis. In this regard, at increasing the weight fraction of pectin in the aqueous phase from 1 % (*w/w*) to 2 % (*w/w*) for a given concentration of Tween 80 (6 % *w/w*) and any concentration of EO, the apparent viscosity remarkably increased regardless the type of EO (supplementary material, Tables 2, 3, 4 and 5). Guerra-Rosas et al. (2016) also observed that the higher the concentration of pectin, the higher its viscosity due to the thickening properties of pectin, which are related with its ability to holding high quantities of water. In this

regard, free pectin molecules in the aqueous phase are able to form gel-like structures, thus increasing the viscosity of the aqueous media (Hansen, Arnebrant, & Bergström, 2001).

3.4. Whiteness Index

The whiteness index of the blends understood as an indicator of their milky appearance ranged between 25.9 ± 0.1 and 79.69 ± 0.02 (supplementary material, Tables 2, 3, 4 and 5 for OR-EO, TH-EO, LG-EO and MN-EO, respectively) depending on the formulation. That is, the higher the WI, the whiter, and the lower the WI, the more transparent (Salvia-Trujillo et al., 2013b). A quadratic model was fitted to experimental results of all the nanoemulsions regardless the EO used, which was statistically significant with a R^2 values above 0.93 and p values of 0.0009, 0.0026, 0.0015 and 0.0138 for OR-EO, TH-EO, LG-EO and MN-EO respectively (Table 1).

The contour plots of the whiteness index were characterized by their curved isolines, which indicate its dependency to multiple variables (Figure 5A, 5B, 5C and 5D). In this regard, the color of these blends was significantly affected by Tween 80 and EOs concentration. Our results evidenced that the transparency of the EOs nanoemulsions diminished when increasing the oil amount or decreasing the Tween 80 concentration (supplementary material, Tables 2,3,4 and 5), which is in agreement with a previously reported work by Rao & McClements (2011). In fact, it was reflected by the negative coefficients of the quadratic terms AB and BD in the polynomial equation (Table 1).

It is known that emulsion whitish appearance is due to the light scattering of the oil droplets. In turn, light scattering of oil droplets depends fundamentally on the refractive index of continuous (water) and dispersed phase (oil), oil concentration and droplet size (McClements, 2002a, 2002b). Therefore, OR-EO nanoemulsions, with the highest refractive index, were those less transparent. In MN-EO contour plot parallel isolines to Tween 80 axis indicate the strong influence of surfactant concentration on the whiteness index of nanoemulsions. Thus, WI of MN-EO nanoemulsions decreased while increasing concentrations of Tween 80 regardless EO or pectin concentration. This can be related to the small particle sizes (29-260 nm) of MN-EO nanoemulsions at high concentrations of Tween 80. The whiteness index is closely correlated with the particle size of nanoemulsions since larger particles scatter the light more intensively causing an increase in the lightness, opacity and whiteness index of emulsions (Rao & McClements, 2011a).

4. Conclusions

The present work reveals that the pseudo-ternary phase experimental design based on a response surface methodology is useful to obtain significant information about the behavior of the individual components on the formation of nanoemulsions containing lipophilic functional compounds, such as EOs. In all cases, linear, quadratic or special cubic models successfully fit experimental data to describe the behavior of the mixtures. In general, the EOs concentration did not dominate the nanoemulsion particle size, being rather the Tween 80 and pectin concentrations the determining factors. A minimum concentration of Tween 80 of 1.8 % (*w/w*) was needed to obtain particle sizes in the nano-range (d < 500 nm). This work also evidenced the role of pectin as emulsifier in the absence of small molecule surfactants, since submicron emulsions (d ≈ 350 - 850 nm) were obtained at a pectin concentration above 1 % (*w/w*) regardless the type of EOs. Nonetheless, in general, increasing the pectin concentration enlarged the particle size and viscosity of emulsions and nanoemulsions. This suggests that high pectin concentrations might reduce the microfluidization

efficiency in decreasing the oil droplet size. Moreover, the ζ-potential values indicate that pectin is not or weakly adsorbed at the oil-water interface as a modest or negligible decrease in the ζ-potential was observed depending on the type of EOs at increasing pectin concentrations. Nevertheless, the transparency of nanoemulsions was achieved mainly when using low EO concentrations, regardless the type of EOs. Therefore, pseudo-ternary diagrams have been used to observe the behavior of nanoemulsions components on their properties. This study has greatly contributed to describe the role of pectin and its interaction with small molecule surfactants in complex systems for the formation of nanoemulsions.

5. Acknowledgments

This study was supported by the Ministry of Science and Innovation (Spain) throughout the project 'Improving quality and functionality of food products by incorporating lipid nanoparticles into edible coatings' **(AGL2012-35635)**. María Artiga-Artigas thanks the University of Lleida for the pre-doctoral grant.

6. References

Acevedo-Fani, A., Salvia-Trujillo, L., Rojas-Graü, M. A., & Martín-Belloso, O. (2015). Edible films from essential-oil-loaded nanoemulsions: Physicochemical characterization and antimicrobial properties. *Food Hydrocolloids*, *47*, 168–177.

Alba, K., & Kontogiorgos, V. (2017). Pectin at the oil-water interface: Relationship of molecular composition and structure to functionality. *Food Hydrocolloids*, *68*, 211–218.

Brar, S. K., & Verma, M. (2011). Measurement of nanoparticles by light-scattering techniques. *TrAC Trends in Analytical Chemistry*, *30*(1), 4–17.

Burt, S. (2004). Essential oils: their antibacterial properties and potential applications in foods--a review. *International Journal of Food Microbiology*, *94*(3), 223–53.

Chan, S. Y., Choo, W. S., Young, D. J., & Loh, X. J. (2017). Pectin as a rheology modifier: Origin, structure, commercial production and rheology. *Carbohydrate Polymers*, *161*, 118–139.

Fisher, K., & Phillips, C. (2008). Potential antimicrobial uses of essential oils in food: is citrus the answer? *Trends in Food Science and Technology*, *19*(3), 156–164.

Gasa-Falcon, A., Odriozola-Serrano, I., Oms-Oliu, G., & Martín-Belloso, O. (2017). Influence of mandarin fiber addition on physico-chemical properties of nanoemulsions containing β-carotene under simulated gastrointestinal digestion conditions. *LWT - Food Science and Technology*, *84*, 331–337.

Goddard, E. D. (2002). Polymer/Surfactant Interaction: Interfacial Aspects. *Journal of Colloid and Interface Science*, *256*(1), 228–235.

Guerra-Rosas, M. I., Morales-Castro, J., Ochoa-Martínez, L. A., Salvia-Trujillo, L., & Martín-Belloso, O. (2016). Long-term stability of food-grade nanoemulsions from high methoxyl pectin containing essential oils. *Food Hydrocolloids*, *52*, 438–446.

Hammer, K. A., Carson, C. F., & Riley, T. V. (1999). Antimicrobial activity of essential oils and other plant extracts. *Journal of Applied Microbiology*, *86*(6), 985–990.

Hansen, P. H. F., Arnebrant, T., & Bergström, L. (2001). Shear induced aggregation of a pectin stabilised emulsion in two dimensions. *Colloid and Polymer Science*, *279*, 153–160.

Hopkins, E. J., Chang, C., Lam, R. S. H., & Nickerson, M. T. (2015). Effects of flaxseed oil concentration on the performance of a soy protein isolate-based emulsion-type film. *Food Research International*, *67*, 418–425.

Jafari, S. M., He, Y., & Bhandari, B. (2007). Optimization of nano-emulsions production by microfluidization. *European Food Research and Technology*, *225*(5–6), 733–741.

Kralova, I., & Sjöblom, J. (2009). Surfactants used in food industry: A review. *Journal of Dispersion Science and Technology*, *30*(9).

Kralova, I., & Sjöblom, J. (2009). Surfactants Used in Food Industry: A Review. *Journal of Dispersion Science and Technology*, *30*(9), 1363–1383.

Kralova, I., Sjöblom, J., Øye, G., Simon, S., Grimes, B. a., & Paso, K. (2011). Heavy crude oils/particle stabilized emulsions. *Advances in Colloid and Interface Science*, *169*(2), 106–127.

Laurent, M. A., & Boulenguer, P. (2003). Stabilization mechanism of acid dairy drinks (ADD) induced by pectin. *Food Hydrocolloids*, *17*(4), 445–454.

Li, P. (2005). Box-Cox Transformations : An Overview.

Lin, D., Lopez-Sanchez, P., & Gidley, M. J. (2016). Interactions of pectins with cellulose during its synthesis in the absence of calcium. *Food Hydrocolloids*, *52*, 57–68.

Marinova, K. G., Alargova, R. G., Denkov, N. D., Velev, O. D., Petsev, D. N., Ivanov, I. B., & Borwankar, R. P. (1996). Charging of Oil−Water Interfaces Due to Spontaneous Adsorption of Hydroxyl Ions. *Langmuir*, *12*(8), 2045–2051.

McClements, D. J. (2002a). Colloidal basis of emulsion color. *Current Opinion in Colloid & Interface Science*, *7*(5–6), 451–455.

McClements, D. J. (2002b). Theoretical prediction of emulsion color. *Advances in Colloid and Interface Science*, *97*(1–3), 63–89.

McClements, D. J. (2005). Theoretical analysis of factors affecting the formation and stability of multilayered colloidal dispersions. *Langmuir*, *21*(21), 9777–9785.

McClements, D. J. (2012). Advances in fabrication of emulsions with enhanced functionality using structural design principles. *Current Opinion in Colloid and Interface Science*, *17*(5), 235–245.

McClements, D. J., & Rao, J. (2011). Food-Grade nanoemulsions: Formulation, fabrication, properties, performance, Biological fate, and Potential Toxicity. *Critical Reviews in Food Science and Nutrition*, *51*(4), 285–330.

Nambam, J. S., & Philip, J. (2012). Competitive adsorption of polymer and surfactant at a liquid droplet interface and its effect on flocculation of emulsion. *Journal of Colloid and Interface Science*, *366*(1), 88–95.

Neumann, M. G., Schmitt, C. C., & Iamazaki, E. T. (2003). A fluorescence study of the interactions between sodium alginate and surfactants. *Carbohydrate Research*, *338*(10), 1109–1113.

Otoni, C. G., Avena-Bustillos, R. J., Olsen, C. W., Bilbao-Sáinz, C., & McHugh, T. H. (2016). Food Hydrocolloids Mechanical and water barrier properties of isolated soy protein composite edible fi lms as affected by carvacrol and cinnamaldehyde micro and nanoemulsions, *57*, 72–79.

Ozturk, B., & McClements, D. J. (2016). Progress in natural emulsifiers for utilization in food emulsions. *Current Opinion in Food Science*, *7*, 1–6.

Pal, R. (2000). Shear viscosity behavior of emulsions of two immiscible liquids. *Journal of Colloid and Interface Science*, *225*(2), 359–366.

Qian, C., & McClements, D. J. (2011). Formation of nanoemulsions stabilized by model food-grade emulsifiers using high-pressure homogenization: Factors affecting particle size. *Food Hydrocolloids*, *25*(5), 1000–1008.

Ramsey, J. (1997). Modeling the Component Linear and Nonlinear Blending Properties in a Two-Stage Mixture Experiment, (96).

Rao, J., & McClements, D. J. (2011). Food-grade microemulsions, nanoemulsions and emulsions: Fabrication from sucrose monopalmitate & lemon oil. *Food Hydrocolloids*, *25*(6), 1413–1423.

Ren, S., Mu, H., Alchaer, F., Chtatou, A., & Müllertz, A. (2013). Optimization of self nanoemulsifying drug delivery system for poorly water-soluble drug using response surface methodology. *Drug Development and Industrial Pharmacy*, *39*(5), 799–806.

Robins, M. M. (2000). Emulsions - creaming phenomena*, *5*, 265–272.

Salvia-Trujillo, L., Rojas-Graü, A., Soliva-Fortuny, R., & Martín-Belloso, O. (2014a). Food Hydrocolloids Physicochemical characterization and antimicrobial activity of food- grade emulsions and nanoemulsions incorporating essential oils. *Food Hydrocolloids*, *43*, 1–10.

Salvia-Trujillo, L., Rojas-Graü, A., Soliva-Fortuny, R., & Martín-Belloso, O. (2015). Physicochemical characterization and antimicrobial activity of food-grade emulsions and nanoemulsions incorporating essential oils. *Food Hydrocolloids*, *43*, 547–556.

Salvia-Trujillo, L., Rojas-Graü, M. A., Soliva-Fortuny, R., & Martín-Belloso, O. (2013). Effect of processing parameters on physicochemical characteristics of microfluidized lemongrass essential oil-alginate nanoemulsions. *Food Hydrocolloids*, *30*(1), 401–407.

Salvia-Trujillo, L., Rojas-Graü, M. A., Soliva-Fortuny, R., & Martín-Belloso, O. (2014b). Formulation of Antimicrobial Edible Nanoemulsions with Pseudo-Ternary Phase Experimental Design. *Food and Bioprocess Technology*, 3022–3032.

Schmidt, U. S. (2016). Citrus pectin as a hydrocolloid emulsifier: Emulsifying and emulsion stabilizing properties, (February), 141.

Schmidt, U. S., Schütz, L., & Schuchmann, H. P. (2017). Interfacial and emulsifying properties of citrus pectin: Interaction of pH, ionic strength and degree of esterification. *Food Hydrocolloids*, *62*, 288–298.

Solans, C., Izquierdo, P., Nolla, J., Azemar, N., & Garcia-Celma, M. (2005). Nano-emulsions. *Current Opinion in Colloid & Interface Science*, *10*(3–4), 102–110.

Suriyarak, S., & Weiss, J. (2014). Cutoff Ostwald ripening stability of alkane-in-water emulsion loaded with eugenol. *Colloids and Surfaces A: Physicochemical and Engineering Aspects*, *446*, 71–79.

Svoboda, K., Brooker, J. D., & Zrustova, J. (2006). Antibacterial and antioxidant properties of essential oils: Their potential applications in the food industries. In *Acta Horticulturae* (Vol. 709, pp. 35–43).

Tadros, T., Izquierdo, P., Esquena, J., & Solans, C. (2004). Formation and stability of nano-emulsions. *Advances in Colloid and Interface Science*, *108–109*, 303–318.

Zeeb, B., Gibis, M., Fischer, L., & Weiss, J. (2012). Influence of interfacial properties on Ostwald ripening in crosslinked multilayered oil-in-water emulsions. *Journal of Colloid and Interface Science*, *387*(1), 65–73.

Supplementary material

Table 2. Mixture design formulations and concentration of the individual components for each mixture based on oregano essential oil (OR-EO), Tween 80 and pectin concentration expressed in weigh fraction (*w/w*; %), and experimental values of droplet size, ζ-potential, viscosity and whiteness index.

Run	OR-EO	Tween 80	Pectin	Water	Size (nm)	ζ-potential (mV)	Color (WI)	Viscosity (mPa·s)
1	0.1	6	2	91.9	345 ± 39	-8.8 ± 1.8	26.86 ± 0.07	129.3 ± 0.5
2	0.6	2	1.5	96.4	225 ± 13	-6 ± 1	46.6 ± 0.2	42.75 ± 0.05
3	0.6	3	2	94.4	362 ± 34	-10 ± 2	27.23 ± 0.09	136 ± 3
4	0.1	0	1	98.9	540 ± 32	-18.9 ± 1.5	29.29 ± 0.01	13.81 ± 0.11
5	0.3	5	1.3	93.9	275 ± 39	-11 ± 3	26.65 ± 0.04	32.8 ± 0.2
6	0.8	5	1.8	93	205 ± 59	-8.2 ± 1.2	27.65 ± 0.13	90.0 ± 0.4
7	1	0	1	98	525 ± 8	-8.0 ± 1.3	74.88 ± 0.03	13.65 ± 0.13
8	0.1	6	1	92.9	242 ± 63	-8.9 ± 1.2	25.9 ± 0.1	19.1 ± 0.4
9	0.1	0	2	97.9	601 ± 36	-17 ± 3	31.83 ± 0.04	103.3 ± 1.3
10	0.1	3	1	95.9	301 ± 57	-12 ± 3	26.0 ± 0.1	16.79 ± 0.11
11	0.6	6	1.5	91.9	253 ± 67	-8.6 ± 1.8	26.67 ± 0.06	69.41 ± 0.15
12	1	0	1.5	97.5	528 ± 6	-8.01 ± 1.12	75.80 ± 0.03	43.6 ± 0.4
13	0.1	3	1.5	95.4	453 ± 95	-13 ± 2	26.08 ± 0.06	61.7 ± 0.2
14	1	3	1	95	120 ± 9	-5.6 ± 0.7	37.05 ± 0.08	18.0 ± 0.4
15	0.1	6	2	91.9	349 ± 28	-8 ± 3	26.6 ± 0.2	178 ± 4
16	1	6	2	91	481 ± 70	-5.8 ± 0.8	29.35 ± 0.04	247 ± 4
17	0.1	0	2	97.9	595 ± 13	-16 ± 4	31.57 ± 0.05	133 ± 2

Table 3. Mixture design formulations and concentration of the individual components for each mixture based on thyme essential oil (TH-EO), Tween 80 and pectin concentration expressed in weigh fraction (*w/w;* %), and experimental values of droplet size, ζ-potential, viscosity and whiteness index.

Run	TH-EO	Tween 80	Pectin	Water	Size (nm)	ζ-potential (mV)	Color (WI)	Viscosity (mPa·s)
1	0. 6	0	1.5	97.9	775 ± 20	-9.9 ± 0.8	66.26 ± 0.03	52.8 ±0.2
2	1	6	1.5	91.5	117 ± 22	-12.8 ± 1.9	28.49 ± 0.02	68.5 ± 0.9
3	0.8	1.5	1.8	96	113 ± 3	-9.1 ± 1.4	38.89 ± 0.05	82.3 ± 0.3
4	1	0	2	97	946 ± 24	-6.5 ± 1.2	73.91 ± 0.03	139 ± 3
5	0.1	3	1.5	95.4	421 ± 27	-16 ± 3	26.38 ± 0.09	54.4 ± 0.5
6	1	3	1	95	137 ± 25	-10.7 ± 1.3	27.99 ± 0.03	17.14 ± 0.18
7	0.6	4.5	1.5	93.4	293 ± 26	-14 ± 3	27.05 ± 0.04	58.5 ± 0.4
8	1	3	1	95	158 ± 27	-11.5 ± 1.8	27.7 ± 0.3	17.5 ± 0.2
9	0.3	1.5	1.3	96.9	385 ± 35	-15.1 ± 1.4	26.88 ± 0.06	30.2 ± 0.4
10	0.1	6	2	91.9	392 ± 39	-13.6 ± 1.1	26.63 ± 0.05	173 ± 2
11	0.6	3	2	94.4	319 ± 26	-14 ± 2	27.86 ± 0.06	154 ± 3
12	1	6	2	91	206 ± 40	-6.4 ± 1.7	27.90 ± 0.05	197 ± 3
13	0.1	3	1	95.9	352 ± 18	-13.2 ± 1.8	26.41 ± 0.17	20.1 ± 0.4
14	0.6	6	1	92.4	140 ± 25	-9 ± 3	26.7 ± 0.3	24.9 ± 0.5
15	0.1	6	2	91.9	407 ± 26	-8.6 ± 1.5	26.85 ± 0.08	193 ± 2
16	0.1	0	2	97.9	644 ± 31	-15 ± 4	35.64 ± 0.07	160 ± 4
17	0.1	0	1	98.9	568 ± 9	-18.6 ± 1.6	33.84 ± 0.05	17.0 ± 0.3

Table 4. Mixture design formulations and concentration of the individual components for each mixture based on lemongrass essential oil (LEO), Tween 80 and pectin concentration expressed in weigh fraction (*w/w;* %), and experimental values of droplet size, ζ-potential, viscosity and whiteness index.

Run	LG-EO	Tween 80	Pectin	Water	Size (nm)	ζ-potential (mV)	Color (WI)	Viscosity (mPa·s)
1	2	6	2	9	224 ± 51	-9 ± 2	27.34 ± 0.18	148 ± 5
2	2	0	2	96	1103 ± 157	-4.4± 0.6	78.38 ± 0.03	121 ± 4
3	0.1	0	1	98.9	524 ± 59	-14 ± 8	29.38 ± 0.04	14.6 ± 0.3
4	2	0	2	96	978 ± 35	-4.7 ± 0.7	78.02 ± 0.08	121 ± 4
5	2	0	1	97	824 ± 15	-4.8 ± 0.9	78.71 ± 0.05	14.85 ± 0.06
6	2	2	1	95	245 ± 69	-14 ± 4	31.87 ± 0.14	13.8 ± 0.4
7	0.1	4	1	94.9	201 ± 37	-14.6 ± 1.8	26.4 ± 0.1	16.1 ± 0.8
8	1.05	3	2	94	411 ± 73	-12 ± 4	27.12 ± 0.08	137 ± 7
9	0.1	2	1.7	96.2	349 ± 30	-15 ± 2	26.42 ± 0.14	66.4 ± 1.8
10	1.1	0	1.5	97.5	737 ± 19	-7.3 ± 1.2	72.36 ± 0.02	41.7 ± 1.3
11	1.4	6	1	91.6	146 ± 6	-10.8 ± 1.0	26.33 ± 0.16	19.8 ± 0.9
12	0.6	4.5	1.5	93.4	322 ± 50	-12.6 ± 1.5	26.48 ± 0.14	49.1 ± 0.7
13	2	6	2	90	226 ± 65	-10 ± 3	26.8 ± 0.2	141 ± 1
14	2	4	1.3	92.7	248 ± 54	-10.8 ± 1.6	28.8 ± 0.1	35.28 ± 0.13
15	0.1	0	2	97.9	453 ± 14	-18 ± 2	28.21 ± 0.07	100.5 ± 1.7
16	0.1	6	1.5	92.4	244 ± 41	-11.2 ± 1.9	26.3 ± 0.2	51.6 ± 1.2
17	0.1	3	1	94	266 ± 56	-9.1 ± 1.0	30.34 ± 0.01	15.2 ± 0.4

Table 5. Mixture design formulations and concentration of the individual components for each mixture based on mandarin essential oil (MN-EO), Tween 80 and pectin concentration expressed in weigh fraction (*w/w;* %), and experimental values of droplet size, ζ-potential, viscosity and whiteness index.

Run	MN-EO	Tween 80	Pectin	Water	Size (nm)	ζ- potential (mV)	Color (WI)	Viscosity (mPa·s)
1	1.1	1.5	1.3	96.1	57 ± 2	-10.7 ± 1.5	29.08 ± 0.04	27.1 ± 0.4
2	3	3	2	92	69 ± 4	-6.8 ± 1.3	44.16 ± 0.12	147 ± 1
3	0.5	0	2	97.5	868 ± 51	-10.2 ± 1.1	60.85 ± 0.03	103.8 ± 0.5
4	0.5	6	2	91.5	243 ± 43	-8.7 ± 1.7	26.62 ± 0.07	141 ± 3
5	1.1	4.5	1.3	93.1	68 ± 20	-12 ± 3	26.72 ± 0.14	29.7 ± 0.4
6	1.8	6	1.5	90.8	60 ± 11	-8.8 ± 1.5	26.8 ± 0.1	52 ± 1
7	3	6	1	90	29.4 ± 1.1	-9.0 ± 1.0	28.95 ± 0.04	18.0 ± 0.2
8	2.4	1.5	1.8	94.4	87.6 ± 1.7	-9.4 ± 1.6	44.62 ± 0.08	71.9 ± 0.2
9	0.5	6	1	92.5	90 ± 17	-8.9 ± 1.4	26.46 ± 0.08	18.28 ± 0.15
10	2.4	4.5	1.3	91.9	35.2 ± 1.7	-8.5 ± 1.1	28.65 ± 0.04	30.2 ± 0.5
11	3	0	1.5	95.5	1602 ± 107	-3.0 ± 0.3	79.69 ± 0.02	50.15 ± 0.13
12	0.5	0	1	98.5	761 ± 185	-12.2 ± 0.7	57.43 ± 0.03	12.98 ± 0.05
13	1.8	3	2	93.3	60 ± 3	-12.6 ± 1.9	30.63 ± 0.04	125.0 ± 1.5
14	0.5	3	1.5	95	172 ± 23	-14 ± 2	26.39 ± 0.04	46.9 ± 0.1
15	3	6	2	89	38.2 ± 1.3	-8 ± 2	28 ± 5	141.8 ± 0.5
16	0.5	0	2	97.5	628 ± 46	-11.0 ± 1.4	56.11 ± 0.09	96.9 ± 0.4
17	0.5	6	2	91.5	260 ± 36	-13.3 ± 1.7	26.36 ± 0.03	129.5 ± 0.6

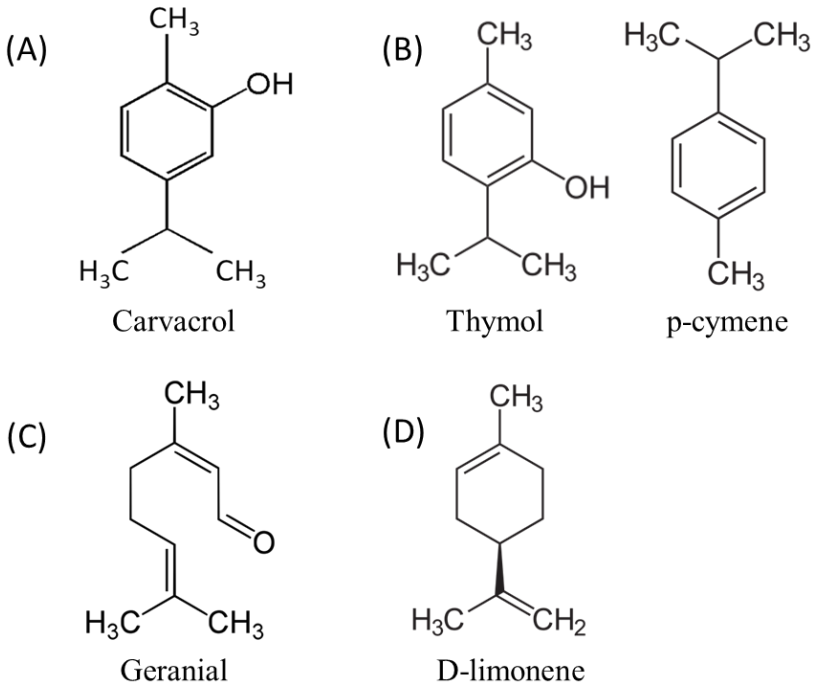

Figure 6 Major components of oregano, thyme, lemongrass and mandarin essential oils being (A) carvacrol, (B) thymol and p-cymene, (C) geranial and (D) D-limonene, respectively.

CHAPTER II: *Curcumin-loaded nanoemulsions stability as affected by the nature and concentration of surfactant*

Artiga-Artigas, M.; Lanjari-Pérez, Y.; Martín-Belloso, O.

Food Chemistry (2018); 266: 466-474

Abstract

Nanoemulsions containing 0.5% *w/w* corn oil enriched with 0.4% *w/w* curcumin, sodium-alginate (1.0% *w/w*) and 0.5, 1.0 or 2.0% *w/w* of surfactant, were assessed, including particle size (nm), ζ-potential (mV) and turbidity over time. Furthermore, nanoemulsions encapsulation efficiency (EE), antioxidant capacity (AC) and release kinetics were studied. Nanoemulsions showed particle sizes ≤ 400±3 nm and effectively reduced droplets interfacial tension with negative ζ-potential values (≤ -37 mV), regardless the concentration of surfactant. Nanoemulsions with 2.0% *w/w* lecithin did not suffer destabilization phenomena during almost 86 days of experiment, whereas those containing Tween 20 or SMP at the same concentrations were destabilized after 5 days or along 24h, respectively. Despite EE of nanoemulsions was above 75%, just in lecithin-stabilized nanoemulsions it was directly correlated to AC. Therefore, this work contributes to elucidate the influence of lecithin, Tween 20 and SMP on curcumin encapsulation and stabilization of curcumin-loaded nanoemulsions.

Keywords: Nanoemulsions; Curcumin; Tween; lecithin; sucrose monopalmitate; release kinetics; encapsulation efficiency.

1. Introduction

Curcumin is a natural polyphenolic flavonoid obtained from *Curcuma longa*, which is known to be an effective bioactive compound to prevent several diseases like cancer, obesity, infectious disease, and cardiovascular illnesses (Aditya et al., 2014). Moreover, since curcumin, considered as a potential antioxidant and antimicrobial agent, does not show toxicity even at high concentrations, its incorporation to food matrices as natural flavoring additive, yellow colorant and preservative is of great interest for the food industry (Borrin, Georges, Moraes, & Pinho, 2016). Curcumin, as the majority of natural pigments, presents high instability under external conditions such as physiological pH, high temperature and light (Schneider, Gordon, Edwards, & Luis, 2015). Moreover, a direct addition of curcumin may cause undesirable changes in the organoleptic properties of some food products providing color, spicy flavor and odor thus decreasing their acceptance by consumers (Borrin et al., 2016). And lastly, the hydrophobic nature of curcumin hinders its incorporation in non-fatty foods and causes the fast elimination of curcumin from the body after its intake, with little absorption in the gastrointestinal tract (Aditya et al., 2014).

Nanostructured delivery systems, however, are useful tools to on one hand, protect, carry and release bioactive compounds; and on the other hand, enhance the bioavailability of lipophilic compounds in aqueous media (Sari et al., 2015). Nanoemulsions, defined as colloidal dispersions with average diameters lower than 500 nm can contain lipophilic ingredients as curcumin in the oil phase and be directly added to aqueous or non-fatty food matrices in liquid state (Otoni et al., 2016).

Nonetheless, the encapsulation and release of bioactive compounds may be influenced by the type of emulsifiers, structural and compositional properties of the emulsion system and other ingredients present within the food matrix (Lee et al., 2017). Therefore, the election of the appropriate surfactant has to be related with the chemical nature of the bioactive compound that will be encapsulated and with the desirable characteristics of the resultant nanostructured system. Regarding the lipophiplic nature of curcumin, surfactants with a high hydrophilic-lipophilic balance (HLB) are the most suitable for the formation of stable oil-in-water (O/W) emulsions (Lee et al., 2017).

Non-ionic polyoxyethylene sorbitan esters, also called Tweens have been frequently used as surfactant due to their ability to rapidly adsorb to the surface of oil droplets and reduce interfacial tension to prevent droplet coalescence (Degner et al., 2014). Similarly, sucrose esters resulted efficient in encapsulating lipid compounds when surfactant-oil ratios are high due to their surface-tension-reducing capacity, dispersion, and exceptional detergent power (Sadtler et al., 2004). Actually, sucrose monoesters such as sucrose monopalmitate, whose chemical structure consists of a lipophilic hydrocarbon tail group (C16:0) and a hydrophilic sucrose head group, are non-ionic emulsifiers that are increasingly utilized by the food and beverage industry as they are biodegradable, non-toxic, with good taste and aroma profile (Szuts & Szabó-Révész, 2012).

Furthermore, there is an increasing interest in using surfactants from natural sources as it is the case of lecithins. Lecithins are amphiphile molecules, which consist of a mixture of phospholipids with adherent glycolipids and oil. They have the capacity of acting as good emulsifiers since their polar head groups, which are bound to lipophilic side chains of esterified fatty acids, contain phosphate and nitrogen moieties that can be ionized. This allows lecithin to form a mechanical barrier around the droplets protecting them against destabilization phenomena such as coalescence or flocculation (Klang & Valenta, 2011).

Therefore, the aim of the present work was to assess the role of three molecularly different surfactants and their concentration on the stability of curcumin-loaded nanoemulsions and evaluate their encapsulation efficiency, antioxidant capacity and physicochemical properties.

2. Materials and methods

2.1.Materials

Corn oil (Koipesol Asua, Deoleo, Spain) enriched with curcumin (from *Curcuma longa*, Sigma-Aldrich, Darmstadt, Germany) was used for preparing all the emulsions. Tween 20 was purchased from Panreac (Barcelona, Spain), whereas L-α-Soybean Lecithin and Sucrose Palmitate (90%) were acquired from Alfa Aesar (Thermo Fisher Scientific, Massachusetts, USA). Sodium alginate (MANUCOL®DH) was obtained from FMC Biopolymer Ltd (Scotland, U.K.). Information provided by the manufacturer indicates that viscosity and pH of a 1% solution is 40-90 mPa·s and 5.0-7.5, respectively. Ultrapure water obtained from a Milli-Q filtration system was used to the preparation of all solutions.

2.2.Methods

2.2.1. Nanoemulsions preparation

Nanoemulsions aqueous phase was prepared by solving 1% *w/w* sodium alginate in ultrapure water at 70ºC for 3 h. After reaching room temperature, the corresponding quantity of Tween 20, lecithin or sucrose monopalmitate at concentrations of 0.5, 1.0 or 2.0% *w/w* was mixed with the aqueous phase until complete dissolution. Secondly, corn oil was enriched with 0.4% *w/w* of curcumin solving the pigment in the oil by magnetic stirring overnight at room temperature in dark conditions. Afterwards, 0.5% *w/w* curcumin-enriched corn oil constituting the lipid phase was added to the aqueous mixture and blended with a high-shear homogenizer (T25 digital Ultra-Turrax, IKA, Staufen, Germany) at 11,000 rpm for 2 min, leading to the formation of coarse emulsions. Lastly, nanoemulsions were formed passing their respective coarse emulsions through a microfluidizer (M110P, Microfluidics, Massachusetts, USA) at 150 MPa for 5 cycles. At the outlet of the interaction chamber of the microfluidizer, the product was refrigerated through an external coil immersed in a water bath with ice maintaining the temperature of the samples below 20 ºC. Nanoemulsions were prepared avoiding the direct contact with light. Besides, pH of all the blends, which remained constant during microfuidization with values around 6.5, was controlled by a pH-meter (Eutech pH 700, Thermo Scientific, Waltham, Massachusetts, USA).

2.2.2. Physicochemical characterization of emulsions and nanoemulsions

2.2.2.1.Droplet size, size distribution and ζ-potential

Particle size distributions and mean droplet diameter (nm) of emulsions and nanoemulsions were measured by a Zetasizer Nano-ZS laser diffractometer (Malvern Instruments Ltd, Worcestershire, UK) working at 633 nm and 25 ºC, equipped with a backscatter detector (173º) (Salvia-Trujillo et al., 2014a).

The ζ-potential (mV), was measured by phase-analysis light scattering (PALS) with a Zetasizer Nano-ZS laser diffractometer (Malvern Instruments Ltd, Worcestershire, UK). It determines the electrical charge at the interface of the droplets dispersed in the aqueous phase.

In both determinations, samples were prior diluted in ultrapure water using a dilution factor of 1:9 sample-to-solvent.

2.2.2.2.Whiteness index

A colorimeter (CR-400, Konica Minolta Sensing Inc., Osaka, Japan) set up for illuminant D65 and 10º observer angle was used to measure the CIE L^*, a^* and b^* parameters of emulsions and nanoemulsions at room temperature. The device was calibrated with a standard white plate (Y =94.0; x = 0.3133; y = 0.3194). The whiteness index (WI) was calculated with equation (1) (Salvia-Trujillo et al., 2014a):

$$WI = 100-((100-L^*)^2+(a^{*2}+b^{*2}))^{0.5} \quad \textbf{eq. (1)}$$

2.2.2.3.Apparent viscosity

Viscosity measurements (mPa·s) were performed by using a vibro-viscometer (SV-10, A&D Company, Tokyo, Japan) vibrating at 30 Hz, with constant amplitude and working at room temperature. Aliquots of 10 mL of each emulsion and nanoemulsion were used for determinations.

2.2.2.4.Turbidity tests

Nanoemulsions turbidity is related to destabilization phenomena such as coalescence, creaming or flocculation among others and was monitored by a Turbiscan Classic (Formulaction, Toulouse, France) during a maximum of 86 days of storage at room temperature. Tests were performed in duplicate.

2.2.2.5.Encapsulation Efficiency (EE, %) and curcumin rate release

Curcumin-loaded nanoemulsion aliquots of 10 mL were placed inside a dialysis tubing cellulose membrane of 43 mm x 27 mm (Sigma-Aldrich, Darmstadt, Germany) and submerged in 20 mL of food grade ethanol. After centrifuging (2000 rpm, 10 min) with a Hettich® Universal 320 centrifuge (Sigma-Aldrich, Darmstadt, Germany) the non-encapsulated curcumin content (free curcumin) was quantified spectrophotometrically with a V-670 spectrophotometer (Jasco, Tokyo, Japan) at 425 nm. Encapsulation efficiency (%) of the obtained nanoemulsions was calculated by equation (2) (Surassmo et al., 2010):

$$\%EE = \frac{Total\ amount\ of\ curcumin - Free\ curcumin}{Total\ amount\ of\ curcumin} \text{ x } 100 \qquad \textbf{eq. (2)}$$

where the total amount of curcumin is the initial concentration of this bioactive compound added to the mixture and the free curcumin is the concentration of compound that was not loaded in nanoemulsions.
All the measurements were performed in triplicate.

In order to monitor the curcumin rate release, aliquots of the samples were taken at times 0, 3, 6 and 24 h and quantified spectrophotometrically with a V-670 spectrophotometer (Jasco, Tokyo, Japan) at 425 nm. The curcumin release was calculated with equation (3) according to Surassmo et al. (2010) and fitted to a rectangular hyperbolic curve according to equation (4):

$$\%CR = (100 - \frac{Total\ amount\ of\ curcumin\ (t=0) - Released\ curcumin(t=t)}{Total\ amount\ of\ curcumin\ (t=0)}) \text{x } 100 \qquad \textbf{eq. (3)}$$

$$CR = \frac{at}{b+t} \qquad \textbf{eq. (4)}$$

where CR is the curcumin release expressed in %, *t* is the time (h), *a* is the maximum curcumin release (%) and *b* is a kinetic constant (h).

2.2.2.6.Antioxidant capacity of curcumin

The antioxidant capacity of curcumin-loaded nanoemulsions was determined by two assays: DPPH and FRAP. Although both methods can properly determine the presence of curcumin, the main difference between them is that DPPH assay is based on the presence of radicals (DPP·), whereas FRAP consists of an electrons exchange (Thaipong et al., 2006).

DPPH procedure was conducted according to the method of Brand-Williams, W.; Cuvelier, M. E. & Berset, (1995) with some modifications. The DPPH radical solution was prepared by dissolving 2.5 mg of DPPH radical in 100 mL of methanol. The absorbance of solution was adjusted to 0.7 ± 0.02 at 515 nm. Aliquots of 20 μL of sample were placed in a microplate and 280 μL of DPPH radical solution was added to each sample. Samples were incubated for 30 min in the dark and the absorbance was measured.

FRAP assay was carried out as described by Benzie & Strain (1996) where 20 μL of sample were placed into each tube and mixed with 280 μL of FRAP solution. The samples were incubated at room temperature in the dark for 30 min and the absorbance was measured at 630 nm after prior filtration.

Results were reported as mg of Trolox equivalents per mL of solution (mg TE/mL) using a standard curve of Trolox (Velderrain-Rodríguez et al., 2015). In both methods, triplicate determinations were made at each dilution of the standard.

2.2.3. Statistics

All the experiments were assayed at least in duplicate, and three replicate analyses were carried out for each parameter. SigmaPlot 12.0 Systat Software was used to perform the analysis of

variance. Tukey test was chosen to determine significant differences among the use of different surfactants and concentrations, at a 5% significance level. Correlation analyses were performed with statistical analysis software (SigmaPlot 12.0 Systat Software, London, UK).

Curcumin release curve was generated and statistically analyzed at a 5% significance level using Statgraphics Centurion XVII (Statgraphics Technologies INC, Virginia, USA). The output showed the results of fitting a nonlinear regression model to describe the relationship between CR and t independent variables. The R-Squared statistic indicates that the model as fitted explains 100.0% of the variability in CR.

3. Results and discussion

3.1.Mean particle size and particle size distribution

Particle sizes of curcumin-loaded nanoemulsions ranged from 322 ± 3 to 400 ± 3 nm in nanoemulsions containing lecithin; from 249 ± 6 to 276 ± 6 nm in the case of using Tween 20 as surfactant and from 350 ± 6 to 380 ± 13 nm if sucrose monopalmitate was used (Table 1). It indicated a clear influence not only of the type of surfactant added but also of its concentration on nanoemulsions particle size. Actually, in nanoemulsions with lecithin and Tween 20, the higher the surfactant concentration, the lower the particle size of nanoemulsion. This is in agreement with literature since low-mass surfactants such as polysorbates (Tween 20) and lecithins are known to rapidly coat the surface of the created oil-water interface during emulsification (Salvia-Trujillo et al., 2014a). Thus, during microfluidization, the newly formed droplets due to mechanical stress are rapidly surrounded by surfactant molecules, which are adsorbed to droplet surface, decreasing interfacial tension between droplets and favoring droplets' disruption (Salvia-Trujillo et al., 2014a).

Moreover, lecithin contains negative charges from its phosphate groups providing repulsive electrostatic interactions needed to avoid coalescence, which is reflected in the low polydispersity index (PdI) of nanoemulsions stabilized by this surfactant (Zhang et al., 2012). As can be observed in Table 1, PdI of curcumin-loaded nanoemulsions containing lecithin did not show significant differences at concentrations ≤ 1.0% *w/w* of surfactant, while it increased when 2.0% *w/w* was added, which fits with the growth of a small peak in the micro-sized region (Figure 1). An excess of lecithin may lead to the formation of aggregates between the surfactant chains themselves or with alginate molecules (Artiga-Artigas, Acevedo-Fani, & Martín-Belloso, 2017). Therefore, it is important to use a lecithin-oil ratio of at least 1:2 necessary to on one hand, assure the complete coating of lipid droplets surface with adsorbed surfactant molecules in order to prevent re-coalescence; and on the other hand, avoid the excess of surfactant able to re-aggregate (Qian & Mcclements, 2011).

Tween 20 is a non-ionic surfactant formed by a polyoxyethilene head group and a single hydrocarbon tail (C12:0 tail) that has widely demonstrated great ability to stabilize nanoemulsions even at low concentrations (Salvia-Trujillo, Soliva-Fortuny, Rojas-Graü, McClements, & Martín-Belloso, 2017). Accordingly, our results showed that nanoemulsions containing this surfactant showed an average PdI value of $0.27 \pm 4 \cdot 10^{-3}$ and monomodal distributions regardless the concentration of Tween 20, which highlighted its emulsifying properties (Table 1).

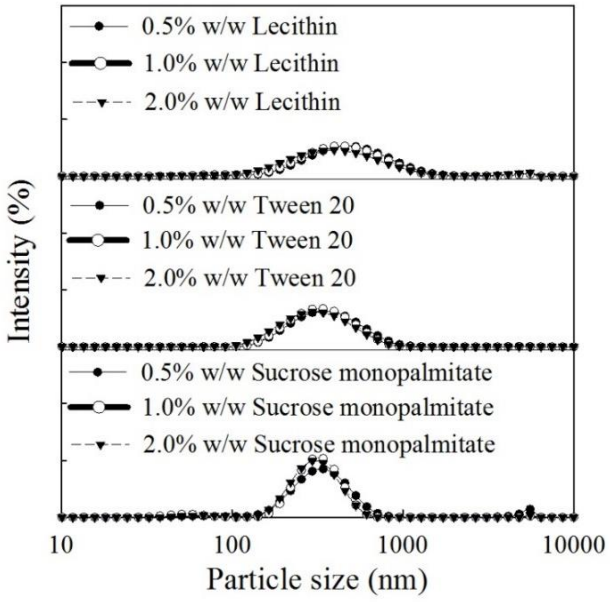

Figure 1. Particle size distributions of curcumin-loaded nanoemulsions containing sodium alginate solution as aqueous phase (1% *w/w*) and 0.5% *w/w* of corn oil enriched with 0.4% *w/w* of curcumin as dispersed phase; stabilized by lecithin, Tween 20 or sucrose monopalmitate at different concentrations: 0.5, 1.0 and 2.0% *w/w*. Microfluidization processes were performed at 150 MPa and for 5 cycles.

Oppositely, particle sizes of curcumin loaded nanoemulsions containing sucrose monopalmitate were the largest and varied in a wide range regardless the concentration of surfactant leading to the highest PdI (0.5 ± 0.02). One possible explanation is that commercial sucrose monopalmitate usually contains a mixture of different molecular species, e.g., diesters as well as monoesters, and other types of fatty acids that can interfere in the proper emulsification process (Rao & McClements, 2011b). In fact, particle size distributions of nanoemulsions containing sucrose monopalmitate shown in Figure 1 confirmed the presence of a small peak in the micro-size region for any concentration of surfactant, which was in accordance with their high PdI values (Table 1). These minor peak can be attributed to the presence of surfactant micelles that were not adsorbed at the oil droplets interface due to an excess of alginate molecules that had been repelled (Artiga-Artigas et al., 2017).

Table 1. Physicochemical properties of curcumin-loaded nanoemulsions containing different concentrations of surfactants.

Surfactant	Concentration (*w/w*)	Droplet diameter (nm)	Polydispersity index (PdI)	ζ-potential (mV)	Color (WI)	Viscosity (mPa·s)	pH
Lecithin	0.5%	400 ± 3^{a}	0.37 ± 0.05^{a}	-85.3 ± 1.7^{a}	57.3 ± 0.3^{a}	25.4 ± 0.9^{a}	6.53 ± 0.02^{a}
	1.0%	354 ± 5^{a}	0.33 ± 0.04^{a}	-85.4 ± 1.5^{a}	57.2 ± 0.3^{a}	29.6 ± 0.3^{a}	6.43 ± 0.02^{a}
	2.0%	322 ± 3^{a}	0.40 ± 0.03^{a}	-85.5 ± 1.8^{a}	59.45 ± 0.15^{a}	33.0 ± 0.7^{a}	6.65 ± 0.02^{a}
Tween 20	0.5%	276 ± 6^{b}	0.270 ± 0.014^{b}	-40 ± 3^{b}	47.0 ± 0.3^{b}	30.1 ± 1.4^{a}	6.627 ± 0.006^{a}
	1.0%	268 ± 5^{b}	0.263 ± 0.012^{b}	-35.0 ± 2.0^{b}	47.7 ± 0.3^{b}	31.3 ± 0.7^{a}	6.55 ± 0.02^{a}
	2.0%	249 ± 6^{b}	0.268 ± 0.010^{b}	-36.0 ± 1.9^{b}	45.75 ± 0.19^{b}	30 ± 2^{a}	6.627 ± 0.006^{a}
Sucrose palmitate	0.5%	350 ± 6^{a}	0.52 ± 0.09^{c}	-70 ± 3^{c}	60.60 ± 0.18^{c}	35.5 ± 0.4^{a}	6.37 ± 0.02^{a}
	1.0%	380 ± 13^{a}	0.53 ± 0.03^{c}	-66.4 ± 1.8^{c}	63.64 ± 0.18^{c}	96.6 ± 0.6^{b}	6.46 ± 0.03^{a}
	2.0%	373 ± 11^{a}	0.54 ± 0.05^{c}	-65 ± 2^{c}	64.57 ± 0.23^{c}	137 ± 5^{c}	6.35 ± 0.02^{a}

[a,b,c] Means in same column with different letters are significantly different at $p < 0.05$ in terms of comparing surfactant type and concentration.

3.2.ζ-potential measurements

All curcumin loaded nanoemulsions exhibited ζ-potential values below -30 mV (Table 1). The presence of sodium alginate, with carboxylate ($-CO_2^-$) and hydroxyl ($-OH^-$) groups, plays a relevant role in the electrostatic stabilization of nanoemulsions. Negative alginate molecules adsorption to the surface of oil droplets may confer them enough negative charge to avoid destabilization phenomena such as coalescence (B Heurtault, 2003). The lowest ζ-potential values were obtained for nanoemulsions containing lecithin with values around -85 ± 1.6 mV without significant differences ($P<0.05$) regardless the concentration of surfactant. Soybean lecithin contains different types of phospholipids including phosphatidylserine (PS), phosphatidic acid (PA), phosphatidylglycerol (PG), phosphatidylinositol (PI), phosphatidylethanolamine (PE), and phosphatidylcholine (PC), whose molecular structures can be observed in Figure 2.

Nanoemulsions containing lecithin showed a pH around 6.5, which means that phosphate groups from these phospholipids are negatively charged, except PE and PC that are zwitterionic and neutral molecules since the nitrogen from the amino group is positively charged (Figures 2E and 2F, respectively). Negative charges from phosphate groups contribute to decrease the droplets surface charge thus making the ζ -potential more negative (Zhang et al., 2012). It is reported that non-ionic surfactants such as Tween 20 and sucrose monopalmitate can contribute to decrease the ζ-potential values even in absence of biopolymer due to the presence of impurities such as free fatty acids from the oil or the surfactants (Celus et al., 2018). Also, the adsorption and orientation of OH^- groups from water in the vicinity of oil droplets can contribute to decrease the surface charge (Marinova et al., 1996). However, huge differences in ζ-potential between both non-ionic surfactants were also observed (Table 1). Indeed, ζ-potential values of nanoemulsions with sucrose monopalmitate were considerably lower than those from nanoemulsions stabilized by Tween 20 (around -67 ± 3 mV against -36 ± 2 mV, respectively). Sucrose monopalmitate can contain some anionic molecules such as impurities (*e.g.* palmitic acid) or those resulting of some chemical degradation as hydrolysis of the surfactant molecule into sucrose and palmitic acid in aqueous solution, which are able to adsorb to the oil droplet surfaces decreasing the ζ-potential (more negative) (Henry, Fryer, Frith, & Norton, 2009).

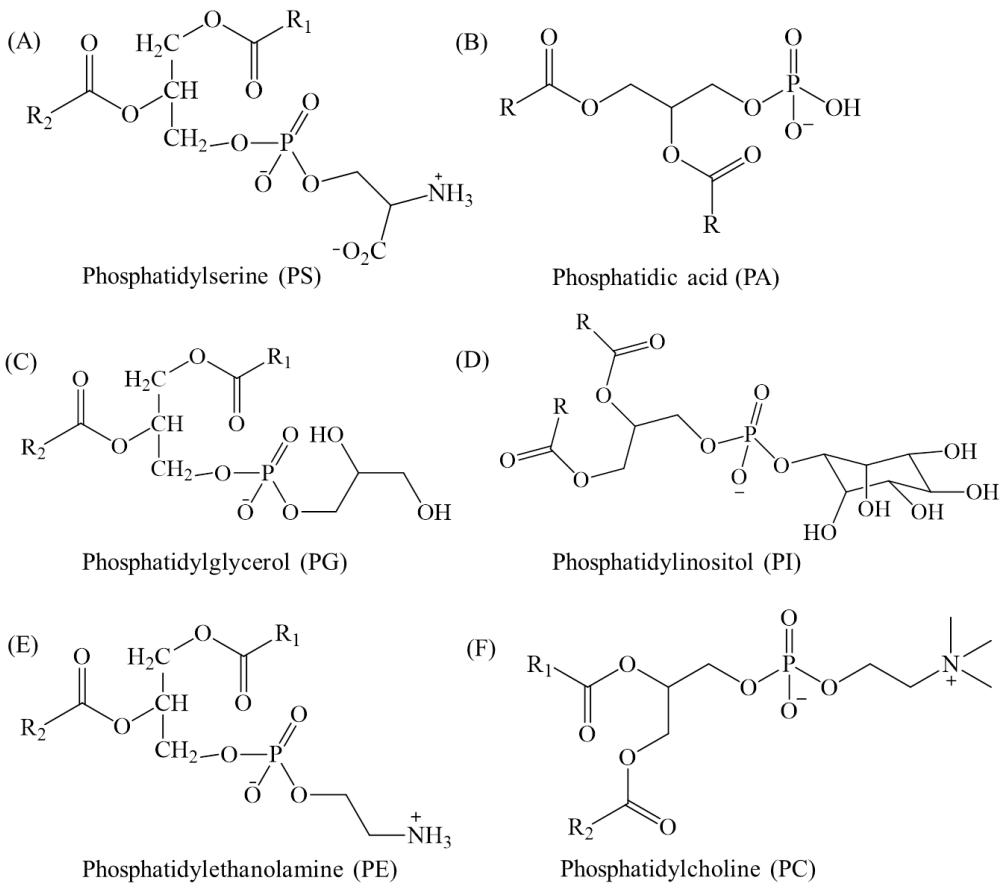

Figure 2. Molecular structure of the lecithin phospholipids drawn with ChemBioDraw® Ultra 12.0 (Cambridgesoft, PerkinElmer Inc., Madrid, Spain): (A) Phosphatidylserine, (B) Phosphatidic acid, (C) Phospatidylglycerol, (D) Phosphatidylinositol, (E) Phophatidylethanolamine and (F) Phosphatidilcoline.

3.3.Whiteness index (WI)

Table 1 compiled the whiteness index (WI) of the prepared curcumin loaded nanoemulsions. All of them presented yellow color and high opacity due to the presence of curcumin and corn oil, respectively. Nanoemulsions containing corn oil as lipid phase usually experiment an increase of the whiteness index after microfluidization due to its intense color (Ekthamasut & Akesowan, 2010; Salvia-Trujillo et al., 2014). Corn oil contains long chain saturated (including palmitic acid (C16:0), stearic acid (C18:0) and arachidic acid (C20:0)), monounsaturated (oleic acid (C18:1)) and polyunsaturated (ω-6 linoleic acid (C18:2)) fatty acids (Beadle, Just, Morgan, & Reiners, 1964). Thus, it presents very low solubility in water, which provoke the increase of blends opacity due to the huge difference between the refractive index of continuous and dispersed phases (Ekthamasut & Akesowan, 2010). Even so, although all the nanoemulsions in the present work contained the same quantity of oil and curcumin, they exhibited variations in their WI depending on the type of surfactant used ranging from 57.2 ± 0.3 to 59.45 ± 0.15, 45.75 ± 0.19 to 47.7 ± 0.3 and between 60.60 ± 0.18 to 64.57 ± 0.23 for lecithin, Tween 20 and sucrose monopalmitate, respectively (Table 1).

In general, the lowest WI values were observed in those nanoemulsions with the smallest particle sizes. Therefore, curcumin loaded nanoemulsions containing 2.0% *w/w* of Tween 20, in which particle sizes of 249 ± 6 nm were observed, showed the lowest WI with a value of 45.75 ± 0.19. In contrast, WI values for nanoemulsions stabilized with lecithin and sucrose monopalmitate, which are colored powders, were higher than those obtained for nanoemulsions containing Tween 20 and increased with the concentration of surfactant. Large molecules such as those from free surfactant chains can scatter the light more intensely than smaller ones causing an increase in the lightness, opacity and whiteness index of emulsions (McClements & Rao, 2011; Salvia-Trujillo et al., 2014a).

3.4.Apparent viscosity

Apparent viscosity of curcumin loaded nanoemulsions ranged from 25.4 ± 0.9 to 137 ± 5 mPa·s. It is well-known that, usually, an increased concentration of surfactant lead to a decrease in the particle size (Salvia-Trujillo et al., 2014a), which according to McClements & Rao (2011) could have an impact on nanoemulsion viscosity. As have been discussed above, low mass surfactants have high mobility at the interface thus promptly adsorbing to droplet surfaces decreasing the surface or interfacial tension between them (Sari et al., 2015). In this regard, lecithin and Tween 20 may facilitate droplet disruption leading to small particle sizes, and protect droplets against destabilization phenomena as re-coalescence or flocculation (Salvia-Trujillo et al., 2014a). Indeed, apparent viscosities of nanoemulsions stabilized by lecithin or Tween 20, were the lowest and not significantly different ($P<0.05$) with mean values of 29.9 ± 2.5 mPa·s regardless the concentration of surfactant (Table 1). That is probably because the apparent viscosity is mainly dominated by the concentration of sodium alginates, which like other hydrocolloids, may lead to a considerable increase in solution viscosities, and/or induce gelation even at low concentrations (Gaonkar, 1991).

Nevertheless, the apparent viscosity of nanoemulsions containing sucrose monopalmitate increased from 35.5 ± 0.4 to 137 ± 5 mPa·s when raised the concentration of surfactant from 0.5 to 2.0% *w/w* (Table 1). This is in agreement with (Sadtler et al., 2004), who observed a gel-liquid transition in the rheological properties of emulsions stabilized by sucrose monopalmitate. That means that sucrose monopalmitate has the capacity of forming viscous or gel-like systems being these systems even more viscous at low temperatures and high concentrations of surfactant. One possible explanation is that nanoemulsions containing 0.5% *w/*w of sucrose monopalmitate showed low viscosities due to almost all surfactant chains will be bound to the oil droplets surfaces and hence, there will be less sucrose monopalmitate available to contribute in the formation of a gel phase (Rao & McClements, 2011b). Other authors also reported an increase in viscosity as the concentration of sucrose monopalmitate raised due to a higher droplets flocculation or the re-aggregation of free surfactant molecules or between the surfactant and sodium alginate chains (Artiga-Artigas et al., 2017).

Moreover, molecular structure of sucrose monopalmitate consist of lipophilic hydrocarbon tail groups (C16:0) bound to sugars that can act as feed source for some microorganisms. This favors their proliferation and biofilms formation and contributes to increase the viscosity of nanoemulsions even in presence of curcumin, which has antimicrobial properties (Raffa, Wever, Picchioni, & Broekhuis, 2015). In this regard, curcumin would not be preventing biofilms formation in these nanoemulsions containing sucrose monopalmitate. It suggests that curcumin is not being effectively protected by this nanostructured system and experiments degradation.

3.5.Turbidity

As it can be observed in Figure 3, those curcumin-loaded nanoemulsions with a concentration of lecithin higher than 1% *w/w* resulted long-term stable because they do not suffer sedimentation and coalescence phenomena until 86 days of storing (Figure 3B and 3C). Lecithin molecules are able to form a multilamellar shell around each oil droplet acting as an effective structural-mechanical barrier that prevents re-coalescence and therefore, preserve the stability of nanoemulsions (Klang & Valenta, 2011). However, at lower concentrations of lecithin (0.5% *w/w*), destabilization occurred after the first 8 days of room temperature storage. It could be probably due to a ratio oil:lecithin lower than 1:2 that may facilitate coalescence since there is a lack of surfactant molecules around droplets. In this regard, oil droplets will tend to come together forming bigger ones thus promoting phase separation (Goddard, 2002; Qian & Mcclements, 2011).

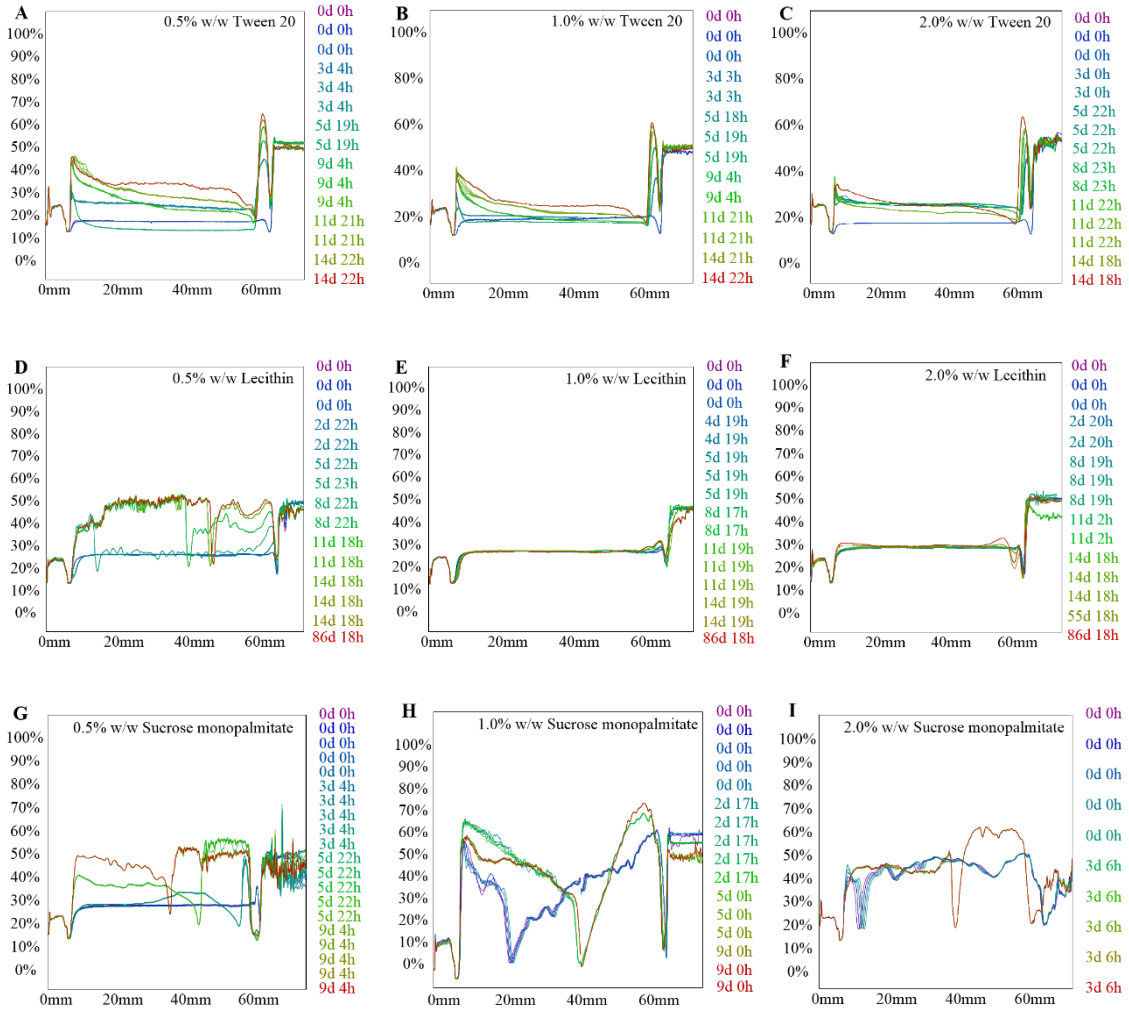

Figure 3. Back scattering distribution of curcumin-loaded nanoemulsions containing sodium alginate solution as aqueous phase (1% *w/w*) and 0.5% *w/w* of corn oil enriched with 0.4% *w/w* of curcumin as dispersed phase; stabilized by 0.5, 1.0 and 2.0% *w/w* Tween 20 (A, B, C), lecithin (D, E, F) or sucrose monopalmitate (G,H,I); during room temperature storage.

Horizontal lines in the Turbiscan images (Figure 3) indicate variations in the particle sizes of nanoemulsions. Therefore, as it can be observed in Figure 3F, horizontal lines in the turbidity test of nanoemulsions containing 2% *w/w* of Tween 20 experimented fewer variations than those with 0.5 or 1.0% *w/w* of this surfactant (Figures 3D and 3E, respectively) regarding the initial line at time 0.

However, Tween 20 could not avoid sedimentation and creaming apparition from the 5 day of storage regardless the concentration of surfactant (Figures 3D, 3E and 3F). According to our prior studies, after microfluidization, sodium alginate chains may suffer a partial hydrolysis. Thus, sodium alginate can re-aggregate over time varying the registered particle sizes and causing phase destabilization phenomena such as creaming or sedimentation (Artiga-Artigas, Acevedo-Fani, & Martín-Belloso, 2017). The most unstable nanoemulsions were those containing sucrose monopalmitate in which the destabilization was almost immediate for any concentration of surfactant observing the appearance of many destabilization phenomena including clarifications, sedimentation, flocculation and coalescence during the first following hours after preparation (Figures 3G, 3H, 3I and 4).

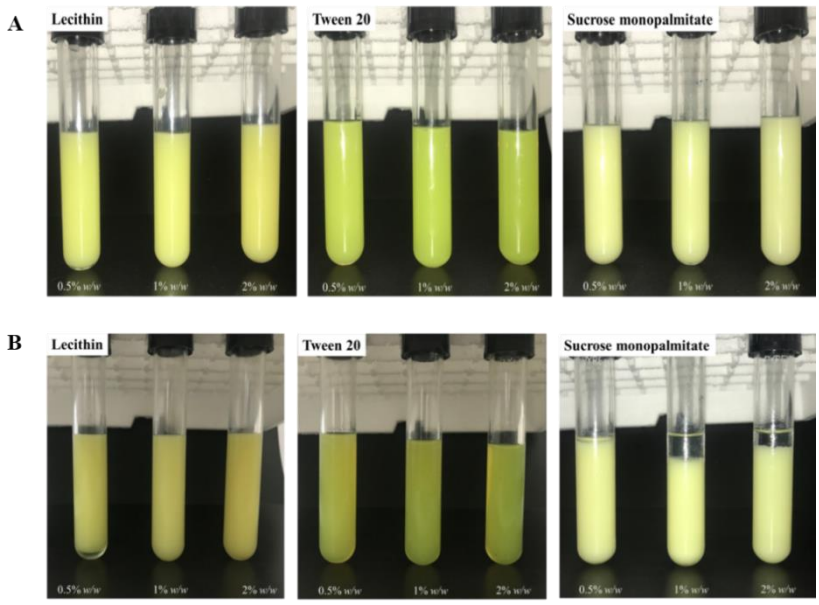

Figure 4. Nanoemulsions stabilized by different concentrations of lecithin, Tween 20 or sucrose monopalmitate when they are fresh (A) and during the first 24 h of storage (B).

For this reason, in nanoemulsions containing 2.0% *w/w* of sucrose monopalmitate, turbidity tests could be just performed during 3 days of room temperature storage (Figure 3I). As discussed in the previous section, the presence of sugars may favor the growth of different microorganisms such as mesophiles that are able to proliferate at room temperature (Sadiq et al., 2017). Therefore, microbial growth may cause changes in the physicochemical properties of curcumin-loaded nanoemulsions due to the production of biofilms, which triggers a phase separation and their immediate destabilization (Raffa et al., 2015).

3.6.Encapsulation efficiency and curcumin release (%)

In general, all the prepared curcumin-loaded nanoemulsions exhibited EE over 75% (Table 2) and high retention of curcumin (Figure 5). The curcumin release (%) after dialysis and centrifugation was monitored during the first 24h and the data obtained from equation (3) was plotted (Figure 6). The resultant curve properly fitted with equation (4) with determination coefficients of 0.99 from which, coefficients *a* and *b* that corresponds to the maximum curcumin release (%) and the kinetic constant (h), respectively; were obtained (Table 3).

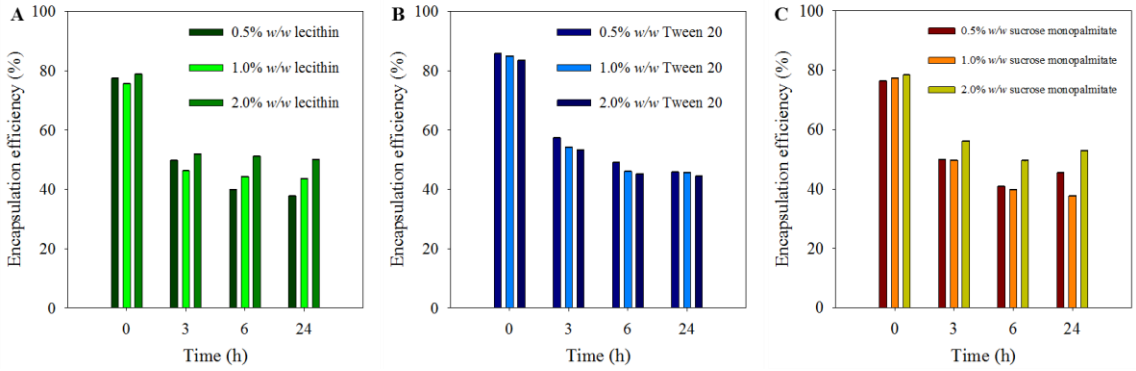

Figure 5. Encapsulation efficiency (%) of curcumin-loaded nanoemulsions containing sodium alginate solution as aqueous phase (1% *w/w*) and 0.5% *w/w* of corn oil enriched with 0.4% *w/w* of curcumin as dispersed phase; stabilized by (A) Lecithin, (B) Tween 20 or (C) Sucrose monopalmitate at different concentrations: 0.5, 1.0 and 2.0% *w/w*. Microfluidization processes were performed at 150 MPa and for 5 cycles.

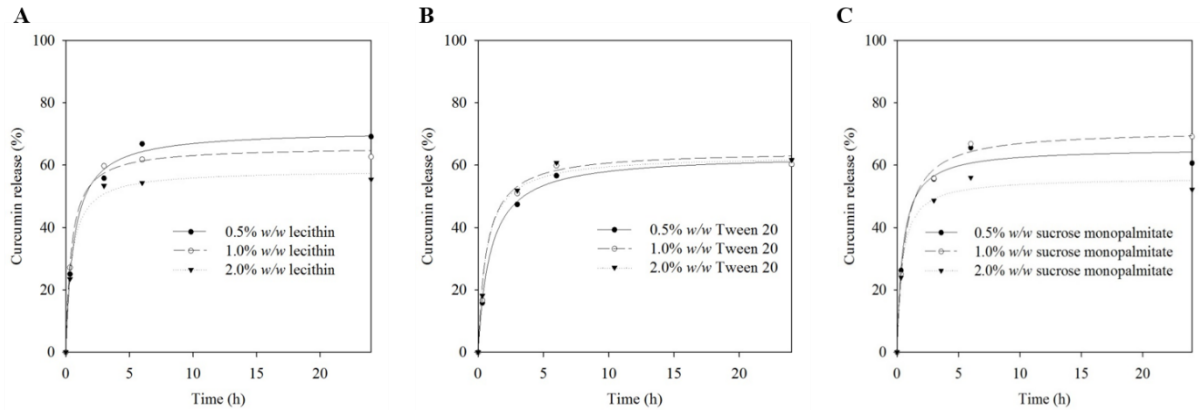

Figure 6. Curcumin release (%) of nanoemulsions during 24h follows equation (4): CR = *at/(*b*+t). Aqueous phase of nanoemulsions contained sodium alginate (1% *w/w*) and their dispersed phase 0.5% *w/w* of corn oil enriched with 0.4% *w/w* of curcumin; and were stabilized by (A) lecithin, (B) Tween 20 or (C) sucrose monopalmitate at different concentrations. Microfluidization processes were performed at 150 MPa and for 5 cycles and curcumin-loaded nanoemulsions were stored at room temperature.**

Table 2. Antioxidant capacity of curcumin-loaded nanoemulsions reported as µg of Trolox equivalents (TE) per g of nanoemulsion, their encapsulation efficiency (EE, %) and Pearson correlation coefficients (r) between both parameters. The control absorbance in the DPPH assay was 0.7930 ± 0.0001 and in the FRAP method it was 0.0915 ± 0.0005.

Surfactant	Concentration (w/w)	DPPH µgTE/g	FRAP µgTE/g	Encapsulation efficiency (%)	$r_{DPPH-EE}$	$r_{FRAP-EE}$
Lecithin	0.5%	1120.3 ± 1.6^{Aa}	99.67 ± 0.15^{Aa}	$77.46 \pm 4 \cdot 10^{-3\ Aa}$		
	1.0%	1503 ± 7^{Ab}	194.97 ± 0.12^{Ab}	$75.56 \pm 4 \cdot 10^{-4\ Aa}$	0.51^{*}	0.23^{*}
	2.0%	1904 ± 4^{Ac}	240.5 ± 0.1^{Ac}	$78.84 \pm 6 \cdot 10^{-3\ Ab}$		
Tween 20	0.5%	792 ± 3^{Ad}	212.1 ± 0.1^{Aa}	$85.74 \pm 3 \cdot 10^{-4\ Ba}$		
	1.0%	1029 ± 4^{Ae}	177.2 ± 0.1^{Ab}	$85 \pm 1 \cdot 10^{-2\ Bb}$	-0.99	0.32^{*}
	2.0%	1279 ± 6^{Af}	195.3 ± 0.1^{Ac}	$83.62 \pm 4 \cdot 10^{-3\ Bc}$		
Sucrose palmitate	0.5%	1239 ± 3^{Ag}	180.1 ± 0.2^{Aa}	$76.41 \pm 8 \cdot 10^{-4\ Bc}$		
	1.0%	1405 ± 3^{Ah}	126.8 ± 0.2^{Ab}	$77.46 \pm 6 \cdot 10^{-5\ Bd}$	-0.45^{*}	-0.5^{*}
	2.0%	1091 ± 3^{Ai}	154.8 ± 0.2^{Ac}	$78.41 \pm 6 \cdot 10^{-4\ Be}$		

Data are means of at least three determinations (n = 3) ± standard deviation. Different letters were assigned to the values of means with significant differences ($p < .05$) within columns. ^{A,B,C} Mean in same column with different capital letters are significantly different at $p < 0.05$ in terms of comparing the type of surfactant at the same concentrations. ^{a,b,c} Mean in same column with different lower case letters are significantly different at $p < 0.05$ in terms of comparing surfactant concentration. *There are no significant relationships between any pair of variables in the correlation table ($P > 0.050$).

Table 3. Coefficients of the mathematical model built to model the curcumin release along the storage.

Surfactant	Concentration (*w/w*)	*a* (%)	*b* (h)	R^2
Lecithin	0.5%	71.3 ± 2.0 [a]	0.65 ± 0.12 [a]	0.996
	1.0%	65.9 ± 1.5 [b]	0.44 ± 0.08 [b]	0.997
	2.0%	58.3 ± 1.6 [c]	0.45 ± 0.09 [c]	0.995
Tween 20	0.5%	63.7 ± 1.3 [b]	0.97 ± 0.109 [a]	0.998
	1.0%	64.9 ± 2.3 [b]	0.84 ± 0.18 [d]	0.994
	2.0%	65.8 ± 1.9 [b]	0.80 ± 0.14 [d]	0.996
Sucrose palmitate	0.5%	65.4 ± 2.9 [b]	0.47 ± 0.15 [e]	0.988
	1.0%	71.3 ± 2.0 [a]	0.65 ± 0.12^{-5} [a]	0.996
	2.0%	56.0 ± 2.1 [d]	0.42 ± 0.12 [e]	0.990

[a,b,c,d,e] Means in same column with different lower case letters are significantly different at $p < 0.05$ in terms of comparing surfactant type and concentration. Curcumin release fits equation (4): $CR = at/(b+t)$ in which, the coefficient *a* referred to the maximum curcumin release (%) and coefficient *b* is the kinetic constant.

Nanoemulsions containing Tween 20 showed the highest EE values at time 0 resulting even more effective at low surfactant concentrations (0.5% *w/w*). Moreover, the maximum curcumin release of these nanoemulsions did not significantly vary with the concentration of surfactant ($a \approx 64\%$) suggesting that Tween 20-stabilized nanoemulsions were able to retain around a 40% of curcumin after 24 h of study. This can be explained due to the low surface tension between droplets covered with Tween 20, which prevented droplets coalescence and improved curcumin solubility ensuring its retention (Ratanajiajaroen, Watthanaphanit, Tamura, Tokura, & Rujiravanit, 2012). This is in accordance with the high stability of nanoemulsions containing over 1% *w/w* of Tween 20 observed in the turbidity evaluation. Indeed, those nanoemulsions containing Tween 20 at 1.0 or 2.0 *w/w* destabilized more slowly than those with 0.5% *w/w* (Figures 3 and 4). In fact, nanoemulsions with surfactant concentrations of 0.5% *w/w* showed the fastest release of curcumin with a kinetic constant (*b*) of 0.97 h, which is specified in Table 3. This trend was also observed by Petchsomrit, Sermkaew, Wiwattanapatapee, & Materials (2013), who reported that low concentrations of Tween produced an incomplete solubilization of curcumin thus provoking its release.

On the contrary, EE of nanoemulsions with lecithin or sucrose monopalmitate increased as the concentration of surfactant raised up to 2% *w/w*. Moreover, nanoemulsions stabilized by lecithin and sucrose monopalmitate at this concentration, were able to maintain EE around 50% during at least the 24 hours of study (Figure 5). In addition, they slowly released the bioactive compound as it can be demonstrated with their small kinetic constants (0.45 ± 0.09 h and 0.42 ± 0.12 h), respectively (Table 3). In the case of nanoemulsions containing lecithin as surfactant the effectiveness in curcumin

retention can be explained because the phenolic hydroxyl of curcumin moiety can form H-bonds with the phosphate ion of PC (Figure 2). Thus, the two long aliphatic chains of this phospholipid are wrapped around the curcumin thus favoring its retention within the droplets (Kumar, Ahuja, & Sharma, 2008). In this regard, the higher the concentration of lecithin, the higher the number of available phosphate ions and hence, the slower the curcumin release, which is in consequent with the great stability of these nanoemulsions. The slow curcumin release of nanoemulsions containing high concentrations of sucrose monopalmitate seems contradictory to what was previously discussed in turbidity section, where a fast destabilization of these nanoemulsions was observed regardless the concentration of surfactant (Figure 3). Nevertheless, Ntawukulilyayo, Demuynck, & Remon (1995) also observed that sucrose esters strongly influenced bioactive compounds release due to the H-bond formation between its hydrophilic groups and those of the ester resulting in a slow release of the bioactive compound. Likewise, hydroxyl groups (OH^-) of curcumin molecule may establish hydrogen bonds with the sugar heads from sucrose monopalmitate thus remaining not encapsulated but held in the surfactant structure (Szuts & Szabó-Révész, 2012).

3.7.Antioxidant capacity

Antioxidant capacity of curcumin-loaded nanoemulsions and nanoemulsions without curcumin (as controls) expressed as μg of Trolox equivalents (TE) per g of nanoemulsion is shown in Table 2 and Table 4, respectively. In general, the nanomeulsions antioxidant capacity measured by FRAP assay did not present significant differences regardless the concentration of surfactant. However, the antioxidant capacity values obtained by FRAP assay were significantly lower than by DPPH. FRAP assay is based on the reducing power of curcumin-loaded nanoemulsions. It consists of detecting the reduction of ferric ion (Fe^{3+}) into ferrous iron (Fe^{2+}) using ferrozine as dye (Cheung, Nigam, & Owusu-Apenten, 2016). In this regard, if some species are reduced, others have to be oxidized. According to Priyadarsini (2014), the three active sites of curcumin can suffer oxidation by electron transfer and hydrogen abstraction. Detailed research by different groups have confirmed that during free radical reactions, the phenol-OH group is the most easily abstractable hydrogen from curcumin, resulting in formation of phenoxyl radicals, which are resonance stabilized across the keto-enol structure. In this regard, curcumin may undergo an autoxidative degradation leading to the formation of bicyclopentadione, ferulic acid and other derivatives, which in fact, could alter the EE of nanoemulsions (Schneider et al., 2015). Moreover, as it is shown in Table 4, the three surfactants presented antioxidant capacity themselves thus suggesting a synergistic effect between them and curcumin on the antioxidant capacity.

Curcumin loaded nanoemulsions containing 2.0% *w/w* of lecithin exhibited the maximum antioxidant capacity for DPPH and FRAP assays (23,800.9 mgTE/g and 3,005.3 mgET/g, respectively). Antioxidant capacity of nanoemulsions containing lecithin was slightly correlated to the EE (Table 2). In this regard, the higher the EE of nanoemulsions, the higher their antioxidant capacity, which indeed can be related to the demonstrated great capacity of lecithin to stabilize nanoemulsions (Kumar et al., 2008). Lecithin contains phosphate ions that are able to interact with phenolic hydroxyls of curcumin through the formation of H-bonds favoring the efficient entrapping of the bioactive compound inside of phospholipids lipophilic chains, especially at lecithin concentrations of 2% *w/w*. As observed by Pan, Tikekar, & Nitin (2013) lecithin is able to reduce the rate of permeation of peroxyl radicals across the emulsion interface suggesting that its interfacial barrier properties conferred lecithin high antioxidant capacity.

Table 4. Antioxidant capacity of nanoemulsions without curcumin reported as µg of Trolox equivalents (TE) per g of nanoemulsion. The control absorbance in the DPPH assay was 0.7088 ± 0.0001 and in the FRAP method it was 0.1662 ± 0.0007.

Surfactant	Concentration (*w/w*)	DPPH µgTE/g	FRAP µgTE/g
Lecithin	0.5%	316 ± 188^{Aa}	2.21 ± 0.15^{Aa}
	1.0%	540 ± 101^{Ab}	1.73 ± 0.07^{Ab}
	2.0%	491 ± 59^{Ab}	3.5 ± 0.7^{Bc}
Tween 20	0.5%	569 ± 58^{ABa}	1.3 ± 0.2^{Aa}
	1.0%	816 ± 182^{ABb}	2.0 ± 0.4^{Ab}
	2.0%	1198 ± 761^{ABc}	1.81 ± 0.25^{Ac}
Sucrose palmitate	0.5%	662 ± 6^{Bab}	3.35 ± 1.42^{Bab}
	1.0%	500 ± 8^{Ba}	3.6 ± 0.3^{Ba}
	2.0%	682 ± 6^{Bb}	2.1 ± 0.1^{Bb}

Data are means of at least three determinations (n = 3) ± standard deviation. Different letters were assigned to the values of means with significant differences (p <.05) within columns.

^{A,B,C} Mean in same column with different capital letters are significantly different at $p < 0.05$ in terms of comparing the type of surfactant at the same concentrations.

^{a,b,c} Mean in same column with different lower case letters are significantly different at $p < 0.05$ in terms of comparing surfactant concentration.

Similarly, in nanoemulsions containing Tween 20 antioxidant capacities varied regarding the concentration of surfactant and depending on the scavenging assay for curcumin determination used. Regarding DPPH method, the highest antioxidant capacity was observed for 2.0% *w/w* of Tween 20, whereas the highest EE was observed by Tween 20 concentrations of 0.5% *w/w*. This inverse proportionality is reflected in their negative correlation coefficients with values of -0.99 regarding DPPH assay. Although based on our results high concentration Tween 20 led to a faster release of curcumin, it has been reported that an excess of this surfactant can form micelles able to entrap the bioactive compound within, which enhance the protection of encapsulated curcumin thus increasing the antioxidant capacity of the system (Ratanajiajaroen et al., 2012).

Curcumin loaded nanoemulsions containing sucrose monopalmitate also exhibited higher antioxidant capacity when it was measured by DPPH method than by FRAP. Likewise, nanoemulsions

containing lecithin as surfactant, those with a 2% *w/w* of sucrose monopalmitate showed the highest EE. However, they did not show the highest antioxidant capacities. This would confirm the fact that, in nanoemulsions containing sucrose monopalmitate, curcumin may be not really encapsulated within their oil phase but retained by the surfactant molecules that are able to form hydrogen bonds with the ketons of curcumin tautomeric form or its phenolic groups (Szuts & Szabó-Révész, 2012). In this regard, curcumin exposed to the aqueous media may suffer its spontaneous auto-oxidation due to its inherent instability leading to the formation of a bicyclopentadione as major product (Wiggers; Zaioncz; Cheleski; Mainardes and Khalil, 2017). Therefore, antioxidant capacity of curcumin-loaded nanoemulsions stabilized by sucrose monopalmitate has a higher time-dependent decay than nanoemulsions containing lecithin or Tween 20 as surfactants.

4. Conclusions

The present study provides useful information about the behavior of lecithin, Tween 20 and sucrose monopamitate when they are used as surfactants in nanoemulsions. The nature and concentration of surfactant affected, on one hand, the physicochemical properties of curcumin-loaded nanoemulsions and specifically their stability. And on the other hand, it has influence on curcumin encapsulation efficiency and release kinetics of these nanostructured systems, which depending on the surfactant used had a direct or inverse correlation with their antioxidant capacities. Curcumin and the three surfactants may have a synergistic effect on nanoemulsions antioxidant capacity since the antioxidant capacities of curcumin-loaded nanoemulsions were significantly higher than those without curcumin. Concentrations of lecithin over 1% *w/w* led to the formation of long-term stable nanoemulsions, which are able to efficiently entrap curcumin within, preventing its autoxidation and hence, maintaining the antioxidant capacity of the bioactive compound. On the other hand, although either Tween 20 or sucrose monopalmitate allowed obtaining nanoemulsions with high EE(%), there is no guarantee that curcumin was encapsulated but remained retained in the surfactant by H-bonding after nanoemulsions destabilization. In this regard, curcumin may be exposed to light and oxidation reactions leading to its degradation and loss of antioxidant capacity. Therefore, results of the present manuscript evidenced the ability of lecithin in a concentration of at least 1% *w/w* to form long-term stable curcumin-loaded nanoemulsions and efficiently entrap curcumin inside the nanostructured system thus protecting it against degradation. In this regard, kinetics study became in a useful tool to model and predict the behavior of the nanoemulsions containing lecithin, Tween 20 or sucrose monopalmitate.

5. Acknowledgments

This study was supported by the Ministry of Economy, Industry and Competitiveness (MINECO/FEDER, UE) throughout project **AGL2015-65975-R**. Author María Artiga-Artigas thanks the University of Lleida for their pre-doctoral fellowship.

6. References

Aditya, N. P., Shim, M., Yang, H., Lee, Y., & Ko, S. (2014). Antiangiogenic effect of combined treatment with curcumin and genistein on human prostate cancer cell line. *Journal of Functional Foods*, *8*(1).

Artiga-Artigas, M., Acevedo-Fani, A., & Martín-Belloso, O. (2017). Effect of sodium alginate incorporation procedure on the physicochemical properties of nanoemulsions. *Food Hydrocolloids*, *70*, 191–200.

Beadle, J. B., Just, D. E., Morgan, R. E., & Reiners, R. A. (1964). Composion of Corn Oil. *The Journal of the American Oil Chemists' Society*, 90–95.

Benzie, I. F. F., & Strain, J. J. (1996). The Ferric Reducing Ability of Plasma (FRAP) as a Measure of "Antioxidant Power": The FRAP Assay. *Analytical Biochemistry*, *239*(1), 70–76.

Borrin, T. R., Georges, E. L., Moraes, I. C. F., & Pinho, S. C. (2016). Curcumin-loaded nanoemulsions produced by the emulsion inversion point (EIP) method: An evaluation of process parameters and physico-chemical stability. *Journal of Food Engineering*, *169*, 1–9.

Brand-Williams, W.; Cuvelier, M. E.; Berset, C. (1995). Use of a free radical method to evaluate antioxidant activity. *Lebensmittel Wissenschaft Und Technologie*, *30*, 25–30.

Celus, M., Salvia-Trujillo, L., Kyomugasho, C., Maes, I., Van Loey, A. M., Grauwet, T., & Hendrickx, M. E. (2018). Structurally modified pectin for targeted lipid antioxidant capacity in linseed/sunflower oil-in-water emulsions. *Food Chemistry*, *241*(August 2017), 86–96.

Cheung, T., Nigam, P., & Owusu-Apenten, R. (2016). Antioxidant Activity of Curcumin and Neem (Azadirachta indica) Powders: Combination Studies with ALA Using MCF-7 Breast Cancer Cells. *Journal of Applied Life Sciences International*, *4*(3), 1–12.

Degner, B. M., Chung, C., Schlegel, V., Hutkins, R., & Mcclements, D. J. (2014). Factors influencing the freeze-thaw stability of emulsion-based foods. *Comprehensive Reviews in Food Science and Food Safety*, *13*(2), 98–113.

Ekthamasut, K., & Akesowan, A. (2010). Effect of Vegetable Oils on Physical Characteristics of Edible Konjac Films. *Water*, (4).

Gaonkar, A. G. (1991). Surface and interfacial activities and emulsion characteristics of some food hydrocolloids. *Topics in Catalysis*, *5*(4), 329–337.

Goddard, E. D. (2002). Polymer/Surfactant Interaction: Interfacial Aspects. *Journal of Colloid and Interface Science*, *256*(1), 228–235.

Henry, J. V. L., Fryer, P. J., Frith, W. J., & Norton, I. T. (2009). Emulsification mechanism and storage instabilities of hydrocarbon-in-water sub-micron emulsions stabilised with Tweens (20 and 80), Brij 96v and sucrose monoesters. *Journal of Colloid and Interface Science*, *338*(1), 201–206.

Heurtault, B. (2003). Physico-chemical stability of colloidal lipid particles. *Biomaterials*, *24*(23), 4283–4300.

Klang, V., & Valenta, C. (2011). Lecithin-based nanoemulsions. *Journal of Drug Delivery Science and Technology*, *21*(1), 55–76.

Kumar, M., Ahuja, M., & Sharma, S. K. (2008). Hepatoprotective study of curcumin-soya lecithin

complex. *Scientia Pharmaceutica*, *76*(4), 761–774.

Lee, L. W., Liu, X., Wong, W. S. E., & Liu, S. Q. (2017). Effects of sucrose monopalmitate (P90), Tween 80 and modified starch on coffee aroma retention and release in coffee oil-based emulsions. *Food Hydrocolloids*, *66*, 128–135.

Marinova, K. G., Alargova, R. G., Denkov, N. D., Velev, O. D., Petsev, D. N., Ivanov, I. B., & Borwankar, R. P. (1996). Charging of Oil−Water Interfaces Due to Spontaneous Adsorption of Hydroxyl Ions. *Langmuir*, *12*(8), 2045–2051.

McClements, D. J., & Rao, J. (2011). Food-Grade nanoemulsions: Formulation, fabrication, properties, performance, Biological fate, and Potential Toxicity. *Critical Reviews in Food Science and Nutrition*, *51*(4), 285–330.

Ntawukulilyayo, J. D., Demuynck, C., & Remon, J. P. (1995). Microcrystalline cellulose-sucrose esters as tablet matrix forming agents. *International Journal of Pharmaceutics*, *121*(2), 205–210.

Otoni, C. G., Avena-Bustillos, R. J., Olsen, C. W., Bilbao-Sáinz, C., & McHugh, T. H. (2016). Mechanical and water barrier properties of isolated soy protein composite edible films as affected by carvacrol and cinnamaldehyde micro and nanoemulsions, *57*, 72–79.

Pan, Y., Tikekar, R. V., & Nitin, N. (2013). Effect of antioxidant properties of lecithin emulsifier on oxidative stability of encapsulated bioactive compounds. *International Journal of Pharmaceutics*, *450*(1–2), 129–137.

Petchsomrit, A., Sermkaew, N., Wiwattanapatapee, R., & Materials, A. (2013). Effect of Alginate and Surfactant on Physical Properties of Oil Entrapped Alginate Bead Formulation of Curcumin, *7*(12), 528–532.

Priyadarsini, K. I. (2014). The chemistry of curcumin: From extraction to therapeutic agent. *Molecules*, *19*(12), 20091–20112.

Qian, C., & Mcclements, D. J. (2011). Food Hydrocolloids Formation of nanoemulsions stabilized by model food-grade emulsi fi ers using high-pressure homogenization : Factors affecting particle size. *Food Hydrocolloids*, *25*(5), 1000–1008.

Raffa, P., Wever, D. A. Z., Picchioni, F., & Broekhuis, A. A. (2015). Polymeric Surfactants: Synthesis, Properties, and Links to Applications. *Chemical Reviews*, *115*(16), 8504–8563.

Rao, J., & McClements, D. J. (2011). Food-grade microemulsions, nanoemulsions and emulsions: Fabrication from sucrose monopalmitate & lemon oil. *Food Hydrocolloids*, *25*(6), 1413–1423.

Ratanajiajaroen, P., Watthanaphanit, A., Tamura, H., Tokura, S., & Rujiravanit, R. (2012). Release characteristic and stability of curcumin incorporated in β-chitin non-woven fibrous sheet using Tween 20 as an emulsifier. *European Polymer Journal*, *48*(3), 512–523.

Sadiq, F. A., Flint, S., Yuan, L., Li, Y., Liu, T. J., & He, G. Q. (2017). Propensity for biofilm formation by aerobic mesophilic and thermophilic spore forming bacteria isolated from Chinese milk powders. *International Journal of Food Microbiology*, *262*(January), 89–98.

Sadtler, V. M., Guely, M., Marchal, P., & Choplin, L. (2004). Shear-induced phase transitions in sucrose ester surfactant. *Journal of Colloid and Interface Science*, *270*(2), 270–275.

Salvia-Trujillo, L., Rojas-Graü, A., Soliva-Fortuny, R., & Martín-Belloso, O. (2014). Food Hydrocolloids Physicochemical characterization and antimicrobial activity of food- grade emulsions and nanoemulsions incorporating essential oils. *Food Hydrocolloids*, *43*, 1–10.

Salvia-Trujillo, L., Soliva-Fortuny, R., Rojas-Graü, M. A., McClements, D. J., & Martín-Belloso, O. (2017). Edible Nanoemulsions as Carriers of Active Ingredients: A Review. *Annual Review of Food Science and Technology*, *8*(1), 439–466.

Sari, T. P., Mann, B., Kumar, R., Singh, R. R. B., Sharma, R., Bhardwaj, M., & Athira, S. (2015). Preparation and characterization of nanoemulsion encapsulating curcumin. *Food Hydrocolloids*, *43*, 540–546.

Schneider, C., Gordon, O. N., Edwards, R. L., & Luis, P. B. (2015). Degredation of curcumin: From mechanism to biological implications. *J Agric Food Chem*, *63*(35), 7606–7614.

Surassmo, S., Min, S. G., Bejrapha, P., & Choi, M. J. (2010). Effects of surfactants on the physical properties of capsicum oleoresin-loaded nanocapsules formulated through the emulsion-diffusion method. *Food Research International*, *43*(1), 8–17.

Szuts, A., & Szabó-Révész, P. (2012). Sucrose esters as natural surfactants in drug delivery systems - A mini-review. *International Journal of Pharmaceutics*, *433*(1–2), 1–9.

Thaipong, K., Boonprakob, U., Crosby, K., Cisneros-Zevallos, L., & Hawkins Byrne, D. (2006). Comparison of ABTS, DPPH, FRAP, and ORAC assays for estimating antioxidant activity from guava fruit extracts. *Journal of Food Composition and Analysis*, *19*(6–7), 669–675.

Velderrain-Rodríguez, G. R., Ovando-Martínez, M., Villegas-Ochoa, M., Ayala-Zavala, J. F., Wall-Medrano, A., Álvarez-Parrilla, E., … González-Aguilar, G. A. (2015). Antioxidant Capacity and Bioaccessibility of Synergic Mango (cv. Ataulfo) Peel Phenolic Compounds in Edible Coatings Applied to Fresh-Cut Papaya. *Food and Nutrition Sciences*, *6*(6), 365–373.

Wiggers, H.J.; Zaioncz, S.; Cheleski, J.; Mainardes, R.M. and Khalil, N. M. (2017). *Studies in Natural Products Chemistry*. Elsevier Science.

Zhang, H. Y., Arab Tehrany, E., Kahn, C. J. F., Ponçot, M., Linder, M., & Cleymand, F. (2012). Effects of nanoliposomes based on soya, rapeseed and fish lecithins on chitosan thin films designed for tissue engineering. *Carbohydrate Polymers*, *88*(2), 618–627.

CHAPTER III: *Factors affecting the formation of highly concentrated emulsions as delivery systems of lipophilic bioactive compounds*

Artiga-Artigas, M.; Montoliu-Boneu, J.; Salvia-Trujillo, L., Martín-Belloso, O.

(Submitted to Journal of Food Engineering)

Abstract

Highly concentrated (HC) emulsions and nanoemulsions arise as an interesting strategy to transport and encapsulate lipophilic bioactive compounds at high concentrations to be further used or diluted in food formulations. Nonetheless, their formation and stabilization in terms of particle size reduction is of crucial importance due to their characteristic high viscosity. HC emulsions containing a 40 % of an oil phase (φ: 0.4) with droplet diameters (d[4;3]) of 520 and 310 nm were produced by ultrasonication (200 s, 100 µm) or microfluidization (2 cycles, 800 bar), respectively. Increasing the surfactant-to-oil ratio (SOR) up to 0.2 led to a particle size reduction down to 240 nm, which in turn led to a dramatic increase in the emulsions viscosity. Interestingly, higher oil volume fractions up to 70 % (φ: 0.7) led to emulsions with smaller particle size, which might be related to the presence highly packed droplets within the aqueous phase. HC-emulsions presented a high curcumin encapsulation efficiency (>70%) and release (> 80 % after 48 h). Therefore, this work contributes in elucidating the factors affecting the formation of HC-emulsions as potential carriers of lipophilic bioactive compounds.

Keywords: highly-concentrated emulsions; curcumin; encapsulation efficiency; volume fraction

1. Introduction

The production of highly concentrated emulsions, whose main characteristic is that the volume fraction of the dispersed phase (φ) is higher or equal to 0.4, is gaining attention because they present some advantages over diluted conventional emulsions and nanoemulsions (Malkin, Zadymova, Skvortsova, Traskine, & Kulichikhin, 2016; Piorkowski & McClements, 2014). On the one hand, concentrated oil-in-water emulsions have the capability to load more quantity of bioactive compounds in their lipid phase than diluted systems and on the other hand, allow reducing storage space and transportation costs (Luo et al., 2017; Muller, Harden, & Keck, 2012). Moreover, this great droplet concentration may have an effect on the physicochemical properties of highly concentrated emulsions (McClements, 2015). Therefore, they can be used to modify the textural, optical, stability and release characteristics to the desired final commercial products (Luo et al., 2017). In addition, according to Osborn & Akoh (2004), the rate of lipid oxidation in oil-in-water emulsions decreases when the total oil level is increased. At high oil concentrations, more unsaturated fatty acids may move to the interior of oil droplets becoming less accessible to direct interaction with the aqueous phase prooxidants (D. J. McClements & Decker, 2000). This suggests that an increase in droplet concentration may improve the shelf-life of chemically labile lipophilic bioactive compounds that may be encapsulated in the lipid inner core.

For instance, curcumin is a natural polyphenolic flavonoid obtained from *Curcuma longa*, which is known to be an effective bioactive compound to prevent several diseases like cancer, obesity, infectious disease, and cardiovascular illnesses (Aditya et al., 2014). Since curcumin is a non-toxic powerful antioxidant and antimicrobial agent, the incorporation of this bioactive compound to food matrices is of great interest to enhance the quality and safety of foods (Artiga-Artigas, Lanjari-Pérez, & Martín-Belloso, 2018). However, its poor solubility, stability, and bioavailability in aqueous media together with its fast elimination from the body after its intake with little absorption in the gastrointestinal tract limits their efficient use as a bioactive compound (Aditya et al., 2014; Bourbon et al., 2016). Therefore, its encapsulation within highly concentrated emulsions is presented as a good alternative to incorporate this bioactive compound to food matrices favoring its diffusion in aqueous media and enhancing its bioavailability after ingestion (Borrin et al., 2016).

In highly concentrated emulsions the volume fraction of the dispersed phase can be increased progressively just to a certain value considered as "critical" until the emulsion breaks or inverts (Princen et al., 1980). Thus, the concentration of oil droplets in the dispersed liquid exceeds the limit of the closest packing of spherical particles (Yakhoub et al., 2011). This tight droplet packing allows the behavior of highly concentrated emulsions to change from elastic to viscoelastic (Calderó, Patti, Llinàs, & García-Celma, 2012). Actually, it is reported that if the volume fraction of the dispersed phase (φ) is lower than 0.74 in a monodisperse emulsion, oil droplets may fit in hexagonal close packing without being deformed (Princen et al., 1980). However, when the volume fraction is over 0.74, droplets may start to deform allowing the continuous phase forming a thin film around them. Despite the fact that at this point each film is subjected to a compressive pressure, equilibrium is maintained due to electrostatic and steric forces thus suggesting the feasibility of preparing stable highly concentrated emulsions (Princen et al., 1980). Therefore, the selection of the most suitable surfactant concentration may be crucial in the stabilization of highly concentrated emulsions based on their ability to avoid droplet aggregation under environmental conditions including pH, ionic strength and temperature (Dickinson, 2003; Garti & Reichman, 1993). Indeed, small molecule surfactants such

as Tween 80 are able to rapidly adsorb at droplet interfaces reducing the interfacial tension, facilitating droplet breakup and avoiding recoalescence (Jafari et al., 2008). Additionally, along with the oil φ and the surfactant-oil ratio (SOR), particle size of highly concentrated nanoemulsions may depend on the homogenizer type (*e.g.*microfluidizer or ultrasonicator) and its operating conditions (Jafari et al., 2008).

Therefore, the aim of this work was to assess the effect of homogenization procedure, oil concentration (φ 0.4 - 0.7) and SOR (0.01 - 0.2) in the design and preparation of highly concentrated submicron emulsions. Additionally, their capacity to act as template carriers for lipophilic bioactive compounds (*e.g.* curcumin) was also evaluated.

2. Material and methods

2.1.Materials

Corn oil (Koipesol Asua, Deoleo, Spain) was used for preparing all the emulsions. Tween 80 was purchased from Panreac (Barcelona, Spain). Ultrapure water obtained from a Milli-Q filtration system was used to the preparation of all solutions. Curcumin (*Curcuma longa*) was obtained from Sigma-Aldrich (Darmstadt, Germany). Ethanol absolute 99.9% purity (Fisher Chemical, Thermo Fisher Scientific, Leicestershire, UK) and n-hexane (≥ 95% purity) (Scharlau, Scharlab S.L., Barcelona, Spain) were used as solvents.

2.2.Methods

2.2.1. Highly concentrated emulsions formation

Different parameters were evaluated for the preparation of highly concentrated emulsions such as high-shear homogenization (HSH) procedure, oil volume fraction (φ) and surfactant-oil ratio (SOR).

Highly concentrated coarse emulsions were prepared by mixing the aqueous phase containing the hydrophilic surfactant and corn oil with a T25 digital Ultra-Turrax (IKA, Staufen, Germany) at 11,000 during 2 min. The oil volume fraction (φ) calculated through eq.(1) ranged from 0.4 to 0.7 and the SOR from 0.01-0.2. Afterwards, highly concentrated submicron emulsions were obtained by ultrasonication (20-300 s, 100 µm of amplitude) with a UP 400S Hielscher sonifier (Hielscher Ultrasound Technology, Teltow, Germany) or by 1-5 microfluidization cycles with a microfluidizer device (M110P, Microfluidics, Massachusetts, USA) working at 800 bar.

$$\varphi = \frac{\text{Coil}}{Cemulsion} \qquad \textbf{eq.(1)}$$

where C_{oil} is the concentration of oil expressed in weight and $C_{emulsion}$ is the total weight of the emulsion.

2.2.2. Physicochemical characterization of highly concentrated emulsions

2.2.2.1.Droplet size and particle size distribution

The emulsion droplet size in terms of volume and surface diameter (d[4;3] and d[3;2], respectively) of all coarse and submicron emulsions expressed in µm was measured by the laser diffraction technique with a Mastersizer 3000^{TM} (Malvern Instruments Ltd., Worcestershire, UK). Refractive index of corn oil was 1.47. For the measurement of particle sizes highly concentrated emulsions were dispersed in distilled water using a dilution factor of 1:150 sample-to-solvent.

2.2.2.2.ζ-Potential

The ζ-potential (mV) was measured by phase-analysis light scattering (PALS) with a Zetasizer Nano-ZS laser diffractometer (Malvern Instruments Ltd, Worcestershire, UK). It determines the electrical charge at the interface of the droplets dispersed in the aqueous phase. Samples were prior diluted in ultrapure water using a dilution factor of 1:150 sample-to-solvent.

2.2.2.3.Apparent Viscosity

Viscosity measurements (mPa·s) were performed by using a vibro-viscometer (SV-10, A&D Company, Tokyo, Japan) vibrating at 30 Hz, with constant amplitude and working at room temperature. Aliquots of 10 mL of each concentrated emulsion and nanoemulsion were used for determinations.

2.2.2.4.Emulsions microstructure

Microscopy images of fresh highly concentrated coarse and submicron emulsions were taken with an optical microscope (BX41, Olympus, Göttingen, Germany) equipped with UIS2 optical system. Phase contrast images were obtained without diluting the samples in order to maintain the original oil droplets packing structure. All images were processed using the instrument software (Olympus cellSense, Barcelona, Spain).

2.2.2.5.Curcumin encapsulation within highly-concentrated emulsions

Curcumin-loaded coarse and submicron emulsions were prepared with a SOR of 0.1 due to the great increase in viscosity presented by the emulsions with a SOR of 0.2 to be sure that the obtained differences were related to SOR and not to viscosity. For the loading of the curcumin, the oil was heated at mild temperature (50 ºC) and mixed with the curcumin powder (0.01% *w/w*). Then, agitation was applied for 10 minutes and the mixture was subjected to 5 minutes of sonication in an ultrasonic bath (J.P Selecta, Barcelona, Spain) to ensure complete dissolution of curcumin.

The coarse emulsions and their respective ultrasonicated or microfluidized emulsions were prepared as mentioned in section 2.2.1 with a SOR of 0.1 and 0.5 φ of corn oil, which was enriched with curcumin (0.01% *w/w*). These emulsions were characterized in terms of particle size, ζ-potential (mV) and viscosity as described in the previous paragraphs of section 2.2.2 to ensure their appropriated formation. Moreover, the encapsulation efficiency (EE) and the curcumin release both expressed in percentage were also assessed.

2.2.2.6.Encapsulation Efficiency (%)

The curcumin EE was measured following the method of Lin et al. (2018) in which 0.5 mL of each emulsion is poured in 2 mL of ethanol absolute and 3 mL of n-hexane, and vortexed (MS 2, Fisher Scientific, Leicestershire, UK). The curcumin was collected in the ethanol fraction and subsequently quantified. The curcumin absorbance was measured with a V-670 spectra photometer (Jasco, Tokyo, Japan) at a 425 nm wavelength and the concentration was calculated from the calibration curve. EE (%) of the obtained emulsions was calculated by eq.(2) (Surassmo et al., 2010):

$$\%EE = \frac{Total\ amount\ of\ curcumin - Free\ curcumin}{Total\ amount\ of\ curcumin} \text{ x } 100 \qquad \textbf{eq.(2)}$$

where the total amount of curcumin is the initial concentration of this bioactive compound added to the mixture and the free curcumin is the concentration of compound that was not loaded in nanoemulsions.

2.2.2.7.Curcumin release

The curcumin release was measured following the method of Behbahani, Ghaedi, Abbaspour, & Rostamizadeh (2017). Aliquots of 10 mL of each sample were loaded into the dialysis bags, which were subsequently submerged in a 100 mL mixture of distilled water and ethanol (50:50), at room temperature and constant agitation (100 rpm). A 2-mL aliquot of the outer extraction medium was used to determine the curcumin concentration at 0.5, 1, 3, 5, 8, 24 and 48 h. In order to maintain the volume constant during the whole experiment, 2 mL of dissolution medium were added to replace each extracted aliquot. Samples were measured with a V-670 spectra photometer (Jasco, Tokyo, Japan) at a 425 nm wavelength. The curcumin release was calculated with eq.(3):

$$Release\ (\%) = \frac{released\ curcumin\ (mg)}{total\ amount\ of\ encapsulated\ curcumin\ (mg)} x100 \qquad \textbf{eq.(3)}$$

where the released curcumin expressed in mg is the amount of curcumin found in each sample and the total amount of encapsulated curcumin is the quantity of compound that was loaded in the emulsions according to encapsulation efficiency results, also expressed in mg.

The curcumin release curve over 24 hours showed a steep increase at short time until reaching a plateau phase fitting with a fractional conversion model to describe the relationship between *CR* and t independent variables as shown in eq.(4). It was statistically analyzed at a 5% significance level using JMP 12 Pro 12 software (Statistical Discovery™, North Carolina, USA).

$$CR = CRmax \cdot (1 - e^{-kt}) \qquad \textbf{eq.(4)}$$

where *CR* is the curcumin release expressed in %, t is the time (h), CR_{max} is the maximum estimated curcumin release (%) and k is the kinetic constant (h^{-1}).

2.2.3. Statistics

All the experiments were assayed in duplicate, and at least three replicate analyses were carried out for each parameter. JMP Pro 12 software (Statistical Discovery™, North Carolina, USA) was used to perform the statistical analysis. Tukey-Kramer test was chosen to determine significant differences among treatments, at a 5% significance level.

3. Results and discussion

Firstly, the effect of emulsification technique (*i.e.* ultrasonication and microfluidization) and its processing conditions (*i.e.* frequency and number of cycles, respectively) on physicochemical properties of highly concentrated submicron emulsions with a φ of 0.4 and a SOR of 0.1 was studied. Once the processing parameters were established for each emulsification technique, the φ was increased in order to observe the influence of oil concentration on the characteristics of highly concentrated coarse emulsions and their subsequent submicron emulsions including particle size and distribution, ζ-potential and apparent viscosity. Afterwards, the impact of surfactant concentration on the physicochemical properties of the prepared concentrated emulsions was also assessed at constant φ. Finally, the feasibility of using highly concentrated emulsions as carriers of curcumin was evaluated.

3.1.Effect of high-shear homogenization procedure on physicochemical characteristics of highly concentrated emulsions

Particle size distribution of submicron emulsions with a φ of 0.4 and a SOR of 0.1, which were prepared by ultrasonication (20-300 s, 100 μm), are shown in Figure 1A. Coarse emulsion exhibited a bimodal distribution and a volume mean droplet diameter (d[4:3]) of 14.46 ± 1.87 μm. However, particle size of the resulting ultrasonicated emulsion decreased as increasing the sonication time leading to monomodal distributions from 200 s of ultrasonication (Figure 1A). Ultrasonicated emulsions reached particle sizes of 0.52 ± 0.03 μm and no significant changes were observed after longer time of sonication (Figure 1B). Salvia-Trujillo, Rojas-Graü, Soliva-Fortuny, & Martín-Belloso (2013) reported that ultrasounds were a feasible technology to produce diluted nanoemulsions with particles sizes lower than 100 nm. Cavitation and high shear forces generated by the sonicator can induce disruption at droplets interface producing stable nanoemulsions in the presence of surfactants (Abbas et al., 2015). In this regard, high concentration of oil (≥ 40 % *w/w*) may interfere in the reduction of particle size since the tight packing of droplets may diminish the efficiency of the high shear device (Calderó et al., 2012).

Microfluidization procedure of the coarse emulsions also led to highly concentrated monomodal submicron emulsions but with particle sizes bellow 0.4 μm after the first cycle (Figures 1D-E). This suggests that the applied high energy procedure to prepare nanoemulsions may affect their particle size and formation (Silva et al., 2012). It could be related to technological differences between the ultrasonicator and the microfluidizer since the latter is able to maintain the outlet temperature of the sample thus being a more gentle technology (Salvia-Trujillo et al., 2014c).

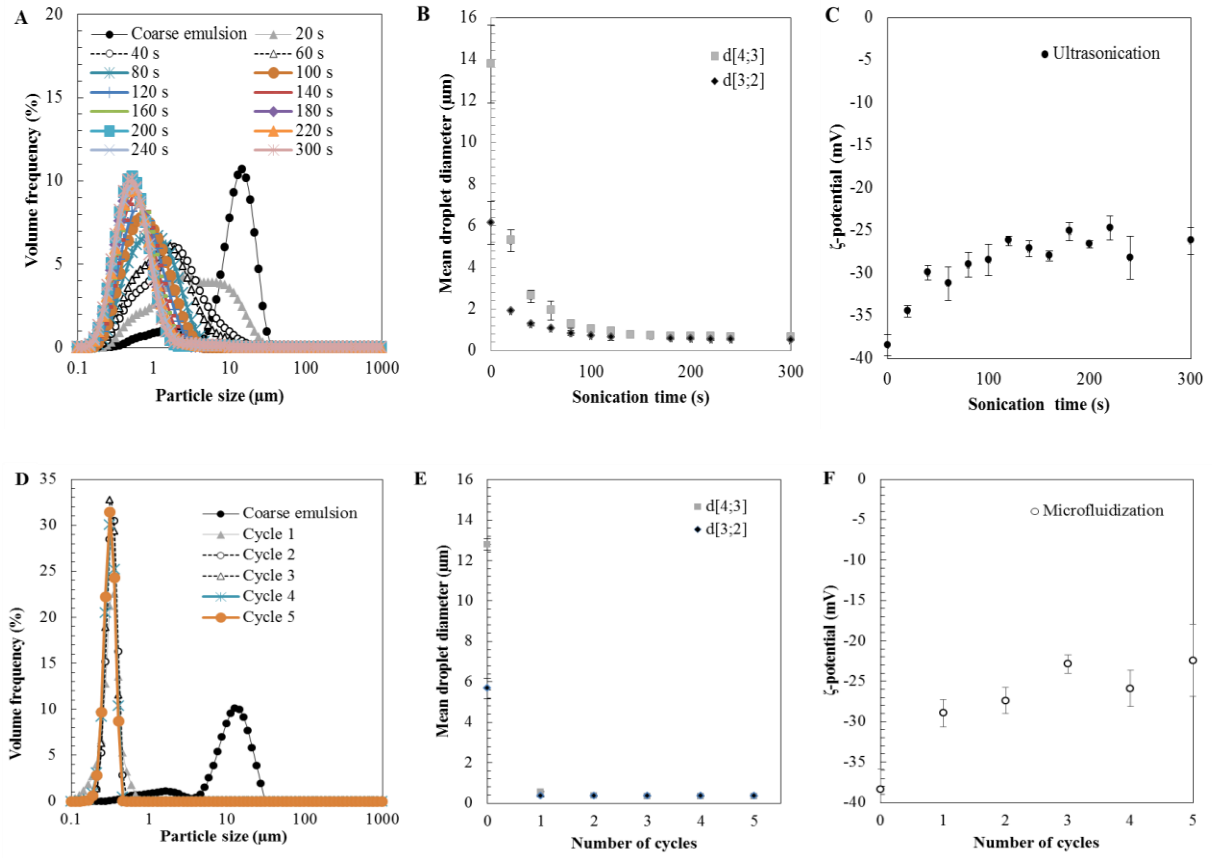

Figure 1. Particle size distribution, volume (d[4;3]) and surface (d[3;2]) mean droplet diameters and ζ-potential of highly concentrated ultrasonicated emulsions (A, B and C, respectively) or microfluidized emulsions (D, E and F, respectively) with a volume fraction of 0.4 and a surfactant-oil ratio of 0.1. Ultrasonication was performed during 20-300 s at 100 µm of amplitude and microfluidiation process was carried out during 1-5 cycles at 800 bar.

It is reported that, in general, high shear stress produced inside the microfluidizer can lead to more homogeneous emulsions with lower particle sizes than other devices (Bonilla, Atarés, Vargas, & Chiralt, 2012a). The coarse emulsion can be passed through the interaction chamber sequentially until obtaining the desired particle size (Bruschi, 2015). However, after the second cycle of microfluidization, highly concentrated nanoemulsions reached a particle size of 0.346 ± 0.003 µm observing a negligible decrease during the following cycles (Figure 2B). In agreement with our results, other works also showed that a further increase in the number of cycles did not lead to a significant reduction of the average droplet size (Qian & McClements, 2011; Salvia-Trujillo et al., 2013b). Provided that droplets have reached their saturation size, subjecting the emulsion at the same pressure might not produce any additional rupturing or change in the size distribution (Wooster, Golding, & Sanguansri, 2008b).

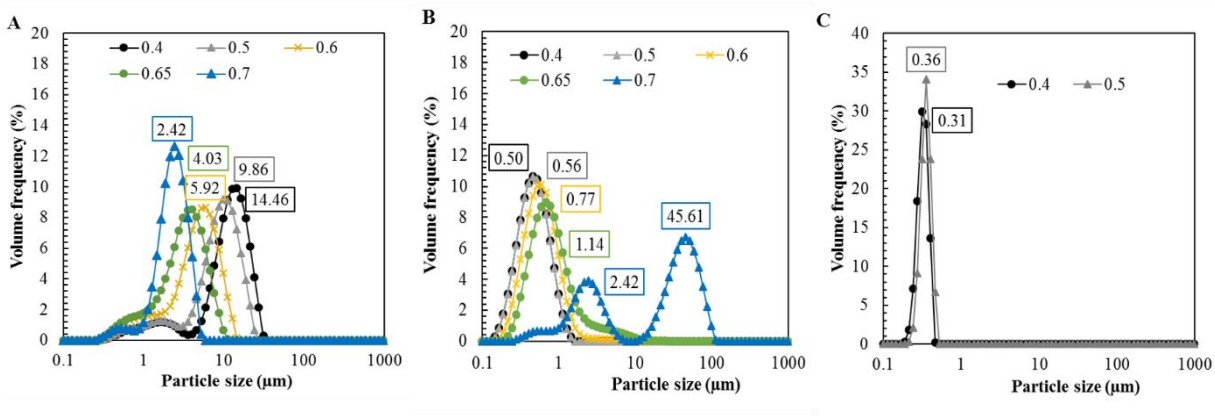

Figure 2. Particle size distributions of highly concentrated coarse emulsions (A) and their subsequent submicron emulsions obtained by ultrasonication (200 s, 100 µm) (B) or microfluidization (2 cycles, 800 bar) (C) prepared with a surfactant-oil ratio of 0.1 and different volume fractions ranging from 0.4 to 0.7.

The ζ-potential of the prepared highly concentrated emulsions was negative and increased from -38 ± 2 mV to -26 ± 2 mV or to -22 ± 4 mV in the case of ultrasonicated or microfluidized nanoemulsions, respectively (Figures 1C or 1F, respectively). Non-ionic surfactants such as Tween 80 may confer negative charge to oil droplets probably due to the orientation towards the oil/water interface of OH^- ions from the aqueous phase or HCO_3^- and CO_3^{2-} ions from the dissolved atmospheric CO_2 (Artiga-Artigas, Guerra-Rosas, Morales-Castro, Salvia-Trujillo, & Martín-Belloso, 2018; Marinova et al., 1996). It is described that if the electrical charge of emulsions is more positive than +30 mV or more negative than -30 mV, it is strong enough to ensure their stability suggesting that repulsive forces between droplets are predominant in the nanoemulsion system (Heurtault, 2003; Salvia-Trujillo et al., 2013a). As can be observed in Figure 3 B-C, highly concentrated submicron emulsions either ultrasonicated or microfluidized showed lower particle sizes than coarse emulsions maintaining their microstructure in spite of the increase of the ζ-potential values after applying the high-shear stress. The spatial repulsive force between interfacial layers allows these emulsions to avoid coalescence even when the droplets follow an adhesive behavior (Foudazi, Qavi, Masalova, & Malkin, 2015).

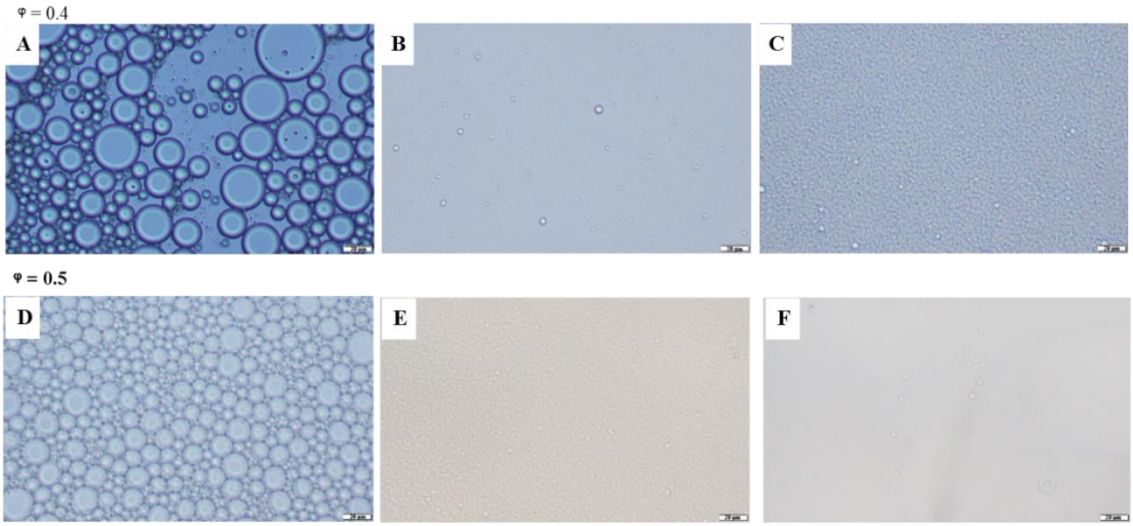

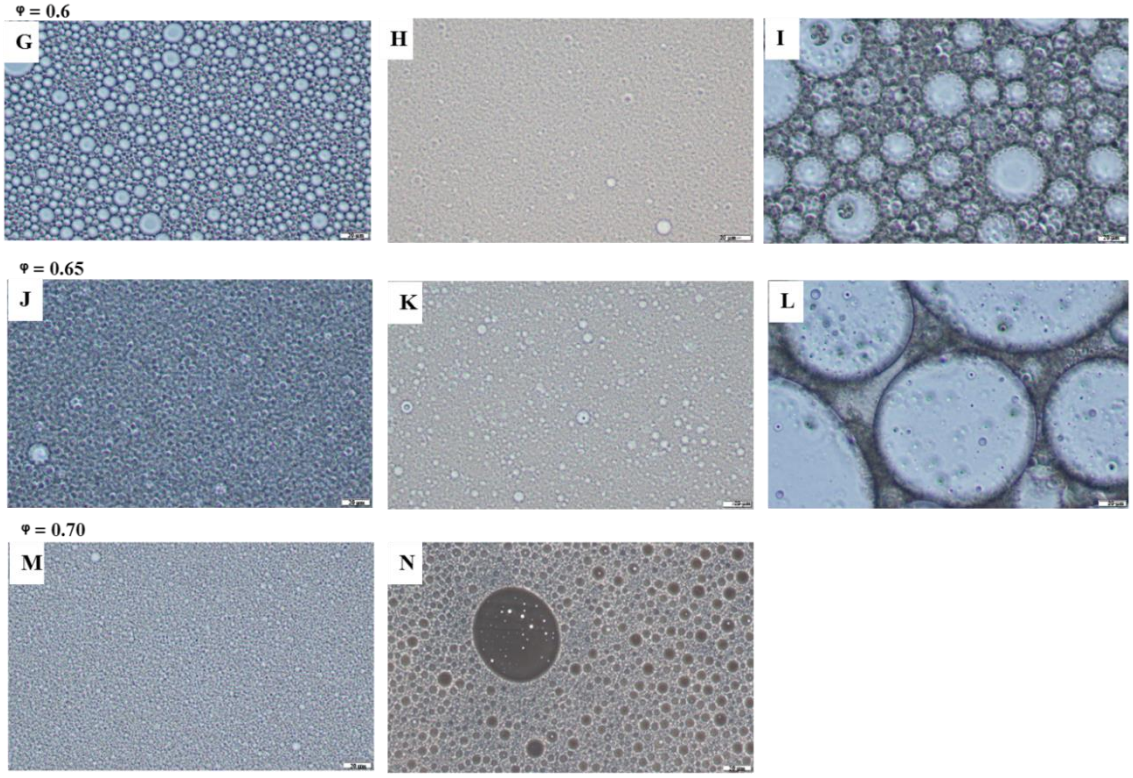

Figure 3. Microscopical phase contrast images of the highly concentrated coarse emulsions (A, D, G, J and M) and their subsequent submicron emulsions obtained by ultrasonication (200 s, 100 µm) (B, E, H, K and N) or microfluidization (2 cycles, 800 bar) (C, F, I and L) prepared by a surfactant-oil ratio of 0.1 and volume fractions of 0.4-0.7. Error bar is equivalent a 20 µm.

3.2.Influence of oil volume fraction on the physicochemical characteristics of highly concentrated emulsions

Mean droplet diameters and particle size distributions of the highly concentrated emulsions as affected by the oil volume fraction are shown in Figures 2A-C. It is observed an opposite tendency between coarse emulsions and ultrasonicated or microfluidized emulsions. As increasing the φ from 0.4 to 0.7, particle size of coarse emulsion decreased from 14.46 ± 2.13 to 2.42 ± 0.01 µm (Figure 2A). However, in the case of ultrasonicated and microfluidized emulsions, the higher the φ, the larger the emulsions particle size. In fact, a φ of 0.7 caused the complete destabilization of ultrasonicated emulsions after homogenization process reaching values of 30.85 ± 1.12 µm (Figure 2B). Something similar occurred with microfluidized emulsions, which suffered fast coalescence and subsequent phase separation after the first cycle when the φ was 0.6 or 0.65.

Moreover, apparent viscosity of coarse emulsion and submicron emulsions increased with the φ being the coarse emulsion with a φ of 0.7 that showed the highest apparent viscosity (624 ± 21 mPa·s) (Table 1). This increase is remarkable because a small increase of φ (0.5%) had a huge impact in the apparent viscosity. In this regard, the apparent viscosity of coarse emulsions containing a φ of 0.7 was around five times higher than those prepared with a φ of 0.65 (Table 1). It has been described

that an increase in the concentration of the lipid phase is decisive in reducing particle size and as dispersed phase content increases, it is the viscosity that commands the droplets reduction phenomenon (Briceño, Salager, & Bertrand, 2001). This higher viscosity caused by a great packing of droplets in coarse emulsions may contribute to reduce their movement thus preventing particle growth (Figures 3A, D, G, J and M).

Table 1. ζ-potential (mV) and apparent viscosity (mPa·s) of highly concentrated coarse, ultrasonicated (200 s, 100 µm) and microfluidized (2 cycles, 800 bar) emulsions with a SOR of 0.1, at different oil volume fractions (φ).

	φ	ζ-potential (mV)	Apparent viscosity (mPa·s)
Coarse emulsion	0.4	-37.9 ± 2.5^{ABb}	6.13 ± 0.73^{Da}
	0.5	-38.6 ± 2.1^{Bb}	11.7 ± 0.8^{Dc}
	0.6	-34.9 ± 2.8^{Ab}	33.3 ± 2.1^{Cb}
	0.65	-38.7 ± 1.9^{Bb}	115 ± 20^{Bb}
	0.7	-39.5 ± 2.6^{Bb}	624 ± 21^{A}
Ultrasonicated emulsion	0.4	-25.75 ± 1.26^{Ba}	7.84 ± 0.48^{Db}
	0.5	-21.43 ± 0.83^{Aa}	19.0 ± 0.7^{Cb}
	0.6	-20 ± 3^{Aa}	55.20 ± 0.27^{Ba}
	0.65	-28.87 ± 0.69^{Ba}	269 ± 52^{Aa}
Microfluidized emulsion	0.4	-43 ± 2^{Ac}	28.1 ± 0.9^{Bb}
	0.5	-41.32 ± 1.52^{Ac}	63 ± 9^{Aa}

^{A,B,C,D} Means in same bar with different letters are significantly different at $p < 0.05$ regarding the φ. ^{a,b,c} Means in same bar with different letters are significantly different at $p < 0.05$ in terms of type of emulsion (coarse, ultrasonicated or microfluidized). Microfluidized emulsions containing $\varphi \geq 0.6$ destabilized after 1 cycle of microfluidization so their physicochemical parameters could not be measured. Likewise, ultrasonicated emulsions with $\varphi = 0.7$ suffered disruption after ultrasonication.

However, the higher the concentration of oil, the greater the apparent viscosity but the less efficient the reduction of particle size during HSH (Table 1). This can be also perceived in the microscopic images corresponding to φ of 0.6 and 0.65, where it is possible to observe the increase in droplets particle size suggesting the destabilization of the system (Figure 3I and 3L). Therefore, the oil volume fraction also played a key role in particle size of highly concentrated emulsions. Indeed, it is reported that although the submicron emulsion sizes at φ below 0.4 usually remained stable, they are expected to grow at higher φ (Wooster et al., 2008a). One possible explanation is that viscous oil phases may difficult the droplets disruption by mechanical forces inside the homogenizer (Jafari et al., 2008; Zeeb et al., 2012). Therefore, the higher the concentration of oil, the greater the apparent viscosity and hence, the less efficient the reduction of particle size. Microscopic images of microfluidized emulsions with φ over 0.5, exhibited the increase of oil droplets probably because coalescence phenomenon after the high shear forces inside the homogenizer device (Figures 3I and 3L). Actually, Figures 3G, 3J and 3M corresponding to coarse emulsions with φ of 0.6, 0.65 and 0.7,

respectively, showed a very high packing (closed to hexagonal) thus suggesting that they are close to breaking after a shear stress.

The ζ-potential of coarse emulsions and nanoemulsions is significantly different (Table 1). Coarse emulsions showed ζ-potential values around -40 mV regardless the concentration of oil fraction. The same occurred with microfluidized emulsions in which, ζ-potential was slightly lower than coarse emulsions (≈ -42 mV) and was independent of φ. This can be related with a higher stabilization of emulsion-based systems after microfluidization. Indeed, microfluidization is considered as a more efficient methodology to prepare homogeneous submicron emulsions with small particle sizes (< 500 nm) (Xu et al., 2014). Oppositely, in ultrasonicated emulsions, ζ-potential values were more positive than those of the coarse or microfluidized emulsions and augmented from -25 to -20 as increasing the φ from 0.4 to 0.6. Then, ζ-potential decreased again almost recovering the initial state (≈ -35 mV). This could be due to the migration of metal ions from the electrode of the ultrasonicator to the sample might alter its electrical charge (ζ-potential). According to the manufacturer, the electrode is made of Titanium (Ti), a highly inert metal due to their passivation capacity. This means that a thin surface titanium oxide layer can be formed and protect the electrode against oxidation. Nonetheless, the addition of aluminum and vanadium traces to commercially pure Ti is a usual practice in order to overcome poor mechanical strength of the pure metal, resulting in an alloy ($TiAl_6V_4$) from which Ti ions can migrate (Joseph, Israel, & Edet, 2009).

3.3.Impact of surfactant concentration on the physicochemical characteristics of highly concentrated emulsions

Particle size of all the prepared highly concentrated emulsions (φ = 0.5) and submicron emulsions decreased as increased the concentration of Tween 80 or what is the same, the SOR (Figures 4A-C). Regarding highly concentrated coarse emulsions, particle sizes ranged from 18.66 ± 0.95 to 6.72 ± 0.16 μm as increasing the SOR from 0.01 to 0.2 (Figure 4A). Tween 80 is a low molecular surfactant that rapidly adsorbs at droplets surface created by emulsification generating a protective layer around droplets (Jafari, He, & Bhandari, 2006). This layer may contribute to reduce the interfacial tension and facilitate droplets disruption preventing them from flocculation or coalescence phenomena (Jafari et al., 2008). Moreover, all the coarse emulsions exhibited bimodal particle size distributions regardless the SOR and significant differences were not observed for coarse emulsions with SOR of 0.05 and 0.07 (Figure 4A). After any type of HSH, all the submicron emulsions prepared with a SOR greater or equal 0.05 presented monomodal distributions (Figures 4B-C). The lowest particle size was shown in microfluidized emulsions with a SOR of 0.2 and 0.1 (0.24 and 0.36 μm, respectively). However, 200 s at 100 μm of ultrasonication only allowed obtaining highly concentrated emulsions with 0.41 μm of diameter (Figure 1B).

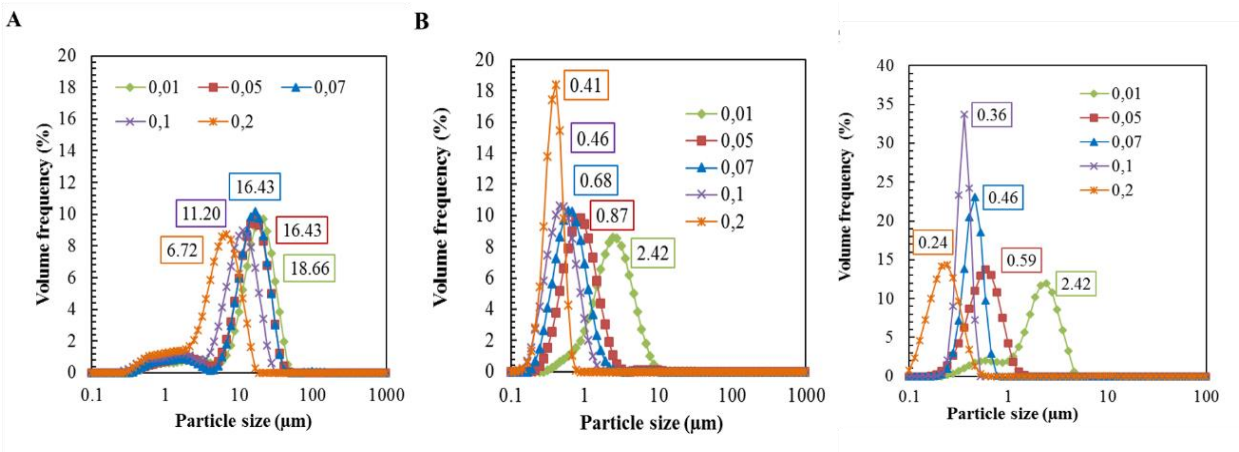

Figure 4. Particle size distributions of highly concentrated coarse emulsions (A) and their subsequent submicron emulsions obtained by ultrasonication (200 s, 100 µm) (B) or microfluidization (2 cycles, 800 bar) (C) prepared with a volume fraction of 0.5 and different surfactant-oil ratio (0.01, 0.05, 0.07, 0.1 or 0.2).

The increase of surfactant concentration clearly decreased droplet size, which in turn contributed to increase the apparent viscosity of emulsions (Table 2). This increase in viscosity parameter was unleashed in microfluidized emulsions prepared with a SOR 0.2, which showed a value of 638 ± 77 mPa·s. The achievement of such small particle sizes involves a very high packing of the droplets, which means that a great apparent viscosity of emulsions is required to control the droplets Brownian motion (Ngan, Basri, Tripathy, Karjiban, & Abdul-Malek, 2014; Sanatkaran, Masalova, & Malkin, 2014). In fact, microscopic images of emulsions showed an increase in packaging either with the concentration of surfactant, or after HSH being this increase even higher when microfluidization was applied (Figure 5). For instance, the microscopic image of coarse emulsion with a SOR of 0.2 (Figure 5M) exhibited a high packaging of droplets that can also be observed in those ultrasonicated (Figure 5N) resulting imperceptible after microfluidization (Figure 5O). Thus, the relationship between the reduction of particle sizes and the increase of their packaging as well as their apparent viscosity was confirmed. This highly packaging was explained by Princen et al. (1980), who proposed that the increase of the surface storage energy in droplet compression was due to osmotic pressure. This hypothesis was later supported by other publications including those of Lacasse, Grest, Levine, Mason, & Weitz (1996) and Mason (1999). Therefore, the concentration of surfactant plays a key role in highly concentrated emulsions formation since interfacial tension is the dominating factor determining their stability and elasticity (Tshilumbu, Ferg, & Masalova, 2010).

Coarse emulsions and nanoemulsions showed negative ζ-potential values regardless the concentration of surfactant (Table 2). According to our results, the tendency of ζ-potential was to increase towards more positive values in all the types of emulsions (coarse, ultrasonicated or microfluidized). Nevertheless, ζ-potential values of coarse emulsions and submicron emulsions were significantly different ($p < 0.05$) becoming less negative after a HSH process (Table 2).

Table 2. ζ-potential (mV) and apparent viscosity (mPa·s) of highly concentrated coarse, ultrasonicated (200 s, 100 µm) and microfluidized (2 cycles, 800 bar) emulsions with a volume fraction of 0.5, at different surfactant-oil ratios (SOR).

	SOR	ζ-potential (mV)	Apparent viscosity (mPa·s)
Coarse emulsion	0.01	-52.6 ± 3.7 ^{Cc}	5.40 ± 0.37 ^{Ca}
	0.05	-47.11 ± 1.42 ^{Bc}	7.68 ± 0.29 ^{Cb}
	0.07	-40 ± 3 ^{Ab}	8.6 ± 0.7 ^{BCc}
	0.1	-42 ± 4 ^{Bc}	11.39 ± 0.84 ^{Bc}
	0.2	-37 ± 3 ^{Ac}	36 ± 5 ^{Ab}
Ultrasonicated emulsion	0.01	-44.1 ± 1.7 ^{Cb}	4.85 ± 0.43 ^{Dab}
	0.05	-25.38 ± 0.72 ^{Bb}	9.22 ± 0.28 ^{CDb}
	0.07	-25.1 ± 1.7 ^{Ba}	13.53 ± 1.68 ^{BCb}
	0.1	-21.9 ± 0.92 ^{Aa}	18.85 ± 0.63 ^{Bb}
	0.2	-25.00 ± 1.75 ^{Bb}	73 ± 9 ^{Ab}
Microfluidized emulsion	0.01	-40.2 ± 2.8 ^{Ca}	4.26 ± 0.38 ^{Cb}
	0.05	-20.1 ± 2.3 ^{Aa}	16.9 ± 2.3 ^{BCa}
	0.07	-25 ± 2 ^{Ba}	32 ± 4 ^{Bca}
	0.1	-27 ± 5 ^{Bb}	69 ± 9 ^{Ba}
	0.2	-22 ± 4 ^{Aa}	638 ± 77 ^{Aa}

^{A,B,C,D} Means in same bar with different letters are significantly different at $p < 0.05$ regarding the φ. ^{a,b,c} Means in same bar with different letters are significantly different at $p < 0.05$ in terms of type of emulsion (coarse, ultrasonicated or microfluidized).

Actually, coarse emulsions presented values ranging from -52.6 ± 3.7 to -37 ± 3 mV as increasing the SOR from 0.01 to 0.2, respectively, whereas ζ-potential of submicron emulsions was approximately between -42 and -24 mV at the same surfactant concentration. It is reported that the adsorption and orientation of negatively charged functional groups from water such as OH^- in the vicinity of oil droplets can contribute to decrease the surface charge (Marinova et al., 1996). In this regard, the higher the concentration of surfactant, the lower the water fraction has to be in order to maintain constant the φ and thus, the lower the presence of these groups contributing to decrease the ζ-potential. Regarding HSH process, the reduction of particle sizes by ultrasonication or microfluidization contribute to increase the surface area available to be covered and hence, there will be less non-adsorbed surfactant molecules in the continuous phase (Chung et al., 2017). Therefore, since it has been described how the presence of impurities such as fatty acids in non-ionic surfactants can contribute to decrease the ζ-potential of emulsions (Celus et al., 2018), a higher concentration of non-adsorbed surfactant molecules may lead to more negative ζ-potential values as it is the case of coarse emulsions.

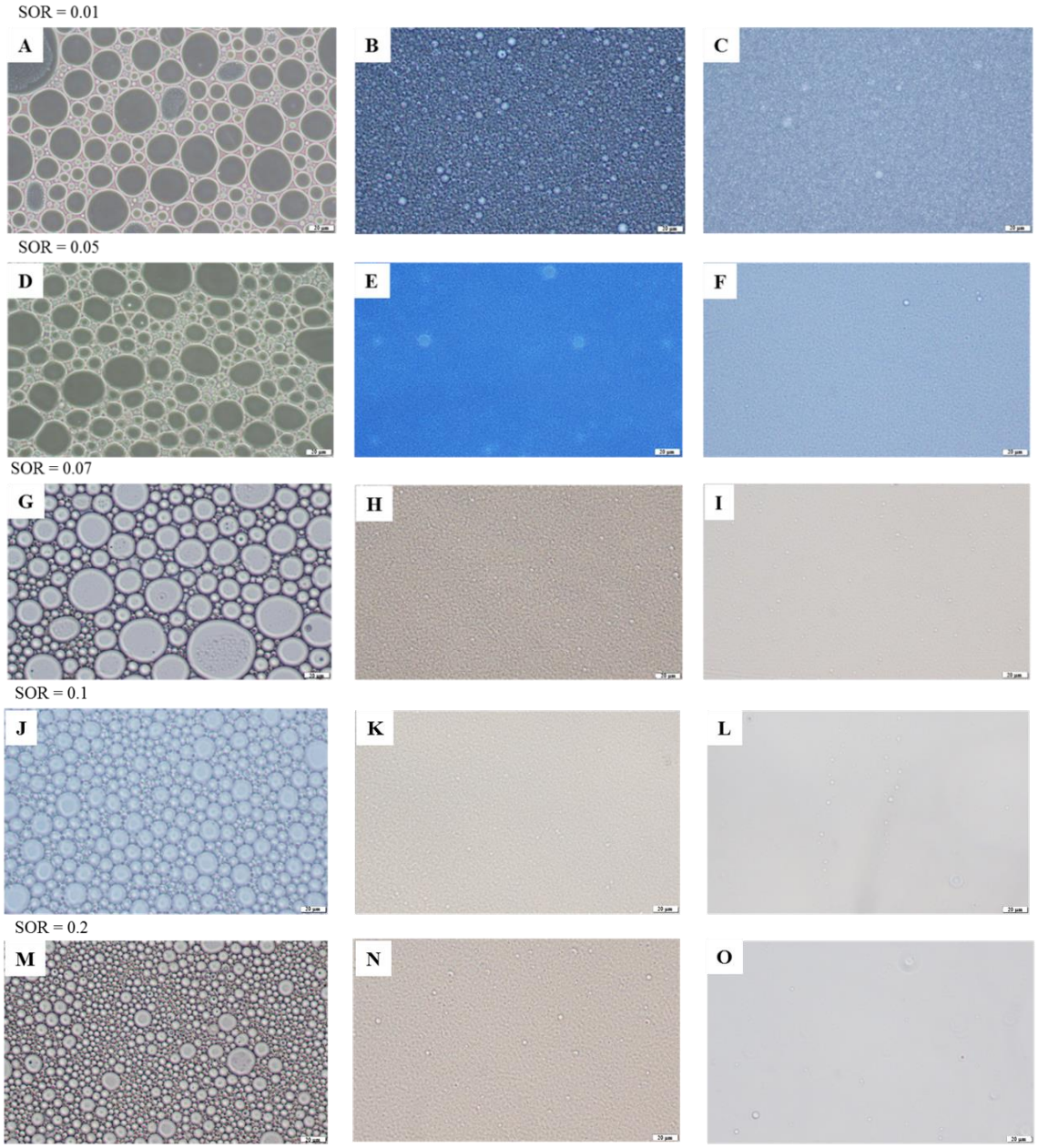

Figure 5. Microscopical phase contrast images of the highly concentrated coarse emulsions (A, D, G, J and M) and their subsequent submicron emulsions obtained by ultrasonication (200 s, 100 µm) (B, E, H, K and N) or microfluidization (2 cycles, 800 bar) (C, F, I, L and O) prepared by a volume fraction of 0.5 and surfactant-oil ratios of 0.01, 0.05, 0.07, 0.1 or 0.2. Error bar is equivalent a 20 µm.

3.4.Encapsulation efficiency and curcumin release kinetics of highly-concentrated emulsions

All the prepared curcumin-loaded emulsions (coarse, ultrasonicated and microfluidized) presented encapsulation efficiency (EE) emulsions higher than 71%, being the coarse emulsion that with the highest EE (78 ± 3%). The significant differences between the EE of coarse emulsion and the

resulting ultrasonicated or microfluidized emulsions (EE of 72.4 ± 1.8 or 71.21 ± 0.01 %, respectively) might be due to the curcumin degradation through the high-shear processing. This bioactive compound is prone to suffer auto-oxidation when it is exposed to the aqueous media due to its inherent instability leading to the formation of a bicyclopentadione as major product (Wiggers, Zaioncz, Cheleski, Mainardes,. & Khalil, 2017). Ultrasonicated emulsions presented in this work reached temperatures over 60ºC at the outlet of the system. Therefore, this temperature might be locally even higher inside the ultrasonic treatment chamber generating species such as hydrogen peroxide able to accelerate the oxidation of curcumin. In fact, Salvia-Trujillo et al. (2014) reported that cavitation phenomena induced by ultrasounds produce the collapse of air bubbles within the fluid. This fact causes a local increase of the pressure and temperature, which in turn results in the dissociation of water into hydroxyl radicals and hydrogen atoms, appearing several molecular species in the media such as hydrogen peroxide (Salvia-Trujillo et al., 2013b). Further research also supported that cavitation forces such as those inside the microfluidizer may lead to high energy molecules like hydroxyl radicals, which can cause chemical degradation (Artiga-Artigas, Acevedo-Fani, & Martín-Belloso, 2017; Feng, Cao, Xu, Wang, & Zhang, 2017).

Curcumin release measured during 48 h is shown in Figure 6 along with their kinetic parameters including the maximum estimated curcumin release (*CRmax*) and the kinetic constant (k). In the period of the first 5h of experiment, significant differences in terms of release were not observed. However, microfluidized emulsion reached the greatest release (70.5%) followed by the coarse emulsion (68.6 %), whereas the ultrasonicated nanoemulsion exhibited the lowest release of curcumin with a value of 62.8% after 48 h of experiment.

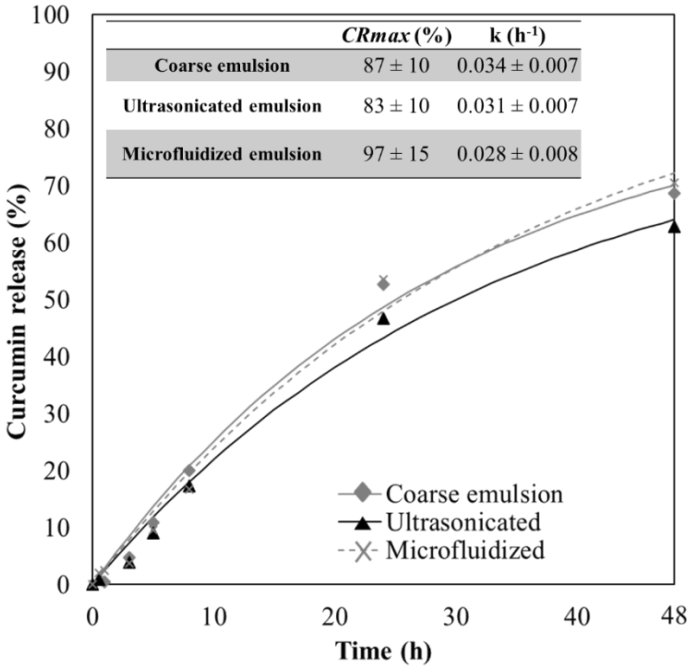

Figure 6. Curcumin release (%) of highly concentrated coarse emulsions and their subsequent submicron emulsions obtained by ultrasonication (200 s, 100 µm) or microfluidization (2 cycles, 800 bar) prepared with a surfactant-oil ratio of 0.1 and a volume fraction of 0.5. Emulsions were loaded with 0.01 % *w/w* of curcumin. The estimated maximum release (*CRmax*) expressed in % and the kinetic constant (k) in h^{-1} both calculated with the model: $CR = CRmax \cdot (1 - e^{-kt})$ are specified within the table.

Concerning the calculated kinetic parameters yielded by the adjusted model showed in eq.(3), neither the *CRmax* values (> 80%) nor k values (≈ 0.031 h^{-1}), were significantly different regardless the type of highly concentrated emulsion. This suggests that both coarse emulsions and submicron emulsions obtained by the two proposed HSH methods, resulted efficient as carriers for curcumin. In our previous research, polysorbates (*e.g.* Tween 20) also were able to retain around a 40% of curcumin after 24 h of study in diluted nanoemulsions (Artiga-Artigas et al., 2018). Low surface tension between droplets covered with Tween 20 prevented their coalescence and improved curcumin solubility ensuring its retention (Ratanajiajaroen et al., 2012).

4. Conclusions

Either ultrasonication (200 s, 100 µm) or microfluidization (2 cycles, 800 bar) led to highly concentrated submicron emulsions (φ = 0.4) with particle sizes lower than 500 nm when the SOR was 0.1. The increase of the φ, contributed to reduce the particle size of coarse emulsions as well as to increase their apparent viscosity. This triggered that HSH process caused the destabilization of the resulting emulsions when φ was higher than 0.5. The particle size of highly concentrated emulsions decreased as the SOR increased from 0.01 to 0.2. This reduction in particle size provoked a sharp increase of submicron emulsions apparent viscosity, especially after microfluidization, factor to take into into account depending on the desired applications. Moreover, all the emulsion-based systems prepared during the present study showed a high capability for the encapsulation and slow release of curcumin according to their low kinetic constants. This indicates the feasibility of these systems to be used as carriers of curcumin after a certain period of time preventing its degradation. Therefore, this manuscript contributes to elucidate the role of processing parameters, φ and SOR in the formation of highly concentrated nanoemulsions with potential ability to act as carriers of lipophilic bioactive compounds such as curcumin.

5. Acknowledgments

This study was funded by the Ministry of Economy, Industry and Competitiveness (MINECO/FEDER, UE) throughout project **AGL2015-65975-R**. Author María Artiga-Artigas thanks the University of Lleida for her pre-doctoral fellowship. Author Laura Salvia-Trujillo thanks the "Secretaria d'Universitats i Recerca del Departament d'Empresa i Coneixement de la Generalitat de Catalunya" for the Beatriu de Pinós post-doctoral grant (**BdP2016 00336)**.

6. References

Abbas, S., Karangwa, E., Bashari, M., Hayat, K., Hong, X., Rizwan, H., & Zhang, X. (2015). Ultrasonics Sonochemistry Fabrication of polymeric nanocapsules from curcumin-loaded nanoemulsion templates by self-assembly. *Ultrasonics - Sonochemistry*, *23*, 81–92.

Aditya, N. P., Shim, M., Yang, H., Lee, Y., & Ko, S. (2014). Antiangiogenic effect of combined treatment with curcumin and genistein on human prostate cancer cell line. *Journal of Functional Foods*, *8*(1).

Artiga-Artigas, M., Acevedo-Fani, A., & Martín-Belloso, O. (2017). Effect of sodium alginate incorporation procedure on the physicochemical properties of nanoemulsions. *Food*

Hydrocolloids, *70*, 191–200.

Artiga-Artigas, M., Guerra-Rosas, M. I., Morales-Castro, J., Salvia-Trujillo, L., & Martín-Belloso, O. (2018). Influence of essential oils and pectin on nanoemulsion formulation: A ternary phase experimental approach. *Food Hydrocolloids*, *81*, 209–219.

Artiga-Artigas, M., Lanjari-Pérez, Y., & Martín-Belloso, O. (2018). Curcumin-loaded nanoemulsions stability as affected by the nature and concentration of surfactant. *Food Chemistry*, *266*(June), 466–474.

Behbahani, E. S., Ghaedi, M., Abbaspour, M., & Rostamizadeh, K. (2017). Optimization and characterization of ultrasound assisted preparation of curcumin-loaded solid lipid nanoparticles: Application of central composite design, thermal analysis and X-ray diffraction techniques. *Ultrasonics Sonochemistry*, *38*, 271–280.

Bonilla, J., Atarés, L., Vargas, M., & Chiralt, A. (2012). Effect of essential oils and homogenization conditions on properties of chitosan-based films. *Food Hydrocolloids*, *26*(1), 9–16.

Borrin, T. R., Georges, E. L., Moraes, I. C. F., & Pinho, S. C. (2016). Curcumin-loaded nanoemulsions produced by the emulsion inversion point (EIP) method: An evaluation of process parameters and physico-chemical stability. *Journal of Food Engineering*, *169*, 1–9.

Bourbon, A. I., Cerqueira, M. A., & Vicente, A. A. (2016). Encapsulation and controlled release of bioactive compounds in lactoferrin-glycomacropeptide nanohydrogels: Curcumin and caffeine as model compounds. *Journal of Food Engineering*, *180*, 110–119.

Briceño, M., Salager, J. L., & Bertrand, J. (2001). Influence of dispersed phase content and viscosity on the mixing of concentrated oil-in-water emulsions in the transition flow regime. *Chemical Engineering Research and Design*, *79*(8), 943–948.

Bruschi, M. L. B. T.-S. to M. the D. R. from P. S. (Ed.). (2015). 6 - Drug delivery systems (pp. 87–194). Woodhead Publishing.

Calderó, G., Patti, A., Llinàs, M., & García-Celma, M. J. (2012). Diffusion in highly concentrated emulsions. *Current Opinion in Colloid and Interface Science*, *17*(5), 255–260.

Celus, M., Salvia-Trujillo, L., Kyomugasho, C., Maes, I., Van Loey, A. M., Grauwet, T., & Hendrickx, M. E. (2018). Structurally modified pectin for targeted lipid antioxidant capacity in linseed/sunflower oil-in-water emulsions. *Food Chemistry*, *241*(August 2017), 86–96.

Chung, C., Sher, A., Rousset, P., & McClements, D. J. (2017). Influence of homogenization on physical properties of model coffee creamers stabilized by quillaja saponin. *Food Research International*, *99*(April), 770–777.

Dickinson, E. (2003). Hydrocolloids at interfaces and the influence on the properties of dispersed systems. *Food Hydrocolloids*, *17*(1), 25–39.

Feng, L., Cao, Y., Xu, D., Wang, S., & Zhang, J. (2017). Ultrasonics Sonochemistry Molecular weight distribution , rheological property and structural changes of sodium alginate induced by ultrasound. *Ultrasonics - Sonochemistry*, *34*, 609–615.

Foudazi, R., Qavi, S., Masalova, I., & Malkin, A. Y. (2015). Physical chemistry of highly concentrated emulsions. *Advances in Colloid and Interface Science*, *220*, 78–91.

Garti, N., & Reichman, D. (1993). Food Structure Hydrocolloids as Food Emulsifiers and Stabilizers. *Food Structure*, *12*(4), 411–426.

Heurtault, B. (2003). Physico-chemical stability of colloidal lipid particles. *Biomaterials*, *24*(23), 4283–4300.

Jafari, S. M., Assadpoor, E., He, Y., & Bhandari, B. (2008). Re-coalescence of emulsion droplets during high-energy emulsification. *Food Hydrocolloids*, *22*(7), 1191–1202.

Jafari, S. M., He, Y., & Bhandari, B. (2006). Optimization of nano-emulsions production by microfluidization. *European Food Research and Technology*, *225*(5–6), 733–741.

Joseph, L. A., Israel, O. K., & Edet, E. J. (2009). Comparative Evaluation of Metal Ions Release from Titanium and Ti-6Al-7Nb into Bio-Fluids. *Dental Research Journal*, *6*(1), 7–11. Retrieved from http://www.ncbi.nlm.nih.gov/pmc/articles/PMC3075453/

Lacasse, M. D., Grest, G. S., Levine, D., Mason, T. G., & Weitz, D. A. (1996). Model for the elasticity of compressed emulsions. *Physical Review Letters*, *76*(18), 3448–3451.

Lin, C., Zhang, X., Chen, H., Bian, Z., Zhang, G., Riaz, M. K., … Yang, Z. (2018). Dual-ligand modified liposomes provide effective local targeted delivery of lung-cancer drug by antibody and tumor lineage-homing cell-penetrating peptide. *Drug Delivery*, *25*(1), 256–266.

Luo, X., Zhou, Y., Bai, L., Liu, F., Zhang, R., Zhang, Z., … McClements, D. J. (2017). Production of highly concentrated oil-in-water emulsions using dual-channel microfluidization: Use of individual and mixed natural emulsifiers (saponin and lecithin). *Food Research International*, *96*, 103–112.

Malkin, A. Y., Zadymova, N. M., Skvortsova, Z. N., Traskine, V. Y., & Kulichikhin, V. G. (2016). Formation of concentrated emulsions in heavy oil. *Colloids and Surfaces A: Physicochemical and Engineering Aspects*, *504*, 343–349.

Marinova, K. G., Alargova, R. G., Denkov, N. D., Velev, O. D., Petsev, D. N., Ivanov, I. B., & Borwankar, R. P. (1996). Charging of Oil−Water Interfaces Due to Spontaneous Adsorption of Hydroxyl Ions. *Langmuir*, *12*(8), 2045–2051.

Mason, T. G. (1999). New fundamental concepts in emulsion rheology [Review]. *Current Opinion in Colloid & Interface Science*, *4*(3), 231–238.

McClements. (2015). *Food Emulsions: Principles, Practices, and Techniques*.

McClements, D. J., & Decker, E. A. (2000). Lipid oxidation in oil-in-water emulsions: Impact of molecular environment on chemical reactions in heterogeneous food systems. *Journal of Food Science*, *65*(8), 1270–1282.

Muller, R. H., Harden, D., & Keck, C. M. (2012). Development of industrially feasible concentrated 30% and 40% nanoemulsions for intravenous drug delivery. *Drug Development and Industrial*

Pharmacy, *38*(4), 420–430.

Ngan, C. L., Basri, M., Tripathy, M., Karjiban, R. A., & Abdul-Malek, E. (2014). Physicochemical characterization and thermodynamic studies of nanoemulsion-based transdermal delivery system for fullerene. *Scientific World Journal*, *2014*.

Osborn, H. T., & Akoh, C. C. (2004). Effect of emulsifier type, droplet size, and oil concentration on lipid oxidation in structured lipid-based oil-in-water emulsions. *Food Chemistry*, *84*(3), 451–456.

Piorkowski, D. T., & McClements, D. J. (2014). Beverage emulsions: Recent developments in formulation, production, and applications. *Food Hydrocolloids*, *42*, 5–41.

Princen, H. M., Aronson, M. P., & Moser, J. C. (1980). Highly Concentrated Emulsions. *Journal of Colloid and Interface Science*, *75*(1), 246–270.

Qian, C., & McClements, D. J. (2011). Formation of nanoemulsions stabilized by model food-grade emulsifiers using high-pressure homogenization: Factors affecting particle size. *Food Hydrocolloids*, *25*(5), 1000–1008.

Ratanajiajaroen, P., Watthanaphanit, A., Tamura, H., Tokura, S., & Rujiravanit, R. (2012). Release characteristic and stability of curcumin incorporated in β-chitin non-woven fibrous sheet using Tween 20 as an emulsifier. *European Polymer Journal*, *48*(3), 512–523.

Salvia-Trujillo, L., Rojas-Graü, A., Soliva-Fortuny, R., & Martín-Belloso, O. (2013a). Physicochemical Characterization of Lemongrass Essential Oil-Alginate Nanoemulsions: Effect of Ultrasound Processing Parameters. *Food and Bioprocess Technology*, *6*(9).

Salvia-Trujillo, L., Rojas-Graü, M. A., Soliva-Fortuny, R., & Martín-Belloso, O. (2013b). Effect of processing parameters on physicochemical characteristics of microfluidized lemongrass essential oil-alginate nanoemulsions. *Food Hydrocolloids*, *30*(1), 401–407.

Salvia-Trujillo, L., Rojas-Graü, M. A., Soliva-Fortuny, R., & Martín-Belloso, O. (2014). Impact of microfluidization or ultrasound processing on the antimicrobial activity against Escherichia coli of lemongrass oil-loaded nanoemulsions. *Food Control*, *37*(1), 292–297.

Sanatkaran, N., Masalova, I., & Malkin, A. Y. (2014). Effect of surfactant on interfacial film and stability of highly concentrated emulsions stabilized by various binary surfactant mixtures. *Colloids and Surfaces A: Physicochemical and Engineering Aspects*, *461*(1), 85–91.

Silva, H. D., Cerqueira, M. Â., & Vicente, A. a. (2012). Nanoemulsions for Food Applications: Development and Characterization. *Food and Bioprocess Technology*, *5*(3), 854–867.

Surassmo, S., Min, S. G., Bejrapha, P., & Choi, M. J. (2010). Effects of surfactants on the physical properties of capsicum oleoresin-loaded nanocapsules formulated through the emulsion-diffusion method. *Food Research International*, *43*(1), 8–17.

Tshilumbu, N. N., Ferg, E. E., & Masalova, I. (2010). Instability of highly concentrated emulsions with oversaturated dispersed phase. Role of a surfactant. *Colloid J.*, *72*(Copyright (C) 2011 American Chemical Society (ACS). All Rights Reserved.), 569–573.

Wiggers, H.J.; Zaioncz, S.; Cheleski, J.; Mainardes, R.M. and Khalil, N. M. (2017). *Studies in Natural Products Chemistry*. Elsevier Science.

Wooster, T. J., Golding, M., & Sanguansri, P. (2008a). Ripening Stability. *Langmuir : The ACS Journal of Surfaces and Colloids*, *24*(10), 12758–12765.

Wooster, T. J., Golding, M., & Sanguansri, P. (2008b). Ripening Stability. *Langmuir : The ACS Journal of Surfaces and Colloids*, *24*(10), 12758–12765.

Xu, J.-H., Ge, X.-H., Chen, R., & Luo, G.-S. (2014). Microfluidic preparation and structure evolution of double emulsions with two-phase cores. *RSC Advances*, *4*(4), 1900.

Yakhoub, H. A., Masalova, I., & Haldenwang, R. (2011). Highly concentrated emulsions: Role of droplet size. *Chemical Engineering Communications*, *198*(2), 147–171.

Zeeb, B., Gibis, M., Fischer, L., & Weiss, J. (2012). Influence of interfacial properties on Ostwald ripening in crosslinked multilayered oil-in-water emulsions. *Journal of Colloid and Interface Science*, *387*(1), 65–73.

CHAPTER IV: *Effect of Sodium alginate incorporation procedure on the physicochemical properties of nanoemulsions*

Artiga-Artigas, M.; Acevedo-Fani, A.; Martín-Belloso, O.

Food Hydrocolloids (2017); 70: 191-200

Abstract

The aim of this work was to evaluate the effect of sodium alginate incorporation procedure on the physicochemical properties of nanoemulsions formed by microfluidization. Emulsions prepared consisted of corn oil and Tween 20 as dispersed phase and sodium alginate solution as continuous phase. In order to obtain nanoemulsion A (N_A), both phases were microfluidized together. On the other hand, coarse emulsion without sodium alginate was microfluidized and mixed with a microfluidized (MA) or non-microfluidized (N-MA) sodium alginate solution leading to nanoemulsions B(MA) and B(N-MA), respectively. N_A exhibited the smallest particle size (261 nm) and monomodal distributions with a polydispersity index of 0.25. The ζ-potential, viscosity and WI of N_A were -37mV, 22.7mPa·s and 57.28, respectively. Spectroscopic, chromatographic and electron microscopic techniques were used to evaluate changes in microfluidized alginate molecules when they were within emulsions. After microfluidization, alginates suffered depolymerization and further rearrangement, changing the disposition of polymer chains around oil droplets and nanoemulsions characteristics. Thus, these results evidence the significant impact of sodium alginate incorporation procedure on the physicochemical properties of nanoemulsions and how it can affect to the stability of the resulting systems once they are applied onto food matrices.

Keywords: Sodium alginate; microfluidization; nanoemulsion; infrared spectroscopy; corn oil.

1. Introduction

Nanoemulsions are described as colloidal dispersions consisting of oil droplets, with a diameter in the nano-range scale, dispersed into an aqueous phase (Rao & McClements, 2011b). Moreover, the presence of a surfactant capable of adsorbing at the oil/water interface of droplets is required to reduce the surface tension and lead to emulsion formation. Oil-in-water nanoemulsions have shown some advantages compared to conventional emulsions. Nanoemulsions present higher physical stability against gravitational processes like flocculation, creaming, sedimentation and coalescence and enhance functionality due to the increase of the surface area of droplets (Guerra-Rosas et al., 2016). Moreover, the use of nanoemulsions let diminish the concentration of each component added to the systems minimizing the alterations in the sensorial properties of the food matrix, and also strong light scattering (McClements, 2011). The incorporation of active compounds like certain vitamins, antioxidants or antimicrobials into food matrices represents a challenge due to their low water solubility and high degradability when they are exposed to external factors such as pH, temperature or light (Borrin et al., 2016). Nanoemulsions appear as systems that could be able to encapsulate, protect and release these compounds effectively (Salvia-Trujillo & McClements, 2015).

On the other hand, the addition of texture modifiers such as biopolymers to the aqueous phase might be useful to improve nanoemulsions stability by reducing droplets movement. Some of these macromolecules, as it is the case of alginates, are capable to interact with surfactant chains disposed around the oil droplets. Hence, they may cause steric and/or electrostatic repulsions between droplet interfaces avoiding destabilization phenomena such as droplets coalescence or gravitational separation (Salvia-Trujillo, Rojas-Graü, Soliva-Fortuny, & Martín-Belloso, 2014). Alginates are linear polysaccharides, which consist of β-D-mannuronic (M) acid and α-L-guluronic (G) acid linked by 1→4 bonds that are able to absorb large quantities of water leading to the formation of hydrogels and hence, facilitating the solubility of the alginate chains in the aqueous phase (Lee & Mooney, 2012; Tao Wang, Sun, Raddatz, & Chen, 2013). In addition, alginates contain functional groups such as carboxylates, which can easily dissociate in the aqueous phase and as a result, provide negative charge to the emulsions (Pereira et al., 2013). Therefore, in presence of multivalent ions, alginates can form polymer networks by a process known as ionic gelation due to their high "gel-forming" capability (Liling et al., 2016). In these networks, linear chains of alginate are connected by ionic interactions resulting in crosslinks called "egg-box". Taking advantage of this property, nanoemulsions containing alginates could be used as films or edible coatings for food matrices (Strobel, Scher, Nitin, & Jeoh, 2016).

The addition procedure of alginate could cause either the increase of nanoemulsions stability or the destabilization of the blends resulting in the loss of functionality. Moreover, it is thought that polysaccharides suffer modifications after microfluidization process due to high shear stress, impact force and hydrodynamic cavitation, which increase the porosity of the biopolymer molecules extending their superficial area (Laneuville, Turgeon, & Paquin, 2013). In this regard, changes in alginate molecules disposed around oil droplets may alter the physicochemical characteristics of nanoemulsions. Therefore, it is necessary to understand the interactions among the alginate and the rest of the components of the nanostructured systems to obtain nanoemulsions with the most appropriated properties according to their further applications.

Thus, the aim of this work was to assess the effect of the incorporation procedure of alginate on the physicochemical properties of nanoemulsions formed by microfluidization to ensure the

stability of the resulting systems once they are added to food matrices. And in turn, what influence may have this process in sodium alginate structure.

2. Materials and methods

2.1.Materials

Corn oil (Koipesol Asua, Deoleo, Spain) and ultrapure water, obtained from a Millipore Milli-Q filtration system (Merck, Darmstadt, Germany) were used for the preparation of all emulsions. Tween 20 was purchased from Panreac (Barcelona, Spain). Sodium alginate (MANUCOL® DH) was provided by FMC Biopolymers Ltd (Scotland, U.K.). Information provided by the manufacturer indicates that viscosity and pH of a solution 1% is 40-90 mPa·s and 5.0-7.5, respectively.

2.2.Methods

2.2.1. Nanoemulsions formation

All the oil-in-water emulsions showed a final formulation consisting of 1% w/w lipid phase (corn oil) with 1% w/w of surfactant (Tween 20) and 98% w/w aqueous phase (1% w/w sodium alginate, 99% w/w water). Sodium alginate solutions were prepared by dissolving the sodium alginate in water at 70ºC for 2 h and then cooling it to room temperature. Concerning nanoemulsions preparation, two different procedures were performed in order to evaluate the effect of the sodium alginate incorporation in the properties of nanoemulsions. After characterizing nanoemulsions in terms of particle size, ζ-potential, viscosity, whiteness index and morphology, those nanoemulsions with the most suitable properties, such as lower particle sizes and ζ-potential values, were more deeply studied to assess the effect of microfluidization in sodium alginate structure.

2.2.1.1.Sodium alginate incorporation before coarse emulsion formation

A coarse emulsion (C_A), was prepared by mixing both lipid and aqueous phases and the surfactant using a high-speed blender (T25 digital Ultra-Turrax, IKA, Staufen, Germany) at 11.000 rpm for 2 min, at room temperature. C_A was treated with a microfluidizer (M110P, Microfluidics, Massachusetts, USA) at 150 MPa and 5 cycles, in order to obtain nanoemulsion A (N_A).

2.2.1.2.Sodium alginate incorporation after coarse emulsion formation

The lipid phase, surfactant and ultrapure water were homogenized with the high-speed blender (T25 digital Ultra-Turrax, IKA, Staufen, Germany) at 11.000 rpm for 2 min, at room temperature. The coarse emulsion (C_B) was passed across the microfluidizer (M110P, Microfluidics, Massachusetts, USA) at 150 MPa for 5 cycles to produce a fine emulsion. This fine emulsion was stirred together with a microfluidized alginate solution (MA) (5 cycles and at 150 MPa) or with a non-microfluidized alginate solution (N-MA), both in the corresponding concentration to obtain a final blend with 1% w/w of sodium alginate, during 1 h at room temperature; this led to nanoemulsion B(MA) ($N_{B(MA)}$) or nanoemulsion B(N-MA) ($N_{B(N-MA)}$), respectively.

2.2.2. Physicochemical characterization

2.2.2.1.Particle size and size distributions

The particle size distribution, polydispersity indexes (PdI) and mean droplet diameters (nm) of coarse emulsions and nanoemulsions as well as the particle size of alginate solutions were measured using a laser diffractometer (Nano-ZS Zetasizer, Malvern Instruments, Worcestershire, U.K.) working at 633 nm, 25 ºC and equipped with a backscatter detector (173º). Samples were prior diluted in ultrapure water using a dilution ratio of 1:9 sample-to-solvent.

2.2.2.2.ζ-potential

The ζ-potential (mV) of oil droplets in emulsions and nanoemulsions was measured by phase-analysis light scattering (PALS) with a Zetasizer NanoZS laser diffractometer (Malvern Instruments Ltd, Worcestershire, UK). Samples were prior diluted in ultrapure water using a dilution ratio of 1:9 sample-to-solvent.

2.2.2.3.Apparent viscosity

Apparent viscosity measurements (mPa·s) of 10 mL aliquots of coarse emulsions, nanoemulsions and alginate solutions were performed by using a vibro-viscometer (SV-10, A&D Company, Tokyo, Japan) vibrating at 30 Hz and constant amplitude (0.4 mm). The device can detect accurate temperature immediately because the fluid and the detection unit (sensor plates) with small surface area/thermal capacity reach the thermal equilibrium in only a few seconds. Therefore, the measurements were performed at controlled room temperature.

2.2.2.4.Whiteness index

The optical properties of coarse emulsions and nanoemulsions were measured using a colorimeter (Konica Minolta CR-400, Konica Minolta Sensing Inc., Osaka, Japan) at room temperature set up for illuminant D65 and 10º observer angle. The device was calibrated with a standard white plate (Y=94.0; x=0.3133; y=0.3194). Once determined the values of CIE L^*, a^* and b^*; the Whiteness Index (WI) was calculated with equation (1) (Salvia-Trujillo, Rojas-Graü, Soliva-Fortuny, & Martín-Belloso, 2013):

$$WI = 100-((100-L)^2+(a^2+b^2))^{0.5} \quad \textbf{eq.(1)}$$

2.2.2.5.Transmission electron microscopy (TEM)

Emulsions were observed by negative-staining electron microscopy as a direct measurement of their droplet size and shape. Conventional emulsions and nanoemulsions were diluted with ultrapure water using a factor of 1:10, and they were adsorbed onto carbon-coated copper/palladium grids for 1 min. Then, the grids were washed three times by floating it face-down on drops of sterilized, deionized water for 1 min. Finally, the sample was negatively stained by floating the grids

face-down on a drop of 2% *w/w* ammonium molybdate at pH 6.5 for 1 min. The grids were observed in a transmission electron microscope (Jeol 2100, FEI Company, Netherlands) at an acceleration voltage of 100 kV.

2.2.3. Molecular characterization

2.2.3.1.Infrared Spectroscopy (ATR)

Infrared spectroscopy through attenuated total reflectance (ATR) was applied to freeze-dried samples of coarse emulsions, nanoemulsions and alginate solutions in order to avoid the interferences caused by water in the –OH signal (3400-3600 cm^{-1}). After freeze-dried process with a Cryodos 50 freeze drier (Telstar Cryodos, Terrassa, Spain) working with a vacuum pressure of 0.128 mBar and a temperature of -45.6 ºC, emulsions and alginate solutions were directly measured in solid state by using an infrared spectrometer (FT-IR 6300 Jasco Series, Easton, USA) in a range of 4000-600 cm^{-1}. All tests were performed in triplicate and data were processed using SpectraManager Software (Jasco Analitica Spain S.L, Madrid, Spain).

2.2.3.2.Nuclear magnetic resonance (^{1}H-NMR)

Samples of emulsions, nanoemulsions and alginate solutions were freeze-dried using a Cryodos 50 freeze drier (Telstar Cryodos, Terrassa, Spain) working with a vacuum pressure of 0.128 mBar and a temperature of -45.6 ºC, weighed in a precision scale (Denver Instrument S-234, Germany) and dissolved in 7.5 mL of D_2O in order to be analyzed with a NMR spectrometer (Mercury Plus AS 400 MHz, Varian; California, USA). Data were processed with MestReNova 10.0.2 Software (Mestrelab Research, Santiago de Compostela, Spain).

2.2.3.3.Gel permeation chromatography (GPC)

Microfluidized and non-microfluidized alginate solutions were prior diluted in water by a 1:1 factor and compared with different dextran solutions of 2 mg/mL acting as patterns (Sigma-Aldrich, USA).

Gel permeation chromatography (GPC) of the alginate solutions was used to study the breaking of alginate molecules. The chromatograph (Waters Alliance 2695, Waters, Barcelona, Spain) was composed by a refraction index detector (Waters 2414, Barcelona, Spain) and a weighing scale (Mettler Toledo AT261 Delta Range, Barcelona, Spain). Chromatographic conditions consisted of an Ultrahydrogel 1000 + Ultrahydrogel 250, 300x7.8 mm column (Waters, Barcelona, Spain) using $NaNO_3$ 0.1M as eluent at 30ºC and the injection volume was 50 µl with a flux of 1.0 mL/min. Data were processed with the Empower GPC Software (Waters, Mildford, USA).

2.3.Statistics

All the procedures were assessed in duplicate, and at least three measurements of each parameter were carried out. The statistical software SigmaPlot 11.0 (Systat Software Inc., Pennsylvania, USA) was used to perform the analysis of variance. To determine differences among means of the different procedures, Tukey test (Two Way ANOVA) was run at a 5% significance level.

In the case of comparing microfluidized and non-microfluidized alginate solutions, a Rank Sum test (One Way ANOVA) was run at a 5% significance level as well.

3. Results

3.1.Average droplet size

Average particle sizes of emulsions and nanoemulsions obtained by the different procedures are shown in Table 1. All coarse emulsions exhibited a dramatic reduction of their average droplet size after creating shear and impact forces caused by microfluidization (Maa & Hsu, 1999). $N_{B(MA)}$ and $N_{B(N\text{-}MA)}$, in which alginate solution (microfluidized or not, respectively) was added in the last step of the nanoemulsion preparation, presented average droplet sizes over 300 nm with values that did not show statistically significant differences ($P>0.05$).

3.2.Polydispersity indexes and droplet size distributions

Polydispersity indexes (PdI) of N_A decreased after microfluidization regarding their respective coarse emulsions (Table 1). In the case of $N_{B(MA)}$ and $N_{B(N\text{-}MA)}$, PdI values increased after microfluidization without significant differences ($P<0.05$) neither between the coarse emulsions nor between the nanoemulsions.

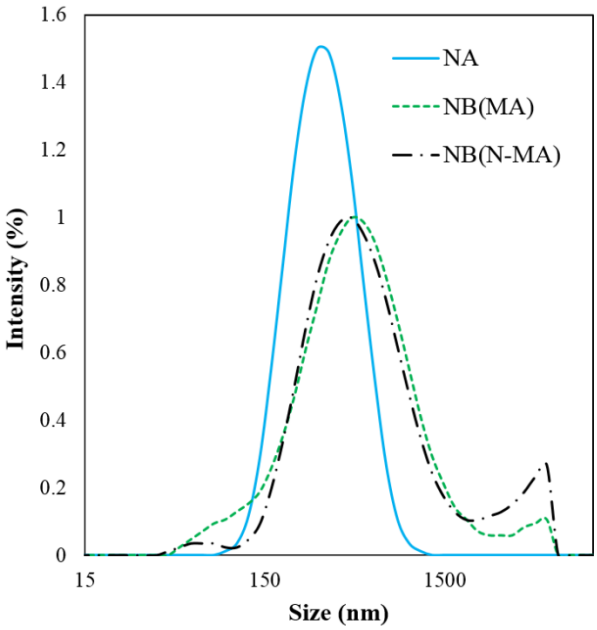

Figure 1. Average droplet size distributions in terms of intensity (%) of nanoemulsions A (N_A) where the incorporation of sodium alginate took place before the coarse emulsion formation; and nanoemulsions B where the incorporation of microfluidized ($N_{B(N\text{-}MA)}$) or non-microfluidized ($N_{B(MA)}$) sodium alginate, respectively, occurred after coarse emulsion formation. Microfluidization processes were performed at 150 MPa and for 5 cycles.

Moreover, as it can be appreciated in Figure 1, $N_{B(MA)}$ and $N_{B(N-MA)}$ exhibited multimodal droplet size distributions with major intensity peaks positioned at the nano-range scale and with minor peaks not only located at the macro-range but above the detection limit of the equipment (more than 10,000 nm), even after microfluidization process of sodium alginate as it is the case of $N_{B(MA)}$. Multimodal distributions led to high polydispersity indexes (PdI), hence, N_A showed the lowest PdI with a value of 0.25 ± 0.01, while the PdI of $N_{B(MA)}$ and $N_{B(N-MA)}$ did not present significant differences with values between 0.41 ± 0.02 and 0.45 ± 0.02, respectively.

3.3.ζ-potential

The ζ-potential values of emulsions and their respective nanoemulsions obtained were all negative as it can be observed in Table 1. Moreover, the negative electrical charge of droplets in N_A and $N_{B(MA)}$ decreased after microfluidization regarding their respective coarse emulsions. However, the ζ-potential of $N_{B(N-MA)}$ did not change significantly ($P<0.05$) concerning their coarse emulsion.

3.4.Apparent Viscosity

C_B, without alginate, presented rather low viscosity values and similar to the water viscosity (≈1 mPa·s), whereas C_A exhibited viscosity values of 42.4 ± 0.8 mPa·s on average (Table 1). The highest increase after microfluidization was observed for $N_{B(N-MA)}$, where the non-microfluidized alginate solution was mixed with the fine emulsion observing a viscosity value of 61.07 mPa·s on average. However, in the case of using microfluidized alginate ($N_{B(MA)}$) the viscosity was lower (Table 1). Oppositely, the viscosity of N_A and alginate solutions (Fig. 2B) decreased on average from 42.43 to 22.73 mPa·s and from 167 to 137 mPa·s, respectively, after microfluidization process.

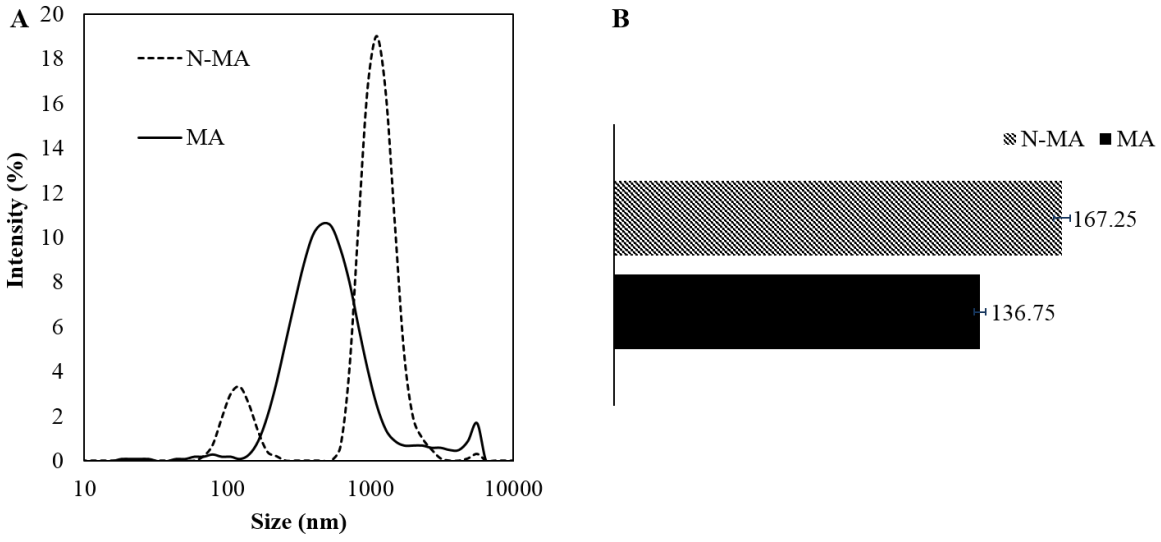

Figure 2. (A) Average particle size distributions (nm) and (B) apparent viscosity mean values (mPa·s) of non-microfluidized (N-MA) and microfluidized (MA) alginate solutions (at 150 MPa and 5 cycles, respectively).

3.5.Whiteness index (WI)

The optical properties of coarse emulsions and nanoemulsions expressed as WI are presented in Table 1. WI values increased after microfluidization process in all cases. Nevertheless, WI of N_A and $N_{B(MA)}$, in which alginate solution underwent to the microfluidization process, did not differ significantly. Oppositely, $N_{B(N-MA)}$ showed the highest WI with a value of 60.28 ± 0.05.

Table 1. Droplet size (nm), polydispersity index (PDI), ζ-potential (mV), viscosity (mPa·s) and whiteness index (WI) of coarse emulsions A (C_A) and B (C_B)-with and without containing sodium alginate, respectively- and nanoemulsions N_A where sodium alginate was added in the first step of emulsions formation; $N_{B(MA)}$ and $N_{B(N-MA)}$ in which a solution of microfluidized or non-microfluidized sodium alginate solution, respectively, was added to a fine emulsion prior prepared. Data shown are the means ± standard deviation.

	Droplet size (nm)	*PdI*	*ζ*-potential (mV)	*Viscosity (mPa·s)*	*Color (WI)*
C_A	8865 ± 588^{a}	0.45 ± 0.14^{a}	-10.3 ± 0.8^{a}	42.4 ± 0.8^{a}	52.84 ± 0.04^{a}
C_B	4012 ± 555^{b}	0.27 ±0.14^{b}	-15.8 ± 2.1^{c}	1.17 ± 0.02^{b}	42.65 ± 1.87^{c}
N_A	261 ± 6^{c}	0.25 ± 0.01^{c}	-39 ± 3^{d}	22.7 ± 0.4^{c}	57.28 ± 0.02^{d}
$N_{B(MA)}$	315 ± 5^{d}	0.41 ±0.02^{d}	-20.9 ± 1.5^{f}	29.5 ± 0.4^{e}	58 ± 2^{d}
$N_{B(N-MA)}$	443 ± 28^{d}	0.45 ± 0.02^{d}	-26.98 ± 0.01^{e}	61.07 ± 0.21^{d}	60.28 ± 0.05^{e}

^{a,b,c,d,e,f} Means in same column with different letters are significantly different at $p < 0.05$.

3.6.Microstructure

The morphology of droplets in N_A, $N_{B(MA)}$ and $N_{B(N-MA)}$ was examined by transmision electron microscopy (TEM) as it can be observed in Figure 3. With this technique, it was possible to observe significant differences regarding the shape and the disposition of the droplets. TEM images revealed a wide range of particle sizes with an average droplet size of 183 ± 45 nm in N_A (Fig.3A), whereas its mean particle size calculated by DLS was higher (261 ± 6 nm). In the case of $N_{B(MA)}$ where alginate solution was microfluidized and added in the last step of emulsion formation, TEM images presented discrete and spherical particles whose droplet diameters ranged between 10 to 500 nm (Fig.3B).

Nevertheless, as in the case of DLS, in TEM images of $N_{B(N-MA)}$ (Fig.3C) it is possible to confirm that the presence of non-microfluidized sodium alginate led to particles with the highest mean droplet diameters 382 ± 209 nm and there were not isolated particles (Table 1).

3.7.Effect of microfluidization on alginate molecular structure.

N_A presented the lowest droplets sizes, ζ-potential, viscosity and WI values, thus, they were expected to be the nanoemulsions with the most suitable properties to be stable during the time. In order to study the effects of microfluidization process on polymer structure, chemical and structural characterizations of coarse emulsions and nanoemulsions A (C_A and N_A, respectively) and alginate solutions by FT-IR and ^{1}H-NMR spectroscopies and gel permeation chromatography (GPC), were achieved.

3.7.1. FT-IR and 1H-NMR spectra

Microfluidized alginate spectrum showed a slight decrease of the –OH (3300 cm-1, stretch, H-bonded) and $–COO^-$ groups (1593 and 1400 cm^{-1}, asymmetric and symmetric stretch, respectively) after microfluidization, being the signal corresponding to –OH groups who experienced the highest decrease (Fig.4A).

Regarding emulsions spectra, Figure 4B showed the disappearance of the peaks at 3002 and 1633 cm^{-1} (alkenes, -C=C-) and 1740 cm^{-1} (together with 1100 cm^{-1}, ester, R'COO-R) that correspond exclusively to corn oil. This could indicate that the corn oil remained within the biopolymer structure. Moreover, the band corresponding to the esters of Tween 20 (1731 cm^{-1}, R'COO-R) decreased in intensity after microfluidization process, whereas those peaks corresponding to alkenes (2919 and 1624 cm^{-1}) did not experiment significant variations ($P>0.05$) in emulsions spectrum (Fig.4B). Nevertheless, it was possible to observe a slight increase in the signal corresponding to O-H bond (3330 cm^{-1}, stretch, H-bonded) and carboxylate groups ($-C=OO^-$, 1595 and 1402 cm^{-1}, asymmetric and symmetric stretch, respectively) of sodium alginate in nanoemulsion spectrum in comparison to the coarse emulsion.

According to proton nuclear magnetic resonance (^{1}H-NMR) technique, microfluidized alginate lost a 31% of the protons in comparison with non-microfluidized alginate spectrum (Fig.5). Likewise, the number of total protons in the spectrum of the coarse emulsion is approximately a 38% higher than that observed in nanoemulsions (Fig.6A and 6B, respectively), being remarkable that differences in peaks integration occurred only in the region corresponding to the main chain of sodium alginate (3.70-4.20 ppm), whereas the rest of integrations remained unaltered (Huang et al., 2015).

3.7.2. Size exclusion chromatography: Gel permeation chromatography (GPC)

Table 2 shows GPC analyses of microfluidized and non-microfluidized alginate solutions. GPC analyses revealed a significant reduction of average molecular weight of microfluidized alginate from 785,656 ± 48,5461 u to 679,809 ± 18,455 u, together with the change in the shape of the GPC profiles (not reported), which indicated the presence of a second polymer distribution after having passed through the microfluidizer. However, the difference in the average values for the rest of studied variables between the two groups was not great enough to exclude the possibility that the difference was due to random sampling variability and therefore, there was not a statistically significant difference ($P= 0.333$).

4. Discussion

Nanoemulsions A (N_A) in which sodium alginate solution was microfluidized at the same time that the rest of components, showed the smallest particle sizes. During microfluidization, creating shear and impact forces may cause a cavitation phenomenon that leads to the reduction of the emulsions droplet size (Maa & Hsu, 1999). In this sense, alginate chains disposition around the droplets may be more homogeneous because the high shear stress occurred on all components of the nanoemulsion at the same time, resulting in a lower PdI (Qian & McClements, 2011). However, in $N_{B(MA)}$ and $N_{B(N\text{-}MA)}$, in which the added alginate was microfluidized or not, respectively; a destabilization phenomenon such as re-coalescence of oil droplets may occur after microfluidization causing an increase in the polydispersity indexes of nanoemulsions (Bonilla et al., 2012a). Nevertheless, microfluidization had an influence on particle sizes promoting the changes of the molecular structure of alginate, which allow obtaining smaller particle sizes. Consequently, the highest particle sizes were observed for $N_{B(N\text{-}MA)}$ in which alginate did not pass through the microfluidizer. Indeed, $N_{B(MA)}$ and $N_{B(N\text{-}MA)}$ size distributions were not monomodals (Fig.1) but they presented another minor peak. These minor peaks observed in Fig.1 could be surfactant micelles that were not adsorbed at the oil droplets interface due to an excess of alginate molecules that had been repelled (Heydenreich, Westmeier, Pedersen, Poulsen, & Kristensen, 2003; Neumann, Schmitt, & Iamazaki, 2003). However, it is more likely that they were aggregates of the biopolymer molecules that do not contain oil within, since particle size distributions of both microfluidized and non-microfluidized alginate solutions (Fig.2A) revealed the same minor peak at the same position.

Moreover, particle size and polidispersity indexes variability between N_A, $N_{B(MA)}$ and $N_{B(N\text{-}MA)}$ observed using light scattering was confirmed by TEM (Fig.3). Certainly, in these images it was possible to observe that the presence of aggregates is higher if alginate molecules are not subjected to high shear stress (Fig.3C). The lack of microfluidization process might cause that alginate molecules maintain their original structure without suffering depolymerization processes, which may cause greater steric impediment among biopolymer chains during their disposition around the oil droplets leading to bigger and non-spherical particles. Thus, microfluidization may also enhance the stability of the blends (Feng, Cao, Xu, You, & Han, 2016; Villay et al., 2012).

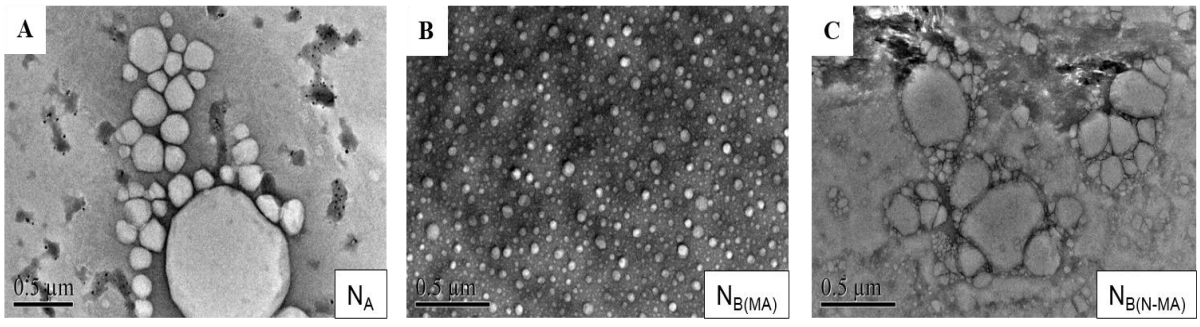

Figure 3. Transmission electron microscopy (TEM) images of nanoemulsions A (N_A) where the incorporation of sodium alginate took place before the coarse emulsion formation (A); and nanoemulsions B where the incorporation of microfluidized ($N_{B(N\text{-}MA)}$) or non-microfluidized ($N_{B(MA)}$) sodium alginate occurred after coarse emulsion formation (B or C, respectively). Microfluidization processes were performed at 150 MPa and for 5 cycles.

On the other hand, Tween 20 is a non-ionic low-mass surfactant that rapidly coats the newly created droplets during emulsification (Kralova & Sjöblom, 2009) giving a neutral or slightly negative electrical charge on oil-water interface (Hsu & Nacu, 2003). Nevertheless, a negative charge was observed in all the emulsions and nanoemulsions in the present work. This is because Tween 20 is preferably adsorbed on the oil surface in the co-presence of polymeric stabilizers, such as sodium alginate molecules, which provided negative charge to oil-water interfaces when dispersed in the aqueous phase (Nambam & Philip, 2012). Therefore, the alginate addition had a really strong influence in the surface charge of oil droplets in emulsions and nanoemulsions due to the presence of carboxylates and hydroxyl groups, which are easily deprotonated at neutral pH (≈ 6-7) (Yang, Jiang, He, & Xia, 2012). Furthermore, the mechanical stress during microfluidization can lead alginate chains to break up or modify its disposition, increasing the number of those molecules able to be potentially adsorbed on the oil-water interface (Chen, Gao, Yang, & Gao, 2013a). In this sense, a partial breaking of alginate molecule may cause the change of its disposition around the oil droplets and increase the concentration of deprotonated groups. In this sense, N_A showed the lowest ζ-potential value and therefore, it could be expected that this nanoemulsion will be less exposed to re-coalescence than $N_{B(MA)}$ and $N_{B(N\text{-}MA)}$.

The increase in viscosity values of the obtained emulsions and nanoemulsions depended on the fact that the alginate has been microfluidized or not. According to Yang et al. (2012), apparent viscosity of emulsions is strongly influenced by the presence of the alginate dispersed in the aqueous phase. In fact, alginate may be a good candidate for chemical functionalization because can present surface activity after being dispersed into the aqueous medium, increasing the viscosity of the solutions. In contrast and based on our results, microfluidization process could cause a significant increase in the porosity of polysaccharide chains due to cavitation forces, which allow chains holding more water leading to the decrease of apparent viscosity (Wang et al., 2013). Harte & Venegas, (2010) also reported a 75-85% viscosity reduction in alginate solutions processed by high-pressure homogenization from 1 to 5 cycles up to 300 MPa. Similarly, Villay et al., (2012) observed a viscosity reduction on sodium alginate solutions when they were microfluidized at 195 MPa for several cycles. They attributed this effect to a decrease in the molar mass of sodium alginate due to a depolymerization of chains caused by covalent bond disruption. This depolymerization is a result of the chemical reaction between the polymers and high energy molecules such as hydroxyl radicals produced from cavitation (Feng et al., 2017). Only when the molecular weight of sodium alginate (M_w) is low enough, particles are able to resist mechanical forces such as shear, turbulence or cavitation, caused by microfluidization. This fact let diminish the heterogeneity of chains, and thus the PdI of this macromolecular species in solution (Villay et al., 2012). Although all the coarse emulsions exhibited a decrease in their average droplet size and size distribution after being microfluidized, none of the nanoemulsions of this study became completely transparent. It is reported that large particles scatter the light more intensely and it produces an increase in lightness (L^*), opacity and WI of emulsions (McClements, 2011).

Therefore, alginate molecules may contribute to raise WI values, probably due to an increase of the number of large particles in dispersion (McClements, 2002). In addition, according to Salvia-Trujillo et al. (2014), the type of oil used in the formulation significantly influenced the WI of the coarse emulsions and nanoemulsions. Corn oil, as other vegetal oils, is intense in color and causes an increase of the WI after microfluidization process (Ekthamasut & Akesowan, 2010; Pereda, Aranguren, & Marcovichs, 2010). It is described that the light scattering of oil droplets depends on the

refractive index of continuous and dispersed phase, oil concentration and droplet size (McClements, 2002a). In this regard, when the refractive index ratio (n_2/n_1) tends to unity, as in the case of corn oil whose refractive index is 1.47 (n_1 = 1.33), the light scattering produced by the lipid droplets dispersed in the emulsion promotes the increase of the opacity of the blends (McClements, 2002a; Yang & Paulson, 2000).

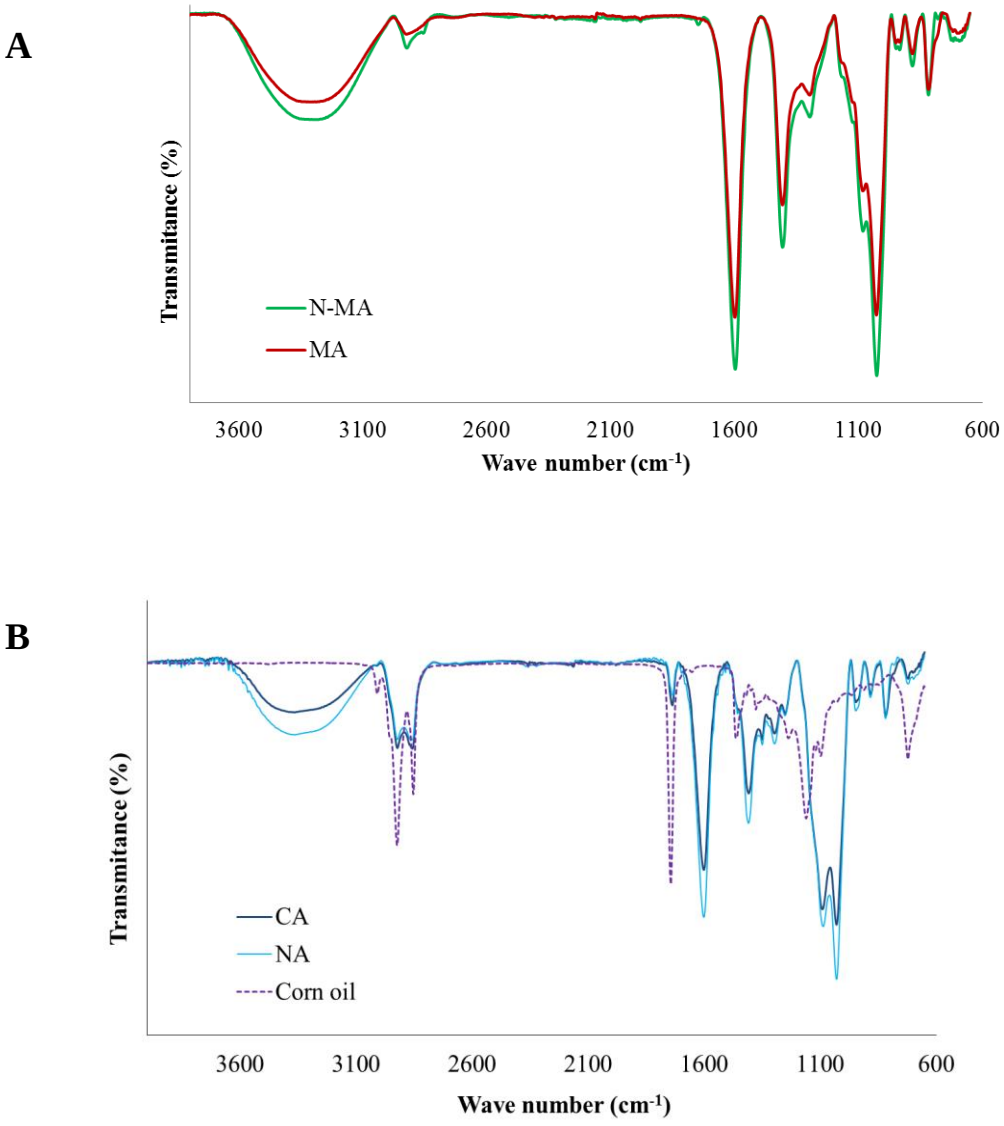

Figure 4. Normalized infrared spectra of (A) freeze-dried non-microfluidized (N-MA) and microfluidized (MA) alginate solutions at 150 MPa and 5 cycles and (B) freeze-dried nanoemulsions A (NA) and coarse emulsions A (CA) containing sodium alginate. Microfluidization was performed at 150 MPa, for 5 cycles.

The increase of hydroxyls observed in alginates spectrum (Fig. 4B) may be due to the breaking of O-glycosidic bonds (depolymerization) or an opening of the alginate structure caused by mechanical forces into the microfluidizer, which increase the ability of sodium alginate for holding

water (Chen et al., 2013a; Mohammad, Hosseini, Emam-djomeh, Hadi, & Meeren, 2013). Nonetheless, in spite of microfluidization may accelerate the collisions between the solvent molecules and sodium alginate molecules causing biopolymer degradation, it has been suggested that alginate is able to rearrange (Chemat & Khan, 2011).

In contrast, in the case of nanoemulsion spectrum, the observed behavior was the opposite because inside these systems mechanical forces can attack the structure of microfluidized molecules, which were not able to restructure (Laneuville et al., 2013). Indeed, the application of these forces may result in some reactions such as sodium alginate conjugation or oxidation (Feng et al., 2017). In this regard, high shear stress caused by microfluidization process could cause the oxidation of hydroxyl groups to carboxylic acids easily deprotonated in aqueous media, able to increase the carboxylate band of nanoemulsion spectrum. This may fit with the hypothesis of a partial breaking of sodium alginate molecule able to react with high energy molecules such as hydroxyl radicals (-$OH^{\cdot}$) produced from cavitation forces into the microfluidizer. This would entail the increase in the amount of exchangeable protons from carboxylic acids or hydroxyl groups (Feng et al., 2017). As a result, those exchangeable protons, which were not observable by ^{1}H-RMN due to the use of deuterium dioxide as the solvent; led to the decrease in the number of relative protons in microfluidized alginate and nanoemulsion spectra. Thus, results from both spectroscopic techniques indicated that after microfluidization, sodium alginate might break and change its conformation influencing the properties of the resultant nanoemulsions.

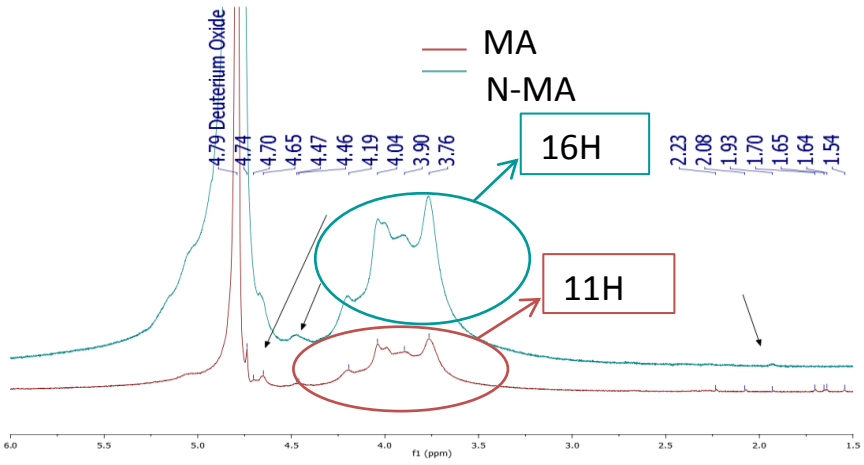

Figure 5. ^{1}H-NMR comparative spectra of microfluidized (MA) and Non-microfluidized (N-MA) alginate solutions in D_2O at room temperature.

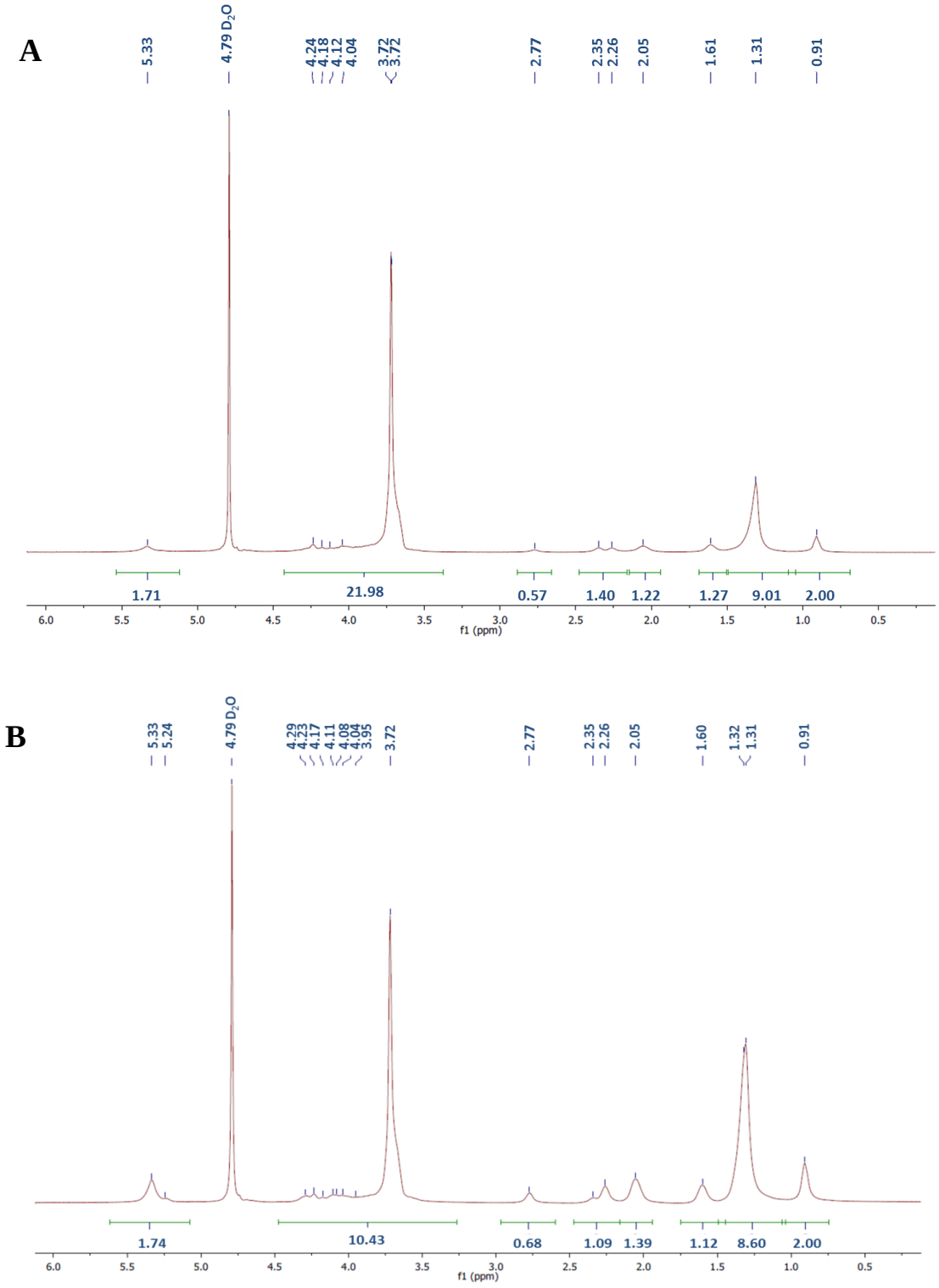

Figure 6. (A) ^{1}H-NMR spectrum of coarse emulsion A (C_A) and (B) ^{1}H-NMR spectrum of nanoemulsion A (N_A) in D_2O at room temperature.

Concerning the results, it could be expected the observation of the breaking of sodium alginate in smaller oligomers through ultra-hydrogel permeation chromatography (GPC). In this regard, although sodium alginate molecule breaks, the re-aggregates formed after microfluidization process may have similar molecular weights than the initial chain.

Those changes might be explained by a partial hydrolysis of alginate molecule that causes higher affinity for water, higher porosity and hence, changes in its molecular weight, which might produce a variation in the disposition of alginate chains around the oil droplets.

5. Conclusions

The present work reveals that physicochemical properties of nanoemulsions can vary depending on their preparation procedure. Mechanical forces from microfluidization caused the breaking of alginate chains reducing the steric impediment between them around the oil droplets. Thus, in terms of particle sizes measured by DLS and TEM, those procedures in which the alginate was microfluidized, either before or after coarse emulsion formation, led to nanoemulsions (N_A and $N_{B(MA)}$) with particle sizes in the nano-scale range. On the other hand, results derived from spectroscopic techniques such as ATR and H^1-NMR also fitted with a partial breaking of sodium alginate molecule after passing through the microfluidizer. Consequently, it was possible to observe that the presence of –OH and $–COO^-$ groups varied changing the interfacial interactions between oil droplets and the rest of the components in the resultant nanoemulsions. Moreover, the GPC analysis highlighted the possibility of rearrangement of the biopolymer after microfluidization since, although the molecular weight of the sodium alginate decreased, a molecular weight distribution similar to the non-microfluidized alginate was obtained. Therefore, further studies such as Scanning electron microscopy (SEM) may help to understand the disposition of the alginate chains in nanoemulsions to obtain stable nanostructured systems able to encapsulate, transport and release biocompounds effectively through food matrices.

6. Acknowledgements

This study was supported by the MINECO (Spain) throughout project **AGL2012-35635** and by the MINECO/FEDER throughout project **AGL2015-65975-R**. Authors María Artiga-Artigas and Alejandra Acevedo-Fani thank the University of Lleida for the pre-doctoral grant.

7. References

Bonilla, J., Atarés, L., Vargas, M., & Chiralt, A. (2012). Effect of essential oils and homogenization conditions on properties of chitosan-based films. *Food Hydrocolloids*, *26*(1), 9–16.

Borrin, T. R., Georges, E. L., Moraes, I. C. F., & Pinho, S. C. (2016). Curcumin-loaded nanoemulsions produced by the emulsion inversion point (EIP) method: An evaluation of process parameters and physico-chemical stability. *Journal of Food Engineering*, *169*, 1–9.

Chemat, F., & Khan, M. K. (2011). Ultrasonics Sonochemistry Applications of ultrasound in food technology : Processing , preservation and extraction. *Ultrasonics - Sonochemistry*, *18*(4), 813–835.

Chen, J., Gao, D., Yang, L., & Gao, Y. (2013). Effect of micro fl uidization process on the functional properties of insoluble dietary fi ber, *54*, 1821–1827.

Ekthamasut, K., & Akesowan, A. (2010). Effect of Vegetable Oils on Physical Characteristics of Edible Konjac Films. *Water*, (4).

Feng, L., Cao, Y., Xu, D., Wang, S., & Zhang, J. (2017). Ultrasonics Sonochemistry Molecular weight distribution , rheological property and structural changes of sodium alginate induced by ultrasound. *Ultrasonics - Sonochemistry*, *34*, 609–615.

Feng, L., Cao, Y., Xu, D., You, S., & Han, F. (2016). Ultrasonics Sonochemistry Influence of sodium alginate pretreated by ultrasound on papain properties : Activity , structure , conformation and molecular weight and distribution. *ULTRASONICS SONOCHEMISTRY*, *32*, 224–230.

Guerra-Rosas, M. I., Morales-Castro, J., Ochoa-Martínez, L. A., Salvia-Trujillo, L., & Martín-Belloso, O. (2016). Long-term stability of food-grade nanoemulsions from high methoxyl pectin containing essential oils. *Food Hydrocolloids*, *52*, 438–446.

Harte, F., & Venegas, R. (2010). A Model for Viscosity Reduction in Polysaccharides Subjected To High-Pressure Homogenization. *Journal of Texture Studies*, *41*(1), 49–61.

Heydenreich, a. V., Westmeier, R., Pedersen, N., Poulsen, H. S., & Kristensen, H. G. (2003). Preparation and purification of cationic solid lipid nanospheres - Effects on particle size, physical stability and cell toxicity. *International Journal of Pharmaceutics*, *254*(1), 83–87.

Hsu, J.-P., & Nacu, A. (2003). Behavior of soybean oil-in-water emulsion stabilized by nonionic surfactant. *Journal of Colloid and Interface Science*, *259*(2), 374–381.

Huang, J., Li, J., Feng, Y., Li, K., Yan, H., & Gao, P. (2015). Colloids and Surfaces A : Physicochemical and Engineering Aspects Aggregation behavior of derivatives of sodium alginate and N-octyl- $^{N}_{L}$ - D -glucopyranoside in aqueous solutions, *479*, 11–17.

Kralova, I., & Sjöblom, J. (2009). Surfactants Used in Food Industry: A Review. *Journal of Dispersion Science and Technology*, *30*(9), 1363–1383.

Laneuville, S. I., Turgeon, S. L., & Paquin, P. (2013). Changes in the physical properties of xanthan gum induced by a dynamic high-pressure treatment. *Carbohydrate Polymers*, *92*(2), 2327–2336.

Lee, K. Y., & Mooney, D. J. (2012). Alginate: Properties and biomedical applications. *Progress in Polymer Science (Oxford)*, *37*(1), 106–126.

Liling, G., Di, Z., Jiachao, X., Xin, G., Xiaoting, F., & Qing, Z. (2016). Effects of ionic crosslinking on physical and mechanical properties of alginate mulching films. *Carbohydrate Polymers*, *136*, 259–265.

Maa, Y. F., & Hsu, C. C. (1999). Performance of sonication and microfluidization for liquid-liquid emulsification. *Pharmaceutical Development and Technology*, *4*(2), 233–240.

McClements, D. J. (2002a). Colloidal basis of emulsion color. *Current Opinion in Colloid & Interface Science*, *7*(5–6), 451–455.

McClements, D. J. (2002b). Colloidal basis of emulsion color. *Current Opinion in Colloid and Interface Science*, *7*(5–6), 451–455.

McClements, D. J. (2011). Edible nanoemulsions: fabrication, properties, and functional performance. *Soft Matter*, *7*(6), 2297–2316.

Mohammad, S., Hosseini, H., Emam-djomeh, Z., Hadi, S., & Meeren, P. Van Der. (2013). Food Hydrocolloids b -Lactoglobulin e sodium alginate interaction as affected by polysaccharide depolymerization using high intensity ultrasound. *FOOHYD*, *32*(2), 235–244.

Nambam, J. S., & Philip, J. (2012). Competitive adsorption of polymer and surfactant at a liquid droplet interface and its effect on flocculation of emulsion. *Journal of Colloid and Interface Science*, *366*(1), 88–95.

Neumann, M. G., Schmitt, C. C., & Iamazaki, E. T. (2003). A fluorescence study of the interactions between sodium alginate and surfactants. *Carbohydrate Research*, *338*(10), 1109–1113.

Pereda, M., Aranguren, M. I., & Marcovich s, N. E. (2010). Caseinate films modified with tung oil. *Food Hydrocolloids*, *24*(8), 800–808.

Pereira, R., Carvalho, A., Vaz, D. C., Gil, M. H., Mendes, A., & Bártolo, P. (2013). Development of novel alginate based hydrogel films for wound healing applications. *International Journal of Biological Macromolecules*, *52*, 221–230.

Qian, C., & McClements, D. J. (2011). Formation of nanoemulsions stabilized by model food-grade emulsifiers using high-pressure homogenization: Factors affecting particle size. *Food Hydrocolloids*, *25*(5), 1000–1008.

Rao, J., & McClements, D. J. (2011). Food-grade microemulsions, nanoemulsions and emulsions: Fabrication from sucrose monopalmitate & lemon oil. *Food Hydrocolloids*, *25*(6), 1413–1423.

Salvia-Trujillo, L., & McClements, D. J. (2015). Influence of Nanoemulsion Addition on the Stability of Conventional Emulsions. *Food Biophysics*.

Salvia-Trujillo, L., Rojas-Graü, A., Soliva-Fortuny, R., & Martín-Belloso, O. (2014). Food Hydrocolloids Physicochemical characterization and antimicrobial activity of food- grade emulsions and nanoemulsions incorporating essential oils. *Food Hydrocolloids*, *43*, 1–10.

Salvia-Trujillo, L., Rojas-Graü, M. A., Soliva-Fortuny, R., & Martín-Belloso, O. (2013). Effect of processing parameters on physicochemical characteristics of microfluidized lemongrass essential oil-alginate nanoemulsions. *Food Hydrocolloids*, *30*(1), 401–407.

Salvia-Trujillo, L., Rojas-Graü, M. A., Soliva-Fortuny, R., & Martín-Belloso, O. (2014). Formulation of Antimicrobial Edible Nanoemulsions with Pseudo-Ternary Phase Experimental Design. *Food and Bioprocess Technology*, 3022–3032.

Strobel, S. A., Scher, H. B., Nitin, N., & Jeoh, T. (2016). In situ cross-linking of alginate during spray-drying to microencapsulate lipids in powder. *Food Hydrocolloids*, *58*, 141–149.

Villay, a., Lakkis de Filippis, F., Picton, L., Le Cerf, D., Vial, C., & Michaud, P. (2012). Comparison of polysaccharide degradations by dynamic high-pressure homogenization. *Food Hydrocolloids*, *27*(2), 278–286.

Wang, T., Sun, X., Raddatz, J., & Chen, G. (2013). Effects of microfluidization on microstructure and physicochemical properties of corn bran. *Journal of Cereal Science*, *58*(2), 355–361.

Yang, J. S., Jiang, B., He, W., & Xia, Y. M. (2012). Hydrophobically modified alginate for emulsion of oil in water. *Carbohydrate Polymers*, *87*(2), 1503–1506.

Yang, L., & Paulson, A. T. (2000). Effects of lipids on mechanical and moisture barrier properties of edible gellan film. *Food Research International*, *33*(7), 571–578.

CHAPTER V: *Decane-in-water nanoemulsions stabilization by whey protein-sugar beet pectin complexes*

Artiga-Artigas, M., Reichert, C., Salvia-Trujillo, L., Zeeb, B., Martín-Belloso, O., Weiss, J.

(Submitted to Food Biophysics)

Abstract

Protein-polysaccharide complexes might enhance the stability of nanoemulsions containing short-chain alkanes, which are very prone to destabilization by Ostwald ripening. The aim of this work was to form interfacially structured nanoemulsions using biopolymer complexes composed of whey protein isolate (WPI) and sugar beet pectin (SBP) and assess their capability against Ostwald ripening. Nanoemulsions with 20% *w/w* of decane and stabilized with 2% *w/w* of the biopolymers alone or the complex were evaluated against Ostwald ripening parameters. Complex-stabilized nanoemulsions exhibited negative ζ-potential with similar values to those stabilized by SBP alone while the interfacial rheology behavior of complex-stabilized systems was more similar to those stabilized by WPI alone. This suggests that the protein fraction may be directly and strongly adsorbed at the oil interface thus dominating the interface rheology, whereas pectin chains located on the periphery of the complex and oriented towards the water phase may confer negative interfacial charge to oil droplets. Complexes showed higher emulsifying capacity than biopolymers alone since particle size of complex-stabilized nanoemulsions remained stable at least 48 hours after their preparation, whereas WPI- or SBP-stabilized nanoemulsions suffered destabilization during the first 24h. Moreover, while the final particle size reached by the latter during the 21 days of storage was around 8 μm, complex-stabilized nanoemulsions exhibited particle sizes up to 2.34 ± 0.86 μm, which had a direct impact in delaying creaming. Overall, WPI:SBP complexes were more effective than the biopolymers alone in preventing Ostwald ripening in decane-in-water nanoemulsions.

Keywords: Whey protein; sugar beet pectin; protein:polysaccharide complexes; interfacial rheology.

1. Introduction

Nanoemulsions have been described as colloidal dispersions of two immiscible phases (*e.g.* oil-in-water) with particle sizes up to 500 nm (Otoni et al., 2016). Nanoemulsions have been intensively studied because of their potential use as delivery systems since they may act as carriers of lipophilic functional compounds including flavor oils or bioactive compounds. Additionally, nanoemulsions may be used as thickening agents due to the presence of biopolymers in their formulation. In this regard, depending on the desired application the nanoemulsions, interface needs to be specifically tailored. However, the main limitation of these nanostructured systems is their thermodynamically instability, thus they tend to experiment destabilization phenomena over time, such as coalescence, flocculation or Ostwald ripening. Instability mechanisms occur due to the tendency of the emulsion to evolve towards a more thermodynamically favorable system, resulting in a decrease of the area of the dispersed lipid phase in the aqueous phase, which ultimately causes phase separation (Suriyarak & Weiss, 2014). Typically, emulsifiers including small-molecular surfactants or biopolymers are required to firstly decrease the interfacial tension between the two immiscible liquids and allow the droplet breakup during homogenization, and secondly, to stabilize the newly created droplets (McClements, Bai, & Chung, 2017). In fact, there is a great interest in the food industry in the use of proteins and polysaccharides to stabilize oil-in-water nanoemulsions since they have shown the potential to adsorb at the oil/water interface thus contributing to the emulsification of oil droplets (Evans, Ratcliffe, & Williams, 2013; Pérez, Carrera Sánchez, Pilosof, & Rodríguez Patino, 2009).

Indeed, proteins such as whey protein isolates (WPI) are known for their emulsification and foaming properties, and polysaccharides like sugar beet pectin (SBP) for their water-holding and thickening properties (Dickinson, 2003). It is reported that the main proteins in WPI being β-lactoglobulin, α-lactalbumin and bovine serum albumin are responsible for the interfacial properties of WPI (Baeza, Carrera Sanchez, Pilosof, & Rodríguez Patino, 2005). Similarly, emulsion-stabilizing properties of SBP are well reported and attributed to their proteinaceous moieties, which may account to their interfacial activity (Akhtar, Dickinson, 2002; Funami et al., 2007). Acetyl groups within the galacturonic backbone and phenolic esters in the side chains could also act as additional anchors to the oil droplets (Nakauma et al., 2008). Nevertheless, not even biopolymers are able to prevent Ostwald ripening in nanoemulsions containing short-chain alkanes since they present partial solubility in water (Chebil, Desbrières, Nouvel, Six, & Durand, 2013; Suriyarak & Weiss, 2014). This phenomenon, which is also responsible for the breakdown of nanoemulsions, is described as the process whereby bigger droplets grow at the expense of those smaller because the solubility of a material within a droplet increases (Zeeb et al., 2012). Therefore, stabilization of these nanoemulsions still remains as a scientific and technological challenge and different approaches need to be considered in order to design optimal interfacial stabilization strategies.

It has been reported that Ostwald ripening could be prevented or reduced by using emulsifiers that are able to sequentially or simultaneously adsorb at droplets surface forming a thick interface. Actually, several works have recently demonstrated the surface-active capacity of biopolymer complexes, also referred as coacervates (Ghosh & Bandyopadhyay, 2012; Gromer, Kirby, Gunning, & Morris, 2009; Zeeb et al., 2018). Complexation is the resultant electrostatic attraction between two biopolymers that are oppositely charged. It can occur between a protein and a polysaccharide when they reach their electrical equivalence at a specific pH, normally between the isoelectric point (pI) of the protein and the pKa of the polysaccharide (Klemmer, Waldner, Stone, Low, & Nickerson, 2012; Liu, Elmer, Low, & Nickerson, 2010; Schmitt & Turgeon, 2011). Therefore, pH and ionic strength of

nanoemulsions influence the charge density of the biopolymers and hence, the complexation process (Zeeb et al., 2016). Nevertheless, the deposition and interaction of these complexes at the droplets interface is a relatively unexplored field.

The aim of this study was to evaluate the hypothesis that stabilization of nanoemulsions by protein-pectin complexes may result more effective in retarding Ostwald ripening, in comparison to the individual biopolymers alone. For this purpose, complexes were formed at pH 3.5 by mixing two biopolymer solutions consisting of a globular protein, namely WPI; and SBP in a ratio 1:1. Nanoemulsions stabilized by WPI, SBP or WPI:SBP complex were characterized in terms of particle size, phase separation, ζ-potential, interfacial density and optical microscopy. In addition, the interaction between decane and WPI, SBP or WPI:SBP complex was assessed by interfacial rheology measurements.

2. Materials and methods

2.1.Materials

WPI was purchased from Fonterra GmbH (Hamburg, Germany). WPI is composed of a mixture of β-lactoglobulin, α-lactalbumin, bovine serum albumin, and other proteins, such as caseins. The pI of β-lactoglobulin is 5.3, whereas the pI of α-lactalbumin is 4.1, and thus the WPI has a pI close to 5 (Dickinson, 1992). Sugar beet pectin (SBP) was a gift of Herbstreith&FoxKG (Neuenbürg, Germany). As stated by the manufacturer the degree of esterification of the beet pectin was 55%. All biopolymers were used without further purification. Decane (Purity > 99.0%) was obtained from Sigma-Aldrich Co. (Steinheim, Germany). Citric acid monohydrate was obtained from Carl Roth GmbH & Co. KG (Karlsruhe, Germany) and sodium citrate dihydrate was purchased from SAFC (St. Louis, MO). Analytical grade hydrochloric acid (HCl) and sodium hydroxide (NaOH) were purchased from Carl RothGmbH& Co.KG (Karlsruhe, Germany). Deionized water was used for the preparation of all samples.

2.2.WPI:SBP complex formation

Initially, the single biopolymers were dissolved in distilled water with magnetic stirring overnight at room temperature to obtain two stock solutions at 2% *w/w* of biopolymer and ensure their complete hydration. Afterwards, solutions were adjusted to pH 7 with 0.1M and 1M of NaOH or HCl (Zeeb et al., 2016). Stock solutions were mixed in a WPI:SBP ratio of 1:1 and the complex formation was induced by decreasing the pH to 3 at regular intervals. According to the procedure described by Zeeb et al. (Zeeb et al., 2016), biopolymers measurements including ζ-potential with a Zetasizer Nano-ZS laser diffractometer (Malvern Instruments Ltd, Worcestershire, UK) and optical microscopy with an Axio Scope optical microscope (A1, Carl Zeiss Microimaging GmbH, Göttingen, Germany) were performed over a pH range of 7 to 3 in order to set the accurate conditions for associative complex formation. Since complexation started at pH 5 and insoluble complex formation followed by the subsequent precipitation was observed at pH 3 (Fig.1B and 1C, respectively), the chosen pH for the formation of simple- and protein:polysaccharide complex-stabilized emulsions throughout the complete experiment was 3.5. The nanoemulsions pH was measured with a laboratory pH meter (inoLab, pH Level 1, WTW, Weilheim, Germany).

2.3.Formation of oil-in-water emulsions with differently structured interfaces

Oil-in-water emulsions with differently structured interfaces: (i) protein- or pectin-stabilized emulsion (simple emulsion) and (ii) coacervate-stabilized emulsion (complex emulsion) were prepared. For the formation of aqueous emulsifier solutions 2% *w/w* WPI or SBP powder was dispersed into 10 mM sodium citrate buffer (pH 3.5). Both solutions were stirred overnight to ensure complete hydration of the biopolymer at room temperature and then readjusted to pH of 3.5 using 1 M HCl and/or 1 M NaOH with a pH-meter (InoLab Level 1, Gemini, Apeldoorn, NL). Single biopolymer-stabilized nanoemulsions were prepared by homogenizing 20% *w/w* of decane with 2% *w/w* WPI or SBP solutions using a high shear laboratory blender (Standard Unit, IKA Werk GmbH, Germany) at 15.000 rpm for 2 min followed by three passes at 1,000 bar (100 MPa) through a high pressure homogenizer (LM10, Microfluidics^{TM}, Westwood, MA). Low temperature of the samples was maintained by using an ice bath.

For the formation of complex-stabilized emulsions two stock solutions, one containing 2 % *w/w* of whey protein isolate (WPI) and the other 2 % *w/w* of sugar beet pectin (SBP), were prepared in citrate buffer (3.5 pH). Both solutions were magnetically stirred overnight to ensure complete hydration of the biopolymers at room temperature and pH was readjusted to 3.5. Afterwards, both solutions were mixed 1:1 (WPI:SBP) ratio and 20% *w/w* of decane was added. The resulting mixture was homogenized by high pressure homogenization as described earlier.

2.4.Characterization of emulsions

2.4.1. Droplet size and droplet growth rate

The particle size and particle size distribution of emulsions were measured using a static light scattering instrument (Horiba LA-950, Retsch Technology GmbH, Haan, Germany) periodically during 21 days at room temperature. Samples were diluted to a droplet concentration of approximately 0.005% *w/w* with citrate buffer (pH 3.5) to prevent multiple scattering effects. The instrument measured the angular dependence of the intensity of the laser beam scattered by the dilute emulsions and then used the Mie theory to calculate the droplet size distributions that gave the best fit between theoretical predictions and empirical measurements. Refractive index (RI) was directly measured from decane-in-water nanoemulsions through the automated RI computation of the static light scattering device, which provided a value of 1.48. The particle size measurements are reported as volume frequency distributions and the mean diameters in terms of the volume (d[4;3]) and number based (d10) mean diameters. The d[4;3] is very sensitive to the presence of large particles in the distribution and the d_{10} describes the diameter where 10% of the distribution has a smaller particle size and 90% has a larger particle size. Particle radii were calculated as the average of measurements made on at least two freshly prepared samples. Particle size and its growth were confirmed by microscopy images taken periodically until day 21 of room temperature storage with an Axio Scope optical microscope (A1, Carl Zeiss Microimaging GmbH, Göttingen, Germany). All the studied samples were diluted in citrate buffer using a dilution factor of 1:30 sample-to-solvent prior to the microscopy analysis. Afterwards, the Ostwald ripening process was modeled by the Lifshitz-Slyozov-Wagner (LSW) theory, which is based on the assumption that the diffusion of oil through water determines the overall Ostwald ripening rate (Santos, Calero, Trujillo-Cayado, Garcia, & Muñoz, 2017). This theory predicts that, at asymptotically long times, there is a constant Ostwald ripening rate determined by the growth in the cube of the number weighted mean droplet radius. Therefore, Ostwald ripening rate was calculated using the following equations:

$$r_t^3 - r_0^3 = \omega t \qquad \textbf{eq.(1)}$$

where, ω is the Ostwald ripening rate, r_t is the mean number droplet radius after time t, r_0 is the initial mean number droplet radius, both calculated from the number based mean diameter (d_{10}).

2.4.2. ζ -potential measurements

The ζ-potential (mV) was measured by phase-analysis light scattering (PALS) with a Zetasizer Nano-ZS laser diffractometer (Malvern Instruments Ltd, Worcestershire, UK). Samples were loaded into an appropriate cuvette and the ζ-potential was determined by measuring the direction and velocity that the droplets moved in the electric field applied. The Smoluchowski equation was utilized to calculate the ζ-potential. The ζ-potential measurements were made from two freshly prepared samples, and were carried out with four readings per sample. All samples were made in duplicate. In all the determinations, samples were prior diluted in citrate buffer (3.5 pH) using a dilution factor of 1:30 sample-to-solvent.

2.4.3. Accelerated creaming index test

The accelerated creaming test was performed by centrifuging 2.5 mL aliquots of nanoemulsions, diluted to 1% in citrate buffer, using a Heraeus Centrifuge (Biofuge 28RS, Osterode, Germany). Samples were centrifuged at 2500 rpm during 1, 5, 10, 15, 30 or 50 min. Pictures of the emulsions were taken periodically with a digital camera (Canon Powershot G10, Tokyo, Japan) and the creaming index provoked by centrifugation was calculated with equation (2):

$$\text{Creaming index (\%)} = (h_{\text{creaming (t)}} - h_{\text{creaming (t0)}})/h_{t0} * 100 \qquad \textbf{eq.(2)}$$

2.4.4. Interfacial rheology

Different biopolymers may lead to interfaces with diverse properties depending on the adsorption mechanism of them at the oil droplets' surface. In general, interfacial rheology describes the relation between an interface deformation and the stresses applied on it, thus being related to the strength of the adsorption as well as unfolding of the biopolymer at the interface (Pelipenko, Kristl, Rošic, Baumgartner, & Kocbek, 2012). Rheological measurements were conducted using a rheometer MCR 502 (Anton Paar GmbH, Graz, Austria; Software: Rheoplus) and were performed with a bicone measuring geometry, where the edge of the disk is located in the interfacial region between the two immiscible liquids. The influence of the bulk and upper phase of the flow field in the bicone system is compensated in an analysis performed using the rheometer software after the measurement. An amplitude sweep was conducted with 100 measuring points in the strain range between 0.01 to 100 % (frequency f = 0.01 Hz; ϑ = 25 °C). At the beginning of each measurement, a relaxation time of 15 min was applied. Each sample was measured in duplicate, whereas the interfacial storage modulus G_i' and loss modulus G_i'' were utilized as a key parameters to determine the rheological properties of the mixtures containing WPI solution (2% *w/w*), SBP solution (2% *w/w*) or complex WPI:SBP (1:1) solution (2% *w/w*) at pH 3.5 and decane as the upper fluid.

2.4.5. Interfacial density

Interfacial density was theoretically calculated in order to determine the concentration of emulsifying biopolymers (*i.e*. WPI and/or SBP) adsorbed. This may contribute to elucidate how is the

adsorption mechanism of WPI and/or SBP at oil/water interfaces, which is in turn linked to the understanding of Ostwald ripening phenomenon. For this purpose, the density of decane oil and decane-in-water nanoemulsions was measured using a Portable Density Meter (DMA™ 35, Anton Paar, Virginia, Ashland, USA).

The complexity of the systems required that some approximations being applied including that all droplets are spherical and with the same size and that there were no free biopolymers. In this regard, the equations used to theoretically calculate interfacial density are the following:

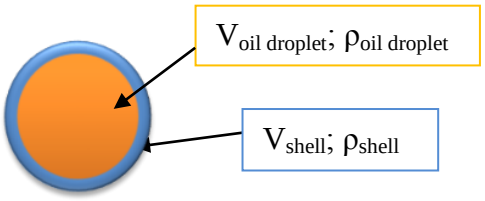

$$V_{emulsion} = n_{droplets} \cdot (V_{oil\ droplet} + V_{shell}) \quad \textbf{eq.(3)}$$

$$n_{droplets} = V_{total\ oil} / V_{oil\ droplet} \quad \textbf{eq.(4)}$$

$$V_{oil\ droplet} = (4/3) \cdot \pi \cdot r^3_{oil\ droplet} \quad \textbf{eq.(5)}$$

$$V_{total\ oil} = m_{total\ oil} / \rho_{total\ oil} \quad \textbf{eq.(6)}$$

$$m_{shell} = m_{biopolymer} / n_{droplets} \quad \textbf{eq.(7)}$$

$$\rho_{droplet\ shell} = m_{shell} / V_{shell} \quad \textbf{eq.(8)}$$

where $V_{emulsion}$, $V_{total\ oil}$ and $V_{oil\ droplet}$ are the volume of nanoemulsion, the total volume of decane and the volume equivalent to one droplet of decane, respectively; $n_{droplets}$ is the number of droplets present in the nanoemulsion; $r_{oil\ droplet}$ is the ratio of the droplets obtained from d[4;3]; m_{shell} and $m_{biopolymer}$ are the weight of the shell or the biopolymer, respectively and $\rho_{droplet\ shell}$ is the density of the shell in each droplet.

2.5.Statistics

All the experiments were performed in duplicate, and at least three replicate analyses were carried out for each parameter. SigmaPlot 11.0 Systat Software was used to perform the analysis of variance. Tukey test was chosen to determine significant differences among the different emulsions, at a 5% significance level.

3. Results and discussion

3.1.Formation of protein:pectin complex

Complexation may occur through attractive interactions between WPI and SBP while reducing the pH from 7 to 3 following the procedure described by Zeeb et al. (2016) (Figure 1). As the pH of biopolymer solutions increased from 3 to 7, the ζ-potential of the complex became more negative, going from values of -25 to -40 mV (Figure 1A). On the one hand, WPI is negatively charged at high pH values (pH 7), and becomes positively charged below its isoelectric point (WPI pI ≈ 5) (Figure 1A).

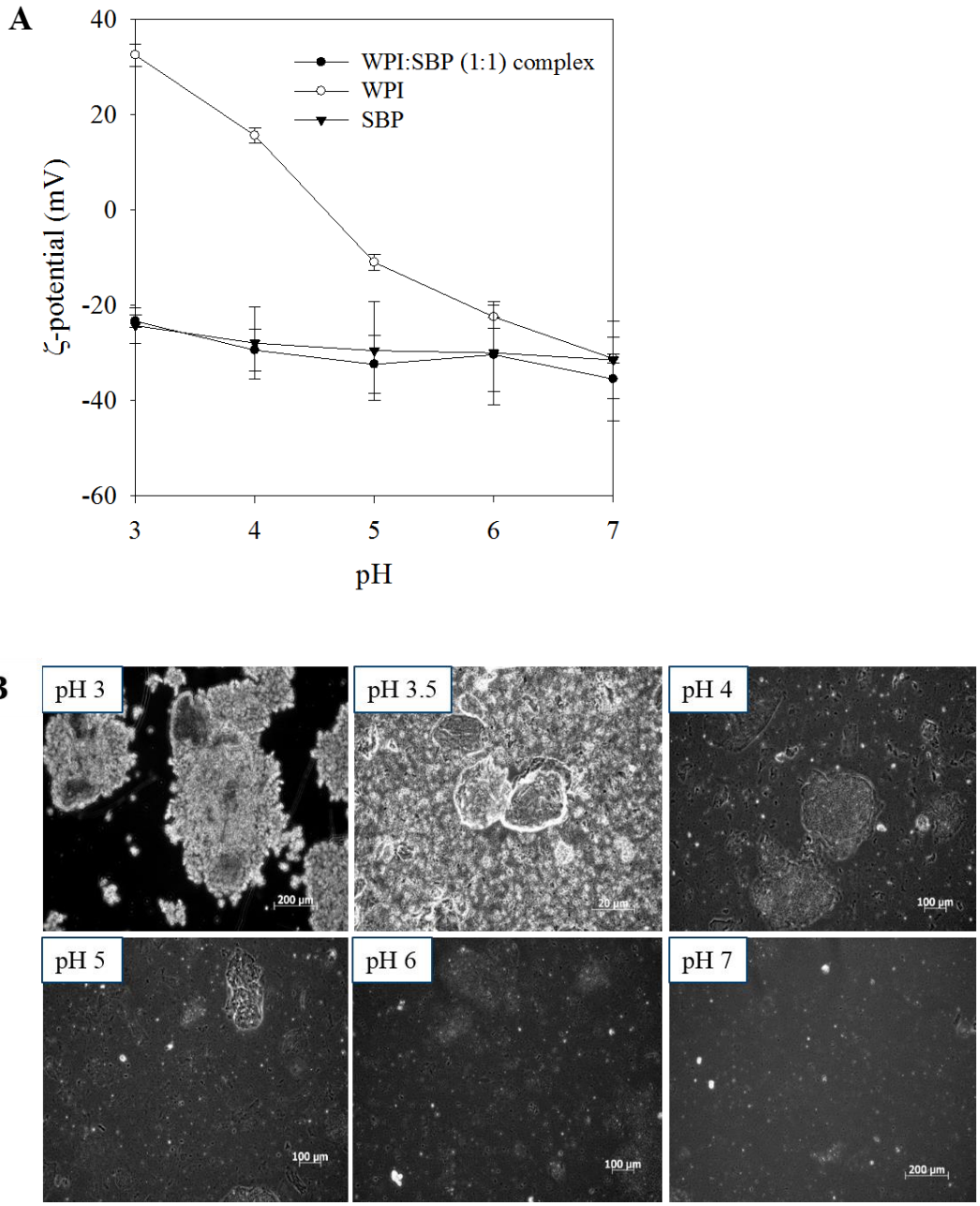

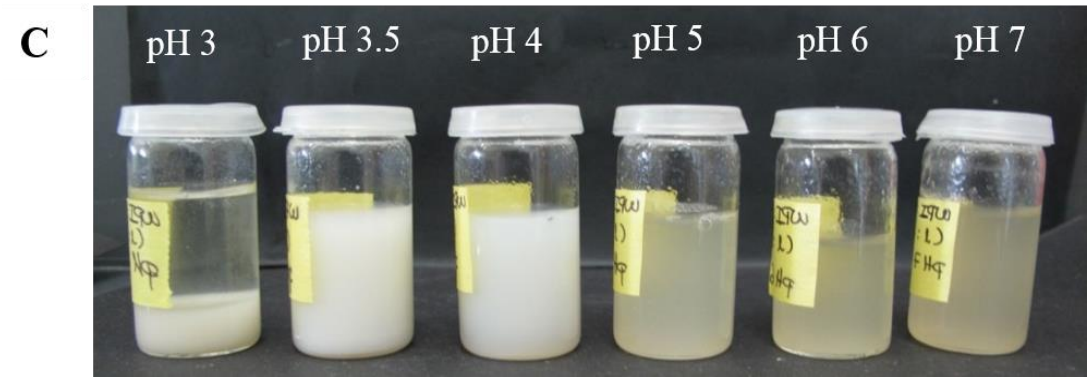

Figure 1. Change in the ζ-potential (mV) of whey protein isolate (WPI), sugar beet pectin (SBP) and WPI:SBP complex formation in distilled water by varying the pH from 7 to 3 (A); optical microstructure of WPI:SBP (1:1) complexes from pH 3 to 7 (B); outward appearance of complexes during their formation (C).

On the other hand, pectin molecules remained negatively charged due to its deprotonated carboxylic groups at a wide range of pH values (Figure 1A). Therefore, at low pH values, positively charged protein molecules and negatively charged pectin are able to electrostatically interact. In fact, microscopic images showed that soluble complexes formation took place from pH 5 (Figure 1B). Afterwards, these complexes grew as the pH decreased (acidic conditions) coinciding with a color change of the solutions probably due to the increase of complexation strength (coacervates formation) (Figures 1B and 1C, respectively). Finally, complexes became insoluble at pH 3 thus causing associative phase separation (Figure 1C). Usually, soluble complexation occurs when the electrostatic interactions are fairly weak and the net charge is relatively high, whereas complex coacervates are formed when the electrostatic interactions between the biopolymers are stronger and the net charge is low (Chen, Li, Ding, & Suo, 2012; Doublier, Garnier, Renard, & Sanchez, 2000). This conditions are met at pH 3.5 since the ζ-potential of WPI and SBP at pH 3.5 were respectively +28 mV and -22 mV, suggesting that at this pH it is possible to control WPI/SBP complex formation.

Therefore, the resulting complex subsequently used as the emulsifying agent during microfluidization was formed at pH 3.5.

3.2.Nanoemulsion stabilization by WPI, SBP or WPI:SBP complexes

Firstly, the capacity of WPI:SBP complexes to act as emulsifiers of nanoemulsions was evaluated and compared to that of WPI or SBP alone. Physicochemical properties of single- (WPI- or SBP-) or WPI:SBP complex-stabilized nanoemulsions were characterized in terms of particle size, particles size distribution, ζ-potential, optical microscopy and interfacial rheology. Secondly, after nanoemulsions formation, their stability over time was assessed through particle size distribution and particle size growth measured by static light scattering, optical microscopy and creaming appearance during 21 days of storage at room temperature.

3.2.1. Particle size, particle size distributions and ζ-potential

Static light scattering was used to measure the mean droplet diameter in terms of d[4;3] and d10 of 20 % *w/w* decane-in-water nanoemulsions stabilized by WPI, SBP or their complex in a ratio 1:1 and the changes in droplet size distribution during 21 days (Figure 2). Initial d[4;3], d10 and ζ-potential values of decane-in water nanoemulsions are shown in Table 1. The smallest particle size (d[4;3]) was exhibited by WPI- and WPI:SBP complex-stabilized nanoemulsions (0.31 ± 0.03 and 0.26 ± 0.07 μm, respectively). Moreover, nanoemulsions stabilized either by WPI or SBP alone experimented rapid changes in their particle size distributions after 24 hours of study, showing a progressive increase in their droplet sizes along time (Figures 2A-B). In the case of complex-stabilized nanoemulsions the growth was slower being significant in day 3 of room temperature storage (Figure 2C).

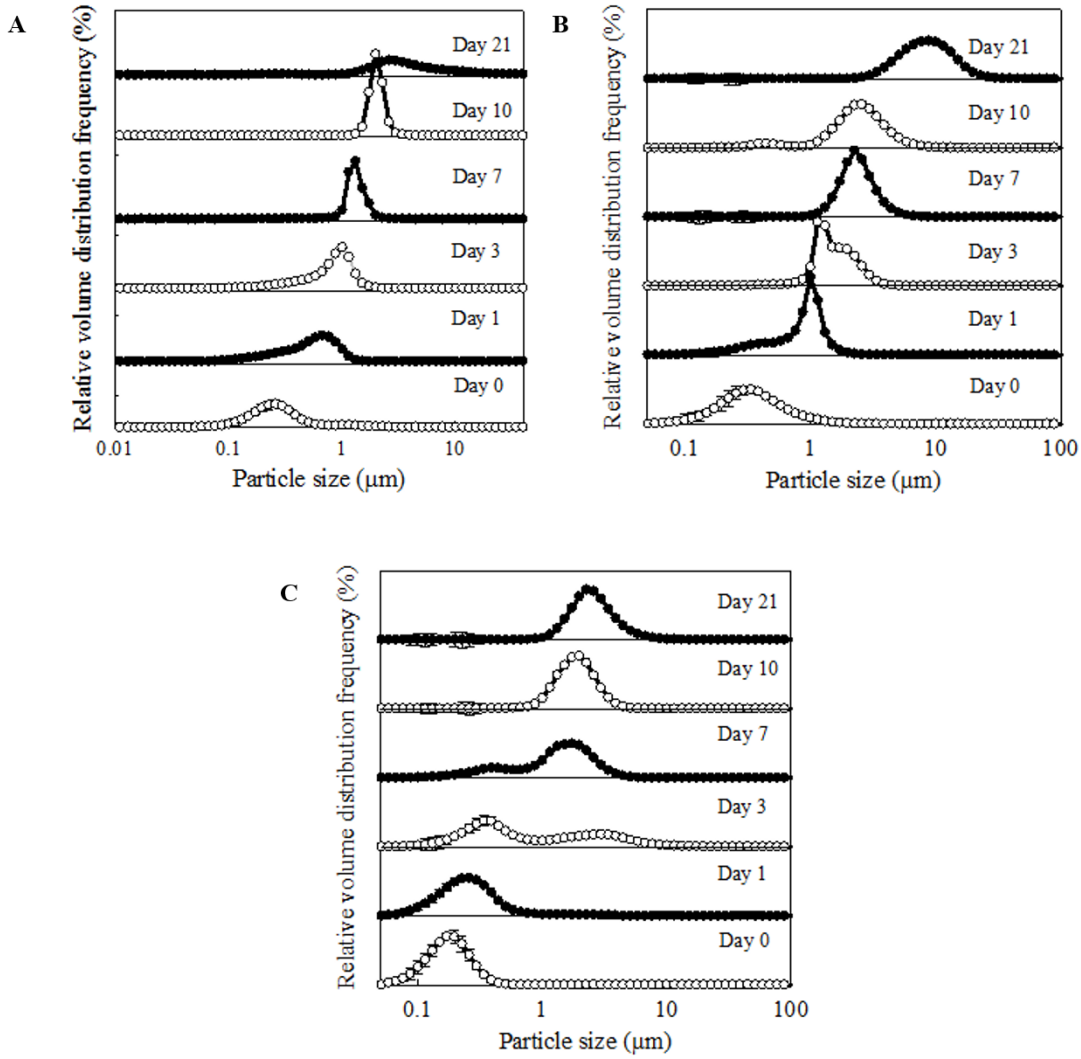

Figure 2. Particle size distribution of nanoemulsions containing 2% *w/w* Whey protein isolate (WPI) (A), 2% *w/w* of Sugar beet pectin (SBP) (B) or 2% *w/w* of the WPI:SBP (1:1) complex (C), acting as emulsifiers; and 20% *w/w* of decane as oil phase. The study was realized during 21 days.

Particle size of WPI-stabilized nanoemulsions in terms of d[4:3], increased from 0.31 ± 0.03 μm to 0.53 ± 0.02 μm during the first 24 hours and reached values of 7.81 ± 0.72 μm after 21 days of storage (Figure 2A). This gradual growth of oil droplets was most likely due to Ostwald ripening, which typically occurs in nanoemulsions of short-chain alkanes, such as decane, due to partial solubility of these oils in the aqueous phase (Santos et al., 2017; Zeeb et al., 2012). Indeed, according to the linear adjustment observed in Figure 3, there was a time-dependent increase of decane diffusion, which is an indicative of Ostwald ripening. It is reported that WPI is able to slow down the ripening process since it forms a greater surface coverage, however, the ripening rate just could be completely stopped under certain conditions such as the presence of insoluble species present in the oily phase (Combrinck, Otto, & du Plessis, 2014; Dickinson, 2009).

Likewise, SBP-stabilized nanoemulsions also experienced an increase in the particle size from 0.37 ± 0.09 to 0.82 ± 0.04 μm during the first 24 hours and continued growing until the appearance of a main intensity peak of oil droplets around 10 μm after 21 days of storage (Figure 2B). According to the observed particle growth, Ostwald ripening of nanoemulsions stabilized with SBP was significantly faster and more pronounced than those containing WPI (Figure 3). The main consequence of Ostwald ripening is the diffusion process that requires the solubility of the dispersed phase into the continuous phase to initiate the diffusion process between droplets (Ghosh & Bandyopadhyay, 2012). SBP can reversibly desorb and adsorb from the interface of the liquid droplet by a mechanism known as depletion-flocculation (Dickinson & Golding, 1997). This may increase the rate of mass transfer between the dispersed droplets and then, favor the Ostwald ripening. As reported by Ghosh & Bandyopadhyay (2012), the chances of desorption of emulsifier is lower in case of the emulsions stabilized by WPI because it provides a thicker layer around the droplets and greater surface coverage of the interfacial area. Particle size of complex-stabilized nanoemulsions remained stable (≈0.29 ± 0.03 μm) at least 48 hours after their preparation showing better emulsifying properties than WPI and SBP alone (Figure 2C). In addition, they exhibited the lowest increase in mean droplet diameters during the study increasing up to 2.34 ± 0.86 μm after 21 days of storage. Although in Figure 3 it can be observed that the slope of the line of Ostwald ripening rate distribution of the complex-stabilized nanoemulsions is similar to that of WPI-stabilized, complexes resulted more efficient in delaying creaming since they maintained small particle population during more time (Figures 2 and 6, respectively). Dickinson (2009) reported that despite the fact that protein:polysaccharide complexes present high surface activity, they mostly behave like a soft polymer, which resembles the protein structures and thus cannot completely avoid the ripening process (Ghosh & Bandyopadhyay, 2012). Therefore, protein:pectin complexation might lead to denser interfaces due to hydrophobic interactions or even biopolymer conjugation, altering interfacial rheology due to high internal stability of the interface and retarding the ripening process (Rodriguez Patino & Pilosof, 2011; Zeeb et al., 2018).

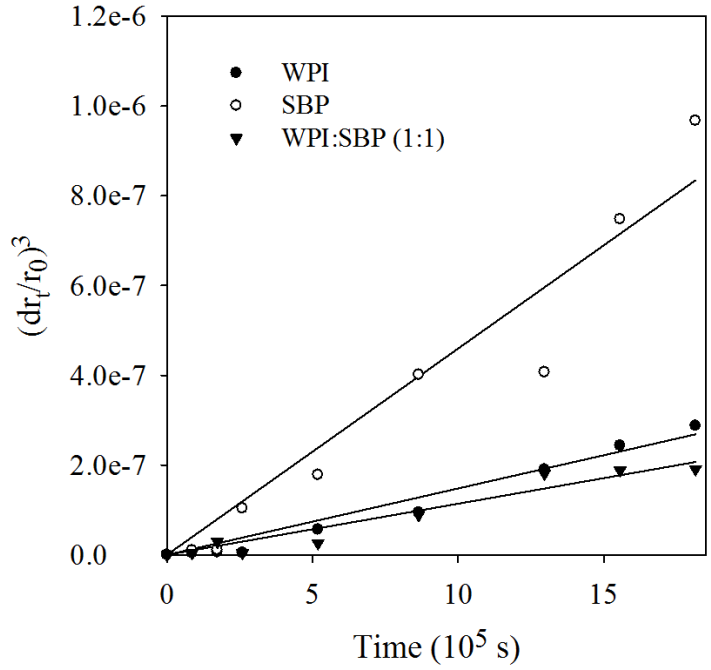

Figure 3. Impact of interfacial structure (biopolymer 0.2 % *w/w*) on the time-dependent growth of decane-in-water nanoemulsions (20 % *w/w* decane) stabilized by whey protein isolate (WPI), sugar beet pectin (SBP), and WPI:SBP complexes.

Regarding ζ-potential, WPI-stabilized nanoemulsions showed positive values of 37.5 ± 0.26 mV at pH 3.5 (Table 1). However, nanoemulsions stabilized with SBP or WPI:SBP complex as emulsifier showed negative charge at pH 3.5, with values of -22.1 ± 0.5 or -20.4 ± 0.5 mV, respectively. These differences can be explained due to WPI is a globular protein whose ζ-potential is slightly negative at physiological pH, yet it is able to change its net charge to positive while decreasing the pH (Ruffin, Schmit, Lafitte, Dollat, & Chambin, 2014).

Table 1. Decane-in water nanoemulsions physicochemical properties in terms of the mean droplet diameter over volume (d[4:3] in µm and ζ-potential (mV).

	d[4:3] (µm)	**d_{10} (µm)**	**ζ-potential (mV)**
2% *w/w* WPI; 20% *w/w* decane	0.31 ± 0.03^{AB}	0.129 ± 0.003^{A}	37.5 ± 0.3^{A}
2% *w/w* SBP; 20% *w/w* decane	0.37 ± 0.09^{A}	0.15 ± 0.09^{B}	-22.1 ± 0.5^{B}
2% *w/w* WPI:SBP (1:1) complex; 20% *w/w* decane	0.26 ± 0.07^{B}	0.11 ± 0.01^{AB}	-20.4 ± 0.5^{C}

^{A,B,C} Means in the same column with different letters are significantly different at $p < 0.05$ in terms of comparing different biopolymers as emulsifiers.

The negative charge of pectin molecules has been previously attributed to the ionization of carboxylic groups, which in turn promotes intra-molecular self-association (Alba & Kontogiorgos, 2017). With regards to the complex-stabilized nanoemulsions, the negative charge of droplets stabilized by protein-pectin complexes may indicate that protein moieties of the complex may be primarily adsorbed at the o/w interface while pectin moieties of the complex may be potentially located at the outer region of the o/w interface. Certainly, the proposed mechanism for complex formation is that the protein nuclei might have increased their hydrophobic properties and therefore grows into larger particles, whereas pectin molecules were simultaneously incorporated (Turgeon, Schmitt, & Sanchez, 2007; Weinbreck, Rollema, Tromp, & De Kruif, 2004; Zeeb et al., 2018). Therefore, the monolayer coverage formed by the protein avoids droplets diffusion and electrostatic and steric repulsion forces from SBP chains may provide the negative surface charge.

3.2.2. Microstructure and macrostructure of nanoemulsions

The microstructure (Figure 4) and macrostructure (Figure 5) of nanoemulsions stabilized by WPI, SBP or the WPI:SBP complex was determined by optical microscopy and visual appearance respectively, immediately after being prepared (day 0) and after 10 and 21 days of storage. After preparing the nanoemulsions (day 0), the three systems showed a uniformly distributed dispersion of oil droplets in the aqueous phase, regardless whether they were stabilized by the biopolymers alone or the complex. Nanoemulsion droplet size was initially in the nanometric range for all the studied samples thus being below the detection limit of the optical microscope, which is in agreement with the particle size results (Table 1). Moreover, despite of the droplet growth observed during storage time, especially in the case of nanoemulsions stabilized by WPI or SBP alone (section 3.2.1), dispersed oil droplets remained undetectable by optical microscopy until 10 days of storage (Figure 4). However, nanoemulsions stabilized by either WPI or SBP presented prominent destabilization after 21 days of storage as seen in the microscopy images (Figure 4A-B), whereas WPI:SBP complex-stabilized was barely beginning to aggregate (Figure 4C).

Nanoemulsions stabilized by WPI alone showed a loose or porous three-dimensional structure with hollow regions of depleted oil droplets (Figure 4A). This structure may be the result of physical bridging formation among droplets due to forces of mutual attraction known as London-Van der Waals forces (Harnsilawat, Pongsawatmanit, & McClements, 2006; Teo et al., 2016). Nevertheless, these forces may predominate when droplet surfaces are close enough resulting in overall attraction and natural aggregation takes place (Forbes, 2014). An increment in particle size may provoke protein desorption and promote flocculation through a depletion mechanism (Chanamai & McClements, 2001). Moreover, macroscopic observations of the WPI-stabilized nanoemulsions after 21 days evidenced a phase separation with a thick and dense layer on the top of the tubes (Figure 5A). This can be explained due to flocculation is able to cause a number of effects that are detrimental to emulsion quality including the enhancement of creaming (Chanamai & McClements, 2001; Dickinson, 1989).

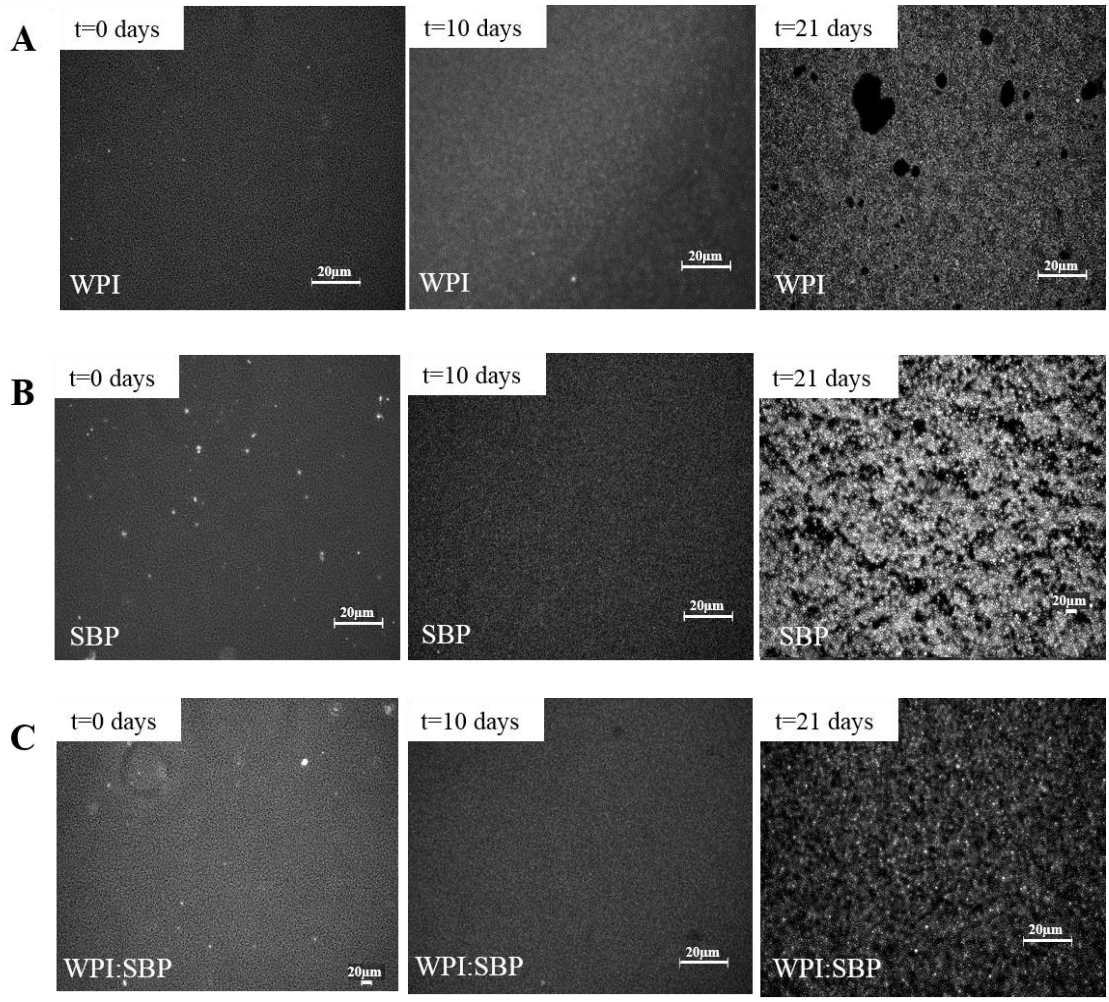

Figure 4. Optical microstructure of decane-in water nanoemulsions stabilized by whey protein isolate (WPI) (A), sugar beet pectin (SBP) (B) or WPI:SBP (1:1) complex (C) during 21 days of room temperature storage. Samples were diluted in citrate buffer in a ratio 1:30 sample-to-solvent.

Likewise, in the case of SBP-stabilized nanoemulsions, the presence of highly aggregated oil droplets with lipid depleted areas after 21 days of storage followed by phase separation was also remarkable (Figure 4B and 5B). As it has been mentioned in the previous section, instability of nanoemulsions containing SBP could be attributed to the placement that biopolymer adopts in the interface, which might favor diffusion (Siew & Williams, 2008). However, Gromer et al. (2009) observed strong aggregation of SBP by atomic force microscopy that can be explained by depletion-flocculation, effect whereby biopolymer molecules are excluded from the gap between adjacent droplets (Dickinson & Golding, 1997). In this regard, the particle growth of SBP-stabilized nanoemulsions over time due to Ostwald ripening might cause desorption of the SBP proteinaceous moiety thus leaving to uncovered regions of the droplet surface and ultimately leading to the emergence of creaming (Figure 5B).

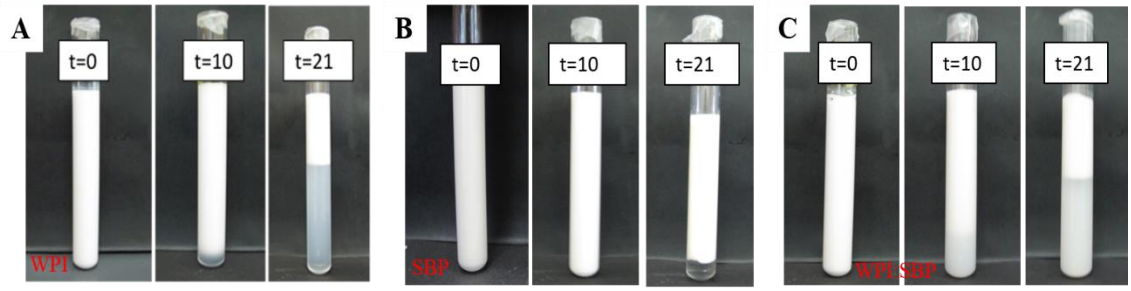

Figure 5. Nanoemulsions stabilized by (A) whey protein isolated (WPI), (B) sugar beet pectin (SBP) or (C) WPI:SBP complexes. Pictures of nanoemulsions stored at room temperature were taken during the 21 days of experiment.

Oppositely, aggregation of complex-stabilized nanoemulsions observed in day 21 was much less than in those WPI- or SBP-stabilized (Figure 4C) agreeing with phase separation observed in Figure 5C. This divergence may also be attributed to the delay in particle growth, which suggests that in complex-stabilized nanoemulsions repulsion forces are higher preventing particles from coming together retarding flocculation and the subsequent phase separation (Forbes, 2014).

3.2.3. Creaming index

An accelerated creaming test of nanoemulsions was conducted during different centrifugation times (0, 5, 10, 15, 30 and 45 min) at 2500 rpm. Rapid creaming was observed in WPI-stabilized emulsions, which reached a plateau when centrifugation was performed during at least 15 min with a creaming index of 11% (Figure 6). This could be attributed to flocculation phenomenon since centrifugation causes a partial phase separation due to a concentration gradient. Centrifugation generates zones with low WPI concentrations, in which the adsorption of the protein is insufficient to yield full surface coverage. Thus, WPI may adsorb onto two different droplets and cause aggregation or bridging flocculation (Jenkins & Snowden, 1996).

In the case of SBP-stabilized nanoemulsions, the increase in creaming index caused by centrifugation was progressive until reaching a constant creaming index of 6% after centrifuging 30 min (Figure 6). As the pH is 3.5, galactosyluronic acid residues from SBP chains are protonated and they acquire compact conformations in which the hydrophobic groups can go towards the oil interface and adsorb (Alba & Kontogiorgos, 2017). Therefore, the interface consists of a mixture of different functional groups and the applying of external forces such as centrifugation may modify the conformational characteristic of pectin thus altering the stability. Like WPI-stabilized nanoemulsions, SBP molecules may be excluded from droplets interface due to centrifuge forces favoring flocculation and then, irreversible creaming formation.

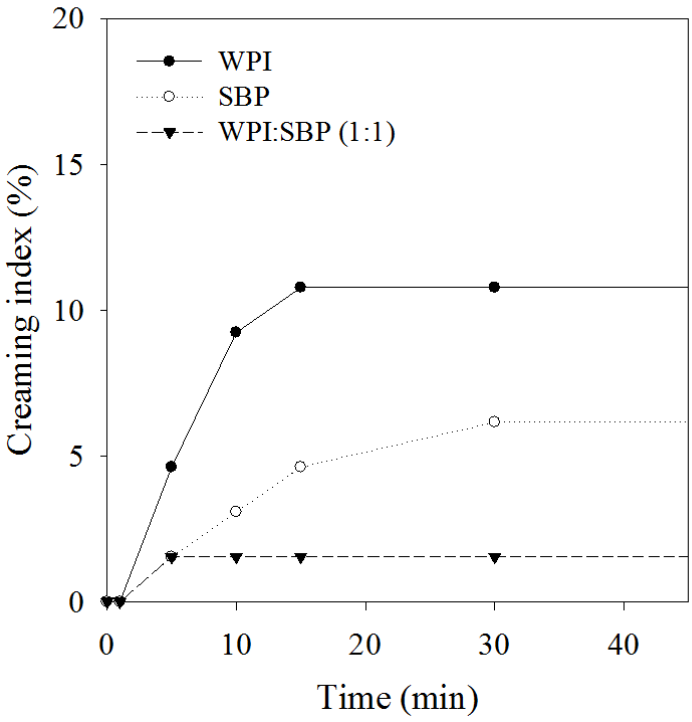

Figure 6. Accelerated creaming test of decane-in water emulsions containing whey protein isolate (WPI), sugar beet pectin (SBP) or their complex (WPI:SBP) in a ratio 1:1, was performed by centrifugation at 2,500 rpm during 0, 5, 15, 20, 30 and 45 min. Samples were diluted till reach an 1% *w/w* of decane.

In complex-stabilized nanoemulsions, the increase of the induced creaming index reached a plateau value (1.5%) after 10 minutes of centrifugation (Figure 6). Therefore, WPI:SBP complexes seem to be effective in preventing creaming even at room temperature. This can be related to the fact that in complex-stabilized nanoemulsions, charged functional groups from both biopolymers are interacting among them forming the complex, so there are fewer intermolecular interactions. In this regard, droplets may be closer each other after centrifugation thus leading to a less thick creaming since there are fewer spaces between them.

3.2.4. Interfacial rheology

Interfacial rheology measurements were performed to elucidate the adsorption mechanisms of the different emulsifiers used at decane droplet interfaces. Interfacial rheology studies the relationship between the deformation of a liquid surface interface and different forces as a function of time (Bos & Van Vliet, 2001). Interfacial characteristics depend on the behavior of the molecules located at the interface including their chemical composition, concentration and interactions (Pelipenko et al., 2012). The interfacial storage modulus (G_i') and the interfacial loss modulus (G_i") determine interfacial rigidity and both contributions constitute the interfacial shear modulus. G_i' represents the recoverable energy stored in the interface, whereas the loss modulus, G_i", accounts for energy lost both through shear dissipation processes (Freer, Yim, Fuller, & Radke, 2004).

On the one hand, the interfacial shear modulus (G_i' and G_i'') of WPI at decane interface remained constant at increasing strain amplitude (Figure 7A). It is reported that proteins adsorb at fluid-fluid interfaces by forming a highly interconnected network at the surface of decane stabilized by hydrogen bonds, hydrophobic and electrostatic interactions and specific covalent bonds between molecules (Murray, 2002). Nonetheless, this adsorption may depend on the polarity of the oil and also on concentration and type of the biopolymer and the interface aging time (Bos & Van Vliet, 2001). Therefore, the lack of an interconnected network observed in our interfacial rheology results might suggest that the aging time was not enough for the entirely formation of the WPI monolayer. Actually, in the study performed by Erni et al. (2003), results were collected after 20 h of aging since longer intervals for recording and averaging have proven beneficial.

Shear rheology measurements of SBP-decane interfaces showed higher values of G_i' compared to those of G_i'' as well as a decay in the G_i' and G_i'' with increasing amplitude after the latter reached a maximum. This behavior, which is characteristic of soft glassy materials and has been attributed to the balance between the breaking and formation of bonds, suggests that the resulting interfacial network generated is elastic (Figure 7B) (Torcello-Gómez & Foster, 2014). In agreement with our results, Gromer et al. (2009) and Rodriguez Patino & Pilosof (2011) also observed that SBP was able to form elastic or viscoelastic films at the air/water or oil/water interface, respectively. The interfacial elasticity has been attributed to the high hydrophobicity of pectin (Pérez et al., 2009). Indeed, acetyl groups of SBP, which enhances its hydrophobic nature and surface-active character favor the formation of elastic interfaces (Rodriguez Patino & Pilosof, 2011). This interface is susceptible to deform at low pH due to a lack of electrostatic repulsive forces between pectin chains causing weak steric repulsion (Alba, Sagis, & Kontogiorgos, 2016).

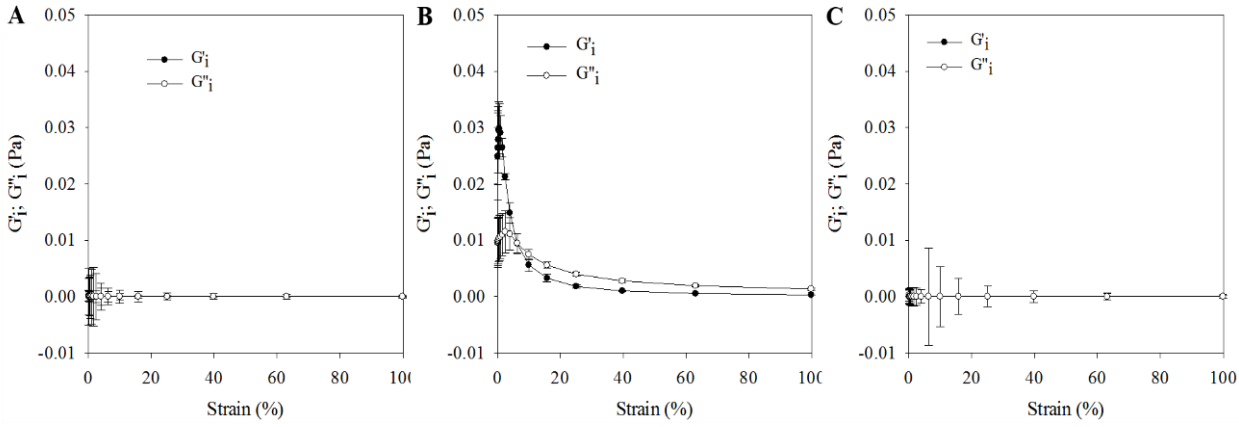

Figure 7. Interfacial rheology of (A) whey protein isolate (WPI), (B) sugar beet pectin (SBP) or (C) their complex (WPI:SBP) in a ratio of 1:1 solutions at the water-decane interface.

Interfacial rheology similarities between WPI- and complex-stabilized nanoemulsions reinforced the previously drawn hypothesis that protein moieties of the complex are adsorbed at the interface leaving the pectin moieties oriented towards the bulk aqueous phase. Indeed, it is reported that complexes may adsorb directly at oil interfaces due to the interaction of protein moieties from their outside with the decane and the pectin remained linked to these adsorbed protein molecules (Rodriguez Patino & Pilosof, 2011). The obtained results concerning interfacial rheology suggested on

the one hand, that probably more aging time is necessary to allow the complete adsorption of WPI at decane interface; and on the other hand, that changes in the protein:pectin ratio would definitely modify the properties of the interface.

3.2.5. Theoretical calculation of interfacial density

In order to determine whether complex-stabilized nanoemulsions present denser interfaces, the interfacial density of the different nanoemulsions was calculated with equations 3-8 (supplementary material). For this purpose, three assumptions were taken into account: (*i*) the shape of droplets is spherical; (*ii*) every droplet has the same diameter; and (*iii*) all biopolymer molecules are located at the interface. However, significant differences were not observed between the interfacial densities of WPI-, SBP- and complex-stabilized nanoemulsions (Table 2).

Table 2. Radius (µm) and density (g/cm^3) of decane-in water nanoemulsions as well as the number and volume (cm^3) of oil droplets necessary to calculate the mass (m_{shell}) in grams, volume (V_{shell}) in cm^3 and densities of the shell (g/cm^3) through equations 1-6; for 100 g of nanoemulsion, 2 g of biopolymer solution and 20 g of decane, whose density is 0.734 g/cm^3 and hence, the oil volume ($V_{total\ oil}$) equals 27.3 ± 1.8·10^{-3} cm^3.

	$r_{[4:3]}$ (µm)	$\rho_{emulsion}$ (g/cm^3)	Number of doplets	$V_{oil\ droplet}$ (cm^3)	m_{shell} (g)	V_{shell} (cm^3)	ρ_{shell} (g/cm^3)
WPI	0.16 ± 0.03	0.950 ± $5\cdot10^{-5}$	$1.7\cdot10^{15}$	$1.6\cdot10^{-14}$ ± $1\cdot10^{-16}$	$1.2\cdot10^{-15}$ ± $2.6\cdot10^{-17}$	$4.6\cdot10^{-14}$ ± $1.2\cdot10^{-16}$	0.026 ± $2\cdot10^{-4}$
SBP	0.19 ± 0.09	0.967 ± $2\cdot10^{-4}$	$9.4\cdot10^{14}$	$2.9\cdot10^{-14}$ ± $9.6\cdot10^{-16}$	$2.1\cdot10^{-15}$ ± $1.5\cdot10^{-18}$	$8.1\cdot10^{-14}$ ± $9.6\cdot10^{-16}$	0.026 ± $8\cdot10^{-4}$
WPI:SBP (1:1) complex	0.11 ± 0.07	0.943 ± $1\cdot10^{-4}$	$5.3\cdot10^{15}$	$5.1\cdot10^{-15}$ ± $1.3\cdot10^{-15}$	$3.8\cdot10^{-16}$ ± $10\cdot10^{-21}$	$1.5\cdot10^{-14}$ ± $1.3\cdot10^{-15}$	0.025 ± $4\cdot10^{-3}$

It may be due to that there the concentration of biopolymer molecules per unit of interfacial surface was the same in all nanoemulsions whether the emulsifier is a single biopolymer or a complex. In general, the mass of biopolymer that is adsorbed at the interface depends on several factors including interactions between the biopolymer and the oil, which in turn will determine the conformation of biopolymer when adsorbed. Siew et al. (Siew & Williams, 2008) reported that 1 mg/m^2 is enough for WPI to form a monolayer coverage, whereas they determined that the required amount of adsorbed SBP onto limonene oil droplets was ~9.5 mg/m^2. In this regard, the higher stability of the complex-stabilized nanoemulsions in comparison with the biopolymers alone might be related to the compactness of the complex at the interface rather than the number of adsorbed molecules of the interfacial layer.

4. Conclusions

Complex-stabilized nanoemulsions showed lower droplet growth than those WPI- or SBP-stabilized with the single biopolymer. The lower viscoelastic properties of the interfaces created by the

complex suggest that protein is adsorbed at the interface while pectin moieties are oriented towards the bulk aqueous phase. This is in agreement with the negative electrical charge observed in nanoemulsions stabilized with the complex, which was similar to the one observed in the pectin-stabilized nanoemulsions. Nanoemulsion stabilization by complexes may take place through a combination of stearic and electrostatic forces by the protein moieties and pectin chains oriented towards the aqueous phase, respectively. WPI:SBP complexes are presented as a good strategy to form nanoemulsions stable during 48 h containing short chain alkanes or short chain triglycerides, although they are very prone to suffer Ostwald ripening.

5. Adknowledgments

This study was funded by the Ministry of Economy, Industry and Competitiveness (MINECO/FEDER, UE) throughout project **AGL2015-65975-R**. Author María Artiga-Artigas thanks the University of Lleida for her pre-doctoral fellowship. Author Laura Salvia-Trujillo thanks the "Secretaria d'Universitats i Recerca del Departament d'Empresa i Coneixement de la Generalitat de Catalunya" for the Beatriu de Pinós post-doctoral grant (**BdP2016 00336)**.

6. References

Akhtar, Dickinson, M. & L. 2002. (2002). Emulsion stabilizing properties of pectin. *Food Hydrocolloids*, *17*(4), 455–462.

Alba, K., & Kontogiorgos, V. (2017). Pectin at the oil-water interface: Relationship of molecular composition and structure to functionality. *Food Hydrocolloids*, *68*, 211–218.

Alba, K., Sagis, L. M. C., & Kontogiorgos, V. (2016). Engineering of acidic O/W emulsions with pectin. *Colloids and Surfaces B: Biointerfaces*, *145*, 301–308.

Baeza, R., Carrera Sanchez, C., Pilosof, A. M. R., & Rodríguez Patino, J. M. (2005). Interactions of polysaccharides with β-lactoglobulin adsorbed films at the air-water interface. *Food Hydrocolloids*, *19*(2), 239–248.

Bos, M. A., & Van Vliet, T. (2001). Interfacial rheological properties of adsorbed protein layers and surfactants: A review. *Advances in Colloid and Interface Science*, *91*(3), 437–471.

Chanamai, R., & McClements, D. J. (2001). Depletion flocculation of beverage emulsions by gum arabic and modified starch. *Journal of Food Science*, *66*(3), 457–463.

Chebil, A., Desbrières, J., Nouvel, C., Six, J. L., & Durand, A. (2013). Ostwald ripening of nanoemulsions stopped by combined interfacial adsorptions of molecular and macromolecular nonionic stabilizers. *Colloids and Surfaces A: Physicochemical and Engineering Aspects*, *425*, 24–30.

Chen, B., Li, H., Ding, Y., & Suo, H. (2012). Formation and microstructural characterization of whey protein isolate/beet pectin coacervations by laccase catalyzed cross-linking. *LWT - Food Science and Technology*, *47*(1), 31–38.

Combrinck, J., Otto, A., & du Plessis, J. (2014). Whey Protein/Polysaccharide-Stabilized Emulsions: Effect of Polymer Type and pH on Release and Topical Delivery of Salicylic Acid. *AAPS PharmSciTech*, *15*(3), 588–600.

Dickinson, E. (1989). Food colloids - An overview. *Colloids and Surfaces*, *42*(1), 191–204.

Dickinson, E. (1992). Faraday research article. Structure and composition of adsorbed protein layers and the relationship to emulsion stability. *Journal of the Chemical Society, Faraday*

Transactions, *88*(20), 2973–2983.

Dickinson, E. (2003). Hydrocolloids at interfaces and the influence on the properties of dispersed systems. *Food Hydrocolloids*, *17*(1), 25–39.

Dickinson, E. (2009). Hydrocolloids as emulsifiers and emulsion stabilizers. *Food Hydrocolloids*, *23*(6), 1473–1482.

Dickinson, E., & Golding, M. (1997). Depletion flocculation of emulsions containing unadsorbed sodium caseinate. *Food Hydrocolloids*, *11*(1), 13–18.

Doublier, J. L., Garnier, C., Renard, D., & Sanchez, C. (2000). Protein-polysaccharide interactions. *Current Opinion in Colloid and Interface Science*, *5*(3–4), 202–214.

Erni, P., Fischer, P., Windhab, E. J., Kusnezov, V., Stettin, H., & Läuger, J. (2003). Stress- and strain-controlled measurements of interfacial shear viscosity and viscoelasticity at liquid/liquid and gas/liquid interfaces. *Review of Scientific Instruments*, *74*(11), 4916–4924.

Evans, M., Ratcliffe, I., & Williams, P. A. (2013). Emulsion stabilisation using polysaccharide–protein complexes. *Current Opinion in Colloid & Interface Science*, *18*(4), 272–282.

Forbes, D. L. (2014). Theory of Flocculation. *WET USA [on Line]*.

Freer, E. M., Yim, K. S., Fuller, G. G., & Radke, C. J. (2004). Interfacial Rheology of Globular and Flexible Proteins at the Hexadecane/Water Interface: Comparison of Shear and Dilatation Deformation. *The Journal of Physical Chemistry B*, *108*(12), 3835–3844.

Funami, T., Zhang, G., Hiroe, M., Noda, S., Nakauma, M., Asai, I., … Phillips, G. O. (2007). Effects of the proteinaceous moiety on the emulsifying properties of sugar beet pectin. *Food Hydrocolloids*, *21*(8), 1319–1329.

Ghosh, A. K., & Bandyopadhyay, P. (2012). Polysaccharide-Protein Interactions and Their Relevance in Food Colloids. *The Complex World of Polysaccharides*, 395–408.

Gromer, A., Kirby, A. R., Gunning, A. P., & Morris, V. J. (2009). Interfacial structure of sugar beet pectin studied by atomic force microscopy. *Langmuir*, *25*(14), 8012–8018.

Harnsilawat, T., Pongsawatmanit, R., & McClements, D. J. (2006). Influence of pH and ionic strength on formation and stability of emulsions containing oil droplets coated by β-lactoglobulin - Alginate interfaces. *Biomacromolecules*, *7*(6), 2052–2058.

Jenkins, P., & Snowden, M. (1996). Depletion flocculation in colloidal dispersions. *Advances in Colloid and Interface Science*, *68*, 57–96.

Klemmer, K. J., Waldner, L., Stone, A., Low, N. H., & Nickerson, M. T. (2012). Complex coacervation of pea protein isolate and alginate polysaccharides. *Food Chemistry*, *130*(3), 710–715.

Liu, S., Elmer, C., Low, N. H., & Nickerson, M. T. (2010). Effect of pH on the functional behaviour of pea protein isolate-gum Arabic complexes. *Food Research International*, *43*(2), 489–495.

McClements, D. J., Bai, L., & Chung, C. (2017). Recent Advances in the Utilization of Natural Emulsifiers to Form and Stabilize Emulsions. *Annual Review of Food Science and Technology*, *8*(1).

Murray, B. S. (2002). Interfacial rheology of food emulsifiers and proteins. *Current Opinion in Colloid and Interface Science*, *7*(5–6), 426–431.

Nakauma, M., Funami, T., Noda, S., Ishihara, S., Al-Assaf, S., Nishinari, K., & Phillips, G. O. (2008). Comparison of sugar beet pectin, soybean soluble polysaccharide, and gum arabic as food emulsifiers. 1. Effect of concentration, pH, and salts on the emulsifying properties. *Food Hydrocolloids*, *22*(7), 1254–1267.

Otoni, C. G., Avena-Bustillos, R. J., Olsen, C. W., Bilbao-Sáinz, C., & McHugh, T. H. (2016). Mechanical and water barrier properties of isolated soy protein composite edible films as

affected by carvacrol and cinnamaldehyde micro and nanoemulsions, *57*, 72–79.

Pelipenko, J., Kristl, J., Rošic, R., Baumgartner, S., & Kocbek, P. (2012). Interfacial rheology: An overview of measuring techniques and its role in dispersions and electrospinning. *Acta Pharmaceutica*, *62*(2), 123–140.

Pérez, O. E., Carrera Sánchez, C., Pilosof, A. M. R., & Rodríguez Patino, J. M. (2009). Surface dilatational properties of whey protein and hydroxypropyl-methyl-cellulose mixed systems at the air-water interface. *Journal of Food Engineering*, *94*(3–4), 274–282.

Rodriguez Patino, J. M., & Pilosof, A. M. R. (2011). Protein-polysaccharide interactions at fluid interfaces. *Food Hydrocolloids*, *25*(8), 1925–1937.

Ruffin, E., Schmit, T., Lafitte, G., Dollat, J. M., & Chambin, O. (2014). The impact of whey protein preheating on the properties of emulsion gel bead. *Food Chemistry*, *151*, 324–332.

Santos, J., Calero, N., Trujillo-Cayado, L. A., Garcia, M. C., & Muñoz, J. (2017). Assessing differences between Ostwald ripening and coalescence by rheology, laser diffraction and multiple light scattering. *Colloids and Surfaces B: Biointerfaces*, *159*, 405–411.

Schmitt, C., & Turgeon, S. L. (2011). Protein/polysaccharide complexes and coacervates in food systems. *Advances in Colloid and Interface Science*, *167*(1–2), 63–70.

Siew, C. K., & Williams, P. A. (2008). Role of protein and ferulic acid in the emulsification properties of sugar beet pectin. *Journal of Agricultural and Food Chemistry*, *56*(11), 4164–4171.

Suriyarak, S., & Weiss, J. (2014). Cutoff Ostwald ripening stability of alkane-in-water emulsion loaded with eugenol. *Colloids and Surfaces A: Physicochemical and Engineering Aspects*, *446*, 71–79.

Teo, A., Goh, K. K. T., Wen, J., Oey, I., Ko, S., Kwak, H. S., & Lee, S. J. (2016). Physicochemical properties of whey protein, lactoferrin and Tween 20 stabilised nanoemulsions: Effect of temperature, pH and salt. *Food Chemistry*, *197*, 297–306.

Torcello-gómez, A., & Foster, T. J. (2014). Interactions between cellulose ethers and a bile salt in the control of lipid digestion of lipid-based systems. *Carbohydrate Polymers*, *113*, 53–61.

Turgeon, S. L., Schmitt, C., & Sanchez, C. (2007). Protein-polysaccharide complexes and coacervates. *Current Opinion in Colloid and Interface Science*, *12*(4–5), 166–178.

Weinbreck, F., Rollema, H. S., Tromp, R. H., & De Kruif, C. G. (2004). Diffusivity of whey protein and gum arabic in their coacervates. *Langmuir*, *20*(15), 6389–6395.

Zeeb, B., Gibis, M., Fischer, L., & Weiss, J. (2012). Influence of interfacial properties on Ostwald ripening in crosslinked multilayered oil-in-water emulsions. *Journal of Colloid and Interface Science*, *387*(1), 65–73.

Zeeb, B., Mi-Yeon, L., Gibis, M., & Weiss, J. (2018). Growth phenomena in biopolymer complexes composed of heated WPI and pectin. *Food Hydrocolloids*, *74*, 53–61.

Zeeb, B., Stenger, C., Hinrichs, J., & Weiss, J. (2016). Formation of concentrated particles composed of oppositely charged biopolymers for food applications - impact of processing conditions. *Food Structure*, *10*, 10–20.

SECTION II. Designing double emulsions as carriers of hydrophilic plant-derived bioactive compounds

CHAPTER VI: *Formation of double emulsions ($W_1/O/W_2$) as carriers of hydrophilic and lipophilic active compounds*

Artiga-Artigas, M.; Molet-Rodríguez, A.; Salvia-Trujillo, L.; Martín-Belloso, O.

Published online in Food Bioprocess and Technology (2018)

(doi.org/10.1007/s11947-018-2221-3)

Abstract

This work aimed at obtaining an optimized formation procedure of water-in-oil-in-water ($W_1/O/W_2$) double emulsions as potential templates to carry hydrophilic (*e.g. chlorophyllin*; CHL) and/or hydrophobic (*e.g.* lemongrass essential oil; LG-EO) active compounds. As a first step, the impact of the hydrophobic surfactant (*i.e.* Span 80 or PGPR), sodium alginate or NaCl concentration as well as the homogenization method (*i.e.* high-shear homogenization, ultrasonication or microfluidization) on the particle size of the primary W_1/O emulsions was evaluated. The inner phase (W_1/O) formulated with PGPR (4% *w/w*) and sodium alginate (2% *w/w*) with NaCl (0.05M) and treated by high-shear homogenization (11,000 rpm, 5 min) presented the smallest particle size (d[4;3] ≈ 0.51 μm). As a second step, the primary W_1/O emulsion was subsequently dispersed in a secondary aqueous phase (W_2) at varying hydrophilic surfactant (*i.e.* lecithin or Tween 20), sodium alginate or NaCl concentrations and magnetic stirring rate (rpm and time) to obtain double emulsions ($W_1/O/W_2$). The formation of stable $W_1/O/W_2$ emulsions with d[4;3] of 7 μm was achieved with the use of lecithin (2% *w/w*), sodium alginate (2% *w/w*) with NaCl (0.05M) and treated by low-intensity UT homogenization (5,600 rpm, 2 min) followed by 24h of magnetic stirring. The incorporation of CHL and LG-EO in the inner aqueous phase and lipid phase respectively did not change the double emulsion characteristics. Overall, this study presents an effective two-step optimized procedure to form stable double emulsions as potential delivery systems for functional compounds.

Keywords: double emulsion; chlorophyllin; lemongrass essential oil; PGPR; two-step procedure.

1. Introduction

Water-in-oil-in-water ($W_1/O/W_2$) double emulsions are emulsion-based systems in which the dispersed phase is an emulsion itself (Dickinson, 2011a). The inner aqueous phase (W_1) is usually miscible with the final external phase (W_2) since they have the same polarity, whereas the intermediate phase (O) is immiscible with the other two (Wang, Zhang, & Hu, 2006). Recently, several applications have been attributed to double emulsions, such as fat replacers or delivery systems of active compounds. The formation of double emulsions is generally achieved with a two-step emulsification procedure in which first a primary water-in-oil emulsion (W_1/O) is formed, and is subsequently emulsified to form the secondary emulsion ($W_1/O/W_2$) (Muschiolik & Dickinson, 2017). However, the fabrication and stabilization of double emulsions remains as a challenge as they are highly susceptible to destabilization phenomena. Several destabilization mechanisms have been described in double emulsions, being (*i*) the coalescence of the lipid dispersed phase; (*ii*) coalescence of the inner aqueous droplets between them or with the external aqueous phase and (*iii*) swelling or shrinkage of the inner water droplets as result of diffusive transport between both aqueous phases (Dickinson, 2011).

For the overall double emulsion stabilization, the stability of both the inner aqueous W_1 and the outer lipid W_1/O dispersed phase and their respective interfaces needs consideration. On the one hand, the presence of a lipophilic surfactant is required for the emulsification and stabilization of the inner aqueous phase. Spans are commonly used for this purpose but their efficiency in primary emulsion stabilization needs to be elucidated. Polymeric surfactants such as polyglycerol polyricinoleate (PGPR) at a 4 to 6% *w/w* concentration are often utilized as an alternative of spans (Su, Flanagan, Hemar, & Singh, 2006). However, its use in food-grade formulations is strictly regulated and it may be detected rapidly due to its unpleasant off-taste when incorporated in the required doses for double emulsion stabilization (Altuntas, Sumnu, & Sahin, 2017). On the other hand, the outer W_1/O dispersed phase may be stabilized by using an hydrophilic surfactant, such as lecithin, Tweens or proteins (Garti & Bisperink, 1998). The formation and stabilization of the secondary emulsion with the dispersed W_1/O droplets depends on two main factors. First, the osmotic balance between the two aqueous phases must be kept in order to avoid diffusive transport of water, which leads to destabilization of double emulsions (Muschiolik, 2007). For instance, the addition of salt in the W_1-droplets may be able to reduce the osmotic differences and avoid swelling of the inner aqueous dispersion (Yan & Pal, 2001). And second, the homogenization method to disperse the oil phase containing the W_1-droplets determines in a high extent the retention of the aqueous inner droplets within the lipid phase. In this regard, moderate emulsification conditions should be applied to prevent intense high shearing hydrodynamic forces that may destabilize the previously formed primary emulsion (Muschiolik & Dickinson, 2017). Due to this mild emulsification conditions, the droplet size of the dispersed W_1/O phase remains relatively large, which in turn allows the retention of the inner W_1 dispersed droplets. However, their large droplet size may result in significant destabilization and phase separation of the W_1/O phase from the W_2 aqueous phase. This effect may be diminished or avoided by the use of thickening agents in the aqueous phases, such as sodium alginate among others, in order to reduce the mobility of the W_1/O phase and as a consequence prevent phase separation. Sodium alginate has a strong defined polarity in the aqueous media since it is deprotonated, which avoids its migration to the internal oil-water interface and may enhance the achievement of aqueous phase rheological control (Artiga-Artigas, Acevedo-Fani, & Martín-Belloso, 2017; Dickinson, 2011a).

Therefore, the aim of this work was to study the formation and stabilization of double emulsions. First of all, the formation of the primary W_1/O emulsion was investigated with regards the effect of the homogenization method (ultrasonication, microfluidization or high-shear mixing) and processing conditions on the particle size of the dispersed W_1 droplets in the oil phase. Moreover, the use of several lipophilic emulsifiers (PGPR or Span 80) at different concentrations was evaluated. Afterwards, the formation of double ($W_1/O/W_2$) emulsions was studied by applying different low-shear homogenization conditions and emulsifiers (lecithin or Tween 20). Additionally, the salt addition in both aqueous phases in order to maintain the osmotic balance between both phases was studied as well as the incorporation of sodium alginate as thickening agent. Finally, the use of the formulated double emulsion as carriers of *chlorophyllin* (CHL) in the W_1 phase and/or lemongrass essential oil (LG-EO) in the oil phase as examples of active compounds due to their high antioxidant capacity to be encapsulated and delivered in food systems was assessed (Cheel et al. 2005; Guerra-Rosas et al. 2017; López-Carballo et al. 2008; Tumolo and Lanfer-Marquez 2012).

2. Material and Methods

2.1.Materials

Sodium alginate (MANUCOL®DH) was obtained from FMC Biopolymer Ltd (Scotland, U.K.). CHL (coppered trisodium salt) with a molecular weight of 724.15 g/mol, copper contain of 3.5-6.5% and a purity of ≥ 95% was purchased from Alfa Aesar (Thermo Fisher Scientific, GmbH, Karlsruhe, Germany). NaCl from POCH S.A. (Gliwice, Poland) was used to improve interfacial thermodynamic stability by controlling the osmotic balance between the two aqueous phases. Corn oil (Koipesol Asua, Deoleo, Spain) and LG-EO (*Cymbopogon citratus*) from Laboratories Dicana (Spain) were used as lipid phase. Sunflower oil, which was kindly donated by Borges (Lleida, Spain), was the dispersant in particle size measurements. Span 80 (***Sorbitane monooleate***) obtained from Alfa Aesar (Thermo Fisher Scientific, GmbH, Karlsruhe, Germany) or Polyglycerol Polyricinoleate (PGPR 90) from castor oil (Grinsted®, DuPont Danisco NHIB Iberica S.L, Barcelona, Spain) were utilized as hydrophobic surfactants. Tween 20 (Polyoxyethylenesorbitan Monoesterate) (Lab Scharlab, Barcelona, Spain) or L-α-Soybean lecithin was acquired from Alfa Aesar (Thermo Fisher Scientific, GmbH, Karlsruhe, Germany) and used as food-grade non-ionic surfactants. Ultrapure water, obtained from Millipore Milli-Q filtration system (0.22 μm) was used for the formulation and analysis of nanoemulsions.

2.2.Water-in-oil emulsions (W_1/O) and double emulsions ($W_1/O/W_2$) formation

$W_1/O/W_2$ nanoemulsions were prepared following a "two-step" emulsification process where first a water-in-oil (W_1/O) emulsion was formed and this one was subsequently dispersed in a second aqueous phase to obtain the so called double emulsion ($W_1/O/W_2$).

Formation of water-in-oil (W_1/O) emulsions

For the formation of the W_1/O emulsions, a ratio aqueous phase (W_1)/oil phase (O) of 30/70 (*w/w*) was used. Different parameters including hydrophobic surfactant type and concentration, emulsification mechanism as well as sodium alginate and salt concentration in the inner aqueous phase were evaluated during the formation of W_1/O emulsions. In addition, the feasibility of incorporating LG-EO as a hydrophobic compound in the lipid phase of W_1/O emulsions was tested.

Firstly, in order to assess the type and concentration of hydrophobic surfactant, the aqueous phase of emulsions was prepared by dissolving 1% *w/w* sodium alginate in ultrapure water at 70 ºC and stirred during 3 hours to ensure its complete hydration. After reaching room temperature, the exact amount of CHL (27 ppm) was added to the alginate solution until its dissolution. This aqueous phase was dispersed into a lipid phase containing corn oil and Span 80 (4, 6 or 10% *w/w*) or PGPR (4, 6 or 10% *w/w*), which were evaluated as hydrophobic surfactants. Both phases were mixed through three different procedures for the formation of W_1/O: A) high shear homogenization (HSH) with a T25 digital Ultra-Turrax (IKA, Staufen, Germany) at 11,000 or 22,000 rpm and during 1, 2, 3 or 5 min; B) HSH (11,000 rpm, 5 min) followed by ultrasonication (US) with a UP 400S Hielscher sonifier (Hielscher Ultrasound Technology, Teltow, Germany) at amplitudes of 30, 60 or 100 μm and for 1, 3 or 5 min and C) HSH (11,000 rpm, 5 min) followed by microfluidization (MF) with a microfluidizer (M110P, Microfluidics, Massachusetts, USA) at 150 MPa and 1-5 cycles.

Secondly, for the establishment of sodium alginate and NaCl concentration W_1/O emulsions containing 0-2% *w/w* of biopolymer and 0-0.25M in their aqueous phase were mixed by HSH at 11,000 rpm during 5 min.

Finally, when the optimization procedure and formulation of the double emulsions as a model of delivery system of bioactive compounds was established, 1% *w/w* lemongrass (as hydrophobic bioactive compound) was incorporated to the lipid phase of W_1/O emulsions.

Formation of double ($W_1/O/W_2$) emulsions

The previously prepared W_1/O emulsion was dispersed in a secondary aqueous phase (W_2) in a ratio 1/4 (primary emulsion/W_2) leading to $W_1/O/W_2$ emulsion formation. The W_2 phase contained 2% *w/w* sodium alginate, NaCl (0-0.25 M) and Tween 20 or lecithin (2-4% *w/w*) as hydrophilic surfactants. $W_1/O/W_2$ emulsions were obtained by HSH with an Ultra Turrax (T25 digital Ultra-Turrax, IKA, Staufen, Germany) at 5,600 rpm and 2 min followed by magnetic stirring at 750 rpm, during 3, 5, 18 and 24h.

2.3.Characterization of water in oil emulsions (W_1/O) and double emulsions ($W_1/O/W_2$)

In order to establish the most suitable processing conditions and formulation for the formation of W_1/O and $W_1/O/W_2$ emulsions, these were characterized in terms of mean droplet diameters (d[4:3]) and particle size distribution. Turbidity measurements were performed on selected double emulsions in order to detect possible flocculation or creaming phenomena. Once the formulation and processing conditions were optimized, apparent viscosity and color with regards to *a**and *b** parameters and whiteness index of W_1/O and $W_1/O/W_2$ emulsions were measured. Also, particle size and morphology of the resultant $W_1/O/W_2$ emulsions were evaluated through confocal microscopy together with the assessment of their turbidity during 21 days of refrigerating storage.

2.3.1. Particle size and particle size distribution

The emulsion droplet size was measured by the laser diffraction technique with a Mastersizer 3000^{TM} (Malvern Instruments Ltd., Worcestershire, UK). The measured droplet size was expressed as volume-weight and surface-weight diameter (d[4;3] and d[3;2] in μm. Refractive indexes (RI) of corn oil and lemongrass essential oil were 1.47 and 1.48, respectively. For the measurement of particle sizes of W_1/O emulsions, sunflower oil, whose RI was the same as corn oil, was used as dispersant, whereas $W_1/O/W_2$ emulsions were dispersed in distilled water (RI=1.33).

2.3.2. Apparent viscosity

A vibro-viscometer (SV-10, A&D Company, Tokyo, Japan) vibrating at 30 Hz was used to measure the viscosity (mPa·s) of 10 mL aliquots of the W_1/O and $W_1/O/W_2$ emulsions. Moreover, the viscosity of water, which was used as dispersant phase, was 0.91 mPa·s. This value was considered with regard to DLS measurements, which were all performed at 25 ± 2 ºC.

2.3.3. Color of W_1/O and $W1/O/W_2$ emulsions

The color of W_1/O and $W_1/O/W_2$ emulsions was measured with a colorimeter (Minolta CR-400, Konica Minolta Sensing, Inc., Osaka, Japan) at room temperature set up for illuminant D65 and 10° observer angle and calibrated with a standard white plate. CIE L^*, a^* and b^* values were determined, and the whiteness index (WI) was calculated with equation 1 (Salvia-Trujillo, Rojas-Graü, Soliva-Fortuny, & Martín-Belloso, 2013a):

$$WI = 100-((100-L)^2+(a^2+b^2))^{0.5} \quad \textbf{eq.(1)}$$

2.3.4. Turbidity over time

The stability of the prepared W_1/O and $W_1/O/W_2$ emulsions containing CHL and/or LG-EO was performed in duplicate through a turbidity study with a Turbiscan Classic (Formulaction, Toulouse, France) during 21 days of refrigerated storage at 4ºC. The turbidity measurement allows the detection of the most common destabilization mechanisms of emulsions such as creaming, sedimentation, flocculation or coalescence by multiple light scattering. Then, the Turbiscan software enables to interpret the obtained data easily.

2.3.5. Confocal fluorescence microscopy

Fresh double emulsions containing CHL and/or LG-EO were dyed with Nile red (Sigma Aldrich, Merk, Darmstadt, Germany), a fat-soluble fluorescent dye that was previously dissolved at 0.1% (w/v) in polyethilenglycol (Sigma Aldrich, Merk, Darmstadt, Germany). Afterwards, double emulsions microstructure was observed with an Olympus Spectral Confocal Microscope (Olympus FV1000, Melville, NY) with 100x oil immersion objective lens. All images were taken and processed using the instrument software program (Olympus FV10-ASW viewer, Melville, NY).

2.3.6. Encapsulation efficiency of double emulsions ($W_1/O/W_2$) containing chlorophyllin

In order to calculate the CHL encapsulation efficiency (EE) of $W_1/O/W_2$ emulsion, aliquots of 10 mL were placed inside a centrifuge tube and 20 mL of food grade methanol were added. After centrifuging (3000 g, 10 min) with a Hettich® Universal 320 centrifuge (Sigma-Aldrich, Darmstadt, Germany) the outer aqueous phase with the non-encapsulated CHL (free CHL) was filtered through a 0.22 mm Vinylidene Polyfluoride (PVDF) syringe filter and quantified by analyzing the solvent spectrophotometrically with a V-670 spectrophotometer (Jasco, Tokyo, Japan) at 405 nm. The EE of the obtained $W_1/O/W_2$ emulsions was calculated by equation (2) (Giroux et al., 2013):

$$\%EE = \frac{C(W1)*X(W1) - Cs*(V+X(W2))}{C(W1)*X(W1)} \text{ x } 100 \qquad \textbf{eq.(2)}$$

where $C(w_1)$ is the initial CHL concentration in the internal aqueous phase of the emulsion (27 ppm), C_S is the CHL concentration in the subphase collected after centrifugation of the diluted emulsion, $X(W_1)$ and $X(W_2)$ are, respectively, the mass fractions of the internal (0.06) and external (0.8) aqueous phases for 1Kg (V) of emulsion. All the measurements were performed in triplicate.

2.3.7. Antioxidant capacity of double emulsions ($W_1/O/W_2$)

The antioxidant capacity of CHL and lemongrass essential oil (LG-EO) both solved in methanol (used as controls), as well as, CHL- and CHL/LG-EO-loaded emulsions was determined by DPPH and FRAP assays. Although both methods are able to measure the antioxidant capacity of a sample, the main difference between them is that DPPH assay is based on the presence of radicals (DPP·), whereas FRAP consists of an electrons exchange (Thaipong et al., 2006).

The DPPH procedure was conducted according to the method of Brand-Williams, Cuvelier, & Berset, (1995) with some modifications. The DPPH radical solution was prepared by dissolving 3.75 mg of DPPH radical in 100 mL of methanol. The absorbance of solution was adjusted to a value between 0.7-0.8 ± 0.02 (measured at 515 nm). Aliquots of 10 μL of sample were placed in a microplate with 90 μL of Milli-Q water and 3900 μL of DPPH radical solution was added to each sample. Samples were incubated for 30 min in the dark and the absorbance at 405 nm was measured.

FRAP assay was carried out as described by Benzie & Strain (1996) with some modifications where 150 μL of sample were placed into each tube and mixed with 2850 μL of FRAP solution. The samples were incubated at room temperature in the dark for 30 min and the absorbance was measured at 630 nm after prior filtration.

Results were reported as mg of Trolox equivalents per mL of solution (mg TE/mL) using a standard curve of Trolox (Velderrain-Rodríguez et al., 2015). In both methods, triplicate determinations were made at each dilution of the standard.

2.4.Statistics

All the procedures were assessed in duplicate, and at least three measurements of each parameter were carried out. The statistical software SigmaPlot 11.0 (Systat Software Inc., Pennsylvania, USA) was used to perform the analysis of variance. To determine differences among means of the different procedures, One Way ANOVA test was run at a 5% significance level.

3. Results and Discussion

First, the formation of the primary (W_1/O) emulsion was studied by determining the influence of the surfactant type and concentration, and homogenization method on the particle size and particle size distribution of the inner W_1-droplets dispersion. Second, the formation of the subsequent double emulsion was evaluated in terms of the surfactant type and concentration and emulsification conditions. The effect of the presence of salt and sodium alginate were assessed both in the primary and double emulsions. Finally, the incorporation of CHL in the inner W_1 phase and LG-EO in the oil phase of the optimized double emulsion formulation was determined and the physicochemical stability and antioxidant capacity of the final double emulsion was determined.

3.1. Water-in-oil emulsions (W_1/O)

Primary W_1/O emulsions were formed at varying Span 80 or PGPR concentrations (4, 6 and 10% *w/w*) (Figure 1A) by HSH (11,000 rpm, 5 min). Subsequently, several homogenization methods and conditions were studied, such as HSH, US or MF (Figure 2). Also the influence of sodium alginate incorporation (0-2% *w/w*) as well as salt addition (0-0.25M) on the particle size of the primary W_1/O dispersion was investigated (Figure 1B and C, respectively).

3.1.1. Effect of type and concentration of the hydrophobic surfactant in the particle size of W_1/O emulsions

The particle size of W_1/O emulsions decreased at increasing the concentration of Span 80 or PGPR from 4% to 10% *w/w* (Figure 1A). Nevertheless, the performance in reducing the particle size of the W_1/O emulsions was significantly different for both surfactants. In this regard, PGPR led to W_1/O emulsions with remarkably smaller particle sizes than Span 80. In fact, particle sizes of PGPR-stabilized W_1/O emulsions ranged between 0.396 and 0.802 μm with monomodal particle size distributions while those with Span 80 exhibited particle sizes above 32 μm for all the tested concentrations. Moreover, particle size distributions of W_1/O emulsions containing Span 80 presented intensity peaks around 1 and 10 μm suggesting a high polydispersity.

Span 80 is a small molecular surfactant that is expected to rapidly adsorb to water droplets thus reducing the interfacial tension and avoiding coalescence (Wooster et al., 2008a). However, Surh et al. (2007) observed that although Span 80 was soluble in vegetable oils such as corn oil at room temperature, the resultant W_1/O rapidly separated after the homogenization process. Therefore, in order to obtain water-in-oil emulsions with particle sizes sufficiently small to be re-encapsulated during the second step, Span 80 needs to be at very high concentrations in the oil (Dickinson, 2011).

One alternative to avoid the use of elevated concentrations of surfactant is to increase the viscosity of the oil phase (Weiss & Muschiolik, 2007). In this regard, polymeric surfactants such as PGPR are potential substitutes to stabilize multiple emulsions. Certainly, the use of PGPR at surfactant concentration of 4% *w/w* led to W_1/O emulsions with particle size bellow 1 μm (Figure 1A). PGPR may be able to better interact with lipid phase due to its higher hydrophobicity compared to Span 80, thus forming a kinetic barrier protecting the emulsion against droplets coalescence (Tabibiazar &

Hamishehkar, 2015). Therefore, the chosen hydrophobic surfactant used for the formation of the subsequent double emulsions was PGPR (4% *w/w*).

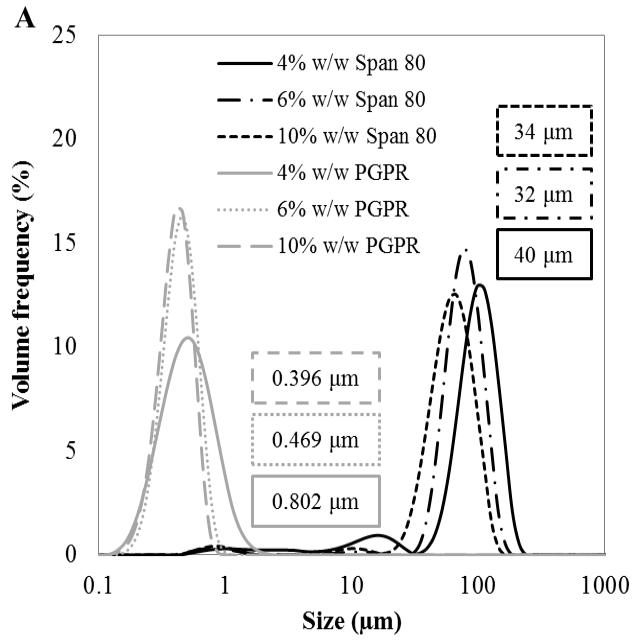

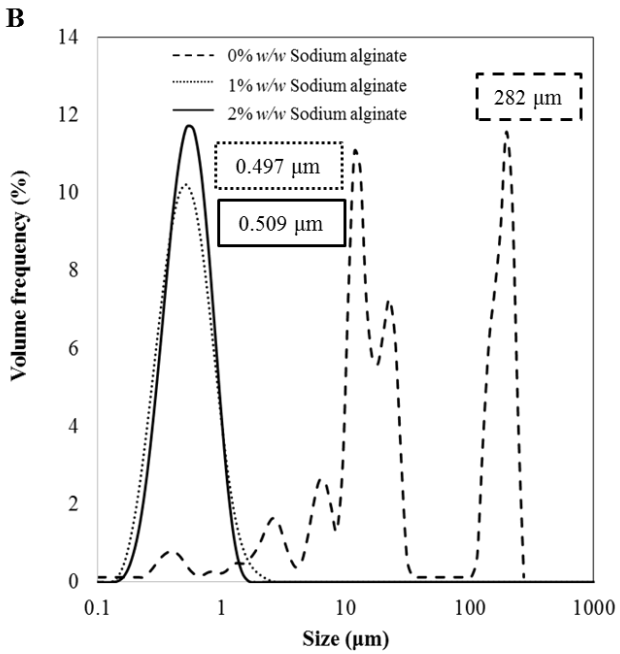

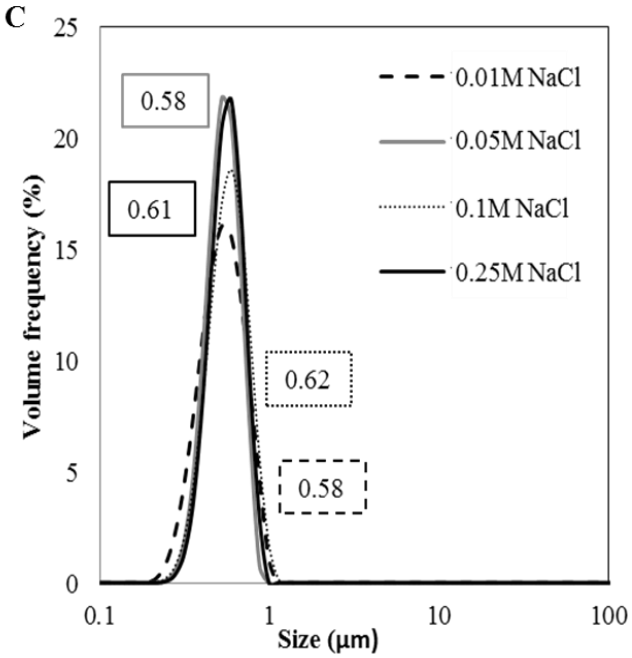

Figure 1. Effect of the type and concentration of hydrophobic surfactant in the particle size of water-in-oil emulsions (W_1/O) produced by high-shear homogenization (11,000 rpm, 5 min) containing 27 ppm of *Chlorophyllin* and 1% *w/w* of sodium alginate in the aqueous phase and corn oil as dispersed phase (A). Influence of sodium alginate concentration (0-2% *w/w*) (B) and NaCl concentration (0-0.25 M) (C) in the inner aqueous phase on the formation W_1/O emulsions, containing 27 ppm of *Chlorophyllin* and 2% *w/w* sodium alginate in the aqueous phase and 4% *w/w* of PGPR in corn oil as dispersed phase. Mean volume-weighed droplet diameters (d[4;3]) of emulsions are specified within boxes.

3.1.2. Influence of the homogenization procedure on the formation of W_1/O emulsions

It has been reported that the fabrication of W_1 dispersed droplets of nanosized range contributes in the overall stability of the resultant $W_1/O/W_2$ emulsion (Fathi, Mozafari, & Mohebbi, 2012; Lamba et al., 2015a). Therefore, three different high energy procedures including laboratory HSH, HSH followed by US or MF were tested in order to obtain W_1/O emulsions with small particle sizes. The first HSH was performed at 11,000 or 22,000 rpm during 1, 2, 3 or 5 minutes. At 11,000 rpm, the longer the processing time, the smaller the mean particle size (d[4:3]) of W_1/O emulsions reaching values of 509 nm after 5 min (Figure 2A). However, as increasing the frequency of HSH processing up to 22,000 rpm, the destabilization of W_1/O emulsions started after the first 2 minutes of processing leading to polydisperse distributions with particles sizes higher than 15 µm. This suggests that HSH frequency significantly affected the reduction of particle size. HSH device produces cavitation, collision and turbulence forces, which causes breakdown of the droplets and uniform dispersion of the dispersed phase (Lamba et al., 2015a). However, under certain conditions, these

forces can cause an over-processing of the emulsions that may provoke re-coalescence due to an increase in the surface area, thus favoring polydispersion (Jafari et al., 2007b). Therefore, the most suitable conditions to obtain nanoparticles and monomodal distributions were 11,000 rpm during 5 min.

After these conditions of HSH, US at amplitudes of 30, 60 and 100 μm during 1, 3 or 5 min; or MF (1-5 cycles at 800 bar) were applied in order to evaluate their effect in W_1/O emulsions particle size. Regarding US application, the longer the processing time, the larger the particle size of W_1/O emulsions regardless the amplitude applied (Figure 2B). In this regard, the smallest particle sizes were obtained after 1 min of US in all the cases being the one prepared with an amplitude of 30 μm, which lead particle sizes below 1 μm, (d[4:3]= 850 nm). Moreover, all the distributions were polydisperse thus suggesting an over-processing of emulsions, which may cause droplets re-coalescence and further emulsions destabilization (Jafari et al., 2007b).

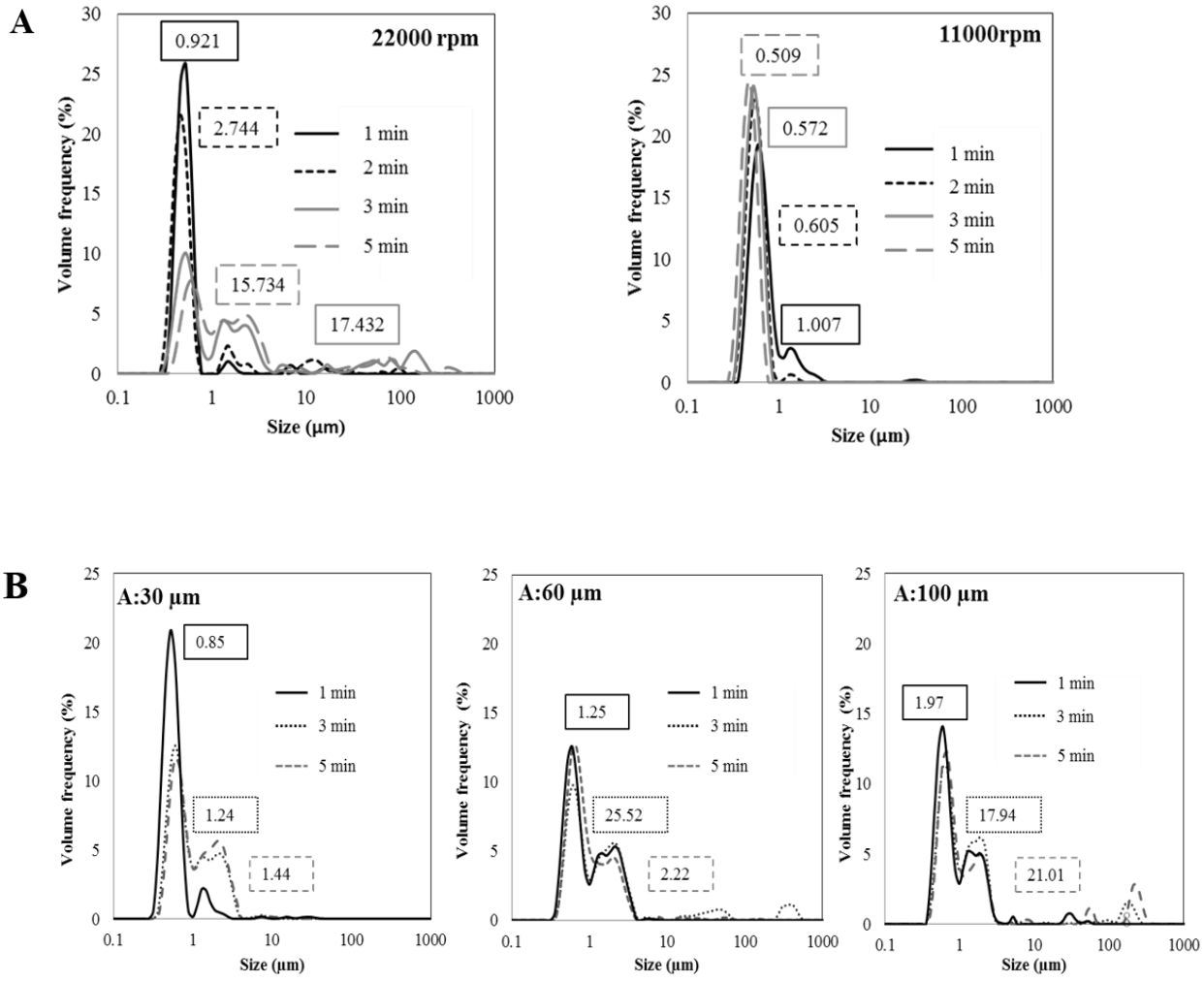

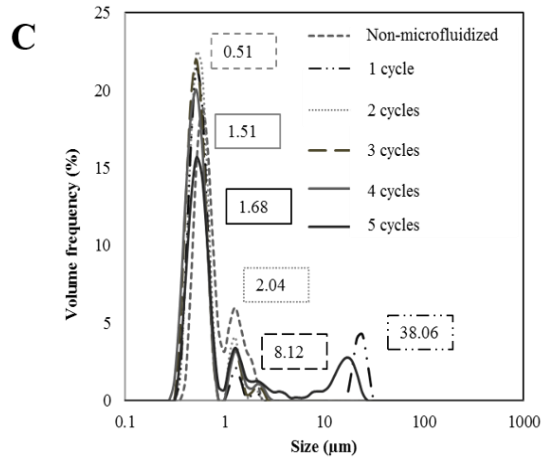

Figure 2. Effect of the homogenization procedure in the formation of W_1/O (3/7) emulsions containing 27 ppm of *chlorophyllin* (CHL) and 1% *w/w* sodium alginate as aqueous phase and 4% *w/w* PGPR in corn oil as lipid phase. (A) Variation of the high shear homogenization frequency and time. (B) High shear homogenization (11,000 rpm, 5 min) followed by sonication at different amplitude and times. (C) High shear homogenization (11,000 rpm, 5 min) followed by microfluidization (150 MPa, 1-5 cycles). Mean droplet diameters (d[4;3]) of emulsions are specified within boxes.

In the case of using MF after HSH, particle size of W_1/O promptly increased immediately after the first cycle of microfluidization from 0.51 to 38.06 μm and it was further reduced during the following cycles (Figure 2C). Despite the fact that MF is considered as the most efficient technique to form fine emulsions, the reduction in particle size it is effective only until a certain limit (Xu et al., 2014). This means that shearing the emulsion at the same pressure may not produce any additional rupturing or change in particle size (Meleson, Graves, & Mason, 2004; Salvia-Trujillo et al., 2013b). Indeed, MF reduced particle size of W_1/O emulsions with increasing cycles up to the 4^{th} one, reaching values of 1.51 μm (Figure 2C). Then, particle size slightly increased after the application of the last cycle (Figure 2C). In agreement with our results, Jafari et al. (2007) observed an increase in the d[4;3] of their submicron emulsions after increase the microfluidization pressure from 20 to 60 MPa. Several authors including Kolb, Viardot, Wagner, & Ulrich (2001) and Schultz, Wagner, Urban, & Ulrich (2004) also observed this over-processing during high-pressure homogenization. This phenomenon has been attributed to the fact that the efficiency of each microfluidization cycle is not complete since shear flow is not equal distributed in all the emulsion being the droplets near the walls who experimented the weakest forces thus resulting in size distributions containing larger particles.

3.1.3. Impact of sodium alginate and NaCl salt incorporation in the stabilization of W_1/O emulsions

Sodium alginate incorporation has a critical impact in the stabilization of W_1/O emulsions since its absence led to emulsions with huge particle sizes (>280 μm), whereas a concentration of 1% *w/w* was enough to obtain monomodal distributions and particle sizes below 1 μm (Figure 1B).

Moreover, at increasing the concentration of sodium alginate up to 2% *w/w* water-in-oil emulsions showed twice of apparent viscosity (data not shown). It is reported that the enhancement of the viscosity of the prior W_1/O emulsion may improve the stability of the subsequent double emulsion (Muschiolik & Dickinson, 2017). In addition, other authors have also observe a positive effect on $W_1/O/W_2$ stabilization after the incorporation of biopolymers to the inner aqueous phase (Dickinson, 2011b; Mezzenga, Folmer, & Hughes, 2004). It is believed that the origin of this enhancement of stability is due to the interaction between polysaccharide and lipophilic surfactant, which provides a viscoelastic barrier thus preventing droplets coalescence (Garti, 1997). Indeed, some authors as Dickinson (2011b) also observed this synergistic stabilizing effect between the biopolymer (*e.g.*sodium caseinate) and PGPR.

Also, the incorporation of electrolytes like NaCl together with biopolymers to the inner water phase of double emulsions (W_1) can improve their thermodynamic stability by controlling the osmotic balance (Benichou et al., 2004). Figure 1C shows that salt incorporation had not a significant effect in the particle size of fresh emulsions. However, Figure 3A revealed that water-in-oil emulsions prepared without NaCl, experimented an increase of particle size (zone II) and creaming (zone III) during the first 72 h. Each backscattering plot generated can be split in three zones named as I (on the left), II (in the middle) and III (on the right) corresponding to the bottom, the intermediate part and the top of the tube, respectively. In this regard, down peaks in zone I mean clarifications and are usually related with up peaks in zone III thus suggesting creaming. Likewise, up peaks in zone I may indicate sedimentation and are often accompanied by down peaks in zone III. The displacement of the horizontal lines from zone II points out variations in emulsions particle size due to flocculation or coalescence. However, those containing 0.05M of NaCl salt did not experiment variation in their turbidity thus suggesting that they were stable during at least a week of refrigerated storage (Figure 3C).

In the case of W_1/O emulsions with concentrations of salt below or over 0.05M, phase separation occurred after 4 days of storage (Figures 3B or 3E and 3F, respectively) being this disruption even more abrupt in emulsions containing NaCl concentrations of 0.25M (zone II). Scherze, Knoth, & Muschiolik (2006) also observed that the addition of NaCl to the inner aqueous phase of W_1/O emulsions containing PGPR as surfactant was essential to prevent coalescence phenomenon. This suggests that the interaction between NaCl and PGPR may contribute to increase droplet size stability since electrolytes can increase the adsorption density of surfactant thus reducing emulsion interfacial tension (Aronson & Petko, 1993; Dickinson, 2011).

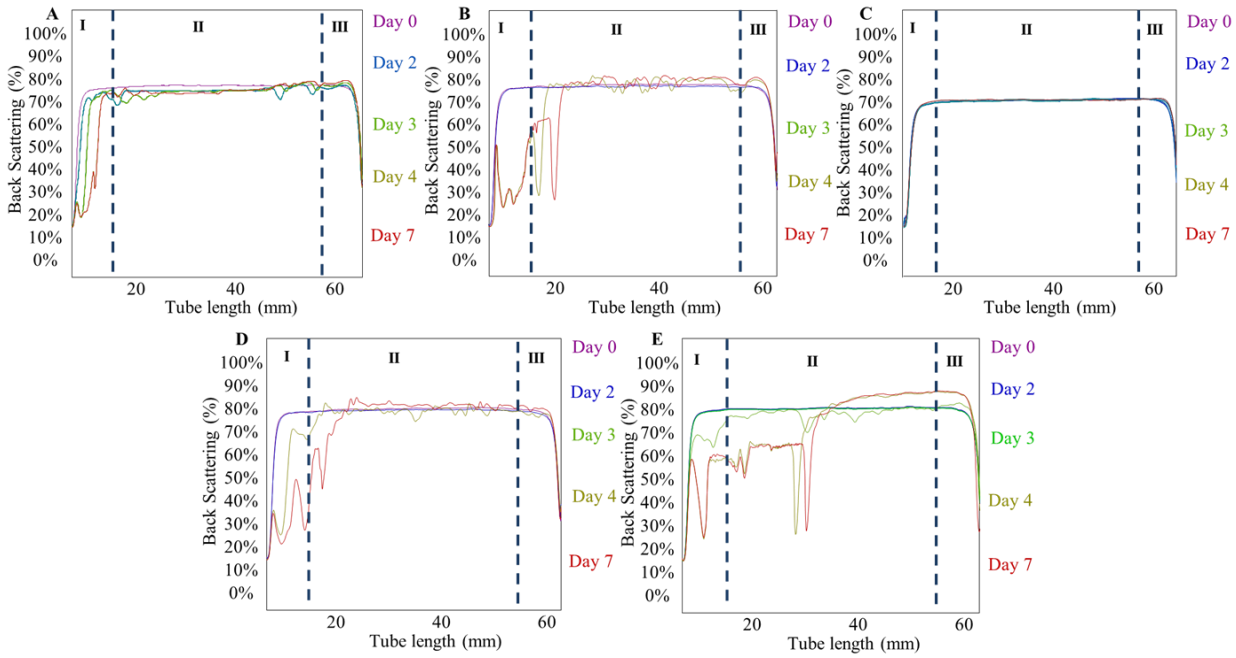

Figure 3. Turbidity assessment expressed as back scatter intensity (%) along a tube (mm) containing water-in-oil emulsions (W_1/O) formulated with 27 ppm of *chlorophyllin,* 2% *w/w* sodium alginate and 4% *w/w* PGPR, after no salt addition (A) or 0.01M NaCl (B); 0.05M NaCl (C), 0.1M NaCl (D) and 0.25M NaCl (E) was added. The destabilization phenomena usually registered by the Turbiscan include clarifications (down peaks in zone I), variations in particle size (displacement of the horizontal lines from zone II: flocculation or coalescence) and creaming (up peaks in zone III).

3.2.Double emulsions ($W_1/O/W_2$)

Iniatially, the prepared W_1/O emulsion containing 2% *w/w* of sodium alginate and NaCl 0.05M in the inner aqueous phase, was dispersed in a second aqueous phase (W_2) and the effect of the time of magnetic stirring (3-24h) on the formation of $W_1/O/W_2$ emulsions was assessed (Figure 4A). Secondly, $W_1/O/W_2$ emulsions were prepared using different concentrations (2-4% *w/w*) of Tween 20 or lecithin as hydrophobic surfactants (Figure 4B-D). Finally, the impact of NaCl incorporation (0-0.25 M) in the W_2 on the particle size of the resultant $W_1/O/W_2$ emulsions was also evaluated (Figure 4E).

3.2.1. Effect of the homogenization procedure on the formation of $W_1/O/W_2$

After dispersing W_1/O emulsion into the W_2 both phases were mixed by HSH at 5,600 rpm and 2 min, followed by magnetic stirring at 750 rpm during different times (3-24h) to the formation of $W_1/O/W_2$ emulsions. Regarding Figure 4A, all the obtained double emulsions were polydisperse probably due to the application of low shear energies required to prevent the disruption of the initial water-in-oil interface (Márquez, Palazolo, & Wagner, 2007; Muschiolik & Dickinson, 2017). As it is shown in Figure 4A, the higher the time of stirring, the lower the particle size of $W_1/O/W_2$ emulsions, reaching a value of 3.6 µm after 24h with regards the initial one of 8.6 µm. It is well-known that lower

particle sizes provide high colloidal stability and large interfacial area to volume ratio thus preventing phenomena such as coalescence (Wooster et al., 2008a). Nonetheless, the final particle size of $W_1/O/W_2$ emulsion has to be large enough to ensure the absence of external (W_1/O globule-W_1/O globule) and internal (W_1 droplet-W_1 droplet) coalescence phenomena (Bonnet, Cansell, Placin, Anton, & Leal-Calderon, 2010). In their study Bonnet et al. (2010) reported that their $W_1/O/W_2$ emulsions, in which W_1/O globules were about eight times larger than W_1 droplets, remained invariant over 30 days. In this regard, concerning our results, W_1 droplets of 509 nm should be able to coexist without coalescing within those W_1/O, whose mean particle sizes were around 4 µm. Therefore, magnetic stirring performed at 750 rpm during 24 h were considered as valid processing conditions to prepare $W_1/O/W_2$ emulsions.

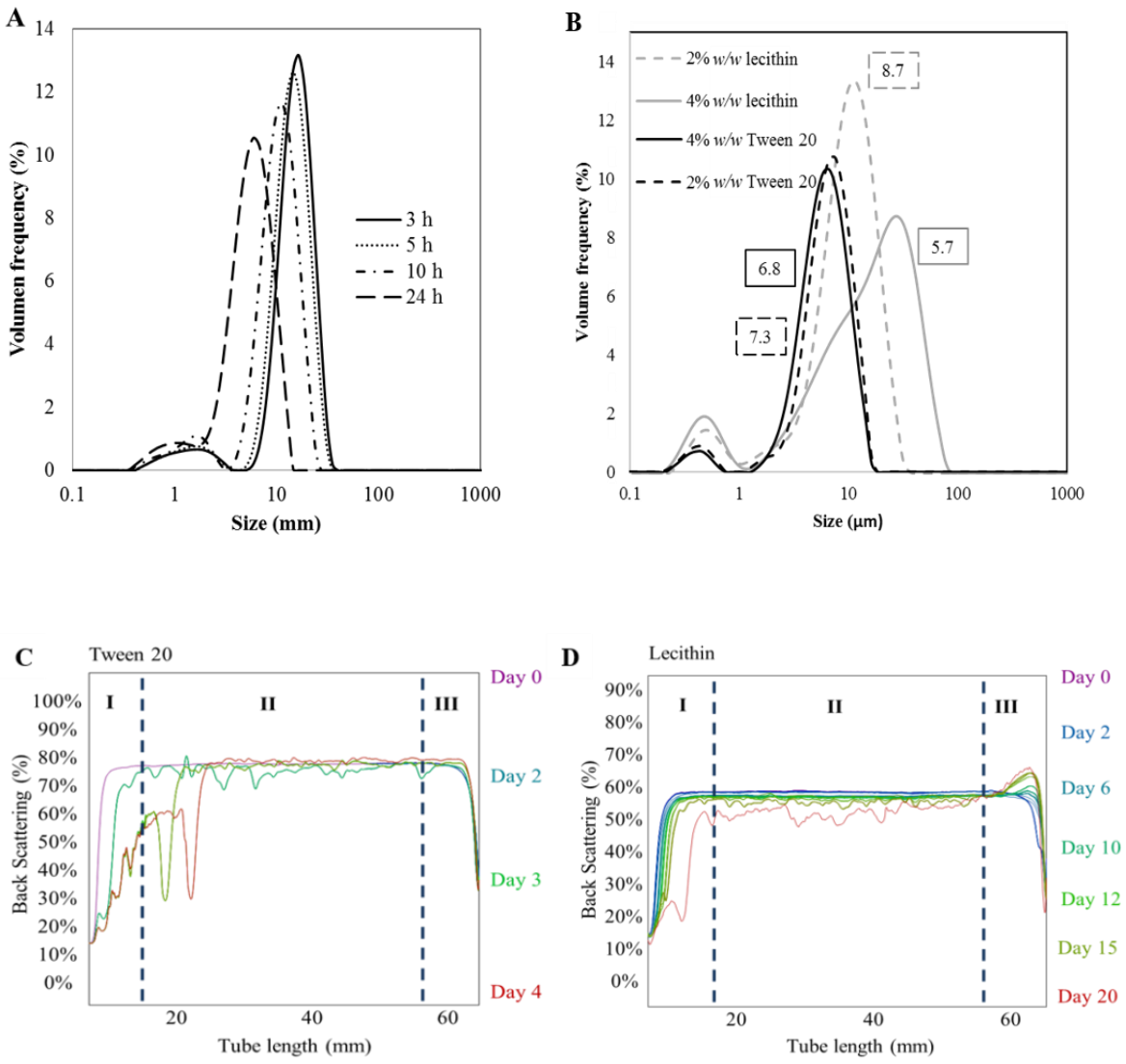

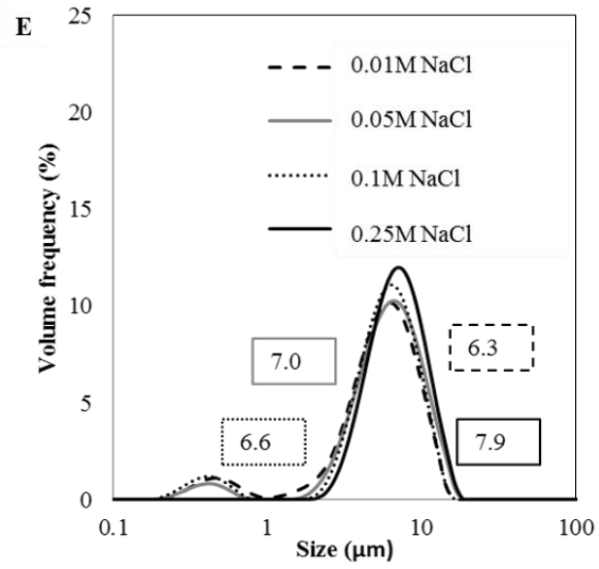

Figure 4. Effect of the magnetic stirring time on the particle size distribution of double emulsions ($W_1/O/W_2$) containing 2% *w/w* sodium alginate, 27 ppm of *chlorophyllin* and 0.05M NaCl in the inner aqueous phase (W_1) and 4% *w/w* PGPR and corn oil as dispersed phase (O). As a model of outer aqueous phase (W_2), 2% *w/w* sodium alginate and 4% *w/w* Tween 20 was used as stabilizing agent and surfactant, respectively (A). Influence of Tween 20 and lecithin concentration in the (B) particle size and (C, D) turbidity during time of $W_1/O/W_2$ emulsions at concentrations of hydrophilic surfactant of 2 and 4% *w/w*. (E) Impact of NaCl incorporation (0-0.25 M) in the particle size of $W_1/O/W_2$ emulsions containing 2% w/w as hydrophilic surfactant.

Overall, W_1/O emulsions had been prepared by high shear homogenization (11,000 rpm, 5 min) and mean volume-weighed droplet diameters (d[4;3]) of emulsions are specified within the boxes. $W_1/O/W_2$ were prepared by low-energy high shear homogenization at 5,600 rpm during 2 min followed by magnetic stirring at 750 rpm, during 3, 5, 10 or 24 h **(A)** or during 24 h in the rest of plots.

3.2.2. Influence of the hydrophilic surfactant type and concentration on the particle size of $W_1/O/W_2$

In order to observe the influence of type and concentration of surfactant on their particle size and stability over time, $W_1/O/W_2$ emulsions containing Tween 20 or lecithin as hydrophilic surfactant at concentrations of 2 and 4% *w/w* were prepared (Figure 4B and C-D, respectively). As increasing the concentration of surfactant from 2 to 4% *w/w*, the mean particle size of $W_1/O/W_2$ emulsions, decreased from 7.3 to 6.8 µm when Tween 20 was used and from 8.7 to 5.7 µm in those lecithin-stabilized. Therefore, only in the case of lecithin the premise that the higher the concentration of surfactant, the smaller the particle size is fulfilled (Zirak & Pezeshki, 2015). In spite of 4% *w/w* lecithin led to smaller particles sizes, at lower concentration of lecithin (2% *w/w*) the minor peak observed in the particle size distribution plot was minor and the major peak was more intense. This suggested a more successful $W_1/O/W_2$ emulsion formation since the polydispersity index was lower (Figure 4B). Moreover, $W_1/O/W_2$ emulsions containing lecithin remained stable during at least 10 days as suggested by the

turbidity measurements, whereas in those containing Tween 20 destabilization occurred after the second day of storage (Figure 4C and 4D, respectively). Indeed, according to Bastida-Rodríguez (2013) lecithin and PGPR have complementary rheological properties, which allows an optimal control in the stability of the prepared systems.

3.2.3. Impact of sodium alginate and NaCl salt incorporation on the stabilization of $W_1/O/W_2$

The effect of NaCl incorporation on the particle size and particle distribution of $W_1/O/W_2$ emulsions is presented in Figure 4E. All of the emulsions showed bimodal distributions regardless the concentration of salt. Moreover, $W_1/O/W_2$ emulsions particle size increased from 6.3 to 7.9 μm when the concentration of NaCl in the W_2 phase incremented from 0.01 to 0.25M. However, significant differences between particle sizes of double emulsions containing 0.05 or 0.1M of NaCl were not observed. In order to ensure the stability of the second interface, a balance between Laplace and osmotic pressures is required, which means between W_1 droplets in oil and between W_1 droplets and the outer aqueous phase (W_2) (Kanouni et al., 2002). Therefore, it is recommended that the concentration of salt in both aqueous phases (W_1 and W_2) was the same. Actually, an excess or lack of salt in one of them may cause droplets migration to or from the other, respectively causing subsequent breaking of $W_1/O/W_2$ emulsions structure (Rosano & Hidrot, 1998). Likewise, sodium alginate contains functional groups such as carboxylates, which can easily dissociate in the aqueous phase and as a result, provide negative charge to the emulsions (Pereira et al., 2013). Therefore, again an excess of a lack of ions in one of the aqueous phases may disrupt the osmotic balance between them leading to $W_1/O/W_2$ emulsion destabilization. Thus, in order to avoid ions migration, which may in turn lead to water diffusion between the inner and outer aqueous phases, 2% *w/w* of sodium alginate and 0.05M NaCl were also added in the W_2 phase.

3.3.Physicochemical characterization of W_1/O and $W_1/O/W_2$ emulsions containing chlorophyllin and/or lemongrass essential oil

$W_1/O/W_2$ emulsions loaded with CHL and/or LG-EO were prepared in order to assess the effectiveness of these systems as carriers of one or more active compounds through the study of their physicochemical properties (*i.e.* particle size and distribution, turbidity, apparent viscosity and color). Also, the encapsulation efficiency of CHL and antioxidant capacity of $W_1/O/W_2$ emulsions were evaluated.

Physicochemical properties of loaded W_1/O and $W_1/O/W_2$ emulsions

The three types of prepared W_1/O emulsions containing *(i)* 27 ppm CHL, *(ii)* 1% *w/w* LG-EO or *(iii)* both, showed particle sizes around 560 nm (d[4;3]), whereas their subsequent $W_1/O/W_2$ emulsions had d[4;3] about 6-7 ± 0.7 μm (Figure 5A). Moreover, droplet sizes of W_1/O and $W_1/O/W_2$ emulsions loaded with CHL and/or LG-EO were not significantly different. The formation of $W_1/O/W_2$ emulsions containing CHL and/or LG-EO and their particle size were confirmed by confocal

images. As it can be observed in Figure 5B, the majority of oil droplets contained several small water droplets within them, proving the successful formation of $W_1/O/W_2$ emulsions (Lamba et al., 2015a).

Moreover, $W_1/O/W_2$ emulsions containing LG-EO exhibited high stability during storage time (Figure 5C), where initiation of creaming was registered (small up peaks in zone III) after 15 or 21 days of refrigerated storage (without or with CHL, respectively). However, particle sizes of $W_1/O/W_2$ emulsions without LG-EO changed over time as indicated by the displacement of horizontal lines in zone II (Figure 5C).

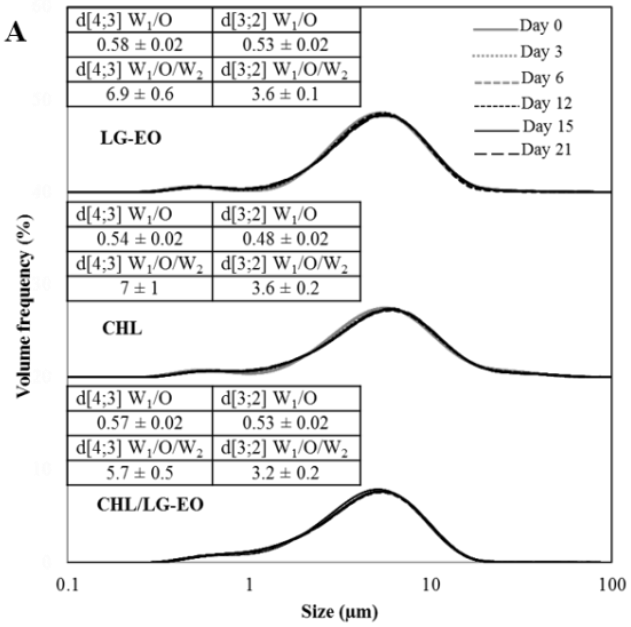

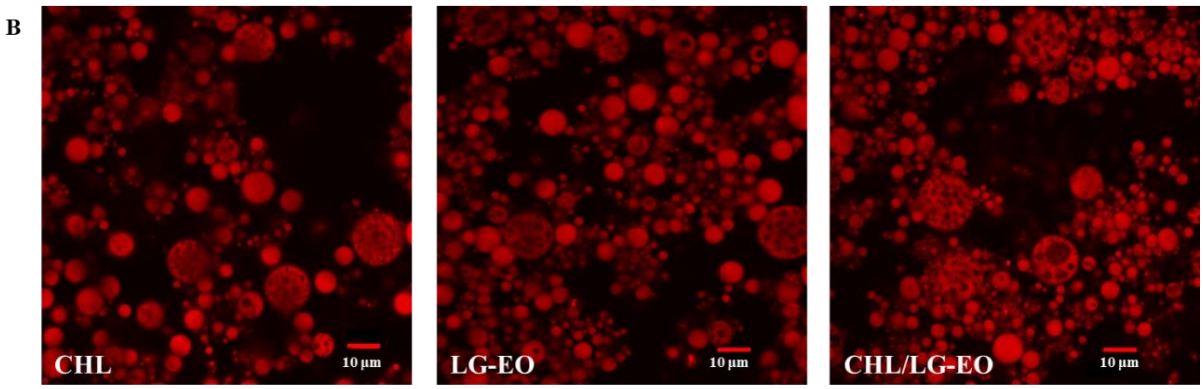

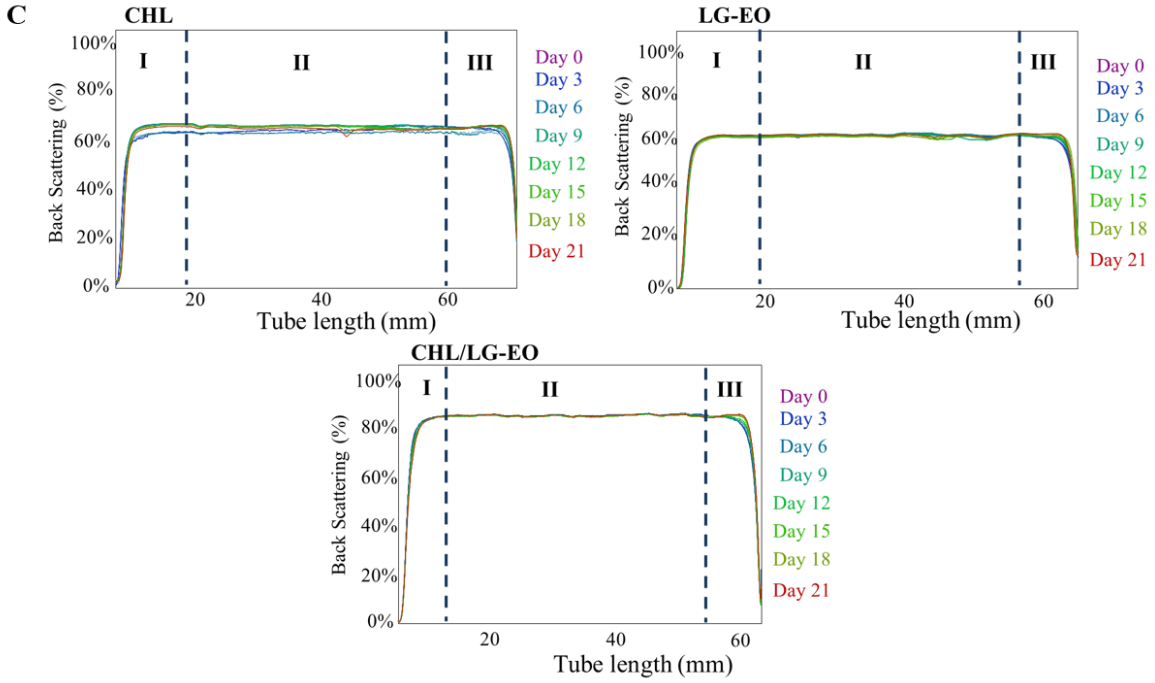

Figure 5. Mean droplet diameters (d[3;2] and d[4;3]) of water-in-oil emulsions (W_1/O) and double emulsions ($W_1/O/W_2$) and particle size distributions (A), confocal images (B) and tubidity measurements during 21 days of refrigerated storage (C) of $W_1/O/W_2$ emulsions containing *chlorophyllin* (CHL) and/or lemongrass essential oil (LG-EO).

Our previous research showed a synergistic effect between LG-EO and the biopolymer (M. Artiga-Artigas et al., 2018). Therefore, the presence of LG-EO in the oil phase of double emulsions might improve $W_1/O/W_2$ emulsions emulsification in presence of sodium alginate thus enhancing their stability. These results are in agreement with the EE, % values since double emulsions containing CHL and LG-EO exhibited higher EE than those without EO (91 ± $6{\cdot}10^{-3}$ and 84 ± $1{\cdot}10^{-2}$, respectively). This suggests that concentrations of 1% *w/w* LG-EO were able to slowdown inner water droplets diffusion. Therefore, a small quantity of LG-EO (1% *w/w*) in the oil phase of $W_1/O/W_2$ emulsions might contribute positively to extend their stability over time by improving emulsification.

Regarding the color of W_1/O and $W_1/O/W_2$ emulsions, it varied significantly depending on the encapsulated bioactive as it can be observed in Tables 1 and 2, respectively. In emulsions containing CHL, *a** values were negative and *b** values positive, which respectively determine green and yellow characteristics. After $W_1/O/W_2$ emulsion formation *a** parameter decreased (became less negative), whereas *b** increased (Tables 1-2). This can be explained because CHL in the $W_1/O/W_2$ emulsion is doubly encapsulated, then if there is no migration of the pigment to the W_2, green color should be less intense. Additionally, this double encapsulation consists of dispersing the primary emulsion containing the CHL into a second water phase (W_2) in a ratio 1/4.

Therefore, the final concentration of CHL in the $W_1/O/W_2$ emulsion is lower than in the W_1/O emulsion. High values of *b** parameter were also expected because of the intense yellow color of corn oil (Ekthamasut & Akesowan, 2010). In addition, WI of $W_1/O/W_2$ emulsion was higher than of the

primary emulsion (Tables 2 and 1, respectively). After homogenization corn oil as many vegetable oils may increase emulsions opacity, which translates as the increase of their WI (Artiga-Artigas et al., 2017). It is described that the light scattering of oil droplets depends on emulsions droplet size (McClements, 2002). Therefore, large particles of $W_1/O/W_2$ emulsion scatter the light more intensely than smaller ones (W_1/O emulsion), which may cause an increase in the lightness, opacity and whiteness index of emulsions (McClements, 2011; Salvia-Trujillo, Rojas-Graü, Soliva-Fortuny, & Martín-Belloso, 2015).

Table 1. Physicochemical properties of water-in-oil (W_1/O) carrying *chlorophyllin* and/or lemongrass essential oil.

Bioactive compound	Viscosity (mPa·s)	*a**	*b**	Whiteness index (WI)
	W_1/O	W_1/O	W_1/O	W_1/O
Chlorophyllin **(CHL)**	144 ± 1^{a}	-5.82 ± 0.05^{a}	3.24 ± 0.08^{a}	73.38 ± 0.03^{a}
Lemongrass EO **(LG-EO)**	$153 \pm 5\cdot10^{-3\ b}$	-0.87 ± 0.03^{b}	4.50 ± 0.04^{b}	79.63 ± 0.03^{b}
CHL/LG-EO	$141 \pm 3\cdot10^{-4\ a}$	$-4 \pm 5\cdot10^{-3\ c}$	$4 \pm 8\cdot10^{-3\ c}$	76.33 ± 0.09^{c}

[a,b,c] Means values in the same column with different letters are significantly different at $p < 0.05$.

Likewise, in those emulsions containing LG-EO, *b** parameter was predominant since both oils (LG-EO and corn oil) are yellow-colored. Moreover, as observed in Tables 1 and 2, this parameter abruptly increased after the formation of $W_1/O/W_2$ emulsion. This increase might be directly related to a decrease in WI according to equation 1. The WI of W_1/O emulsions containing LG-EO was higher than that of those prepared with just corn oil. This parameter depends fundamentally on the RI of continuous and dispersed phases thus since the RI of LG-EO is 1.48 while corn oil's RI is 1.47, LG-EO contributed to increase emulsions opacity (McClements, 2002). However, the second HSH and following magnetic stirring did have a positive effect in reducing WI. Similarly to our results, Guerra-Rosas, Morales-Castro, Ochoa-Martínez, Salvia-Trujillo, & Martín-Belloso (2016) and Salvia-Trujillo et al. (2013a) also reported a decrease of WI in nanoemulsions containing LG-EO and alginate in the aqueous phase after HSH procedures.

Table 2. Physicochemical properties of double emulsions ($W_1/O/W_2$) carrying *chlorophyllin* and/or lemongrass essential oil.

Bioactive compound	Viscosity (mPa·s) $W_1/O/W_2$	*a** $W_1/O/W_2$	*b** $W_1/O/W_2$	Whiteness index (WI) $W_1/O/W_2$
Chlorophyllin **(CHL)**	253 ± 23[ab]	-4.72 ± 0.01[a]	6.34 ±0.04[a]	74.89 ± 0.05[a]
Lemongrass EO **(LG-EO)**	279 ± 2[a]	-2.32 ± 0.07[b]	13.48 ± 0.07[b]	73.65 ± 0.04[b]
CHL/LG-EO	266 ± 26[b]	-4.60 ± 0.06[c]	13.7 ± 0.2[b]	72.3 ± 0.1[c]

[a,b,c] Means values in the same column with different letters are significantly different at $p < 0.05$.

Antixidant capacity of loaded $W_1/O/W_2$ emulsions

Antioxidant capacity (AC) of $W_1/O/W_2$ emulsions and the two prepared controls expressed as mg of Trolox equivalents (TE) per g of emulsion is shown in Table 3. Regarding the solutions of pure bioactive compounds in MeOH, both assays showed that AC of LG-EO was higher than the AC of CHL. Based on the results obtained by DPPH assay, all $W_1/O/W_2$ emulsions presented high AC and similar among them and to both control solutions (≈ 8,000,000 mgTE/g). However, when FRAP assay was performed, AC of $W_1/O/W_2$ emulsions containing LG-EO was significantly higher than the other two types of double emulsions (Table 3) being those containing both bioactive compounds which exhibited the lowest AC (1,696.4 ± 643.9 mgTE/g). It could be due to FRAP assay is based on the reducing power of double emulsions and more specifically, of bioactive compounds within them.

Table 3. Antioxidant capacity of two controls of chlorophyllin and lemongrass in methanol and of double emulsions ($W_1/O/W_2$) containing *chlorophyllin* and/or lemongrass essential oil.

	DPPH mg TE/g	FRAP mg TE/g
$W_1/O/W_2$ with *chlorophyllin* (CHL**)**	7,974,625.2 ± 26,333.2[a]	7,446.4 ± 530.3[a]
$W_1/O/W_2$ with Lemongrass EO (LG-EO)	7,867,557.2 ± 31,413.4[b]	56,142.9 ± 2323.4[b]
$W_1/O/W_2$ with CHL/LG-EO	7,963,989.3 ± 17,508.9[a]	1,696.4 ± 643.9[c]
CHL 27 ppm in Methanol (MeOH)	8,203,297.0 ± 59,093.9[c]	22,339.3 ± 277.8[d]
LG-EO (1% *w/w*) in MeOH	8,250,449.5 ± 11,715.6[c]	88,821.4286 ± $1 \cdot 10^{-7}$ [e]

[a,b,c,d,e] Means values in the same column with different letters are significantly different at $p < 0.05$.

Thus, this assay consists of detecting the reduction of ferric ion (Fe^{3+}) into ferrous iron (Fe^{2+}) using ferrozine as dye (Cheung et al., 2016). In this regard, if some species are reduced, others have to be oxidized being the LG-EO the most exposed bioactive compound in double emulsions. After catalytic oxidation, the essential oils show stronger antioxidant effects than before oxidation, as measured by both methods, DPPH and FRAP (Jukić & Miloš, 2005). Thus, the lower AC of LG-EO in presence of CHL suggests that the latter is preventing essential oil oxidation.

4. Conclusions

Summarizing, neither US nor MF techniques combined with HSH were able to reduce W_1/O emulsion particle size as much as the HSH alone since they cause an over-processing of the emulsions. This HSH (11,000 rpm, 5 min) followed by HSH (5,600 rpm, 2 min) and magnetic stirring (750 rpm, 24h) allowed stable $W_1/O/W_2$ emulsion preparation. PGPR acted more efficiently than Span 80 as emulsifier of the first interface probably because of the higher hydrophobicity of the polymeric surfactant. Sodium alginate and NaCl (0.05M) incorporated in the W_1 of W_1/O emulsions were absolutely necessary to reduce particle size and better stabilize W_1/O emulsions. In this regard, the outer aqueous phase had to contain the same concentrations of sodium alginate and salt as W_1 to prevent ions migration from one phase to the other causing the disruption of $W_1/O/W_2$ emulsion.

Furthermore, template $W_1/O/W_2$ emulsions allowed the successful incorporation of CHL and LG-EO without suffering destabilization. Both active compounds loaded in the prepared dual systems not only maintained their AC but showed a synergic behavior. Indeed, LG-EO incorporation increased the EE, % of CHL, suggesting that the oil was able to slowdown inner water droplets diffusion and in turn, CHL delayed essential oil oxidation according to AC values, which is of great importance from the technological and nutritional point of view. Moreover, LG-EO and sodium alginate contributed positively to reduce particle size and extending the stability of $W_1/O/W_2$ emulsions over time.

Therefore, this study presents an effective two-step optimized procedure to form stable $W_1/O/W_2$ emulsions and evidences their potential capacity as delivery system templates to encapsulate and carry two or more active compounds with different polarity and diverse functionality.

5. Acknowledgments

This study was funded by the Ministry of Economy, Industry and Competitiveness (MINECO/FEDER, UE) throughout project **AGL2015-65975-R**. Authors María Artiga-Artigas and Anna Molet-Rodríguez thank the University of Lleida for their pre-doctoral fellowship. Author Laura Salvia-Trujillo thanks the "Secretaria d'Universitats i Recerca del Departament d'Empresa i Coneixement de la Generalitat de Catalunya" for the Beatriu de Pinós post-doctoral grant **BdP2016 00336**.

6. References

Altuntas, O. Y., Sumnu, G., & Sahin, S. (2017). Preparation and characterization of W/O/W type double emulsion containing PGPR–lecithin mixture as lipophilic surfactant. *Journal of Dispersion Science and Technology*, *38*(4), 486–493.

Aronson, Michael P.; Petko, M. F. (1993). Highly Concentrated Water-inOil Emulsions: Influence of

Electrolyte on Their Properties and Stability. *Journal of Colloid and Interface Science, 159*, 134–149.

Artiga-Artigas, M., Acevedo-Fani, A., & Martín-Belloso, O. (2017). Effect of sodium alginate incorporation procedure on the physicochemical properties of nanoemulsions. *Food Hydrocolloids*, *70*, 191–200.

Artiga-Artigas, M., Guerra-Rosas, M. I., Morales-Castro, J., Salvia-Trujillo, L., & Martín-Belloso, O. (2018). Influence of essential oils and pectin on nanoemulsion formulation: A ternary phase experimental approach. *Food Hydrocolloids*, *81*, 209–219.

Bastida-Rodríguez, J. (2013). The Food Additive Polyglycerol Polyricinoleate (E-476): Structure, Applications, and Production Methods. *ISRN Chemical Engineering*, *2013*, 1–21.

Benichou, A., Aserin, A., & Garti, N. (2004). Double emulsions stabilized with hybrids of natural polymers for entrapment and slow release of active matters. *Advances in Colloid and Interface Science*, *108–109*, 29–41.

Benzie, I. F. F., & Strain, J. J. (1996). The Ferric Reducing Ability of Plasma (FRAP) as a Measure of "Antioxidant Power": The FRAP Assay. *Analytical Biochemistry*, *239*(1), 70–76.

Bonnet, M., Cansell, M., Placin, F., Anton, M., & Leal-Calderon, F. (2010). Impact of sodium caseinate concentration and location on magnesium release from multiple W/O/W emulsions. *Langmuir*, *26*(12), 9250–9260.

Brand-Williams, W.; Cuvelier, M. E.; Berset, C. (1995). Use of a free radical method to evaluate antioxidant activity. *Lebensmittel Wissenschaft Und Technologie*, *30*, 25–30.

Cheel, J., Theoduloz, C., Rodríguez, J., & Schmeda-Hirschmann, G. (2005). Free radical scavengers and antioxidants from lemongrass (Cymbopogon citratus (DC.) Stapf.). *Journal of Agricultural and Food Chemistry*, *53*(7), 2511–2517.

Cheung, T., Nigam, P., & Owusu-Apenten, R. (2016). Antioxidant Activity of Curcumin and Neem (Azadirachta indica) Powders: Combination Studies with ALA Using MCF-7 Breast Cancer Cells. *Journal of Applied Life Sciences International*, *4*(3), 1–12.

Dickinson, E. (2011a). Double Emulsions Stabilized by Food Biopolymers. *Food Biophysics*, *6*(1), 1–11.

Dickinson, E. (2011b). Double Emulsions Stabilized by Food Biopolymers. *Food Biophysics*, *6*(1), 1–11.

Dickinson, E. (2011). Mixed biopolymers at interfaces: Competitive adsorption and multilayer structures. *Food Hydrocolloids*, *25*(8), 1966–1983.

Ekthamasut, K., & Akesowan, A. (2010). Effect of Vegetable Oils on Physical Characteristics of Edible Konjac Films. *Water*, (4).

Fathi, M., Mozafari, M. R., & Mohebbi, M. (2012). Nanoencapsulation of food ingredients using lipid based delivery systems. *Trends in Food Science & Technology*, *23*(1), 13–27.

Garti, N. (1997). Progress in stabilization and transport phenomena of double emulsions in food applications. *LWT - Food Science and Technology*, *30*(3), 222–235.

Garti, N., & Bisperink, C. (1998). Double emulsions: Progress and applications. *Current Opinion in Colloid & Interface Science*, *3*(6), 657–667.

Giroux, H. J., Constantineau, S., Fustier, P., Champagne, C. P., St-Gelais, D., Lacroix, M., & Britten, M. (2013). Cheese fortification using water-in-oil-in-water double emulsions as carrier for water soluble nutrients. *International Dairy Journal*, *29*(2), 107–114.

Guerra-Rosas, M. I., Morales-Castro, J., Cubero-Márquez, M. A., Salvia-Trujillo, L., & Martín-Belloso, O. (2017). Antimicrobial activity of nanoemulsions containing essential oils and high methoxyl pectin during long-term storage. *Food Control*, *77*.

Guerra-Rosas, M. I., Morales-Castro, J., Ochoa-Martínez, L. A., Salvia-Trujillo, L., & Martín-Belloso, O. (2016). Long-term stability of food-grade nanoemulsions from high methoxyl pectin containing essential oils. *Food Hydrocolloids*, *52*, 438–446.

Jafari, S. M., He, Y., & Bhandari, B. (2007). Production of sub-micron emulsions by ultrasound and microfluidization techniques. *Journal of Food Engineering*, *82*(4), 478–488.

Jukić, M., & Miloš, M. (2005). Catalytic Oxidation and Antioxidant Properties of Thyme Essential Oils (Thymus vulgarae L.). *Croatica Chemica Acta*, *78*(1), 105–110.

Kanouni, M., Rosano, H. L., & Naouli, N. (2002). Preparation of a stable double emulsion (W1/O/W2): Role of the interfacial films on the stability of the system. *Advances in Colloid and Interface Science*, *99*(3), 229–254.

Kolb, G., Viardot, K., Wagner, G., & Ulrich, J. (2001). Evaluation of a new high-pressure dispersion unit (HPN) for emulsification. *Chemical Engineering and Technology*, *24*(3), 293–296.

López-Carballo, G., Hernández-Muñoz, P., Gavara, R., & Ocio, M. J. (2008). Photoactivated chlorophyllin-based gelatin films and coatings to prevent microbial contamination of food products. *International Journal of Food Microbiology*, *126*(1–2), 65–70.

Lamba, H., Sathish, K., & Sabikhi, L. (2015). Double Emulsions: Emerging Delivery System for Plant Bioactives. *Food and Bioprocess Technology*, *8*(4), 709–728.

Márquez, A. L., Palazolo, G. G., & Wagner, J. R. (2007). Water in oil (w/o) and double (w/o/w) emulsions prepared with spans: Microstructure, stability, and rheology. *Colloid and Polymer Science*, *285*(10), 1119–1128.

McClements, D. J. (2002). Theoretical prediction of emulsion color. *Advances in Colloid and Interface Science*, *97*(1–3), 63–89.

McClements, D. J. (2011). Edible nanoemulsions: fabrication, properties, and functional performance. *Soft Matter*, *7*(6), 2297–2316.

Meleson, K., Graves, S., & Mason, T. G. (2004). Formation of concentrated nanoemulsions by extreme shear. *Soft Materials*, *2*(2–3), 109–123.

Mezzenga, R., Folmer, B. M., & Hughes, E. (2004). Design of double emulsions by osmotic pressure tailoring. *Langmuir*, *20*(9), 3574–3582.

Muschiolik, G. (2007). Multiple emulsions for food use. *Current Opinion in Colloid and Interface Science*, *12*(4–5), 213–220.

Muschiolik, G., & Dickinson, E. (2017). Double Emulsions Relevant to Food Systems: Preparation, Stability, and Applications. *Comprehensive Reviews in Food Science and Food Safety*, *16*(3), 532–555.

Muschiolik, G., & Dickinson, E. (2017). Double Emulsions Relevant to Food Systems: Preparation, Stability, and Applications. *Comprehensive Reviews in Food Science and Food Safety*, *16*(3), 532–555.

Pereira, R., Carvalho, A., Vaz, D. C., Gil, M. H., Mendes, A., & Bártolo, P. (2013). Development of novel alginate based hydrogel films for wound healing applications. *International Journal of Biological Macromolecules*, *52*, 221–230.

Rosano, H. L., & Hidrot, J. P. (1998). Stability of W /O/W multiple emulsions 1 2 In uence of ripening and interfacial interactions, *138*, 109–121.

Salvia-Trujillo, L., Rojas-Graü, A., Soliva-Fortuny, R., & Martín-Belloso, O. (2013a). Physicochemical Characterization of Lemongrass Essential Oil-Alginate Nanoemulsions: Effect of Ultrasound Processing Parameters. *Food and Bioprocess Technology*, *6*(9).

Salvia-Trujillo, L., Rojas-Graü, A., Soliva-Fortuny, R., & Martín-Belloso, O. (2015). Physicochemical characterization and antimicrobial activity of food-grade emulsions and nanoemulsions incorporating essential oils. *Food Hydrocolloids*, *43*, 547–556.

Salvia-Trujillo, L., Rojas-Graü, M. A., Soliva-Fortuny, R., & Martín-Belloso, O. (2013b). Effect of processing parameters on physicochemical characteristics of microfluidized lemongrass essential oil-alginate nanoemulsions. *Food Hydrocolloids*, *30*(1), 401–407.

Scherze, I., Knoth, A., & Muschiolik, G. (2006). Effect of emulsification method on the properties of lecithin- and PGPR-stabilized water-in-oil-emulsions. *Journal of Dispersion Science and Technology*, *27*(4), 427–434.

Schultz, S., Wagner, G., Urban, K., & Ulrich, J. (2004). High-pressure homogenization as a process for emulsion formation. *Chemical Engineering and Technology*, *27*(4), 361–368.

Su, J., Flanagan, J., Hemar, Y., & Singh, H. (2006). Synergistic effects of polyglycerol ester of polyricinoleic acid and sodium caseinate on the stabilisation of water-oil-water emulsions. *Food Hydrocolloids*, *20*(2–3 SPEC. ISS.), 261–268.

Surh, J., Vladisavljević, G. T., Mun, S., & McClements, D. J. (2007). Preparation and characterization of water/oil and water/oil/water emulsions containing biopolymer-gelled water droplets. *Journal of Agricultural and Food Chemistry*, *55*(1), 175–184.

Tabibiazar, M., & Hamishehkar, H. (2015). Formulation of a food grade water-in-oil nanoemulsion: Factors affecting on stability. *Pharmaceutical Sciences*, *21*(4), 220–224.

Thaipong, K., Boonprakob, U., Crosby, K., Cisneros-Zevallos, L., & Hawkins Byrne, D. (2006). Comparison of ABTS, DPPH, FRAP, and ORAC assays for estimating antioxidant activity from guava fruit extracts. *Journal of Food Composition and Analysis*, *19*(6–7), 669–675.

Tumolo, T., & Lanfer-Marquez, U. M. (2012). Copper chlorophyllin: A food colorant with bioactive properties? *Food Research International*, *46*(2), 451–459.

Velderrain-Rodríguez, G. R., Ovando-Martínez, M., Villegas-Ochoa, M., Ayala-Zavala, J. F., Wall-

Medrano, A., Álvarez-Parrilla, E., … González-Aguilar, G. A. (2015). Antioxidant Capacity and Bioaccessibility of Synergic Mango (cv. Ataulfo) Peel Phenolic Compounds in Edible Coatings Applied to Fresh-Cut Papaya. *Food and Nutrition Sciences*, *6*(6), 365–373.

Wang, Y., Zhang, T., & Hu, G. (2006). Structural evolution of polymer-stabilized double emulsions. *Langmuir*, *22*(1), 67–73.

Weiss, J., & Muschiolik, G. (2007). Factors affecting the droplet size of water-in-oil emulsions (W/O) and the oil globule size in Water-in-oil-in-water emulsions (W/O/W). *Journal of Dispersion Science and Technology*, *28*(5), 703–716.

Wooster, T. J., Golding, M., & Sanguansri, P. (2008). Ripening Stability. *Langmuir : The ACS Journal of Surfaces and Colloids*, *24*(10), 12758–12765.

Xu, J.-H., Ge, X.-H., Chen, R., & Luo, G.-S. (2014). Microfluidic preparation and structure evolution of double emulsions with two-phase cores. *RSC Advances*, *4*(4), 1900.

Yan, J., & Pal, R. (2001). Osmotic swelling behavior of globules of W/O/W emulsion liquid membranes. *Journal of Membrane Science*, *190*(1), 79–91.

Yang, J. S., Jiang, B., He, W., & Xia, Y. M. (2012). Hydrophobically modified alginate for emulsion of oil in water. *Carbohydrate Polymers*, *87*(2), 1503–1506.

Zirak, M. B., & Pezeshki, A. (2015). <. *International Journal of Current Microbiology and Applied Sciences*, *4*(9), 924–932.

SECTION III. Application of emulsion-based nanoestructures to foods

CHAPTER VII: *Improving the shelf life of low-fat cut cheese using nanoemulsion-based edible coatings containing essential oil and mandarin fiber*

Artiga-Artigas, M.; Acevedo-Fani, A.; Martín-Belloso, O.

Food Control (2017); 76: 1-12

Abstract

Nanoemulsion-based edible coatings containing oregano essential oil (OR-EO) as antimicrobial were applied onto low-fat cut cheese to extend its shelf life. Nanoemulsions formulation was 2.0% *w/w* sodium alginate, 0.5% *w/w* mandarin fiber, 2.5% *w/w* Tween 80 and 1.5%, 2.0% or 2.5% *w/w* of OR-EO. Particle size, ζ-potential, apparent viscosity and whiteness index of nanoemulsions were assessed. Water vapor resistance of coatings was evaluated as well as their antimicrobial efficiency against inoculated *Staphylococcus aureus* and native microbiota growth during refrigerated storage. Headspace gases were measured as an indicator of bacterial activity and sensory alterations such as color and texture of cheese pieces were studied. Coatings with at least 2.0% *w/w* OR-EO decreased *Staphylococcus aureus* population from 6.0 to 4.6 log CFU/g after 15 days. Coated-cheese pieces containing 2.5% *w/w* OR-EO inhibited psychrophilic bacteria or molds and yeasts growth during 6 or 24 days of storage, respectively. Consequently, the atmosphere into the sealed tracks was stabilized and the outward appearance of cheese pieces was preserved. Thus, the present work evidences the feasibility of using mandarin fiber with high nutritional properties and sodium alginate acting as texturizing agents, to form OR-EO-loaded coatings onto low-fat cut cheese in order to extend its shelf life.

Keywords: Nanoemulsions; mandarin fiber; cheese; edible coatings; *Staphylococcus aureus*; molds; oregano essential oil.

1. Introduction

Low-fat cheese is characterized by containing low quantities of calories and salt. The shelf life of this kind of cheeses is limited due to the uncontrolled and extensive fungal and bacterial development on its surface reducing their quality, especially if they are cut. The need of bacterial cultures to obtain the suitable form, taste and texture of cheese introduces a potential risk of infection from cheese-borne species like *Staphylococcus aureus*, *Listeria monocytogenes*, *Salmonella enterica* and *Escherichia coli* (Kuorwel, Cran, Sonneveld, Miltz, & Bigger, 2011). In this regard, consumers' demand for safe and high-quality foods has motivated the scientific community and food industry in finding new strategies that allow increasing the shelf life of highly perishable foods, but with slight effect on the organoleptic properties of the product.

Over the past few years, it has been an increasing interest in using natural antimicrobials for food preservation, due to the general consumer rejection of synthetic additives such as sulfites, benzoic acid or its derived salts, commonly used to control the microbial growth in foods. Essential oils (EOs) are secondary metabolites produced by aromatic plants that have shown potent antimicrobial effect against several pathogenic and spoilage microorganisms. EOs contain a complex mixture of different constituents (non-volatile and volatile), whose composition is highly variable (Adorjan & Buchbauer, 2010; Bonilla, Atarés, Vargas, & Chiralt, 2012; Salvia-Trujillo et al., 2014). In particular, oregano essential oil (OR-EO) has been previously utilized to control the microbial growth in foods (Raybaudi-Massilia, Mosqueda-Melgar, & Martín-Belloso, 2006; Tajkarimi, Ibrahim, & Cliver, 2010). Its active compound carvacrol presents strong antifungal capacity and high inhibitory effect against *Listeria monocytogenes*, *Salmonella*, *Escherichia coli* and *Staphylococcus aureus* (Burt, 2004; Rojas-Graü et al., 2009; Tajkarimi et al., 2010). Nonetheless, despite these remarkable properties, EOs have poor water solubility, intense aroma, high volatility and may be toxic at high concentrations, which mainly jeopardize their application as natural preservatives (Svoboda et al., 2006).

The great challenge of incorporating EOs into food matrices could be overcome if they are incorporated into nanoemulsions. These oil-in-water systems have been described as colloidal dispersions with an extremely small droplet size (< 200 nm) (Li, Zheng, Xiao, & McClements, 2012), which can contain lipophilic ingredients in the oil phase (McClements, 2011; Solans et al., 2005). Nanoemulsions can be directly added to food matrices in liquid state or instead, they can be applied as edible coatings onto food surfaces (solid state) if a biopolymer is incorporated in the aqueous phase of nanoemulsions. Moreover, the combination of different biopolymers (for instance, alginate-pectin or alginate-chitosan), can be used to enhance the physicochemical properties of emulsions (George & Abraham, 2006). In this regard, this combination could be even more interesting if one of these biopolymers is also able to provide added-value to the food product, as in the case of dietary fibers (González-Molina, Domínguez-Perles, Moreno, & García-Viguera, 2010). Specifically, mandarin fiber has been used as functional food additive due to its prebiotic properties (Moreira et al., 2015). It has been reported that the intake of mandarin fiber significantly reduce the risk of developing coronary heart disease, stroke, hypertension, diabetes, obesity, and certain gastrointestinal diseases (Grigelmo-Miguel & Martín-Belloso, 1999; Wang, Sun, Zhou, & Chen, 2012).

Furthermore, mandarin fiber, which contains a high percentage of soluble fiber (mainly pectin), has been shown to have high water holding capacity and apparent viscosity in combination with sodium alginate, which may lead to the formation of nanoemulsion-based edible coatings

(Lundberg, Pan, White, Chau, & Hotchkiss, 2014). Edible coatings are defined as thin layers of eatable material, which are applied in liquid form on the food surface, usually by immersing the product in a solution formed by the structural matrix (carbohydrate, protein, lipid or multicomponent mixture) (Rojas-Graü, et al., 2009). Some of its functions are to protect the product from mechanical damage and chemical reactions acting as moisture barriers (Miller & Krochta, 1997). Otherwise, if the coatings contain antimicrobial agents, they are able to protect high perishable food products, such as low-fat cheese, from the microbial growth extending their shelf life (Raybaudi-Massilia, Mosqueda-Melgar, & Martín-Belloso, 2008; Rojas-Grau et al., 2007).

In this regard, nanoemulsions containing EOs could be used to form antimicrobial coatings on the cheese surface, as a way to limit the negative changes that occur during the time. Thus, the aim of the current work was to assess the antimicrobial effectiveness of nanoemulsions-based edible coatings containing OR-EO and enriched with mandarin fiber against inoculated *Staphylococcus aureus*, and their capability to improve the shelf life of a highly perishable low-fat cut cheese.

2. Materials and methods

2.1.Materials

Low-fat cheese (CADICOOP light) was kindly donated by CADÍ® (Lleida, Spain). Oregano essential oil was supplied by Essential arôms (Lleida, Spain). Tween 80 was purchased from Panreac (Barcelona, Spain). Sodium alginate (MANUCOL®DH) was obtained from FMC Biopolymer Ltd (Scotland, U.K.). Information provided by the manufacturer indicates that viscosity and pH of a solution 1% is 40-90 mPa·s and 5.0-7.5, respectively. Mandarin fiber containing 231.30 *g/kg* of soluble fiber (mainly pectin), 202.38 *g/kg* of insoluble fiber, 81.25 g/kg of proteins, 7,74 *g/kg* of lipids, 29.61 g/kg of ashes and 423.76 *g/kg* of carbohydrates was kindly donated by Indulleida (Lleida, Spain). Ultrapure water obtained from a Milli-Q filtration system was used to the preparation of all solutions.

2.2.Methods

2.2.1. Nanoemulsions preparation

Formulation of oil-in-water nanoemulsions contained OR-EO (1.5–2.5% *w/w*), Tween 80 (2.5% *w/w*), sodium alginate (2.0% *w/w*) and mandarin fiber (0.5% *w/w*).

The aqueous phase was prepared by solving sodium alginate in ultrapure water at 70ºC for 3 h. After reaching room temperature, mandarin fiber was added to alginate solution and mixed using a laboratory high-shear homogenizer (T25 digital Ultra-Turrax, IKA, Staufen, Germany) at 9,600 rpm for 3 min. Ultimately, the aqueous phase was filtered in order to remove the fiber in excess. An accurate amount of the lipid phase consisted of the mixture of OR-EO and Tween 80 at room temperature was added to the aqueous phase, and blended with the high-shear homogenizer at 11,000 rpm for 2 min, leading to coarse emulsions. Lastly, nanoemulsions were formed passing the respective coarse emulsion through a microfluidizer (M110P, Microfluidics, Massachusetts, USA) at 150 MPa for 5 cycles.

2.2.2. Physicochemical characterization of emulsions and nanoemulsions.

2.2.2.1.Droplet size, size distribution and ζ-potential

The particle size distribution and mean droplet diameter (nm) of emulsions and nanoemulsions were measured by a Zetasizer Nano-ZS laser diffractometer (Malvern Instruments Ltd, Worcestershire, UK) working at 633 nm and 25 ºC, equipped with a backscatter detector (173º) (L. Salvia-Trujillo et al., 2015b).

The ζ-potential (mV), was measured by phase-analysis light scattering (PALS) with a Zetasizer Nano-ZS laser diffractometer (Malvern Instruments Ltd, Worcestershire, UK). It determines the electrical charge at the interface of the droplets dispersed in the aqueous phase.

In both types of determinations, samples were prior diluted in ultrapure water using a dilution factor of 1:9 sample-to-solvent.

2.2.2.2.Apparent viscosity and whiteness index

Viscosity measurements (mPa·s) were performed by using a vibro-viscometer (SV-10, A&D Company, Tokyo, Japan) vibrating at 30 Hz, with constant amplitude and working at room temperature. Aliquots of 10 mL of each emulsion and nanoemulsion were used for determinations.

A colorimeter (CR-400, Konica Minolta Sensing Inc., Osaka, Japan) set up for illuminant D65 and 10º observer angle was used to measure the CIE L^*, a^* and b^* parameters of emulsions and nanoemulsions at room temperature. The device was calibrated with a standard white plate (Y =94.0; x = 0.3133; y = 0.3194). The whiteness index (WI) was calculated with eq. (1) (Vargas et al., 2008):

$$WI= 100-((100-L^*)^2+(a^{*2}+b^{*2}))^{0.5} \quad \textbf{eq.(1)}$$

2.2.3. Cheese coating and sampling

Sealed cheese bars were stored at 4ºC before processing. Immediately after opening the cheese bars, identical cylindrical pieces (diameter: 1.5 cm, height: 2.4 cm) were cut in order to make reproducible experiments.

Cheese pieces were immersed into the corresponding nanoemulsion for 1 min, and allowed to dry at room temperature for 5 min. The addition of $CaCl_2$, which acts as cross-linker was not needed since cheese contains calcium itself. On the other hand, the uncoated pieces were immersed into ultrapure water following the procedure explained above. Lastly, 50 grams of either coated or uncoated cut cheese were packed polypropylene (PP) trays (ATS packaging, Barcelona, Spain) of 170 mm length x 25 mm height x 110 mm width, using a tray sealer (Basic V/G, Ilpra systems, Barcelona, Spain). Afterwards a cover film made of polyamide and polyethylene (Tecnopack, Girona, Spain) was used to heat seal the trays. Lastly, sealed trays were stored at 4ºC during 15 days.

Separate trays were prepared with cheese pieces inoculated with *Staphylococcus aureus* to evaluate the antimicrobial effect of the antimicrobial coating and to assess the changes in quality attributes along 24 days of refrigerated storage. Two trays of each set were prepared, and two replicates for each sealed package were performed.

2.2.4. Water Vapor Resistance (WPR) and weight loss

Water vapor resistance (WVR) of cheese pieces was evaluated gravimetrically at 25 ºC using a modified version of ASTM standard method E96-00 (ASTM, 2000). The method and experimental set up following to determine the water loss of coated cheese pieces was described by García et al. (1998). Cheese cylinders were placed in small test cups (internal diameter of 2.7 cm and depth of 1.3 cm) and weighed in an analytical laboratory scale (AT261 Delta Range, Mettler Toledo, Barcelona, Spain). Initial weights of coated cheese pieces were 8.3 ± 0.12, 8.4 ± 0.23 and 8.5 ± 0.20g for coatings with 1.5% OR-EO, 2.0% OR-EO and 2.5% OR-EO, respectively and 7.8 ± 0.14 g for those uncoated. Cheese cylinders were placed in sealed chambers that were equilibrated at 33% RH with a saturated $MgCl_2 \cdot 6H_2O$ solution (Panreac Quimica SA, Barcelona, Spain) at 25 ºC. Cups weights were recorded at 60 min intervals during 6 h. Weight loss was calculated by difference using equation (2) and plotted versus time. Data were analyzed by lineal regression to obtain the slope (d_s/d_t) of the curve in g/s.

Water activity of the coated and uncoated cheese pieces (0.974 ± 0.001 and 0.947 ± 0.001, respectively) was measured twice for each sample with a water activity meter (Acqualab CX-2, Decagon Devices Inc., Pullman, WA).

$$WL = W_i - W_f \quad \textbf{eq. (2)}$$

where WL is the weight loss of cheese pieces (in mg); W_i and W_f, are initial and final weights of cheese pieces (in mg).

Afterwards, WVR of the coatings was calculated using a modified Fick's first law equation as described in equations (3), (4) and (5) (Ben-Yehoshua et al., 1985; Kaya & Kaya, 2000; Park & Chinnan, 1995; Rojas-Graü et al., 2007):

$$\Delta C = (P_i - P_a)/(R_c \cdot T) \quad \textbf{eq.(3)}$$

$$A = \pi \cdot r \cdot (2 \cdot h + r) \quad \textbf{eq.(4)}$$

$$WVR = (A \cdot \Delta C)/(d_s/d_t) \quad \textbf{eq.(5)}$$

where P_i - P_a is the difference in water vapor pressure (Pa) inside and outside of the cheese piece ($P_i = a_w$ of the cheese x P_0 – that is the vapor pressure of liquid water at 25ºC and P_a = partial water pressure in the environment with 33.3% RH at 25ºC, in Pa x P_0); ΔC is the concentration of gas (g/cm^3) inside and outside the cheese piece at time t; A is the exposed area of cylindrical cheese pieces (5.65 cm^2) taking into account that only one of the bases was in contact with the environment; (d_s/d_t) is the rate of gas exchange (slope) in g/s; Rc is the universal gas constant(3.46 L·mmHg/K g) and T is the temperature in degrees Kelvin.

2.2.5. Antimicrobial efficiency of edible coatings

2.2.5.1.Inoculum preparation

A strain of *Staphylococcus aureus* (CECT 240) (University of Valencia, Spain) was provided by the culture collection of the Department of Food Technology, University of Lleida, Spain. The *Staphylococcus aureus* culture was kept in slant tubes with Tryptone Soy Agar (TSA) (Biokar Diagnostics, France) at 5 ºC. The strain was then inoculated in Tryptone Soy Broth (TSB) (Biokar Diagnostics, France) and incubated at 35 ºC, 200 rpm for 6 h, to obtain cells in stationary growth

phase. The inoculum concentration was diluted from 10^8 CFU/mL to 10^6 CFU/mL for cheese inoculation.

2.2.5.2.Antimicrobial activity against inoculated Staphylococcus aureus

Cheese pieces (10 g) were inoculated with 50 µL aliquots of the culture and left dry for 20 min. Cheese pieces were coated with nanoemulsions that contained OR-EO, packed in heat sealed PP trays and stored at 4ºC for 15 days. In order to corroborate that no one of the other components of edible coating had also antimicrobial activity, nanoemulsions containing corn oil instead of OR-EO in the same concentrations were prepared and applied onto cheese pieces.

The content of each tray (10 g) was put into a sterile stomacher bag (Strainer bag stomacher® lab system, Seward, UK) with 90 mL of buffer peptone (Biokar Diagnostics, France). Bags were homogenized for 1 min in a Stomacher blender (BagMixer®, Interscience, France). Serial dilutions with saline peptone (Peptic Digest of meat USP, Biokar, Diagnostics, France) were prepared and spread onto Baird-Parker agar (BP) (Biokar Diagnostics, France). Plates were incubated at 37 ºC for 48 h and colonies were counted. Results were expressed as $\log_{10}$ CFU/g.

2.2.6. Quality assessment of coated cheese pieces

2.2.6.1.Microbial stability

Psychrophilic bacteria and molds and yeasts growth in cheese pieces was examined along 24 days under refrigeration. Cheese samples of 10 grams randomly chosen in aseptic conditions were put into sterile bags with 90 mL of peptone buffer (Biokar Diagnostics, France). Bags were homogenized for 1 min in a Stomacher blender (BagMixer®, Interscience, France). Serial dilutions with saline peptone (Peptic Digest of meat USP, Biokar, Diagnostics, France) were prepared, and 100 µL were spread onto Plate Count Agar (PCA) (Biokar Diagnostics, France) and Cloranfenicol Glucosa Agar (CGA) (Biokar Diagnostics, France) for psychrophilic bacteria and molds and yeast counts, respectively. PCA plates were incubated at 4 ºC for 15 days, whereas CGA plates were maintained at room temperature during 5 days. Afterwards, colonies were counted and the results were expressed as $\log_{10}$ CFU/g.

2.2.6.2.Headspace gas analysis

The composition of the headspace of each tray was analyzed with a gas chromatograph (Varian 490-CG) equipped with a thermal conductivity detector (Micro-GC CP 2002 gas analyzer, Chromatography Systems, Middelburg, The Netherlands). A 10 mL sample was automatically withdrawn from the tray headspace atmosphere and injected in the gas chromatograph. The oxygen (O_2) content expressed in percentage was analyzed with a 10 m packed column (CP-Molsieve 5Å, Varian, Middelburg, The Netherlands) at 60 ºC and 100 kPa. For quantification of carbon dioxide (CO_2) expressed in percentage, and ethanol (C_2H_5OH) concentration reported in ppm, a column PoraPLOT Q (Varian, Middelburg, The Netherlands) (10 m x 0.32mm, df = 10 mm) held at 70 ºC and 200 kPa was used.

2.2.6.3.Color (WI)

The color of coated and uncoated cheese pieces was measured with a colorimeter (CR-400, Konica Minolta Sensing Inc., Osaka, Japan) set up for illuminant D65 and 10º observer angle and calibrated with a standard white plate. Measurements were taken at room temperature. CIE *L**, *a** and *b** values were determined and the Whiteness Index (WI) was calculated through equation (1).

2.2.6.4.Texture profile analysis (TPA)

TPA of cheese pieces was carried out using a texture analyzer (TA-TX2, Stable Micro Systems, Goldaming, UK) equipped with a 5 kg load cell and the 36R probe, operating with two compression-decompression cycles and 2 $mm \cdot s^{-1}$ of crosshead speed (Diamantino et al., 2014). The hardness, cohesiveness, gumminess, elasticity, adhesiveness and chewiness of the cylindrical cheese pieces were calculated according to Szczesniak (2002). Eight replicates of each tray were performed at each sampling time.

2.2.7. Statistics

All the experiments were assayed in duplicate, and at least three replicate analyses were carried out for each parameter. SigmaPlot 11.0 Systat Software was used to perform the analysis of variance. Tukey test was chosen to determine significant differences among treatments, at a 5% significance level.

Correlation analyses were performed with statistical analysis software (JMP Pro 12, Statistical Discovery™, North Carolina, USA).

3. Results and discussion

3.1.Particle size and ζ-potential of nanoemulsions

Microfluidization process caused a droplet disruption leading to nanoemulsions with smaller droplet sizes than their respective coarse emulsions (particle sizes over 700 nm) (Table 1). In fact, the smallest size (169 ± 23 nm) was obtained in nanoemulsions with 2.0% *w/w* of OR-EO, whereas those with OR-EO percentages of 1.5% or 2.5% *w/w* led to particle sizes of 214 ±14 nm or 337 ±79 nm, respectively. The obtained results are in accordance with previous research in which the average droplet diameter of nanoemulsions containing OR-EO and polysaccharides such as pectin or alginate, were also in the nanorage scale (Guerra-Rosas et al., 2016; Salvia-Trujillo et al., 2014).

Differences in particle size may be related to the observed polydisperse particle distributions in all nanoemulsions (Figure 1). There was a minor peak in the macro range that indicates the presence of particles with greater size, which may cause an increase in the mean particle size values. These minor peaks could be the outcome of an excess or a lack of OR-EO. When the concentration of OR-EO is too low, two possible phenomena can occur: the excess of surfactant molecules adsorbed at the interface of droplets may repel biopolymer chains and/or these biopolymer chains may bind free surfactant molecules rather than those that are in the surface of oil droplets (Goddard, 2002; Neumann et al., 2003). On the other hand, an excess of OR-EO droplets might cause the coalescence phenomenon in which two or more small oil droplets come in contact forming a single bigger droplet (Victoria Klang, Matsko, Valenta, & Hofer, 2012).

Regarding the electrical charge of oil droplets, all nanoemulsions showed ζ-potential values lower than -30 mV regardless the concentration of OR-EO used (-35 ± 5 mV, -47 ± 3 mV and -42 ± 3 mV for 1.5%, 2.0% and 2.5% *w/w* of OR-EO, respectively), whereas coarse emulsions had higher ζ-potential (from -14 to -22 mV) (Table 1). It is known that when ζ-potentials are below -30 mV, the electrical charge of droplets is strong enough to assume that repulsive forces between droplets are predominant in the system, keeping them stable (Béatrice Heurtault, Saulnier, Pech, Proust, & Benoit, 2003). Therefore, nanoemulsions obtained in the current work presented higher stability than coarse emulsions regardless the concentration of OR-EO.

Despite the fact that a neutral or slightly negative electrical charge was expected at the oil-water interface, according to the non-ionic low-mass nature of Tween 80 (Hsu & Nacu, 2003), the presence of the anionic groups of sodium alginate and mandarin fiber molecules dispersed in the aqueous phase has a strong influence in the ζ-potential values. When emulsions are exposed to mechanical treatment such as microfluidization, it might cause the opening of the biopolymer chain by mechanical shear, releasing free hydroxyl and carboxyl groups from their molecular structures available to bind with water (Chen et al., 2013). These deprotonated alcohols or carboxylic acids ($R\text{-}O^-$ or $R'CO_2^-$, respectively) contributed to increase the negative charge in the interface of the droplets. Therefore, the higher the biopolymer concentration, the higher was the presence of $R\text{-}O^-$ or $R'CO_2^-$ and the more negative ζ-potential values.

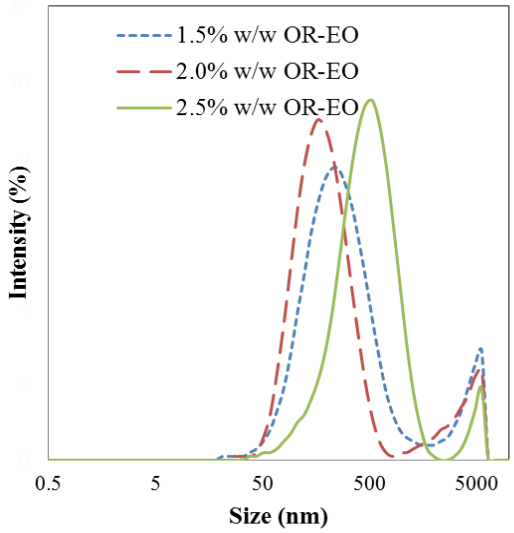

Figure 1. Particle size distribution (nm) of the nanoemulsions with different concentrations of oregano essential oil (OR-EO).

3.2.Apparent viscosity and whiteness index (WI)

Apparent viscosity values of nanoemulsions regarding coarse emulsions increased after microfluidization (Table 1), probably due to the non-Newtonian behavior of the pair mandarin fiber–alginate (Lundberg et al., 2014). This behavior let biopolymer structures hold additional water after a shear stress, increasing their gel-forming capacity, which consists of the formation of a gelatinous mass through water absorption (Dikeman, Murphy, &Jr, 2006; Wang et al., 2015). Regarding the viscosity values of both coarse emulsions and nanoemulsions, significant differences ($P<0.05$) between 1.5% *w/w* OR-EO emulsions and those with more concentration of OR-EO (2.0 and 2.5% *w/w*) were observed. The lower the percentage of OR-EO, the higher the viscosity of emulsions probably due to aggregation phenomena between biopolymers and surfactant molecules (Neumann et al., 2003). In this regard, apparent viscosity of emulsions might be strongly influenced by the presence of alginate and mandarin fiber dispersed in the aqueous phase.

The whiteness indexes (WI) of emulsions significantly decreased ($P<0.05$) in all cases after microfluidization process (Table 1). In fact, nanoemulsions have been defined as slightly turbid systems because small droplets scatter light weakly. Therefore, with the increase of droplet size, the light scattering is stronger and the WI of emulsions tends to be higher (Acevedo-Fani et al., 2015; McClements, 2002a).

On the other hand, nanoemulsions with a concentration of OR-EO over 2% w/w scattered the light significantly ($P<0.05$) more intensely than those with less concentration of OR-EO, causing an increase in the WI of the former (McClements, 2011; Salvia-Trujillo et al., 2013). This is because the emulsion appearance is highly determined by the physicochemical characteristics of oil droplets such as their size, refractive index or concentration. Specifically, if the concentration of oil droplets rises, L^* value also increased (Table 1) and hence, WI of emulsions become higher (eq.1) (Chantrapornchai, Clydesdale, & McClements, 1999).

Table 1. Physicochemical properties of coarse emulsions (CE) and their respective nanoemulsions (NE) in terms of Z-average (nm), ζ-potential (mV), Viscosity (mPa·s), Whiteness index (WI) and parameter *L. Data shown are the means ± standard deviation.**

	EO concentration (w/w)	ζ-average (nm)	ζ-potential (mV)	Viscosity (mPa·s)	WI	*L**
CE	1.5%	1851 ± 592^{Aa}	-17 ± 3^{a}	341 ± 6^{a}	60.42 ± 0.04^{a}	65.6 ± 0.1^{a}
	2.0%	1442 ± 529^{Ca}	-14 ± 3^{a}	250 ± 4^{b}	63.90 ± 0.05^{b}	69.09 ± 0.09^{b}
	2.5%	707 ± 242^{Eb}	-22.51 ± 1.48^{b}	237 ± 3^{b}	71.4 ± 0.3^{c}	75.7 ± 0.3^{c}
NE	1.5%	214 ± 14^{Bc}	-34 ± 5^{c}	366 ± 4^{c}	59.49 ± 0.16^{d}	62.59 ± 0.21^{d}
	2.0%	169 ± 23^{Dd}	-47 ± 3^{d}	270 ± 6^{d}	60.91 ± 0.17^{e}	62.73 ± 0.21^{e}
	2.5%	337 ± 79^{Fe}	-42 ± 4^{d}	265 ± 1^{d}	67.80 ± 0.10^{f}	71.17 ± 0.19^{e}

^{a,b,c,d,e,f} Means in same column with different letters are significantly different at $p < 0.05$ in terms of comparing OR-EO concentration.

3.3.Water Vapor Resistance (WVR) and water loss of coated-cheese pieces

As it is shown in Table 2, the highest weight loss was observed in cheese pieces with coatings containing 1.5% and 2.0% *w/w* of OR-EO (205.4 ± 0.1 mg and 216.4 ± 0.2 mg, respectively) without significant differences ($P<0.05$). However, the uncoated cheese presented the lowest weight loss value (156.5 ± 0.1 mg). The fact that the presence of a coating increased the weight loss of cut cheese can be explained by the higher water activity (a_w) of coated cheese pieces, compared with those uncoated (0.974 versus 0.947, respectively). In the coated product, the concentration of water on the matrix surface is higher, so it is easily captured by saturated $MgCl_2 \cdot 6H_2O$ solution situated in a sealed chamber, causing a greater loss of water from the coating. Regarding the different coatings, those with the highest content of EO resulted more effective as barriers showing a weight loss of 195.3 ± 0.2 mg, which is lower than in the case of using coatings with less concentration of OR-EO.

Coated cheese pieces exhibited greater values of WVR, compared to those uncoated (Table 2). Moreover, as the concentration of OR-EO in nanoemulsions increased, the WVR of coatings was higher. Although, polysaccharide-base coatings exhibit limited water vapor barrier ability owing to their hydrophilic and hygroscopic nature (Gennadios et al., 1997), OR-EO-based coatings, reducing water loss and avoiding cheese dehydration. On the other hand, there was a solid correlation ($r = 0.73$) between the water loss of coated product and calculated WVR values of nanoemulsion-based coatings. It suggested that those edible coatings that presented a higher WVR, experimented a lower water loss.

Table 2. Initial and final weights (g) of cheese pieces, weight loss (%) of coated and uncoated cheese pieces and water vapour resistance (WVR) expressed in s/cm of edible coatings based on oregano essential oil (OR-EO) from nanoemulsions (NE) applied onto cylindrical cut cheese pieces. Data shown are the means ± standard deviation.

	OR-EO concentration (w/w)	Initial weight (g)	Final weight (g)	Weight loss (%)	WVR (s/cm)
NE	1.5%	8. 26 ± 0.12^{a}	8.06 ± 0.12^{a}	2.49 ^{a}	8.40 ± 0.13 ^{a}
	2.0%	8.44 ± 0.23^{ab}	8.22 ± 0.24^{ab}	2.56 ^{a}	8.40 ± 0.24 ^{a}
	2.5%	8.50 ± 0.20^{b}	8.30 ± 0.18^{b}	2.30 ^{b}	10.08 ± 0.19 ^{b}
Uncoated		7.80 ± 0.14^{c}	7.65 ± 0.13^{c}	2.00 ^{c}	12.06 ± 0.14 ^{c}

^{a,b,c} Means in same column with different letters are significantly different at $p < 0.05$.

3.4.Antimicrobial efficiency of edible coatings against inoculated Staphylococcus aureus

The effectiveness of the antimicrobial edible coatings in inhibiting *Staphylococcus aureus* growth inoculated on low-fat cut cheese during refrigerated storage is shown in Figure 2. Initial

microbial load (10^6 CFU/g) inoculated on the surface of cylindrical cheese pieces decreased 0.9 ± 0.1 log CFU/g on average, just after applying the different coatings or after their submersion in ultrapure water (uncoated cheese pieces). The antimicrobial effectiveness of coatings with 1.5%, 2.0% or 2.5% *w/w* of OR-EO applied on the surface of cylindrical cheese pieces was compared with the formulations loaded with corn oil at the same concentrations confirming the lack of antimicrobial activity of coatings in absence of OR-EO (Fig.2).

The concentration of OR-EO used in the formulation of edible coatings had a significant effect on their bactericidal activity against inoculated *Staphylococcus aureus* over time. The microbial population decreased 1.4 and 1.5 log CFU/g in coated cheese pieces containing 2.0 % or 2.5% *w/w* of OR-EO, respectively, during 15 days of refrigerated storage. However, coatings with an OR-EO concentration of 1.5% *w/w* were not effective in reducing *Staphylococcus aureus* population.

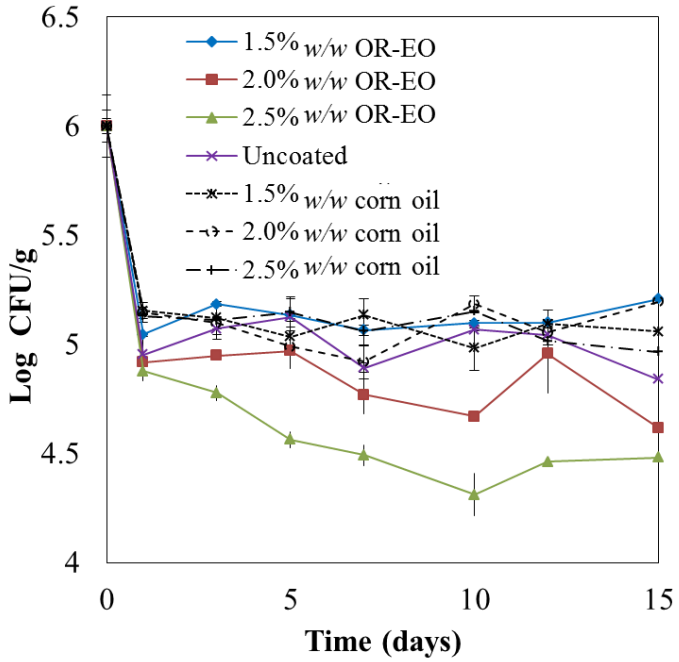

Figure 2. Effect of the edible coatings from nanoemulsions containing different concentrations of oregano essential oil (OR-EO) against *Staphylococcus aureus* (log CFU/g) inoculated onto cheese pieces. Data shown are the means ± standard deviation.

OR-EO can alter the fatty acid composition of cytoplasmic membranes of pathogenic and spoilage microorganisms (Pasqua, Hoskins, Betts, & Mauriello, 2006). Specifically, carvacrol, the major active compound from OR-EO, is able to modify the cell membrane of Gram-positive bacterial species such as *Staphylococcus aureus* (La Storia et al., 2011). Nevertheless, the antimicrobial activity of coatings against this pathogen was found to be dependent on the concentration of carvacrol contained in them (Kuorwel et al., 2011). Therefore, neither in coated-cheese pieces with an OR-EO concentration of 1.5% *w/w* nor in uncoated cheese pieces or in those with the coating based on corn oil, was possible to inactivate or inhibit the growth of *Staphylococcus aureus*.

3.5.Microbial growth and quality changes along storage.

3.5.1. Psychrophilic bacteria, molds and yeast

Figure 3 shows the growth of psychrophilic bacteria (A) and molds and yeast (B) in uncoated and coated cheese pieces during refrigerated storage. The results revealed that coatings with a concentration of OR-EO higher than 2.0% *w/w* clearly had an antimicrobial effect. However, a concentration of 1.5% *w/w* of OR-EO was not enough to inhibit the development of neither psychrophilic bacteria nor molds and yeast in cheese pieces.

Indeed, the most effective microbial inhibition of psychrophilic bacteria was obtained for cheese pieces coated by the nanoemulsion with the highest percentage of OR-EO (2.5% *w/w*). In this case, the growth began after the 6^{th} day of storage and reached the equilibrium with values lower than 6.7 log CFU/g at the 13^{th} day (Fig.3A). Although coatings with 2.0% *w/w* resulted effective in slowing down the psychrophilic bacteria growth, it was not enough to stop it. The microbial growth in the cheese pieces with a 2.0% *w/w* of OR-EO was lower than in those coated containing 1.5% *w/w* of OR-EO, reaching the maximum microbial population at the 17^{th} day with a 7.3 log CFU/g. On the other hand, microbial counts of psychrophilic bacteria in uncoated cheese pieces and in those coated with 1.5% OR-EO increased until 8.3 log CFU/g from the first day to the 17^{th} day of storage before reaching the equilibrium (Fig.3A).

Regarding molds and yeast (Fig. 3B), the growth started after the 13^{th} day in uncoated cheese pieces and in those coated with the lowest percentage of OR-EO (1.5% w/w). However, the fungi growth for uncoated pieces was greater than for those coated. In the case of coatings prepared with a 2.0% *w/w* of OR-EO, the growth began after 17 days of storage. Lastly, cheese pieces coated with 2.5% *w/w* of OR-EO did not show molds and yeast growth at least during 24 days of experiment. Lipids like EOs have many biological functions in microbial cells (La Storia et al., 2011), however, their effectiveness not only depend on the concentration but also on the active compound (Moore-Neibel et al., 2013). According to the results, both psychrophilic bacteria and molds and yeast were especially sensitive to carvacrol (main component of OR-EO) (Microbiology & Andrews, 2001). In this regard, OR-EO coatings may require less concentration of essential oil to extend the microbiological shelf life of low-fat cheese pieces (2.0% *w/w*) than in the case of using other type of EOs (Kavas & Kavas, 2014).

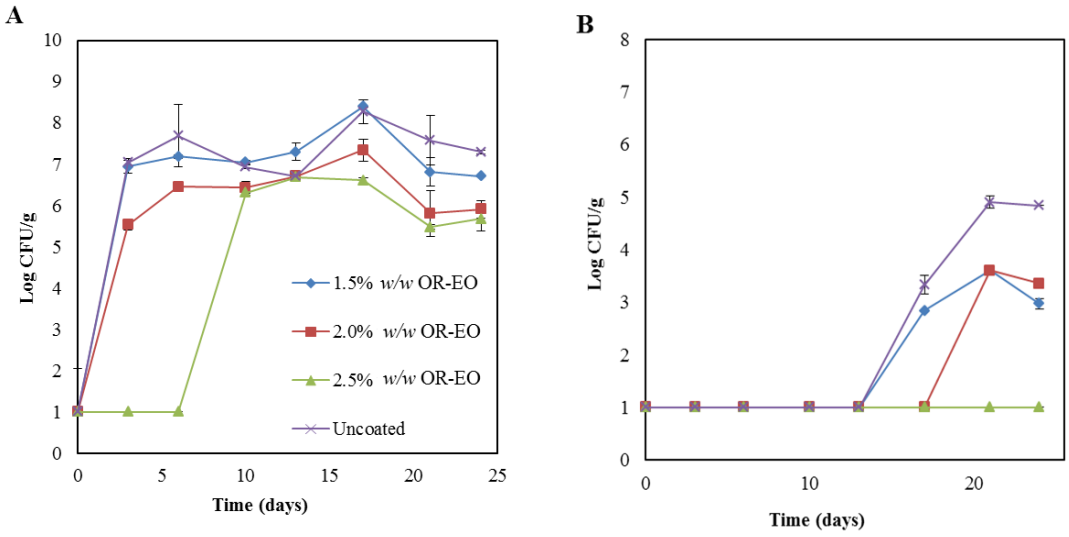

Figure 3. Effect of the nanoemulsion-based edible coatings containing oregano essential oil (OR-EO) on the microbial growth (log CFU/g) of psychrophilic bacteria (A) and molds and yeasts (B) in cheese pieces. Data shown are the means ± standard deviation.

3.5.2. Headspace gas composition

As it can be appreciated in Figure 4A, coatings based on nanoemulsions with OR-EO caused a decrease of O_2 consumption compared with the uncoated pieces from the 3th day, probably as a result of the control of the microbial growth (Raybaudi-Massilia et al., 2008). On the contrary, the production of CO_2 increased gradually until reaching the equilibrium because of the gas produced by cheese itself (Acerbi, Guillard, Guillaume, Saubanere, & Gontard, 2016). Nonetheless, significant variations ($P<0.05$) were observed during the first 13 days regarding the concentration of OR-EO (Fig.4B). Although it was supposed that coatings with a higher percentage of EO ought to have a higher resistance to gas diffusion due to their lipophilic nature (Salvia-Trujillo et al., 2015b), the presence of some carbohydrates such as alginate and mandarin fiber contributes to increase gas permeability (Rojas-Graü et al., 2007). This is related to the capability of alginate or mandarin fiber chains of holding water in their structures, which together with the fact that EO concentration was low, could cause a decrease in the ability of coatings to act as barriers to the transport of humidity, gases, and aroma compounds (Espitia, Du, Avena-Bustillos, Soares, & McHugh, 2014; Miller & Krochta, 1997).

Regarding ethanol production, there were not significant differences ($P>0.05$) between cut cheese coated by nanoemulsions containing 1.5% *w/w* OR-EO and uncoated pieces (Fig.4C). The same occurred for 2.0% and 2.5% *w/w* OR-EO coatings between them probably because both resulted effective in the control of microbial growth. Moreover, despite the fact that cheese produces CO_2 and ethanol during propionic and acid fermentation due to the action of lactic bacteria (Acerbi et al., 2016; Fröhlich-Wyder et al., 2013), it was possible to observe a fast decrease of ethanol concentration during the first three days of storage before reaching the equilibrium, because the alcohol may react with different derivatives of primary or secondary biochemical processes that occur during cheese shelf life

(Mei, Guo, Wu, Li, & Yu, 2015). In this regard, lipolysis reactions lead to several free fatty acids whose esters are able to react with ethanol. In addition, the reaction between some acids such as acetic or lactic acid with ethanol molecule produces the corresponding acetates resulting in the chemical equilibrium of equation (6):

$$RCO_2H + CH_3CH_2OH \leftrightarrow RCO_2CH_2CH_3 \qquad \textbf{eq.(6)}$$

Therefore, ethanol acts as a reaction intermediate, so its production and consumption are in equilibrium and thus, it is likely that an increase of ethanol could not be detected by gas chromatography.

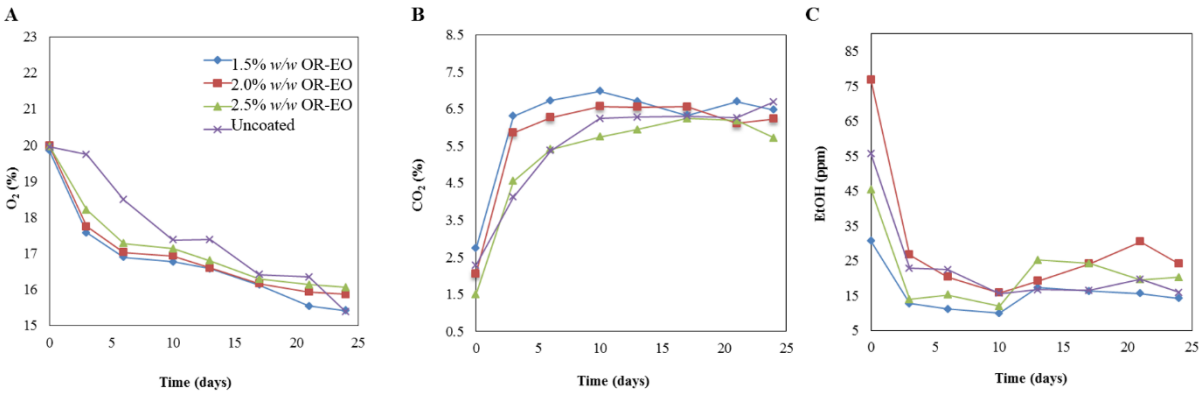

Figure 4. (A) Oxygen (O_2), (B) Carbon dioxide (CO_2) and (C) Ethanol (EtOH) headspace gas concentration of sealed trays containing uncoated or coated cheese samples during storage at 4ºC. Data shown are the means ± standard deviation.

3.5.3. Color (WI)

As has been discussed before, the optical properties of nanoemulsions depended on OR-EO concentration, thus when they are applied as edible coatings the color of the coated cheese pieces could be altered. Uncoated cheese pieces exhibited the highest WI value (76.32 ± 0.98) and there were no significant differences during the time (Fig.5A). Regarding coated cut cheese, a concentration of over 2.0% *w/w* OR-EO did not affect the WI values during storage time. However, when coatings with less OR-EO concentration (1.5% *w/w*) were used, the color of the cheese pieces increased progressively until the 13th day, probably because a lack of oil droplets might cause biopolymer or surfactant aggregation leading to more instable coatings (Neumann et al., 2003).

According to experimental data, the WI was influenced by the rise of the *b** coordinate value, which indicates the increase of yellow color (Fig.5B). The higher the *b** value, the more yellow the cheese pieces and therefore, the lower the WI (eq.1). The increase of the *b** parameter can be explained by the orange color of mandarin fiber that was incorporated to nanoemulsions. Even though coated pieces seemed to be more yellow than uncoated, they were able to maintain the brightness and the external properties of cheese during the time. In fact, the preservation of the outward appearance of coated cheese pieces is very important in terms of being unnoticed for consumers (Stintzing & Carle, 2004).

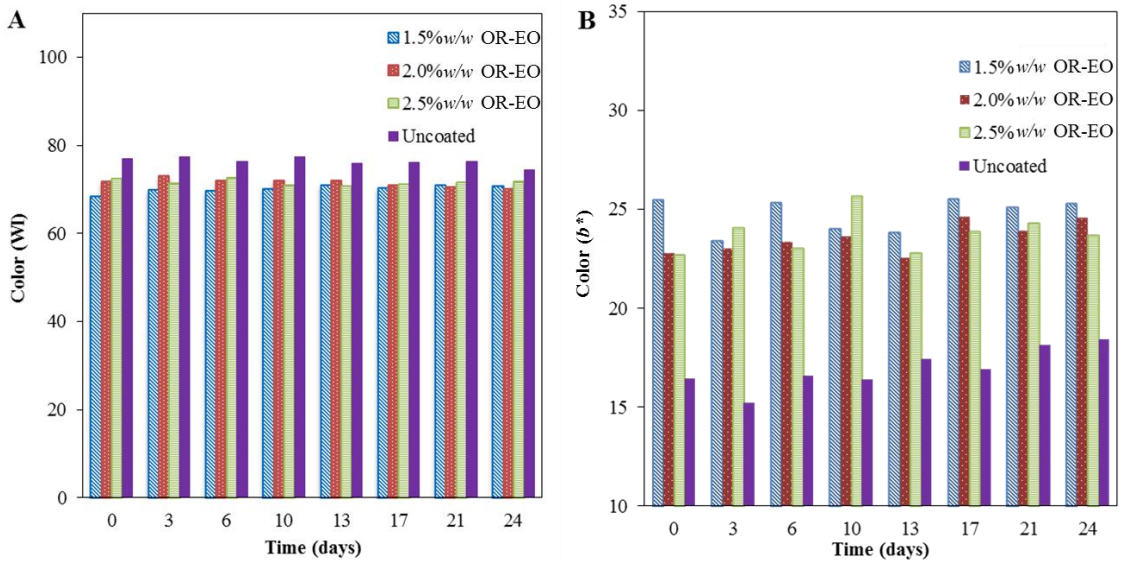

Figure 5. (A) Color changes in terms of whiteness index (WI) values of coated and uncoated cheese pieces during storage. (B) Changes in *b parameter values of coated and uncoated cheese pieces during storage. Data shown are the means ± standard deviation.**

3.5.4. Cheese Texture Profile Analysis (TPA)

Coated cheese pieces showed similar values of hardness, cohesiveness, gumminess and elasticity regardless the EO percentage incorporated in nanoemulsions, whereas these parameters were higher in uncoated cut cheese (Fig.6). The highest values of adhesiveness were observed in the uncoated product, and it remains constant during the time (Fig.6D). In the case of coated pieces, adhesiveness values gradually decreased during 24 days.

Cheese hardness usually increases over time as a result of water loss and proteolysis (Bourne, 2002). Hence, the product may require a major force in the process of chewing due to a lack of elasticity (Segnini, Dejmek, & Öste, 1999). In the current work, the percentage of high water-content edible coatings allowed maintaining, not only the elasticity of coated cheese pieces but also cheese pieces' softness (Fig. 6C, 6A, respectively).

Szczesniak (2002) pointed out that gumminess and chewiness (defined as the energy required to masticate a solid food) are mutually exclusive (Bourne, 2002) so, as elasticity remained constant over time, the two properties must vary proportionally. Nevertheless, although coatings did not exert any effect on chewiness, which was maintained constant during the time (data not shown), the gumminess of the uncoated cheese pieces started to increase from the 7th day of storage (Fig.6E). Probably because gumminess, understood as the energy required to disintegrate a semisolid food to a state of readiness for swallowing, is dependent on hardness; hence, if the latter increases, the former does (Bourne, 2002).

On the other hand, the cohesiveness of cheese pieces, defined as the limit point to which the material can deform itself before breaking, did not vary over time regardless the concentration of OR-EO (Fig.6B). Nevertheless, uncoated pieces showed higher cohesiveness values, which decreases

during the time; hence, coated cheese may break easily. The cheese becomes a cohesive material along the time because the particles are closer after the product dehydration (Szczesniak, 2002). However, the edible coatings helped to preserve the water into the food matrix maintaining the cohesiveness, whereby the disintegration of the product is less probable.

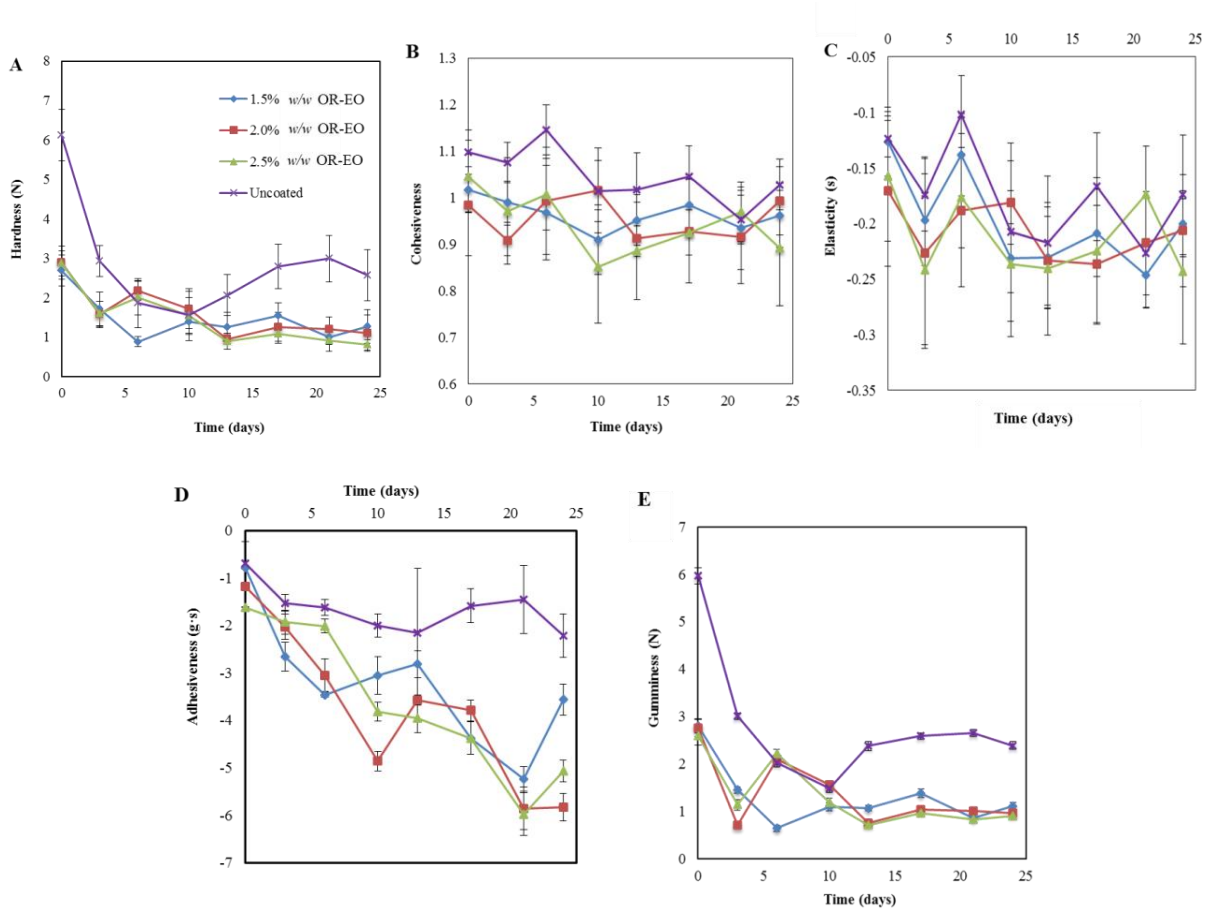

Figure 6. Texture Profile Analysis of coated and uncoated cheese pieces. (A) Hardness (N); (B) Cohesiveness (N·s/N·s); (C) Elasticity (s); (D)Adhesiveness (g·s) and (E) Gumminess (N). Data shown are the means ± standard deviation.

Lastly, adhesiveness, which is the work necessary to overcome the attractive forces between the surface of the food and the surface of the other materials in contact (Szczesniak, 2002), did not correlate with the other properties studied by TPA (Segnini et al., 1999). In fact, coated cheese pieces experienced a loss of adhesion, whereas this property remained constant over time in the uncoated product (Fig.6D). Therefore, coated cheese pieces might be less sticky during the days than those uncoated.

4. Conclusions

The combination of mandarin fiber with prebiotic properties, and sodium alginate let the formation of stable OR-EO-loaded nanoemulsions able to act as edible coatings onto cheese pieces. Thus, the incorporation of fiber to the coatings may become in an interesting alternative for increasing the nutritional value of coated cheese pieces. In addition, edible coatings with at least 2.0% w/w of OR-EO improved the microbial stability of the cheese pieces, resulted effective in the decontamination of external pathogens such as *Staphylococcus aureus* and preserved cheese outward appearance during the time. As a consequence, the incorporation of nanoemulsions-based edible coatings containing OR-EO onto low-fat cut cheese extended the shelf life of this product. These results evidence the potential advantages of using OR-EO as natural antimicrobial within edible coatings acting as preservatives and enhancing the safety, quality and nutritional properties of high perishable low-fat cut cheese.

5. Acknowledgments

This study was supported by the Ministry of Science and Innovation (Spain) throughout project **AGL2009-11475** and by the MINECO (Spain) throughout project **AGL2012-35635**. Authors María Artiga-Artigas and Alejandra Acevedo-Fani thank the University of Lleida for their pre-doctoral fellowship.

6. References

Acerbi, F., Guillard, V., Guillaume, C., Saubanere, M., & Gontard, N. (2016). An appraisal of the impact of compositional and ripening parameters on CO2 diffusivity in semi-hard cheese. *Food Chemistry*, *194*, 1172–1179.

Acevedo-Fani, A., Salvia-Trujillo, L., Rojas-Graü, M. A., & Martín-Belloso, O. (2015). Edible films from essential-oil-loaded nanoemulsions: Physicochemical characterization and antimicrobial properties. *Food Hydrocolloids*, *47*, 168–177.

Adorjan, B., & Buchbauer, G. (2010). Biological properties of essential oils: an updated review. *Flavour and Fragrance Journal*, *25*(6), 407–426.

Ben-Yehoshua, S., Burg, S. P., & Young, R. (1985). Resistance of citrus fruit to mass transport of water vapor and other gases. *Plant Physiology*, *79*(4), 1048–1053.

Bonilla, J., Atarés, L., Vargas, M., & Chiralt, A. (2012). Effect of essential oils and homogenization conditions on properties of chitosan-based films. *Food Hydrocolloids*, *26*(1), 9–16.

Bourne, M. C. (2002). Principles of Objective Texture Measurement. *Food Texture and Viscosity: Concept and Measurement, 2nd Edition*, (1961), 107–188.

Burt, S. (2004). Essential oils: their antibacterial properties and potential applications in foods--a review. *International Journal of Food Microbiology*, *94*(3), 223–53.

Chantrapornchai, W., Clydesdale, F., & McClements, D. J. (1999). Influence of droplet characteristics on the optical properties of colored oil-in-water emulsions. *Colloids and Surfaces A: Physicochemical and Engineering Aspects*, *155*(2–3), 373–382.

Chen, J., Gao, D., Yang, L., & Gao, Y. (2013). Effect of microfluidization process on the functional properties of insoluble dietary fiber. *Food Research International*, *54*(2), 1821–1827.

Diamantino, V. R., Beraldo, F. A., Sunakozawa, T. N., & Penna, A. L. B. (2014). Effect of octenyl succinylated waxy starch as a fat mimetic on texture, microstructure and physicochemical properties of Minas fresh cheese. *LWT - Food Science and Technology*, *56*(2), 356–362.

Dikeman, C. L., Murphy, M. R., & Jr, G. C. F. (2006). Nutrient Physiology , Metabolism , and Nutrient-Nutrient Interactions Dietary Fibers Affect Viscosity of Solutions and Simulated Human Gastric and Small Intestinal Digesta, (September 2005), 913–919.

Espitia, P. J. P., Du, W. X., Avena-Bustillos, R. de J., Soares, N. de F. F., & McHugh, T. H. (2014). Edible films from pectin: Physical-mechanical and antimicrobial properties - A review. *Food Hydrocolloids*, *35*, 287–296.

Fisher, K., & Phillips, C. (2008). Potential antimicrobial uses of essential oils in food: is citrus the answer? *Trends in Food Science and Technology*, *19*(3), 156–164.

Fröhlich-Wyder, M. T., Guggisberg, D., Badertscher, R., Wechsler, D., Wittwer, A., & Irmler, S. (2013). The effect of Lactobacillus buchneri and Lactobacillus parabuchneri on the eye formation of semi-hard cheese. *International Dairy Journal*, *33*(2), 120–128.

García, M., Jergel, M., Conde-Gallardo, A., Falcony, C., & Plesch, G. (1998). Optical properties of Co and Co-Fe-Cr thin films deposited from an aerosol on glass substrates. *Materials Chemistry and Physics*, *56*(1), 21–26.

Gennadios, a, Hanna, M. a, & Kurth, L. B. (1997). Application of edible coatings on meats, poultry and seafoods: A review. *Food Science and Technology-Lebensmittel-Wissenschaft & Technologie*, *30*(4), 337–350.

George, M., & Abraham, T. E. (2006). Polyionic hydrocolloids for the intestinal delivery of protein drugs: Alginate and chitosan - a review. *Journal of Controlled Release*, *114*(1), 1–14.

Goddard, E. D. (2002). Polymer/Surfactant Interaction: Interfacial Aspects. *Journal of Colloid and Interface Science*, *256*(1), 228–235.

González-Molina, E., Domínguez-Perles, R., Moreno, D. A., & García-Viguera, C. (2010). Natural bioactive compounds of Citrus limon for food and health. *Journal of Pharmaceutical and Biomedical Analysis*, *51*(2), 327–345.

Grigelmo-Miguel, N., & Martín-Belloso, O. (1999). Characterization of dietary ® ber from orange juice extraction. *Food Research International*, *31*(5), 355–361.

Guerra-Rosas, M. I., Morales-Castro, J., Ochoa-Martínez, L. A., Salvia-Trujillo, L., & Martín-Belloso, O. (2016). Long-term stability of food-grade nanoemulsions from high methoxyl pectin containing essential oils. *Food Hydrocolloids*, *52*, 438–446.

Heurtault, B., Saulnier, P., Pech, B., Proust, J. E., & Benoit, J. P. (2003). Physico-chemical stability of colloidal lipid particles. *Biomaterials*, *24*(23), 4283–4300.

Hsu, J.-P., & Nacu, A. (2003). Behavior of soybean oil-in-water emulsion stabilized by nonionic surfactant. *Journal of Colloid and Interface Science*, *259*(2), 374–381.

Kavas, G., & Kavas, N. (2014). The effects of mint (Mentha spicata) essential oil fortified edible films on the physical, chemical and microbiological characteristics of lor cheese. *Journal of Food, Agriculture and Environment*, *12*(3–4), 40–45.

Kaya, S., & Kaya, A. (2000). Microwave drying effects on properties of whey protein isolate edible films. *Journal of Food Engineering*, *43*(2), 91–96.

Klang, V., Matsko, N. B., Valenta, C., & Hofer, F. (2012). Electron microscopy of nanoemulsions: An essential tool for characterisation and stability assessment. *Micron*, *43*(2–3), 85–103.

Kuorwel, K. K., Cran, M. J., Sonneveld, K., Miltz, J., & Bigger, S. W. (2011). Antimicrobial activity of natural agents coated on starch-based films against Staphylococcus aureus. *Journal of Food Science*, *76*(8), M531-7.

La Storia, A., Ercolini, D., Marinello, F., Di Pasqua, R., Villani, F., & Mauriello, G. (2011). Atomic force microscopy analysis shows surface structure changes in carvacrol-treated bacterial cells. *Research in Microbiology*, *162*(2), 164–172.

Li, Y., Zheng, J., Xiao, H., & McClements, D. J. (2012). Nanoemulsion-based delivery systems for poorly water-soluble bioactive compounds: Influence of formulation parameters on Polymethoxyflavone crystallization. *Food Hydrocolloids*, *27*(2), 517–528.

Lundberg, B., Pan, X., White, A., Chau, H., & Hotchkiss, A. (2014). Rheology and composition of citrus fiber. *Journal of Food Engineering*, *125*(1), 97–104.

McClements, D. J. (2002). Colloidal basis of emulsion color. *Current Opinion in Colloid & Interface Science*, *7*(5–6), 451–455.

McClements, D. J. (2011). Edible nanoemulsions: fabrication, properties, and functional performance. *Soft Matter*, *7*(6), 2297–2316.

Mei, J., Guo, Q., Wu, Y., Li, Y., & Yu, H. (2015). Study of proteolysis, lipolysis, and volatile compounds of a Camembert-type cheese manufactured using a freeze-dried Tibetan kefir co-culture during ripening. *Food Science and Biotechnology*, *24*(2), 393–402.

Microbiology, A., & Andrews, S. (2001). A study of the Minimum Inhibitory Concentration and mode of action of Oregano Essential Oil , Thymol and Carvacrol, (October), 453–462.

Miller, K. S., & Krochta, J. M. (1997). Oxygen and aroma barrier properties of edible films: carboxymethylated konjac glucomannan blend films. *Journal of Applied Polymer Science*, *88*(July), 1095–1099.

Moore-Neibel, K., Gerber, C., Patel, J., Friedman, M., Jaroni, D., & Ravishankar, S. (2013). Antimicrobial activity of oregano oil against antibiotic-resistant Salmonella enterica on organic leafy greens at varying exposure times and storage temperatures. *Food Microbiology*, *34*(1), 123–129.

Moreira, M. R., Cassani, L., Martín-Belloso, O., & Soliva-Fortuny, R. (2015). Effects of polysaccharide-based edible coatings enriched with dietary fiber on quality attributes of fresh-cut apples. *Journal of Food Science and Technology*, *52*(12), 7795–7805.

Neumann, M. G., Schmitt, C. C., & Iamazaki, E. T. (2003). A fluorescence study of the interactions between sodium alginate and surfactants. *Carbohydrate Research*, *338*(10), 1109–1113.

Park, H. J., & Chinnan, M. S. (1995). Gas and water vapor barrier properties of edible films from protein and cellulosic materials. *Journal of Food Engineering*, *25*(4), 497–507.

Pasqua, R. D., Hoskins, N., Betts, G., & Mauriello, G. (2006). Changes in membrane fatty acids composition of microbial cells induced by addiction of thymol, carvacrol, limonene, cinnamaldehyde,and eugenol in the growing media. *Journal of Agricultural and Food Chemistry*, *54*, 2745–2749.

Raybaudi-Massilia, R. M., Mosqueda-Melgar, J., & Martín-Belloso, O. (2006). Antimicrobial activity of essential oils on Salmonella enteritidis, Escherichia coli, and Listeria innocua in fruit juices. *Journal of Food Protection*, *69*(7), 1579–1586.

Raybaudi-Massilia, R., Mosqueda-Melgar, J., & Martín-Belloso, O. (2008). Edible alginate-based coating as carrier of antimicrobials to improve shelf-life and safety of fresh-cut melon. *International Journal of Food Microbiology*, *121*(3), 313–327.

Rojas-Graü, M. A., Avena-Bustillos, R. J., Olsen, C., Friedman, M., Henika, P. R., Martín-Belloso, O., … McHugh, T. H. (2007). Effects of plant essential oils and oil compounds on mechanical, barrier and antimicrobial properties of alginate-apple puree edible films. *Journal of Food Engineering*, *81*(3), 634–641.

Rojas-Graü, M. A., Avena-Bustillos, R. J., Olsen, C., Friedman, M., Henika, P. R., Martín-Belloso, O., … McHugh, T. H. (2007). Effects of plant essential oils and oil compounds on mechanical, barrier and antimicrobial properties of alginate–apple puree edible films. *Journal of Food Engineering*, *81*(3), 634–641.

Rojas-Graü, M. A., Soliva-Fortuny, R., & Martín-Belloso, O. (2009). Edible coatings to incorporate active ingredients to fresh-cut fruits: a review. *Trends in Food Science & Technology*, *20*(10), 438–447.

Rojas-Graü, M. a., Tapia, M. S., Rodríguez, F. J., Carmona, a. J., & Martin-Belloso, O. (2007). Alginate and gellan-based edible coatings as carriers of antibrowning agents applied on fresh-cut Fuji apples. *Food Hydrocolloids*, *21*(1), 118–127.

Salvia-Trujillo, L., Rojas-Graü, A., Soliva-Fortuny, R., & Martín-Belloso, O. (2014). Food Hydrocolloids Physicochemical characterization and antimicrobial activity of food- grade emulsions and nanoemulsions incorporating essential oils. *Food Hydrocolloids*, *43*, 1–10.

Salvia-Trujillo, L., Rojas-Graü, M. A., Soliva-Fortuny, R., & Martín-Belloso, O. (2013). Effect of processing parameters on physicochemical characteristics of microfluidized lemongrass essential oil-alginate nanoemulsions. *Food Hydrocolloids*, *30*(1), 401–407.

Salvia-Trujillo, L., Rojas-Graü, M. A., Soliva-Fortuny, R., & Martín-Belloso, O. (2015). Use of

antimicrobial nanoemulsions as edible coatings: Impact on safety and quality attributes of fresh-cut Fuji apples. *Postharvest Biology and Technology*, *105*, 8–16.

Segnini, S., Dejmek, P., & Öste, R. (1999). Relationship Between Instrumental and Sensory Analysis of Texture and Color of Potato Chips. *Journal of Texture Studies*, *30*(6), 677–690.

Solans, C., Izquierdo, P., Nolla, J., Azemar, N., & Garcia-Celma, M. (2005). Nano-emulsions. *Current Opinion in Colloid & Interface Science*, *10*(3–4), 102–110.

Stintzing, F. C., & Carle, R. (2004). Functional properties of anthocyanins and betalains in plants, food, and in human nutrition. *Trends in Food Science and Technology*, *15*(1), 19–38.

Svoboda, K., Brooker, J. D., & Zrustova, J. (2006). Antibacterial and antioxidant properties of essential oils: Their potential applications in the food industries. In *Acta Horticulturae* (Vol. 709, pp. 35–43).

Szczesniak, A. S. (2002). Texture is a sensory property, *13*, 215–225.

Tajkarimi, M. M., Ibrahim, S. a., & Cliver, D. O. (2010). Antimicrobial herb and spice compounds in food. *Food Control*, *21*(9), 1199–1218.

Vargas, M., Cháfer, M., Albors, A., Chiralt, A., & González-Martínez, C. (2008). Physicochemical and sensory characteristics of yoghurt produced from mixtures of cows' and goats' milk. *International Dairy Journal*, *18*(12), 1146–1152.

Wang, L., Xu, H., Yuan, F., Pan, Q., Fan, R., & Gao, Y. (2015). Physicochemical characterization of five types of citrus dietary fibers. *Biocatalysis and Agricultural Biotechnology*, *4*, 250–258.

Wang, T., Sun, X., Zhou, Z., & Chen, G. (2012). Effects of microfluidization process on physicochemical properties of wheat bran. *Food Research International*, *48*(2), 742–747.

Ziani, K., Chang, Y., McLandsborough, L., & McClements, D. J. (2011). Influence of surfactant charge on antimicrobial efficacy of surfactant-stabilized thyme oil nanoemulsions. *Journal of Agricultural and Food Chemistry*, *59*(11), 6247–6255.

General Discussion

In this Doctoral Thesis, oil-in-water nanoemulsions and double emulsions have been designed, prepared and characterized to be used as delivery systems of lipophilic and/or hydrophilic bioactive compounds, respectively. The resulting emulsion-based nanostructures were able to efficiently encapsulate, transport and release plant-derived bioactive compounds including antimicrobials (*i.e.* essential oils) and bioactive compounds (*e.g.* curcumin and chlorophyllin). Moreover, the prepared essential oil-in-water nanoemulsions were applied as edible coatings onto food matrices in order to extend the shelf-life of a highly perishable low-fat cut cheese.

SECTION I: Designing nanoemulsions as carriers of lipophilic plant-derived bioactive compounds.

Effect of formulation in the physicochemical properties of nanoemulsions

Nanoemulsions are thermodynamic unstable systems so that the selection of the appropriated formulation is a crucial step to obtain stable systems over time. In this regard, the type and concentration of each component: (i) surfactant, (ii) oil and (iii) stabilizing agents such as biopolymers or polymeric complexes may influence the final properties of nanoemulsions. Moreover, the ratio between the concentrations of each component in the formulation has to be taken into account since the lack or the excess of any of them could provoke the destabilization of the nanostructures.

Hence, the starting point of this work (chapter I) consisted of using a surface-response experimental design, specifically a D-optimal, to study the influence of four types of essential oils (EOs) (oregano, thyme, lemongrass or mandarin), Tween 80 and pectin concentrations on the oil droplet diameter (nm), ζ-potential (mV), apparent viscosity (mPa·s) and color of emulsions. Pseudo-ternary phase experimental designs built during this experiment provided significant information about the behavior of the individual components on the formation of nanoemulsions through microfluidization.

The models built showed that the EOs concentration did not dominate the particle size of nanoemulsion, being rather the Tween 80 and pectin concentrations the determining factors. Actually, a minimum concentration of Tween 80 (1.8% *w/w*) was required for the preparation of nanoemulsions ($d < 500$ nm), whose oil droplet diameters decreased as the concentration of surfactant increased regardless the type of EO. Additionally, pseudo-ternary phase diagrams revealed the role of pectin as an emulsifier since in absence of Tween 80, biopolymer concentrations over 1% *w/w* led to submicron nanoparticles (350-850 nm) being this emulsification even more effective depending on the EO used. Indeed, an increase of pectin concentration in the aqueous phase caused the enlargement in particle size of nanoemulsions containing oregano, thyme or mandarin EOs (OR-EO, TH-EO or MN-EO, respectively), whereas the opposite behavior was observed in the case of emulsions containing lemongrass essential oil (LG-EO). This suggested that pectin contributed positively to the emulsification of LG-EO-loaded nanoemulsions. Other authors have also observed a certain surface activity of pectin at oil-water interfaces since it contains functional units including acetyl and methyl groups, which are able to act as hydrophobic anchors that facilitate adsorption of biopolymer chains at the interface resulting in the reduction of interfacial tension (Alba & Kontogiorgos, 2017).

Despite the fact that EO and Tween 80 poorly influenced nanoemulsions apparent viscosity, specifically in the case of LG-EO loaded nanomeulsions, a slight decrease of viscosity was observed when the concentration of surfactant increased. This may be related to a reduction in nanoemulsions

particle size. In fact, droplet size has been reported to impact the rheology of emulsions and depends on the properties of the dispersed phase (Pal, 2000). In this regard, MN-EO nanoemulsions present lower overall viscosity values in comparison with the rest of the EOs since they also had the smallest droplet sizes. Nonetheless, our results suggested that nanoemulsion viscosity was mainly determined by pectin concentration. Actually, at increasing the weight fraction of pectin in the aqueous phase up to 2% *w/w* for a given concentration of Tween 80 (6% *w/w*) the apparent viscosity remarkably increased regardless the type and concentration of EO. Guerra-Rosas, Morales-Castro, Ochoa-Martínez, Salvia-Trujillo, & Martín-Belloso (2016) also observed that the higher the concentration of pectin, the higher its viscosity. This is related to the thickening properties of pectin due to its ability to holding high quantities of water. Therefore, free pectin molecules in the aqueous phase are able to form gel-like structures, thus increasing the viscosity of the aqueous media (Hansen, Arnebrant, & Bergström, 2001).

Furthermore, contour plots of OR-EO and LG-EO showed that an increase of the pectin concentration from 1% to 2% *w/w* caused the decrease of ζ-potential values becoming more negative from -10 to -15 mV or from -9 to -15 mV, respectively. Pectin is a linear polysaccharide consisting of covalently linked galacturonic acid (GalA) units with methylester groups along the backbone. The ionization of the carboxylic groups of the methyesters contributes to the negative charge of pectin (Lin, Lopez-Sanchez, & Gidley, 2016). Although Tween 80 is a non-ionic small molecule surfactant, which rapidly adsorbs at the oil/water interface stabilizing the newly created oil droplets, Jafari, He, & Bhandari (2007) reported that pectin chains present in the bulk aqueous phase can compete with Tween 80 molecules. This may cause the displacement of the previously-adsorbed surface active species and it would be the biopolymer that dominates the interfacial charge. Nevertheless, in the contour plots of TH-EO and MN-EO, ζ-potential values remained practically unaltered after increasing the concentration of pectin, ranging from -12 to -15 mV and from -10 to -11 mV, respectively. Thus, there was a preferential adsorption of Tween 80 at the oil droplet surface. It is known that, in the absence of any anionic biopolymer, non-ionic surfactants such as Tween 80 may confer negative charge to oil droplets probably due to the orientation towards the oil/water interface of OH^- ions from the aqueous phase or HCO_3^- and CO_3^{2-} ions from the dissolved atmospheric CO_2 (Marinova et al., 1996). These results suggested that pectin adsorption at the oil/water interface depends on the type of EO.

Tween 80 and EOs concentration significantly affected the color of nanoemulsions. Indeed, high Tween 80 or low EO concentrations led to transparent nanoemulsions regardless the type of oil. Light scattering of oil droplets depends fundamentally on the refractive index of continuous (water) and dispersed phase (oil), oil concentration and droplet size (McClements, 2002; McClements & Rao, 2011). Hence, OR-EO nanoemulsions, with the highest refractive index, were those less transparent. It is known that larger particles scatter the light more intensively causing an increase in the lightness, opacity and whiteness index of emulsions. Therefore, MN-EO nanoemulsions, which presented the smallest particle sizes (29-260 nm) also, exhibited the lowest whiteness index.

Effect of type and concentration of surfactant on the physicochemical properties of nanoemulsions

Emulsifiers play a relevant role in the formation and stabilization of nanostructures. Typically, small and high molecular surfactants have been used as emulsifiers for the stabilization of nanoemulsions. These molecules, which locate themselves around the internal droplets, are able to interact with all the components present in the nanoemulsions, even with the encapsulated bioactive compound through H-bond formation. Therefore, the selection of the surfactant may be related on the one hand, to the characteristics of the nanostructured system and on the other hand, to the nature of the bioactive compound that is going to be encapsulated. In this regard, the influence of three surfactants (lecithin, Tween 20 and sucrose monopalmitate) on the formation and stabilization of curcumin-loaded nanoemulsions was assessed during the second chapter of this nanoemulsions design, preparation and characterization study. The particle size of curcumin-loaded nanoemulsions was lower than 400 nm regardless the type of surfactant and decreased with an increase of Tween 20 or lecithin concentration. Oppositely, the particle size of nanoemulsions containing sucrose monopalmitate were highly polydisperse (PdI = 0.5) probable due to this surfactant contains diesters as well as monoesters and other type of fatty acids in its composition that may influence the emulsification process (Rao & Mcclements, 2011). This is in agreement with literature since low-mass surfactants such as polysorbates (Tween 20) and lecithins are known to rapidly coat the surface of the created oil-water interface during emulsification (Salvia-Trujillo, Rojas-Graü, Soliva-Fortuny, & Martín-Belloso, 2014). Also, phosphate groups from lecithin provided negative charge favoring electrostatic interactions needed to avoid coalescence, which is reflected in the low polydispersity index (PdI) of nanoemulsions stabilized by this surfactant (Zhang et al., 2012).

Overall, there has to be enough surfactant molecules to completely cover the oil droplets surface. The lack or excess of surfactant may lead to respectively, droplets coalescence or aggregates formation between the surfactant chains themselves or with alginate molecules present in the bulk phase (Artiga-Artigas, Acevedo-Fani, & Martín-Belloso, 2017).

All the nanoemulsions presented ζ-potential values bellow -30 mV since they contained sodium alginate in their formulation. The presence of sodium alginate, with carboxylate (CO_2^-) and hydroxyl (OH^-) groups played a relevant role in the electrostatic stabilization of nanoemulsions. Differences in ζ-potential values between the surfactants are related to their nature. For instance, lecithin and sucrose monopalmitate contributed to decrease the electrical charge since they contain negative functional groups in their structure, whereas in Tween 20-stabilized nanoemulsions the electrical charge was dominated by the biopolymer.

Also the whiteness index was influenced by the type of surfactant used since the smaller the nanoemulsions particle size, the lower their whiteness index (Salvia-Trujillo et al., 2014). This reduction in particle size is also related to an increase of nanoemulsions apparent viscosity, which restricted droplets mobility preventing coalescence. Nanoemulsions containing sucrose monopalmitate as surfactant destabilized almost instantaneously, whereas those with concentrations of lecithin over 1% w/w remained stable during at least 3 months. Moreover, lecithin-stabilized nanoemulsions were able to efficiently entrap curcumin within them, preventing its autoxidation and hence, maintaining the antioxidant capacity of the bioactive compound. Oppositely, although either Tween 20 or sucrose monopalmitate allowed obtaining nanoemulsions with high encapsulation efficiencies (EE), it does not mean that curcumin was encapsulated but retained in the surfactant structure by H-bonding after nanoemulsions destabilization. In this case, curcumin was exposed to light and oxidation reactions

leading to its degradation and loss of antioxidant capacity.

Moreover, it is reported that high oil concentrations contribute to decrease the rate of lipid oxidation (Osborn & Akoh, 2004). Therefore, an increase in droplet concentration may improve the shelf-life of chemically labile products such as curcumin. Highly concentrated emulsions are presented in chapter III as an alternative to encapsulate higher quantities of bioactive compounds. These systems contain at least 40% w/w oil and are able to modify the textural, optical, stability and release characteristics to the desired final commercial products, as well as reduce storage and transportation costs (Luo et al., 2017). However, several factors can affect the physicochemical properties of concentrated systems. For these reasons, the effect of high-shear homogenization (HSH) procedure (ie. ultrasonication or microfluidization), the oil volume fraction (φ: 0.4-0.7) and the hydrophilic surfactant-oil-ratio (SOR: 0.01-0.2) on highly concentrated emulsions formation were evaluated.

Either ultrasonication (200 s, 100 µm) or microfluidization (2 cycles, 800 bar) led to highly concentrated submicron emulsions (φ = 0.4) with particle sizes lower than 500 nm when the SOR was 0.1. The increase of the φ, contributed to reduce the particle size of coarse emulsions, as well as to increase their apparent viscosity (Sanatkaran, Masalova, & Malkin, 2014). This triggered that HSH procedures caused the destabilization of the resulting emulsions when φ was higher than 0.5. The particle size of all the studied highly concentrated emulsions decreased as the SOR increased from 0.01 to 0.2. However, a SOR of 0.2 provoked a prompt increase of submicron emulsions apparent viscosity, especially after microfluidization, which has to be taken into account depending on the desired final applications. Moreover, the emulsion-based systems prepared during the present study showed a high capability for curcumin encapsulation (> 70%) and slow release of this bioactive pigment according to their low kinetic constants (≈ 0.0031 h^{-1}). This indicates the feasibility of these systems to be used as carriers of curcumin during a certain period of time preventing its degradation.

Effect of biopolymer incorporation procedure on the physicochemical properties of naneomulsions

The incorporation of biopolymers such as proteins and polysaccharides to emulsion-based systems is currently gaining attention. These natural macromolecules have been widely used as texturizing agents; however, they have also shown emulsifying capacity. Nonetheless, their structure might be altered after homogenization processes changing their disposition around droplets and modifying the final physicochemical characteristics of nanoemulsions. Therefore, the effect of sodium alginate incorporation procedure on the physicochemical properties of nanoemulsions formed by microfluidization was assessed along chapter IV of this study. Nanoemulsion in which sodium alginate solution was microfluidized at the same time that the rest of components, showed the smallest particle sizes. Microfluidization had an influence on particle sizes promoting changes in the sodium alginate molecular structure, which allow obtaining more homogeneous droplets distribution and smaller particle sizes. Consequently, the highest particle sizes were observed for those nanoemulsions in which alginate did not pass through the microfluidizer.

Certainly, in transmission electron microscopical images of nanoemulsions, it was observed that the presence of aggregates was higher when alginate molecules were not subjected to high shear stress. Non-microfluidized alginate molecules maintained their original structure without suffering depolymerization. According to our results, non-depolymerizer chains placed at droplets interface experimented a steric impediment among them greater than those partially depolymerized leading to big and non-spherical particles.

On the other hand, the observed electrical charge was negative in all the emulsions and nanoemulsions suggesting that Tween 20 is preferably adsorbed on the oil surface in the co-presence of polymeric stabilizers, such as sodium alginate molecules. These molecules provided negative charge to oil-water interfaces when dispersed in the aqueous phase due to the presence of OH^- and CO_3^- groups in their structures (Nambam & Philip, 2012). Moreover, the mechanical stress during microfluidization caused a partial breaking of alginate molecule in agreement with ^{1}H-magnetic resonance and infrared spectra. This occurred probably as a result of the chemical reaction between the polymers and high energy molecules such as hydroxyl radicals produced from cavitation (Feng, Cao, Xu, Wang, & Zhang, 2017). This partial breaking may provoke the change of biopolymer chains disposition around the oil droplets and the increase of the concentration of deprotonated groups. Microfluidization also caused a decrease in nanoemulsions apparent viscosity, which fit with a decrease in the molar mass of sodium alginate due to a depolymerization of chains caused by covalent bond disruption. The increase of hydroxyls groups observed in alginates infrared spectrum may be due to the breaking of O-glycosidic bonds (depolymerization) or an opening of the alginate structure caused by mechanical forces into the microfluidizer, which increase the ability of sodium alginate for holding water (Chen, Gao, Yang, & Gao, 2013; Mohammad, Hosseini, Emam-djomeh, Hadi, & Meeren, 2013). Nonetheless, in spite of microfluidization may accelerate the collisions between the solvent molecules and sodium alginate molecules causing biopolymer degradation, depolymerized alginate chains were able to rearrange (Chemat & Khan, 2011). In the case of nanoemulsion infrared spectrum, the observed behavior was the opposite because inside these systems mechanical forces can attack the structure of microfluidized molecules, which were not able to restructure (Laneuville, Turgeon, & Paquin, 2013). The application of these forces may result in some reactions such as sodium alginate conjugation or oxidation (Feng et al., 2017). In this regard, high shear stress caused by microfluidization process could cause the oxidation of hydroxyl groups to carboxylic acids easily deprotonated in aqueous media, able to increase the carboxylate band of nanoemulsion spectrum. This fitted with the initial hypothesis that sodium alginate molecule is able to react with high energy molecules such as hydroxyl radicals ($-OH^\cdot$) produced from cavitation forces into the microfluidizer, which may cause the biopolymer partial breaking. This entailed the increase in the amount of exchangeable protons from carboxylic acids or hydroxyl groups (Feng et al., 2017).

As a result, those exchangeable protons, which were not observable by ^{1}H-RMN due to the use of deuterium dioxide as solvent; led to the decrease in the number of relative protons in microfluidized alginate and nanoemulsion spectra. Thus, results from both spectroscopic techniques indicated that, after microfluidization, sodium alginate might break and change its conformation influencing the properties of the resultant nanoemulsions. Concerning the results, it could be expected the breaking of sodium alginate in smaller oligomers through ultra-hydrogel permeation chromatography (GPC). In this regard, although sodium alginate molecule partially breaks, the re-aggregates formed after microfluidization process may have similar molecular weights than the initial chain. Those changes might be explained by a partial hydrolysis of alginate molecule that causes higher affinity for water, higher porosity and hence, changes in its molecular weight, which might produce a variation in the disposition of alginate chains around the oil droplets.

.

Effect of using protein-polysaccharide complexes on preventing Ostwald ripening in nanoemulsions

The understanding of interfacial biopolymers disposition is of great relevance in order to obtain stable emulsion-based nanostructured systems. It is believed that thicker interfaces may contribute to better stabilize molecules prone to easily suffer destabilization phenomena due to Oswald ripening effect such as short chain fatty acids (*eg.* alkanes, EOs). According to their structure, short-chain fatty acids are slightly water-soluble oils favoring their migration to the continuous phase (Suriyarak & Weiss, 2014). In this regard, biopolymer complexes are presented in chapter V as a potential alternative to build stronger and thicker interfaces that protect droplets against coalescence, flocculation or Ostwald ripening. For this purpose, differences between interfacially structured decane-in-water nanoemulsion single (protein or polysaccharide) or complex-stabilized were studied. Complexes containing whey protein isolate (WPI) and sugar beet pectin (SBP) in a ratio 1-1 (protein-pectin) were prepared at pH 3.5 in order to be used as decane-in-water nanoemulsions stabilizers. Decane was used as a model to predict the behavior of EOs against Ostwald ripening since it has resulted better in preventing the phenomenon than other alkanes (Zeeb, Gibis, Fischer, & Weiss, 2012).

Both single biopolymers and the complex led to nanoemulsions formation, therefore, all the droplets were below the detection limit of the optical microscope. In spite of the droplet growth observed during storage time, especially in the case of nanoemulsions stabilized by WPI or SBP alone, dispersed oil droplets remained undetectable by optical microscopy until 10 days of storage. However, nanoemulsions stabilized by either WPI or SBP presented prominent destabilization after 21 days of storage, whereas WPI:SBP complex-stabilized was barely starting to aggregate. Complex-stabilized nanoemulsions repulsion forces were higher than those produced at single-stabilized nanoemulsions interface preventing particles from coming together retarding flocculation and the subsequent phase separation.

Likewise, although complexes could not completely avoid Ostwald ripening, they resulted more effective in retarding it. According to our results, Dickinson (2009) reported that despite the fact that protein-polysaccharide complexes present high surface activity, they mostly behave like a soft polymer, which resembles the protein structures and thus cannot completely avoid the ripening process (Ghosh & Bandyopadhyay, 2012). WPI and SBP could desorb from droplets interface through depletion-flocculation mechanism, favouring coalescence phenomenon. For this reason, single-stabilized nanoemulsions exhibited a fast droplet growth.

With regards to the complex-stabilized nanoemulsions, the negative charge of droplets stabilized by protein-pectin complexes indicated that protein moieties of the complex may be primarily adsorbed at the o/w interface while pectin moieties might be potentially located at the outer region of the o/w interface. Certainly, the proposed mechanism for complex formation is that the protein nuclei might have increased their hydrophobic properties and therefore grows into larger particles, whereas pectin molecules were simultaneously incorporated (Turgeon, Schmitt, & Sanchez, 2007; Weinbreck, Rollema, Tromp, & De Kruif, 2004; Zeeb, Mi-Yeon, Gibis, & Weiss, 2018). Therefore, the monolayer coverage formed by the protein avoids droplets diffusion and electrostatic and steric repulsion forces from SBP chains may provide the negative surface charge. This was also confirmed by interfacial rheology measurements since just SBP exhibited an elastic interface, whereas the complexes and WPI showed a similar interaction with the decane.

SECTION II: Designing double emulsions as carriers of hydrophilic plant-derived bioactive compounds.

Effect of processing parameters and formulation on the physicochemical properties of double emulsions

The design and preparation of double emulsions ($W_1/O/W_2$) is complicated since it is required to stabilize at least two types of interfaces. There are four principal forms of double emulsions instability including coalescence of inner water droplets, coalescence of oil droplets, the rupture of oil film that separates the inner and outer phases due to high packing density both causing the leakage of the encapsulated bioactive compound and migration of inner water droplets or their water soluble materials through a process called "reverse micellar transport" (Hino, Shimabayashi, Tanaka, Nakano, & Okochi, 2001; Lamba, Sathish, & Sabikhi, 2015). Moreover, another practical concern is that inner droplets are prone to suffer swelling and rupture induced by osmotic transport and hence, this phenomenon has to be controlled in order to avoid their coalescence.

Therefore, the type and concentration of surfactant, the emulsification procedure and the incorporation of stabilizing agents are crucial for the effective formation of double emulsions. In this regard, the chapter VI of the present work aimed at obtaining an optimized formation procedure of water-in-oil-in-water ($W_1/O/W_2$) double emulsions as potential templates to carry hydrophilic (*e.g.* chlorophyllin; CHL) and/or hydrophobic (*e.g.* lemongrass essential oil; LG-EO) active compounds. First of all, primary W_1/O emulsions were formed at varying Span 80 or PGPR concentrations (4, 6 and 10% *w/w*) by HSH (11,000 rpm, 5 min). Subsequently, several emulsification methods and conditions were studied, such as high-shear homogenization (HSH), ultrasonication or microfluidization. Also the influence of sodium alginate incorporation (0-2% *w/w*) as well as salt addition (0-0.25M) on the particle size of the primary W_1/O dispersion was investigated. The particle size of W_1/O emulsions decreased at increasing the concentration of Span 80 or PGPR from 4% to 10% *w/w*. Nevertheless, the performance in reducing the particle size of the W_1/O emulsions was significantly different for both surfactants. In this regard, PGPR led to W_1/O emulsions with remarkably smaller particle sizes (< 1 μm) than Span 80 (> 32 μm), regardless the surfactant concentration. According to Tabibiazar & Hamishehkar (2015), PGPR may be able to better interact with the lipid phase due to its higher hydrophobicity compared to Span 80 forming a kinetic barrier protecting the emulsion against droplets coalescence.

Primary emulsions prepared by HSH (11,000 rpm, 5 min) with a 4% *w/w* PGPR led to particle sizes of 509 nm. Either HSH at higher energy, ultrasonication or microfluidization caused the breaking of primary emulsions. This "over-processing" was also reported by other authors like Jafari, He, & Bhandari (2007b), who observed a re-coalescence due to an increase in the droplets surface area, which favored polydispersion. Moreover, the incorporation of NaCl (0.05M) and sodium alginate (2% *w/w*) in the inner aqueous phase was vital for double emulsions destabilization. It is reported that the enhancement of the viscosity of the prior W_1/O emulsion may improve the stability of the subsequent double emulsion (Muschiolik & Dickinson, 2017) In addition, other authors have also observed a positive effect on $W_1/O/W_2$ stabilization after the incorporation of biopolymers to the inner aqueous

phase (Dickinson, 2011; Mezzenga, Folmer, & Hughes, 2004). It is believed that the origin of this improvement of stability is due to the interaction between polysaccharide and lipophilic surfactant, which provides a viscoelastic barrier thus preventing droplets coalescence (Garti, 1997). Indeed, some authors such as Dickinson (2011) also described the synergistic stabilizing effect between the biopolymer (*e.g.* sodium caseinate) and PGPR. The incorporation of electrolytes like NaCl together with biopolymers extended the thermodynamic stability of double emulsions by controlling the osmotic balance (Benichou, Aserin, & Garti, 2004). Primary emulsions containing 0.05M of NaCl remained stable during one week, whereas those with less or more concentration of salt destabilized during the third day of storage. The same behavior was observed by Aronson & Petko (1993), who proposed that electrolytes can increase the adsorption density of surfactant thus reducing emulsion interfacial tension and preventing destabilization.

For the formation of double emulsions, the prepared W_1/O emulsion containing 2% *w/w* of sodium alginate and NaCl 0.05M in the inner aqueous phase was dispersed in a second aqueous phase (W_2). The effect of *(i)* magnetic stirring time (3-24h), *(ii)* type and concentration of hydrophilic surfactant (*i.e.* Tween 20 or lecithin at 2-4% *w/w*) and *(iii)* impact of NaCl incorporation (0-0.25 M) in the W_2 on the formation of $W_1/O/W_2$ emulsions was evaluated. First of all, the higher the time of stirring, the lower the particle size of $W_1/O/W_2$ emulsions, reaching a value of 3.6 μm after 24h with regards the initial one of 8.6 μm. In agreement with our results, Bonnet, Cansell, Placin, Anton, & Leal-Calderon (2010) reported that their $W_1/O/W_2$ emulsions, in which W_1/O globules were about eight times larger than W_1 droplets, remained invariant over 30 days. Secondly, the increase of surfactant concentration contributed to reduce the particle size of lecithin-stabilized double emulsions, which in turn remained stable during at least 10 days. This surfactant seemed to have complementary rheological properties with PGPR allowing a better control in the stability of double emulsions (Bastida-Rodríguez, 2013). Finally, in order to ensure the stability of the second interface, a balance between Laplace and osmotic pressures was required. Therefore, the concentration of ions from salt and biopolymer in both aqueous phases (W_1 and W_2) had to be the same (0.05M and 2% *w/w*, respectively) preventing migration and subsequent breaking of $W_1/O/W_2$ emulsions structure.

The loading of stable double emulsions with hydrophilic (*e.g.* CHL) and/or lipophilic (*e.g.* LG-EO) active compounds did not have an impact in the physicochemical properties of emulsion-based systems. Particle size of primary emulsions containing CHL and/or LG-EO was 0.56 μm, while the mean droplet diameter of double emulsions was about 6-7 ± 0.7 μm. Double emulsions were of type C, in which, a single droplet contains several droplets with opposite polarity within thus acting as a highly efficient delivery system. Moreover, LG-EO at 1% *w/w* was able to slowdown inner water droplets diffusion regarding the higher EE of emulsions containing EO than those without ($91 \pm 6 \cdot 10^{-3}$ % and $84 \pm 1 \cdot 10^{-2}$ %, respectively). Additionally, the antioxidant capacity (AC) measured by DPPH and FRAP assays of double emulsions containing CHL and LG-EO was lower than in the case of those carrying only one of them. It is reported that after catalytic oxidation produced during the antioxidant activity tests, the essential oils show stronger antioxidant effects than before oxidation (Jukić & Miloš, 2005). Therefore, our results indicated that CHL prevented LG-EO oxidation.

$W_1/O/W_2$ emulsions were twice viscous than their starting primary emulsions with apparent viscosities greater than 250 mPa·s due to the presence of sodium alginate in both aqueous phases. Yang, Jiang, He, & Xia (2012) also observed a strong influence of sodium alginate dispersed in the aqueous phase in the apparent viscosity of emulsions, which can increase until sixty times when the biopolymer was not microfluidized (Artiga-Artigas et al., 2017).

The encapsulated active compound determined the final color of W_1/O and $W_1/O/W_2$ emulsions. Consequently, emulsions containing CHL tended to the green, whereas in those containing LG-EO, the predominant color was yellow.

SECTION III: Application of emulsion-based nanostructures to foods

Use of edible coatings from nanoemulsions to extend the shelf-life of a low-fat cut cheese

Nanoemulsions containing 1.5%, 2.0% or 2.5% *w/w* oregano essential oil (OR-EO) and enriched with 0.5% *w/w* mandarin fiber were applied as antimicrobial edible coatings onto a low-fat cut cheese surface in order to assess their antimicrobial effectiveness against inoculated *Staphylococcus aureus*; and their capability to improve the shelf life of a highly perishable product. The combination of sodium alginate and mandarin fiber, a prebiotic, resulted interesting to enhance the physicochemical properties of emulsions and provide added-value to the food product.

Coated cheese pieces prepared during chapter VII suffered a higher weight loss than those uncoated since in the coated product; the concentration of water on the matrix surface was grater according to the measured water activity (a_w) that was 0.974 for coated cheese pieces and 0.947 for the uncoated. Regarding the different coatings, those with the highest content of EO resulted more effective as barriers showing a weight loss of 195.3 ± 0.2 mg, and a higher water vapor resistance (WVR) than those with less concentration of OR-EO.

In order to evaluate the antimicrobial effectiveness of coatings, an initial microbial load of 10^6 CFU/g was inoculated on the surface of cylindrical cheese pieces. The initial load decreased 0.9 ± 0.1 log CFU/g on average, just after applying the different coatings or after their submersion in ultrapure water (uncoated cheese pieces). The concentration of OR-EO used in the formulation of edible coatings had a significant effect on their bactericidal activity against inoculated *Staphylococcus aureus* over time. The microbial population decreased 1.4 and 1.5 log CFU/g in coated cheese pieces containing 2.0 % or 2.5% w/w of OR-EO, respectively, during 15 days of refrigerated storage. However, coatings with a lower OR-EO concentration were not effective in reducing *Staphylococcus aureus* population. This is due to the higher the OR-EO concentration, the greater the carvacrol content. Carvacrol is the major active compound from OR-EO, which is able to modify the cell membrane of Gram-positive bacterial species such as *Staphylococcus aureus* (La Storia et al., 2011).

Likewise, results revealed that coatings with a concentration of OR-EO higher than 2.0% w/w clearly had an antimicrobial effect against psychrophilic bacteria and molds and yeast. However, the most effective microbial inhibition of psychrophilic bacteria was obtained for cheese pieces coated by the nanoemulsion with the highest percentage of OR-EO (2.5% w/w). In this case, the growth began after the 6^{th} day of storage and reached the equilibrium with values lower than 6.7 log CFU/g at the 13^{th} day. Regarding molds and yeast, the growth started after the 13^{th} day in uncoated cheese pieces and in those coated with the lowest percentage of OR-EO (1.5% *w/w*). However, the fungi growth for uncoated pieces was greater than for those coated. In the case of coatings prepared with a 2.0% *w/w* of OR-EO, the growth began after 17 days of storage. Lastly, cheese pieces coated with 2.5% *w/w* of OR-EO did not show molds and yeast growth at least during 24 days of experiment. Therefore, both psychrophilic bacteria and molds and yeast were also sensitive to carvacrol.

Moreover, coatings based containing OR-EO caused a decrease of O_2 consumption compared with the uncoated pieces from the 3th day of storage as a result of the control of the microbial growth. Although it has been observed that coatings with an upper percentage of EO had a higher resistance to gas diffusion due to their lipophilic nature, the presence of some carbohydrates such as alginate and mandarin fiber contributed to increase gas permeability (Rojas-Graü et al., 2007). This agrees with literature where it is reported that the capability of alginate or mandarin fiber chains of holding water in their structures together with the fact that EO concentration was low, could cause a decrease in the ability of coatings to act as barriers to the transport of humidity, gases, and aroma compounds (Espitia, Du, Avena-Bustillos, Soares, & McHugh, 2014; Miller & Krochta, 1997; Rojas-Graü et al., 2007).

Regarding ethanol production, there were not significant differences ($P>0.05$) between cut cheese coated by nanoemulsions containing 1.5% OR-EO and uncoated pieces. The same occurred for 2.0% and 2.5% OR-EO coatings probably because both resulted effective in the control of microbial growth. Moreover, it was observed that ethanol produced by cheese during propionic and acid fermentation due to the action of lactic bacteria (Acerbi, Guillard, Guillaume, Saubanere, & Gontard, 2016; Fröhlich-Wyder et al., 2013), reacted with different derivatives of primary or secondary biochemical processes that occur during cheese shelf life since its concentration was diminishing during storage.

Optical properties of nanoemulsions depended on OR-EO concentration, thus when they are applied as edible coatings the color of the coated cheese pieces was slightly altered. Indeed, WI was influenced by the rise of the *b** coordinate value, which indicates the increase of yellow color. In this regard, uncoated cheese pieces exhibited the highest WI value (76.32 ± 0.98) and there were no significant differences during the time. However, although coated cheese pieces were more yellow than uncoated, they were able to maintain the brightness and the external properties of cheese during the time.

Regarding textural properties, edible coatings allowed maintaining, not only the elasticity of coated cheese pieces but also their softness. Coated cheese pieces showed similar values of hardness, cohesiveness, gumminess and elasticity regardless the EO percentage incorporated in nanoemulsions. Nonetheless, uncoated pieces showed higher cohesiveness values, which decreases during the time; hence, coated cheese may break easily. The cheese becomes a cohesive material along the time because the particles are closer after the product dehydration (Szczesniak, 2002). Therefore, edible coatings helped to preserve the water into the food matrix maintaining the cohesiveness, whereby the disintegration of the product is less probable.

References

Acerbi, F., Guillard, V., Guillaume, C., Saubanere, M., & Gontard, N. (2016). An appraisal of the impact of compositional and ripening parameters on CO2 diffusivity in semi-hard cheese. *Food Chemistry*, *194*, 1172–1179.

Alba, K., & Kontogiorgos, V. (2017). Pectin at the oil-water interface: Relationship of molecular composition and structure to functionality. *Food Hydrocolloids*, *68*, 211–218.

Aronson, Michael P.; Petko, M. F. (1993). Highly Concentrated Water-inOil Emulsions: Influence of Electrolyte on Their Properties and Stability. *Journal of Colloid and Interface Science*, *159*, 134–149.

Artiga-Artigas, M., Acevedo-Fani, A., & Martín-Belloso, O. (2017). Effect of sodium alginate incorporation procedure on the physicochemical properties of nanoemulsions. *Food Hydrocolloids*, *70*, 191–200.

Artiga-Artigas, M., Guerra-Rosas, M. I., Morales-Castro, J., Salvia-Trujillo, L., & Martín-Belloso, O. (2018). Influence of essential oils and pectin on nanoemulsion formulation: A ternary phase experimental approach. *Food Hydrocolloids*, *81*, 209–219.

Bastida-Rodríguez, J. (2013). The Food Additive Polyglycerol Polyricinoleate (E-476): Structure, Applications, and Production Methods. *ISRN Chemical Engineering*, *2013*, 1–21.

Benichou, A., Aserin, A., & Garti, N. (2004). Double emulsions stabilized with hybrids of natural polymers for entrapment and slow release of active matters. *Advances in Colloid and Interface Science*, *108–109*, 29–41.

Bonnet, M., Cansell, M., Placin, F., Anton, M., & Leal-Calderon, F. (2010). Impact of sodium caseinate concentration and location on magnesium release from multiple W/O/W emulsions. *Langmuir*, *26*(12), 9250–9260.

Bourne, M. C. (2002). Principles of Objective Texture Measurement. *Food Texture and Viscosity: Concept and Measurement, 2nd Edition*, (1961), 107–188.

Chemat, F., & Khan, M. K. (2011). Ultrasonics Sonochemistry Applications of ultrasound in food technology : Processing , preservation and extraction. *Ultrasonics - Sonochemistry*, *18*(4), 813–835.

Chen, J., Gao, D., Yang, L., & Gao, Y. (2013). Effect of microfluidization process on the functional properties of insoluble dietary fiber. *Food Research International*, *54*(2), 1821–1827.

Dickinson, E. (2009). Hydrocolloids as emulsifiers and emulsion stabilizers. *Food Hydrocolloids*, *23*(6), 1473–1482.

Dickinson, E. (2011). Double Emulsions Stabilized by Food Biopolymers. *Food Biophysics*, *6*(1), 1–11.

Espitia, P. J. P., Du, W. X., Avena-Bustillos, R. de J., Soares, N. de F. F., & McHugh, T. H. (2014). Edible films from pectin: Physical-mechanical and antimicrobial properties - A review. *Food Hydrocolloids*, *35*, 287–296.

Feng, L., Cao, Y., Xu, D., Wang, S., & Zhang, J. (2017). Ultrasonics Sonochemistry Molecular weight distribution , rheological property and structural changes of sodium alginate induced by ultrasound. *Ultrasonics - Sonochemistry*, *34*, 609–615.

Fröhlich-Wyder, M. T., Guggisberg, D., Badertscher, R., Wechsler, D., Wittwer, A., & Irmler, S. (2013). The effect of Lactobacillus buchneri and Lactobacillus parabuchneri on the eye formation of semi-hard cheese. *International Dairy Journal*, *33*(2), 120–128.

Garti, N. (1997). Progress in stabilization and transport phenomena of double emulsions in food applications. *LWT - Food Science and Technology*, *30*(3), 222–235.

Ghosh, A. K., & Bandyopadhyay, P. (2012). Polysaccharide-Protein Interactions and Their Relevance in Food Colloids. *The Complex World of Polysaccharides*, 395–408.

Guerra-Rosas, M. I., Morales-Castro, J., Ochoa-Martínez, L. A., Salvia-Trujillo, L., & Martín-Belloso, O. (2016). Long-term stability of food-grade nanoemulsions from high methoxyl pectin containing essential oils. *Food Hydrocolloids*, *52*, 438–446.

Hansen, P. H. F., Arnebrant, T., & Bergström, L. (2001). Shear induced aggregation of a pectin stabilised emulsion in two dimensions. *Colloid and Polymer Science*, *279*, 153–160.

Hino, T., Shimabayashi, S., Tanaka, M., Nakano, M., & Okochi, H. (2001). Improvement of encapsulation eæ ciency of water-in-oil-in- water emulsion with hypertonic inner aqueous phase.

Hopkins, E. J., Chang, C., Lam, R. S. H., & Nickerson, M. T. (2015). Effects of flaxseed oil concentration on the performance of a soy protein isolate-based emulsion-type film. *Food Research International*, *67*, 418–425.

Jafari, S. M., He, Y., & Bhandari, B. (2007a). Effectiveness of encapsulating biopolymers to produce sub-micron emulsions by high energy emulsification techniques. *Food Research International*, *40*(7), 862–873.

Jafari, S. M., He, Y., & Bhandari, B. (2007b). Production of sub-micron emulsions by ultrasound and microfluidization techniques. *Journal of Food Engineering*, *82*(4), 478–488.

Jukić, M., & Miloš, M. (2005). Catalytic Oxidation and Antioxidant Properties of Thyme Essential Oils (Thymus vulgarae L.). *Croatica Chemica Acta*, *78*(1), 105–110.

La Storia, A., Ercolini, D., Marinello, F., Di Pasqua, R., Villani, F., & Mauriello, G. (2011). Atomic force microscopy analysis shows surface structure changes in carvacrol-treated bacterial cells. *Research in Microbiology*, *162*(2), 164–172.

Lamba, H., Sathish, K., & Sabikhi, L. (2015). Double Emulsions: Emerging Delivery System for Plant Bioactives. *Food and Bioprocess Technology*, *8*(4), 709–728.

Laneuville, S. I., Turgeon, S. L., & Paquin, P. (2013). Changes in the physical properties of xanthan gum induced by a dynamic high-pressure treatment. *Carbohydrate Polymers*, *92*(2), 2327–2336.

Lin, D., Lopez-Sanchez, P., & Gidley, M. J. (2016). Interactions of pectins with cellulose during its synthesis in the absence of calcium. *Food Hydrocolloids*, *52*, 57–68.

Lundberg, B., Pan, X., White, A., Chau, H., & Hotchkiss, A. (2014). Rheology and composition of citrus fiber. *Journal of Food Engineering*, *125*(1), 97–104.

Luo, X., Zhou, Y., Bai, L., Liu, F., Zhang, R., Zhang, Z., … McClements, D. J. (2017). Production of highly concentrated oil-in-water emulsions using dual-channel microfluidization: Use of individual and mixed natural emulsifiers (saponin and lecithin). *Food Research International*, *96*, 103–112.

Marinova, K. G., Alargova, R. G., Denkov, N. D., Velev, O. D., Petsev, D. N., Ivanov, I. B., & Borwankar, R. P. (1996). Charging of Oil−Water Interfaces Due to Spontaneous Adsorption of

Hydroxyl Ions. *Langmuir*, *12*(8), 2045–2051.

McClements, D. J. (2002). Theoretical prediction of emulsion color. *Advances in Colloid and Interface Science*, *97*(1–3), 63–89.

McClements, D. J., & Rao, J. (2011). Food-Grade nanoemulsions: Formulation, fabrication, properties, performance, Biological fate, and Potential Toxicity. *Critical Reviews in Food Science and Nutrition*, *51*(4), 285–330.

Mei, J., Guo, Q., Wu, Y., Li, Y., & Yu, H. (2015). Study of proteolysis, lipolysis, and volatile compounds of a Camembert-type cheese manufactured using a freeze-dried Tibetan kefir co-culture during ripening. *Food Science and Biotechnology*, *24*(2), 393–402.

Mezzenga, R., Folmer, B. M., & Hughes, E. (2004). Design of double emulsions by osmotic pressure tailoring. *Langmuir*, *20*(9), 3574–3582.

Miller, K. S., & Krochta, J. M. (1997). Oxygen and aroma barrier properties of edible films: carboxymethylated konjac glucomannan blend films. *Journal of Applied Polymer Science*, *88*(July), 1095–1099.

Mohammad, S., Hosseini, H., Emam-djomeh, Z., Hadi, S., & Meeren, P. Van Der. (2013). Food Hydrocolloids b -Lactoglobulin e sodium alginate interaction as affected by polysaccharide depolymerization using high intensity ultrasound. *FOOHYD*, *32*(2), 235–244.

Muschiolik, G., & Dickinson, E. (2017). Double Emulsions Relevant to Food Systems: Preparation, Stability, and Applications. *Comprehensive Reviews in Food Science and Food Safety*, *16*(3), 532–555.

Nambam, J. S., & Philip, J. (2012). Competitive adsorption of polymer and surfactant at a liquid droplet interface and its effect on flocculation of emulsion. *Journal of Colloid and Interface Science*, *366*(1), 88–95.

Neumann, M. G., Schmitt, C. C., & Iamazaki, E. T. (2003). A fluorescence study of the interactions between sodium alginate and surfactants. *Carbohydrate Research*, *338*(10), 1109–1113.

Osborn, H. T., & Akoh, C. C. (2004). Effect of emulsifier type, droplet size, and oil concentration on lipid oxidation in structured lipid-based oil-in-water emulsions. *Food Chemistry*, *84*(3), 451–456.

Pal, R. (2000). Shear viscosity behavior of emulsions of two immiscible liquids. *Journal of Colloid and Interface Science*, *225*(2), 359–366.

Rao, J., & Mcclements, D. J. (2011). Food-grade microemulsions, nanoemulsions and emulsions: Fabrication from sucrose monopalmitate & lemon oil. *Food Hydrocolloids*, *25*(6), 1413–1423.

Raybaudi-Massilia, R., Mosqueda-Melgar, J., & Martín-Belloso, O. (2008). Edible alginate-based coating as carrier of antimicrobials to improve shelf-life and safety of fresh-cut melon. *International Journal of Food Microbiology*, *121*(3), 313–327.

Rojas-Graü, M. A., Avena-Bustillos, R. J., Olsen, C., Friedman, M., Henika, P. R., Martín-Belloso, O., … McHugh, T. H. (2007). Effects of plant essential oils and oil compounds on mechanical,

barrier and antimicrobial properties of alginate–apple puree edible films. *Journal of Food Engineering*, *81*(3), 634–641.

Rojas-Graü, M. A., Soliva-Fortuny, R., & Martín-Belloso, O. (2009). Edible coatings to incorporate active ingredients to fresh-cut fruits: a review. *Trends in Food Science & Technology*, *20*(10), 438–447.

Salvia-Trujillo, L., Rojas-Graü, M. A., Soliva-Fortuny, R., & Martín-Belloso, O. (2014). Formulation of Antimicrobial Edible Nanoemulsions with Pseudo-Ternary Phase Experimental Design. *Food and Bioprocess Technology*, 3022–3032.

Sanatkaran, N., Masalova, I., & Malkin, A. Y. (2014). Effect of surfactant on interfacial film and stability of highly concentrated emulsions stabilized by various binary surfactant mixtures. *Colloids and Surfaces A: Physicochemical and Engineering Aspects*, *461*(1), 85–91.

Segnini, S., Dejmek, P., & Öste, R. (1999). Relationship Between Instrumental and Sensory Analysis of Texture and Color of Potato Chips. *Journal of Texture Studies*, *30*(6), 677–690.

Stintzing, F. C., & Carle, R. (2004). Functional properties of anthocyanins and betalains in plants, food, and in human nutrition. *Trends in Food Science and Technology*, *15*(1), 19–38.

Suriyarak, S., & Weiss, J. (2014). Cutoff Ostwald ripening stability of alkane-in-water emulsion loaded with eugenol. *Colloids and Surfaces A: Physicochemical and Engineering Aspects*, *446*, 71–79.

Szczesniak, A. S. (2002). Texture is a sensory property, *13*, 215–225.

Tabibiazar, M., & Hamishehkar, H. (2015). Formulation of a food grade water-in-oil nanoemulsion: Factors affecting on stability. *Pharmaceutical Sciences*, *21*(4), 220–224.

Turgeon, S. L., Schmitt, C., & Sanchez, C. (2007). Protein-polysaccharide complexes and coacervates. *Current Opinion in Colloid and Interface Science*, *12*(4–5), 166–178.

Weinbreck, F., Rollema, H. S., Tromp, R. H., & De Kruif, C. G. (2004). Diffusivity of whey protein and gum arabic in their coacervates. *Langmuir*, *20*(15), 6389–6395.

Yang, J. S., Jiang, B., He, W., & Xia, Y. M. (2012). Hydrophobically modified alginate for emulsion of oil in water. *Carbohydrate Polymers*, *87*(2), 1503–1506.

Zeeb, B., Gibis, M., Fischer, L., & Weiss, J. (2012). Influence of interfacial properties on Ostwald ripening in crosslinked multilayered oil-in-water emulsions. *Journal of Colloid and Interface Science*, *387*(1), 65–73.

Zeeb, B., Mi-Yeon, L., Gibis, M., & Weiss, J. (2018). Growth phenomena in biopolymer complexes composed of heated WPI and pectin. *Food Hydrocolloids*, *74*, 53–61.

Zhang, H. Y., Arab Tehrany, E., Kahn, C. J. F., Ponçot, M., Linder, M., & Cleymand, F. (2012). Effects of nanoliposomes based on soya, rapeseed and fish lecithins on chitosan thin films designed for tissue engineering. *Carbohydrate Polymers*, *88*(2), 618–627.

Conclusions

The main findings obtained based on the results observed in the present Doctoral Thesis are described below organized according to the three proposed sections. The following statements can be concluded:

SECTION I: Designing nanoemulsions as carriers of lipophilic bioactive compounds.

- Pectin influenced the physicochemical properties of the nanoemulsions where it is included. At concentrations over 1% *w/w*, pectin acted as an emulsifier even in absence of small molecule surfactants leading to submicron emulsions formation (d ≈ 350-850 nm). Nonetheless, the ζ-potential values indicated that pectin is weakly adsorbed at the oil-water interface as a modest or negligible decrease in the ζ-potential was observed depending on the type of oil (*e.g.* essential oils) at increasing biopolymer concentrations.

- Tween 20, lecithin and sucrose monopalmitate led to nanoemulsions with particle sizes below 400 nm. Moreover, although the three surfactants exhibited high encapsulation efficiencies (> 75%), just lecithin efficiently entrapped curcumin inside the nanostructured system thus protecting it against degradation. Lecithin in a concentration of at least 1% *w/w* was able to form long-term stable curcumin-loaded nanoemulsions (3 months of room temperature storage). Oppositely, sucrose monopalmitate was not effective in nanoemulsions stabilization, since phase separation occurred during the first 24h after preparation regardless its concentration.

- Ultrasonication (200 s, 100 μm) and microfluidization (2 cycles, 800 bar) allowed the preparation of highly concentrated submicron emulsions with particle sizes of 0.56 and 0.36 μm, respectively. The increase of oil volume fraction (φ) or surfactant-oil ratio (SOR) contributed to decrease the particle size of concentrated systems, which in turn increased their apparent viscosity and thus, the droplets spatial packing. High shear forces caused destabilization of emulsions with φ over 0.5. Highly concentrated emulsions (φ 0.5; SOR 0.1) exhibited high capacity to encapsulate curcumin regardless the particle size and the emulsification process used.

- Mechanical forces due to microfluidization caused the partial breaking of alginate chains leading to the formation of nanoemulsions with lower particle sizes than those prepared with non-microfluidized biopolymer. This breaking was irreversible but microfluidized biopolymer chains were able to rearrange according to gel permeation chromatography results.

- Nanoemulsions stabilized by whey protein isolate (WPI):sugar beet pectin (SBP) complexes showed lower droplet growth than those WPI- or SBP-stabilized. WPI is preferably adsorbed at droplet interface, whereas pectin chains are oriented towards the bulk aqueous phase since the interfacial rheology of WPI-SBP complexes was similar to that of the WPI alone. WPI:SBP complexes are a good strategy to form nanoemulsions stable during 48h containing decane, although as other short-chain triglycerides, it is very prone to suffer Ostwald ripening.

SECTION II: Designing double emulsions as carriers of hydrophilic bioactive compounds.

- The formation of double ($W_1/O/W_2$) emulsions requires the use of a two-step emulsification procedure, in which the primary emulsion may be formed by high-shear mixing (11,000 rpm, 5 min) and the subsequent secondary emulsion formation shall be formed by mild shear mixing (5,600 rpm, 2 min) followed by magnetic stirring (750 rpm, 2 min) in order to preserve their structure. The use of alginate as stabilizing agent and NaCl in both aqueous phases to maintain the osmotic balance between the internal and external water phases is of crucial importance to formulate stable double emulsions.

- Template $W_1/O/W_2$ emulsions allowed the successful incorporation of chlorophyllin (CHL) and lemongrass essential oil (LG-EO) without suffering destabilization. Both active compounds loaded in the prepared dual systems not only maintained their antioxidant capacity (AC) but showed a synergic behavior. Indeed, LG-EO incorporation increased the encapsulation efficiency of CHL, suggesting that the oil was able to slowdown inner water droplets diffusion and in turn, CHL delayed essential oil oxidation according to AC values. Moreover, LG-EO and sodium alginate contributed positively to reduce particle size and extending the stability of $W_1/O/W_2$ emulsions over time.

SECTION III: Application of emulsion-based nanostructures to foods

- The combination of mandarin fiber, and sodium alginate let the formation of stable antimicrobial nanoemulsions containing oregano essential oil (OR-EO) able to act as edible coatings onto cheese pieces.

- Edible coatings with concentration of OR-EO over 2.0% *w/w* improved the microbial stability of the cheese pieces, resulted effective in the decontamination of external pathogens such as *Staphylococcus aureus*, retarded the microbial growth of psychrophilic bacteria, molds and yeasts during at least 11 days regarding uncoated cheese pieces; and preserved cheese outward appearance during the time. As a consequence, the incorporation of nanoemulsions-based edible coatings containing OR-EO onto low-fat cut cheese extended the safety, quality, nutritional value and ultimately, the shelf life of this product.

Future Research

The results obtained in this Doctoral Thesis contributed to elucidate the main factors affecting the formation and stability of emulsion-based nanostructures that can be used as delivery systems of plant-derived bioactive compounds. Indeed, nanoemulsions and double emulsions prepared during the present work have demonstrated effective potential to encapsulate and protect lipophilic and/or hydrophilic bioactive compounds such as curcumin, chlorophyllin and essential oils. Nonetheless, further investigations are required in order to be used in the food industry including a deep study of these systems digestibility, the bioaccesibility and bioavailability of the encapsulated bioactive pigments and the feasibility of scaling up the preparation methodologies. Therefore, the following research is proposed:

- Study the functionality of encapsulated bioactive pigments using *in vitro* and *in vivo* models.

- Incorporate nanoemulsions and double emulsions to food matrices in order to assess their efficiency as delivery systems and explain the possible interactions with the components of food products.

- Evaluate the feasibility of extrapolating the formation procedure of emulsion-based nanostructures on a large scale in order to be introduced these systems into the industry field.

- Confirm the consumers' acceptance of food products containing emulsion-based systems, either as coatings or in liquid state.